ANALYTICA CHIMICA ACTA

International monthly devoted to all branches of analytical chemistry
Revue mensuelle internationale consacrée à tous les domaines de la chimie analytique
Internationale Monatsschrift für alle Gebiete der analytischen Chemie

ELSEVIER SCIENTIFIC PUBLISHING COMPANY

AMSTERDAM

Anal. Chim. Acta, Vol. 84, 1–230, June 1976

Published monthly

ANALYTICA CHIMICA ACTA

Publication Schedule for 1976

Vol. 81, No. 1	January 1976	
Vol. 81, No. 2	February 1976	**(completing Vol. 81)**
Vol. 82, No. 1	March 1976	
Vol. 82, No. 2	April 1976	**(completing Vol. 82)**
Vol. 83	May 1976	**(complete in one issue)**
Vol. 84, No. 1	June 1976	
Vol. 84, No. 2	July 1976	**(completing Vol. 84)**
Vol. 85, No. 1	August 1976	
Vol. 85, No. 2	September 1976	**(completing Vol. 85)**
Vol. 86	October 1976	**(complete in one issue)**
Vol. 87, No. 1	November 1976	
Vol. 87, No. 2	December 1976	**(completing Vol. 87)**

Subscription price for 1976 (covering November '75/December '76, Vols. 80–87): Dfl. 840.00 plus Dfl. 96.00 postage. Subscribers in the U.S.A. and Canada receive their copies by airmail. Additional charges for airmail to other countries are available on request. For advertising rates apply to the publishers.

Subscriptions should be sent to:
Elsevier Scientific Publishing Company, P.O. Box 211, Amsterdam, The Netherlands.

GENERAL INFORMATION

Languages

Papers will be published in English, French or German.

Detailed information

Authors should consult Vol. 73, p. 435 for detailed instructions. Reprints of this information are obtainable from Dr. Macdonald or from: Elsevier Editorial Services Ltd., Mayfield House, 256 Banbury Road, Oxford (Great Britain)

Submission of papers

Papers should be sent to:

Prof. Philip W, West,
Coates Chemical Laboratories,
College of Chemistry and Physics,
Louisiana State University,
Baton Rouge 3,
La. 70803 (U.S.A.)

or to:

Dr. A.M.G. Macdonald,
Department of Chemistry,
The University,
P O. Box 363,
Birmingham B15 2TT (Great Britain)

Reprints

Fifty reprints will be supplied free of charge. Additional reprints (minimum 100) can be ordered at quoted prices. They must be ordered on order forms which are sent together with the proofs.

ANALYTICA CHIMICA ACTA
Vol. 84 (1976)

ANALYTICA CHIMICA ACTA

International monthly devoted to all branches of analytical chemistry
Revue mensuelle internationale consacrée à tous les domaines de la chimie analytique
Internationale Monatsschrift für alle Gebiete der analytischen Chemie

ELSEVIER SCIENTIFIC PUBLISHING COMPANY

AMSTERDAM

PRINTED IN THE NETHERLANDS

Analytica Chimica Acta, 84 (1976) 1—13

MOLECULAR EMISSION CAVITY ANALYSIS PART VIII*. THE DETERMINATION OF ORGANOPHOSPHORUS COMPOUNDS

R. BELCHER, S. L. BOGDANSKI, O. OSIBANJO and A. TOWNSHEND

Chemistry Department, Birmingham University, P.O. Box 363, Birmingham B15 2TT (England)

(Received 12th December 1975)

SUMMARY

Optimal conditions for the rapid determination of nanogram amounts of organophosphorus compounds by MECA, based on HPO emission, are discussed. The effect of solvents on the emission characteristics is evaluated, and simultaneous determinations of some binary mixtures of organophosphorus compounds by the temporal resolution of the MECA peaks are described. Water cooling of the cavity can be used to enhance sensitivity and to improve the resolution of mixtures.

Phosphorus has its principal atomic resonance lines at 177.5 nm and 213.6 nm. Because of the absorption of radiation of such wavelengths by flame gases and ambient air, it is not possible to determine this element sensitively by atomic emission or absorption spectrophotometry in their usual flame modes. Recent flame photometric methods for the determination of phosphorus rely on the measurement of a band emission at 528 nm derived from HPO molecules which form in a cool, hydrogen-rich flame. In this manner, sub-p.p.m. amounts of inorganic and organic phosphorus compounds have been determined [1—5] by aspiration of their liquid samples into the flame.

Similarly, gas chromatographic detectors specific for phosphorus compounds have been developed which are based on detection of the HPO emission [6—8]. Although the green emission has been observed for more than a century [9], the source of the emission was first identified as arising from an HPO emitting species in 1963 [10]. The HPO emission for phosphorus compounds has also been detected within the MECA cavity [11], when introduced into a hydrogen—nitrogen flame. This was first observed by Bogdanski [12], who obtained a detection limit for phosphoric acid of 10 p.p.m. of phosphorus.

This paper describes a detailed investigation of the MECA responses of a number of organophosphorus compounds, nanogram amounts of which may be

*Part VII, R. Belcher, S. L. Bogdanski, I. H. B. Rix and A. Townshend, Anal. Chim. Acta, 83 (1976) 119.

determined. In addition, mixtures of certain phosphorus compounds may be determined because of the temporal resolution of their MECA peaks. Further resolution of certain organophosphorus compounds can be achieved by employing a recently developed, water-cooled MECA cavity.

EXPERIMENTAL

Reagents and chemicals

The organophosphorus compounds used (British Drug Houses, Ltd.) are listed in Table 5. Stock solutions containing 1000 p.p.m. of phosphorus were prepared for each compound; the solvents used were ethanol for aliphatic compounds, benzene for aromatic compounds, and methyl isobutyl ketone (MIBK) for all compounds, except for nicotinamide adenine dinucleotide (NAD) which was dissolved only in water. All experiments with mixtures were made with ethanolic solutions. Solutions containing lower concentrations of phosphorus were prepared by appropriate dilution.

Apparatus

A modified Evans Electroselenium (EEL) 240 atomic absorption spectrophotometer operating in the emission mode was used, as described previously [11]. The sample holder assembly used was that described previously for candoluminescence measurements [13]. The cavities employed in this study were made from (316) stainless steel and aluminium cylinders, 19 mm long and having a diameter of 12.5 mm. The optimal size of flat-bottomed cavity (8 mm diam. × 5 mm deep, 0.25 cm^3 volume) was drilled into one flat end of each cylinder and a small threaded hole (2BA) was formed in the other end, allowing the cylinder containing the cavity to be screwed on to a 2BA threaded brass rod coming from a cavity-holding assembly. In this manner, each cylinder could be attached to the holding assembly, so that the cavity could be positioned reproducibly above the burner in line with the detector.

The water-cooled cavity (Fig. 1) was constructed from an aluminium cylinder 39.5 mm long and 12.5 mm in diameter. A cavity of the same dimensions as above was drilled into one end, and a hole (4 mm diameter) was bored 30 mm into the other end, the outer 10 mm being threaded with a 2BA thread. Another hole (4 mm diam.) was drilled through one side of the cylinder 12 mm from the cavity end, and threaded to allow a threaded copper tube to be screwed into position, making a side-arm to the inner compartment of the cylinder. The threaded brass rod coming from the cavity-holding assembly was then pushed through and the aluminium cylinder screwed into position as before (see Fig. 1). The device contains the cavity which can be positioned above the burner, and can be cooled whilst in the flame by water flowing through.

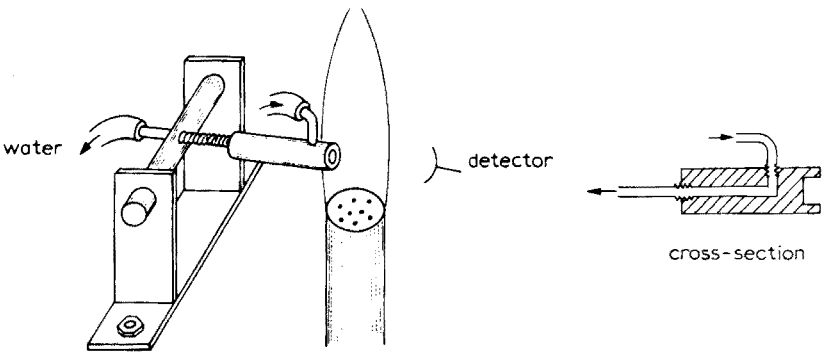

Fig. 1. Water-cooled cavity. The cavity is 5 mm deep and of 8 mm diameter.

General procedure

A 5-μl aliquot of stock solution containing phosphorus as a single compound or as a mixture of compounds was injected into the cavity, and the solvent was evaporated by a stream of nitrogen and air from the burner head for a predetermined time. Hydrogen gas was turned on and the flame ignited. The intensity of the green HPO emission at 528 nm, contained within the cavity, was recorded as a function of time. The emission intensity was measured as peak height obtained on a chart recorder (10 mV full scale deflection). The optimal gas flow rates were 4.1 l min^{-1} for nitrogen, 5.3 l min^{-1} for hydrogen and 6.2 l min^{-1} for air. The hydrogen was shut off after 30 s, before which time all phosphorus emission had ceased, leaving air and nitrogen and cold air from an air blower to cool the cavity for 3 min. This procedure was repeated for each sample injection.

Optimization of analytical parameters

Flame composition. The effect of flame composition on the HPO emission was studied by changing the flow rates of the constituent gases. In each experiment, a 5-μl aliquot of tri-n-butyl phosphate solution (containing 20 p.p.m. of phosphorus) in ethanol was injected into the aluminium cavity. The solvent was evaporated off for 10 s, and the emission intensity was measured. The results are shown in Tables 1 and 2. The optimal flame composition was considered, on the basis of these results, to be 4.1 l N_2 min^{-1}, 5.3 l H_2 min^{-1}, and 6.2 l min^{-1} for air. This optimal fuel-rich flame was used for the remainder of the work.

Position of the cavity in the flame. The cavity was pitched 7° below the horizontal [11]. The effect of changing the position of the cavity in the flame at a burner-cavity distance of 25 mm, on the emission from a 5-μl aliquot of the tri-n-butyl phosphate solution as described above, is shown in Table 3. The effect of changing the distance between cavity and burner head

TABLE 1

Effect of hydrogen and nitrogen flows on peak emission intensity for tri-n-butyl phosphate (Air = 5.4 l min^{-1}; results in mV)

Nitrogen (l min^{-1})	Hydrogen (l min^{-1})				
	2.0	3.5	5.3	7.0	9.0
0.0	2.5	3.0	4.3	13.0	9.8
2.8	5.3	13.3	20.0	22.0	10.3
4.1	8.0	18.3	31.0	3.8	0.0
5.5	4.3	24.0	21.5	0.3	0.0

TABLE 2

Effect of air flow on peak emission intensity for tri-n-butyl phosphate (N_2 = 4.1 l min^{-1}, H_2 = 5.3 l min^{-1})

Air flow (l min^{-1})	0.0	⩽3.0	4.0	4.5	5.4	6.2	7.0
Intensity (mV)	0.0	0.0	7.0	15.0	28.8	30.8	25.0

TABLE 3

Effect of the horizontal position of the cavity on peak emission intensity for tri-n-butyl phosphate
(Optimal flame 18 mm in diam., 25 mm above burner)

Distance into flame from edge (mm)	3.0	6.0	9.0	12.0	15.0
Intensity (mV)	19.0	32.0	40.0	38.0	32.0
t_m (s)	2.5	2.5	2.5	2.0	2.0

is shown in Table 4. Tables 3 and 4 indicate no significant change in t_m value (time from flame ignition to maximal emission) with change in burner–cavity distance and for different positions inside the flame. The central position in the flame (9 mm into the flame from the edge), 25 mm above the burner top was found to be optimal for the cavity. For mixtures of organophosphorus compounds, the cavity was positioned 30 mm above the burner top at the edge of the flame, because this gave an improved resolution, though at the expense of some sensitivity.

Effect of solvent evaporation

Solvent effects have been observed in flame studies of phosphorus compounds when aspiration systems are used. Certain solvents have been found to enhance the HPO emission, chemiluminescence [14] being given as the major reason. Syty and Dean [3] aspirated aqueous solutions of phosphoric

TABLE 4

Effect of cavity—burner distance on peak emission intensity for tri-n-butyl phosphate (Optimal flame; cavity 9 mm into the flame)

Distance (mm)	15.0	20.0	25.0	30.0	35.0	40.0
Intensity (mV)	1.5	19.5	39.0	31.0	21.0	17.0
t_m(s)	2.0	2.0	2.5	2.5	2.5	2.5

acid, and phosphoric acid and different organophosphorus compounds dissolved in MIBK, into a shielded fuel-rich air—hydrogen flame. All compounds gave similar relative HPO emission intensities, except for trimethyl phosphite which gave no emission; with MIBK they found a 3- to 4-fold enhancement for phosphoric acid compared to the aqueous solution.

It has also been shown that certain organic solvents can suppress the HPO emission in hydrogen flames. Dagnall et al. [2] found that addition of ethanol, to give a 10 % (v/v) solution, to an aqueous phosphoric acid solution, reduced the HPO emission in a nitrogen-diluted hydrogen diffusion flame. Belcher et al. [11] found that the presence of a 50 % hexane—propanol solvent suppressed the MECA S_2 emission from diphenyl sulphide. This effect was eliminated by allowing the solvent to evaporate before the cavity was inserted into the flame. As similar effects were possible for organophosphorus compounds, the effects of solvents were studied for each of the compounds investigated. The experiments were carried out with aluminium and stainless steel cavities.

The variation of the emission response with respect to the time allowed for solvent evaporation before flame ignition was studied first. Figure 1 shows how emission intensity and t_m vary with solvent evaporation time for trimethyl phosphite in MIBK and in ethanol. When the flame is ignited almost immediately after sample injection, the HPO emission is inhibited. Maximal HPO emission intensity is obtained after the solvent has evaporated (20 s for MIBK and 10 s for ethanol) from both cavities. Further evaporation time results only in loss of sample with a resultant decrease in emission intensity. Figure 1 also shows that the t_m values at maximal intensities for the MIBK and ethanol solutions are about the same for a particular cavity, as would be expected if all the solvent had been evaporated. The results indicate that when solvent is present the HPO emission is delayed (larger t_m values), but as more of the solvent is evaporated, the HPO response is faster and more intense, and at maximal emission intensity, t_m reaches a value which remains constant, and presumably characteristic of trimethyl phosphite alone, with further evaporation time. The greatest sensitivity is achieved with ethanol rather than MIBK as solvent, and the aluminium cavity.

There are several possible reasons for the quenching effect of the solvent in analyte emission. Hydrogen atoms, which are needed to form and excite

the HPO molecules, are consumed in the decomposition of the organic solvent. Further removal of hydrogen atoms may occur by formation of hydrogen molecules promoted by carbon-containing molecules. In addition to these chemical effects, the concurrent vaporization of the solvent and analyte would be expected to have a pronounced physical effect. The great volume of gas released as the solvent vaporizes reduces the residence time of any analyte vapour in the cavity. The time reduction would have a greater effect on the emission intensity of those phosphorus compounds which are easily vaporized but are slow in forming the HPO emitting species from the form being vaporized.

The boiling point of trimethyl phosphite (111 °C) is lower than that of MIBK (119 °C) but considerably higher than that of ethanol (78.5 °C). Thus it would be expected that much of the trimethyl phosphite would be lost during the evaporation of MIBK, which accounts for the relatively poor sensitivity obtained with this solvent. The evaporation of ethanol should be completed with an appreciable proportion of the analyte remaining in the cavity.

To avoid the above solvent effects, in all experiments with other compounds, the solvent was allowed to evaporate for 10 s (ethanol or benzene) or 20 s (MIBK), without water cooling where relevant. This was found to be sufficient to minimize the solvent effect for all the compounds studied.

Calibration

Calibration graphs were prepared for all the compounds investigated, under the optimal conditions for trimethyl phosphite, with ethanol, benzene and MIBK solutions; the above evaporation times were used. The results are summarized in Table 5, where the sensitivities given are the slopes of the calibration graphs. The graphs of peak height versus phosphorus concentration were linear for each compound over at least one order of magnitude; some calibration graphs are given in Fig. 3. The procedure described can be used to determine the most sensitive compounds in the range 0.5—10 p.p.m. of phosphorus and the less sensitive compounds in the range 5—200 p.p.m.

DISCUSSION

Previous workers using cool flames [2, 3, 6] found that different organophosphorus compounds gave emission responses of almost the same relative magnitude. Table 5 shows that the MECA emission response depends on the nature of the compound, the solvent and the cavity material. In most instances better sensitivities are obtained in ethanol or benzene, i.e. solvents with lower boiling points, than in MIBK, and in an aluminium rather than stainless steel cavity.

The order of sensitivity of the groups of compounds in either aluminium or stainless steel cavities is generally phosphine $\geqslant$ phosphine oxide $>$ phosphite $>$ phosphate, the sensitivity thus increasing with decreasing oxygen

TABLE 5

HPO emission from various organophosphorus compounds

Compound	B.p. (°C)	Stainless steel cavity				Al cavity	
		MIBK soln.		Ethanol (e) or benzene (b) soln.		Ethanol soln.	
		t_m(s)	Sens. (mV/ p.p.m.)	t_m(s)	Sens. (mV/ p.p.m.)	t_m(s)	Sens. (mV/ p.p.m.)
Trimethyl phosphate	197.2	4.0	0.02	4.0(e)	0.01	2.0	0.06
Triethyl phosphate	216.0	4.5	0.01	4.0(e)	0.02	2.0	0.26
Tri-n-butyl phosphate	289.0	5.0	0.08	4.5(e)	0.08	2.5	1.63
Triphenyl phosphate	245.0	13.0	0.02	12.0(b)	0.03	5.0	0.22
Tritolyl phosphate	244.0	13.0	0.02	13.0(b)	0.03	8.0	0.12
Di-(2-ethylhexyl) phosphate	—	14.0	0.01	13.5(e)	0.02	11.0	0.16
Trimethyl phosphite	111.2	4.0	0.01	4.0(e)	0.25	2.0	0.30
Diethyl phosphite	87.0	4.0	0.09	4.0(e)	0.25	2.0	0.36
Triphenyl phosphite	360.0	4.0	0.20	4.0(b)	0.17	3.0	0.34
Tri-n-butyl phosphine	236.0	4.0	0.43	3.0(e)	0.64	2.5	1.82
Triphenylphosphine	377.0	4.5	0.13	4.0(b)	0.39	2.5	2.92
Triphenylphosphine oxide	>360.0	7.0	0.15	6.5(b)	0.16	5.0	1.12

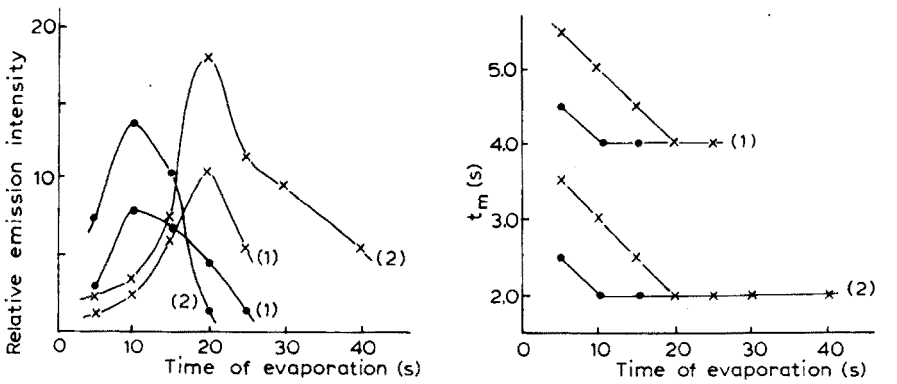

Fig. 2. Effect of solvent evaporation time on HPO emission from trimethyl phosphite in (•) MIBK (5 μg P) and (×) ethanol (0.25 μg P) in (1) stainless steel and (2) aluminium cavities.

content of the compounds. This is probably a consequence of the strong bond formed between phosphorus and oxygen (P=O ≃ 140 kcal mol^{-1}; P—O ≃ 95 kcal mol^{-1}). The mild hydrogen flame will have difficulty in breaking such bonds, so that compounds with more than one oxygen atom bound to the phosphorus will be much less likely to be converted to the emitting HPO species than those containing one or no oxygen atoms bound

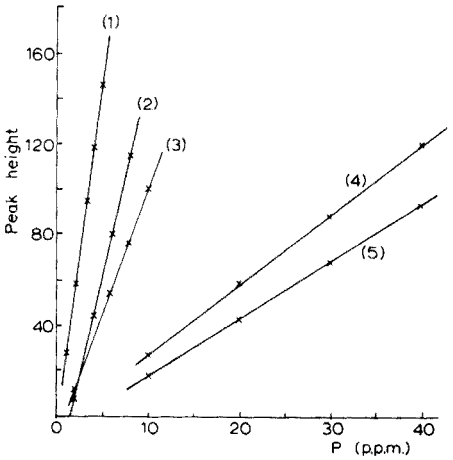

Fig. 3. Calibration graphs for (1) triphenylphosphine; (2) tri-n-butyl phosphate; (3) triphenylphosphine oxide; (4) trimethyl phosphite; (5) triethyl phosphate. Aluminium cavity.

to the phosphorus. The much weaker P—C bond (63 kcal mol^{-1}) ensures much easier breakdown in order to produce HPO molecules. It is interesting to note that a similar sequence of sensitivities is shown by the various inorganic sulphur anions, where an S_2 emitting species is formed [16].

For substances of boiling point greater than that of trimethyl phosphite, Table 5 shows that it makes little difference to the sensitivity whether the solvent is ethanol or MIBK, as one would expect because the compound would not be lost during solvent evaporation. (Triphenylphosphine is an exception to this statement.) In all instances, the compounds emit faster and give enhanced sensitivities in aluminium cavities compared to those of stainless steel, with enhancement factors (peak height), after solvent evaporatic ranging from about 3-fold for tri-n-butylphosphine to more than 20-fold for tri-n-butyl phosphate. This indicates that the aluminium cavity heats up faster than a stainless steel cavity of identical dimensions, as a result of the greater thermal conductivity of the aluminium, and of the greater density of the steel. Eventually, the greater thermal conductivity of aluminium, which causes more rapid heat transfer from the cavity to the bulk of the apparatus, ensures that the ultimate temperature of the aluminium cavity is appreciably lower than that of the steel cavity.

Detection limits (the least discernible signal above the flame background) of 0.1 p.p.m. phosphorus were obtained for triphenylphosphine, tri-n-butylphosphine and tri-n-butyl phosphate, although the sensitivities of these compounds differ. The relative standard deviation was 2—3 % (10 results) for all compounds investigated, at the 10—15-ng level.

A preliminary study of the MECA response of NAD was also carried out. An aqueous solution of NAD containing 500 p.p.m. of phosphorus gave an emission intensity of 2 mV and a t_m of 20 s in the stainless steel cavity. This insensitivity can be directly linked with its large t_m value and resistance to thermal breakdown.

The sensitivity and rapidity of the technique should make it useful for the detection and determination of trace amounts of a wide variety of organophosphorus compounds in pesticides, fungicides and petroleum fractions.

The effect of cooling the cavity

The enhancement of HPO emission in a hydrogen diffusion flame near a cool surface introduced into the flame was first observed by Salet [9] and has since been confirmed, and applied analytically [1, 6, 15]. Enhanced S_2 emission has been observed when the MECA cavity has been water-cooled [11]. Therefore, the effect of water cooling of the cavity on the emission of the twelve organophosphorus compounds listed in Table 5 was investigated. A cross-section of the water-cooled aluminium cavity is shown in Fig. 1. The effect of water flow rate (and thus decreasing cavity surface temperature) on the emission characteristics of the compounds is shown in Figs. 4 and 5.

Figure 4 shows that the HPO emissions from trimethyl phosphate, triethyl phosphate, triphenyl phosphite and trimethyl phosphite are enhanced by the external cooling, with the emission intensity remaining constant at water

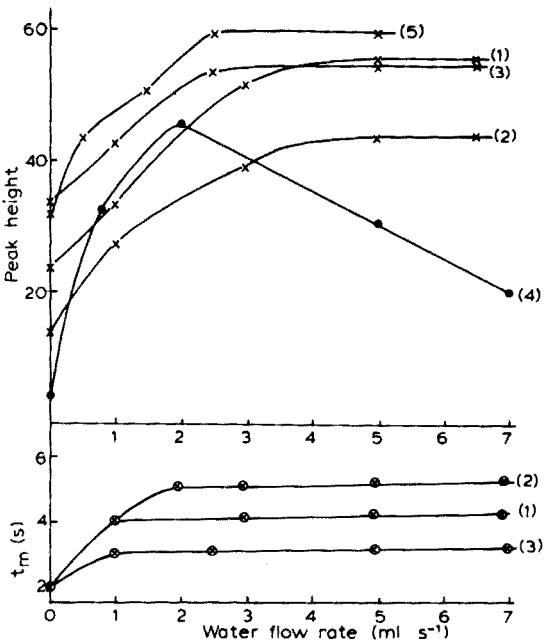

Fig. 4. Effect of water cooling on MECA response characteristics of: (1) trimethyl phosphate (100 p.p.m. P); (2) trimethyl phosphite (20 p.p.m. P); (3) triethyl phosphate (25 p.p.m. P); (4) diethyl phosphite (12 p.p.m. P); (5) triphenyl phosphate (20 p.p.m. P).

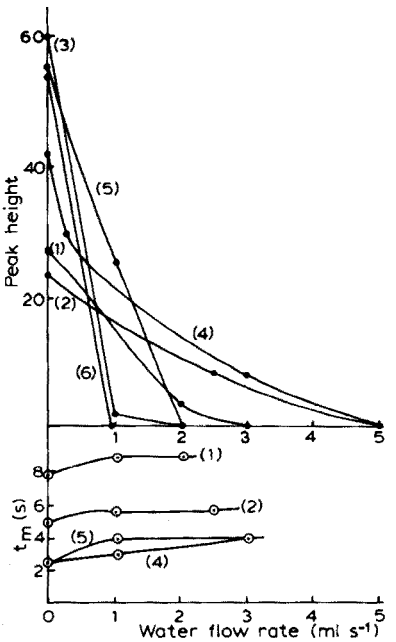

Fig. 5. Effect of water cooling on MECA response characteristics of: (1) tritolyl phosphate (50 p.p.m. P); (2) triphenyl phosphate (50 p.p.m. P); (3) di-(2-ethylhexyl) phosphate (100 p.p.m. P); (4) tri-n-butyl phosphate (5 p.p.m. P); (5) triphenylphosphine (5 p.p.m. P); (6) triphenylphosphine oxide (40 p.p.m. P).

flow rates greater than 5 ml s^{-1}. The t_m values also increase as the cavity is cooled. Emission from diethyl phosphite is also enhanced by moderate cooling, but greater cooling decreases the emission. The results for tritolyl phosphate, triphenyl phosphate, di-(2-ethylhexyl) phosphate, tri-n-butyl phosphate, triphenylphosphine and triphenylphosphine oxide (Fig. 5) show that the emission intensity of these compounds decreases and is eventually extinguished as the cooling of the cavity is increased. The t_m values are slightly increased on cooling the cavity. Tri-n-butyl phosphine also behaves in this way.

In general, the compounds which show enhanced emissions are those with the lower boiling points, and those which show supressed emissions are those with the higher boiling points; but although triphenyl phosphite has a very high boiling point, its emission is enhanced by cooling. Thus, the cooled cavity is too cold to volatilize the samples which give no emission. This was confirmed by removing the water cooling after a run with a less-volatile compound (tritolyl or di-(2-ethylhexyl) phosphate). Although no emission was observed under cooled conditions, the emission appeared when the cooling was removed (see below).

The cooled cavity may be used to enhance the sensitivity (2—6 times) for those compounds described above. Calibration graphs remain linear under these conditions.

Determination of mixtures of organophosphorus compounds

Because the t_m value of each compound is characteristic of that compound under the experimental conditions appertaining, it is possible to obtain resolved MECA peaks from compounds with sufficiently different t_m values. Thus, mixtures of sulphur anions, such as sulphite and sulphate [17], and mixtures of organotin compounds, such as dibutyltin oxide and tributyltin oxide [18], give resolved peaks, and both components can be determined. Similar resolution of certain organophosphorus compounds can be achieved in an aluminium cavity. Figure 6 shows the resolved peaks from a mixture of trimethyl phosphate (t_m = 2.0 s) and di-(2-ethylhexyl) phosphate (t_m = 11.5 s). Trimethyl phosphite (t_m = 2.0 s) can likewise be resolved from di-(2-ethylhexyl) phosphate. Trimethyl phosphate can also be resolved from tritolyl phosphate (t_m = 9.0 s) and from triphenyl phosphate (t_m = 7.0 s), although in the latter case there is slight overlapping of peaks. This indicates that a t_m difference of about 5.0 s is necessary under the present conditions to resolve peaks from nanogram amounts of organophosphorus compounds, when one of the compounds has a small t_m value. When both compounds have larger t_m values, a t_m difference of 4.5 s is insufficient to resolve the peaks satisfactorily; a mixture of triphenyl phosphate (t_m = 7.0 s) and di-(2-ethylhexyl) phosphate (t_m = 11.5 s) shows poor resolution. However, Fig. 7(a) shows that when trimethyl phosphate is also present, it is partly resolved from the peaks of the other two compounds. When peaks are resolved, there is no effect of one component on the peak height of the other compound, and the calibration graphs coincide with those obtained for single substances.

For some of those mixtures which cannot completely be resolved in the normal aluminium cavity, water cooling can be of assistance. Figure 7 shows the change in emission profile for a mixture of trimethyl phosphate, triphenyl phosphate and di-(2-ethylhexyl) phosphate as the flow of cooling water increases. As was expected from the effect of cooling on the emission of the

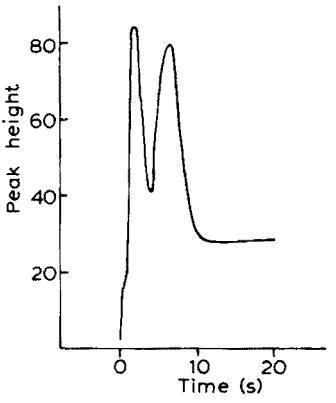

Fig. 6. MECA response from a mixture of trimethyl phosphate (100 p.p.m. P, t_m = 2.0 s) and triphenyl phosphate (60 p.p.m. P, t_m = 7.0 s).

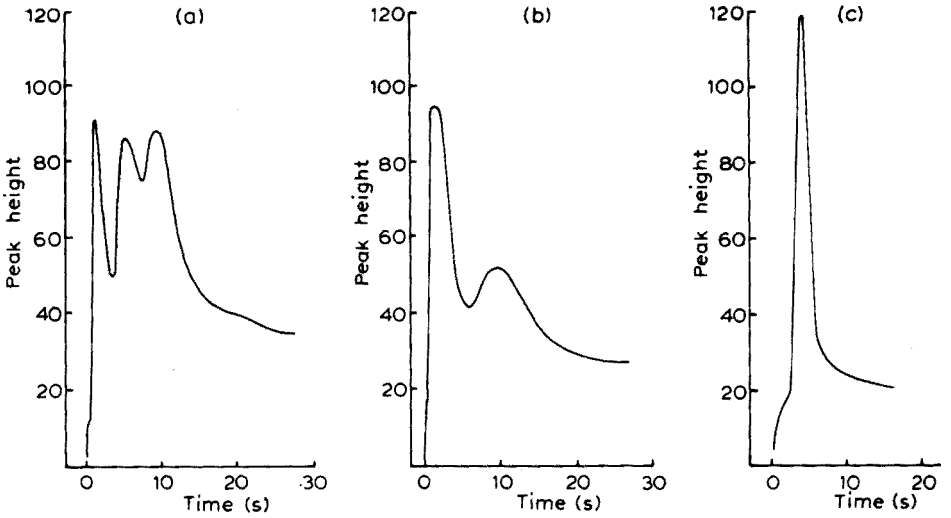

Fig. 7. Effect of water cooling on the MECA response from a mixture of trimethyl phosphate (100 p.p.m. P), triphenyl phosphate (50 p.p.m. of P) and di-(2-ethylhexyl) phosphate (50 p.p.m. of P).
(a), no water flowing; (b), 1 ml s^{-1} water flow; (c), 10 ml s^{-1} water flow.

individual compounds, the response of trimethyl phosphate is enhanced, whereas that of the other two compounds is eliminated when the cooling water flow is 10 ml s^{-1}. When the water is turned off, the peaks for the two remaining compounds are again obtained, only partially resolved as before (Fig. 8). These peaks are spread out because of the cooling effect of the water remaining, but not flowing, in the cooling chamber. There is no interference of the less volatile compounds on the response of trimethyl phosphate.

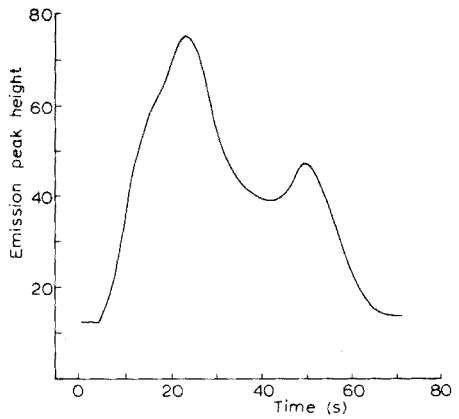

Fig. 8. HPO emission obtained from a mixture of triphenyl phosphate and di-(2-ethylhexyl) phosphate when water flow was stopped.

O. O. wishes to thank the Federal Government of Nigeria for the provision of a research scholarship.

REFERENCES

1 H. Dräger and B. Dräger, German Pat. 1,133,918 (July 1962).
2 R. M. Dagnall, K. C. Thompson and T. S. West, Analyst (London), 93 (1968) 72.
3 A. Syty and J. A. Dean, Appl. Opt., 7 (1968) 1331.
4 W. N. Elliott, C. Heathcote and R. A. Mostyn, Talanta, 19 (1972) 359.
5 G. L. Everett, T. S. West and R. W. Williams, Anal. Chim. Acta, 68 (1974) 387.
6 S. S. Brody and J. E. Chaney, J. Gas Chromatogr., 4 (1966) 42.
7 M. C. Bowman and M. Beroza, Anal. Chem., 40 (1968) 1448.
8 B. Versino and G. Rossi, Chromatographia, 4 (1971) 331.
9 G. Salet, Compt. Rend., 68 (1869) 404; Bull. Soc. Chim. Fr., 11 (1869) 302; Ann. Phys., 137 (1869) 171.
10 Lam Than My and M. Peyron, J. Chim. Phys., 60 (1963) 1289.
11 R. Belcher, S. L. Bogdanski and A. Townshend, Anal. Chim. Acta, 67 (1973) 1.
12 S. L. Bogdanski, Ph.D. Thesis, Birmingham Univ., 1973.
13 R. Belcher, S. L. Bogdanski and A. Townshend, Talanta, 19 (1972) 1049.
14 B. E. Buell, Anal. Chem., 34 (1962) 635.
15 C. Veillon and J. Y. Park, Anal. Chim. Acta, 60 (1972) 293.
16 R. Belcher, S. L. Bogdanski, D. J. Knowles and A. Townshend, Anal. Chim. Acta, 77 (1975) 53.
17 R. Belcher, S. L. Bogdanski, D. J. Knowles and A. Townshend, Anal. Chim. Acta, 79 (1975) 292.
18 C. O. Akpofure, R. Belcher, S. L. Bogdanski and A. Townshend, Anal. Lett., 8 (1975) 921.

Analytica Chimica Acta, 84 (1976) 15—22

AN ION-SELECTIVE ELECTRODE FOR METHYLAMINE

K. P. HSIUNG, S. S. KUAN and G. G. GUILBAULT

Department of Chemistry, University of New Orleans, New Orleans, Louisiana 70122 (U.S.A.)

(Received 11th November 1975)

SUMMARY

A simple electrode is described for the assay of methylamine in the concentration range 10^{-5}—10^{-2} M. The electrode is based on the air-gap sensor principle. In the range of linear response, the relative standard deviation is about 1.4 % when the measurement time is 24 min, and about 5 % when the equilibration time is 12 min. Some interference is noted from dimethylamine and ammonium chloride.

Numerous publications have described the determination of higher amines but relatively few publications have dealt with the small volatile aliphatic amines. The colorimetric method of Dubin [1] estimates simple primary amines spectrophotometrically as their DNP (2, 4-dinitrophenyl) derivatives An enzymatic method developed by Murden et al. [2] successfully distinguishes small primary amines in mixtures with secondary amines or amino acids. Ninhydrin has been used [3] in a colorimetric estimation of volatile methylamine in fresh sea food products. Ion-exchange chromatographic techniques have been employed to determine amines in biological fluids [4—6]. A specific gas chromatographic procedure for lower volatile amines has been developed [7], as has one with modified packings [8, 9] that allowed C_1—C_4 aliphatic amines to be determined. An iodimetric method by Grabowicz [10] was developed to measure methylamine in the presence of ammonia having a concentration less than 5 %. A new reagent synthesized for spectrometric analysis of ammonia and aliphatic amines by Kramer [11, 12] showed great potential for volatile amines.

Růžička and Hansen [13] recently developed the air-gap electrode, a modification of the potentiometric gas sensor, in which the hydrophobic gas-permeable membrane separating the inner electrolyte from the sample solution is replaced by an air gap. The response toward carbon dioxide and ammonia is fast and fairly sensitive. Air-gap electrodes have been used to determine the ammonia content of waste waters [14] the sulfite content of wine [15] and urea in urine and blood [16, 17]. Fiedler et al. [18] used the air-gap electrode successfully to measure the carbon dioxide content in water.

The present methylamine electrode described is based on the same type of

air-gap sensor. The purpose of this work was to find a direct and simple method for the detection and determination of N-methylcarbamate pesticide residues, via the sensing of the resulting methylamine moiety after either a chemical or an enzymatic decomposition.

EXPERIMENTAL

Apparatus

The Radiometer Type E 503610 glass electrode and the construction of the air-gap sensor were the same as described previously [16, 17]. The internal filling solution of the reference electrode used was the same as the electrolyte solution (see below). A Corning digital 110 pH meter and a Heath strip-chart recorder (model EU-205-11) with a d.c. offset module (EU-200-20) and a potentiometric amplifier (EU-200-10) were used for measuring and recording the electrode responses. A glass electrode (Sargent S-20070-10) and Beckman Zeromatic II pH meter were used for monitoring the pH values of the samples and preparing the buffer solutions. Before every series of analyses, the Radiometer flat-bottom combination glass electrode used in the air-gap electrode, was checked to ensure that a constant level of electrolyte filling solution was present.

All calibration curves were calculated by means of a least-squares analysis of the linear portions with a PDP-10 computer.

Reagents

Double-distilled water was used for all the sample preparations. All chemicals used were reagent or analytical grade: methylamine hydrochloride (Columbia Organic Chemical Co., Inc., Columbia, S. C.); dimethylamine (aqueous 40 % solution, Aldrich Chemical Co., Inc., Milwaukee, Wis.); ammonium chloride (MCB Chemical Co., Norwood, Ohio); sodium borate, potassium hydrogen and dihydrogen phosphate (J. T. Baker Chemical Co., Phillipsburg, N. J.); Tris (tris(dihydroxymethyl)-aminomethane, Sigma Chemical Co., St. Louis, Mo.); and the wetting agent (Victawet 12, Stauffer Chemical Co.).

Procedure

A cone-shaped polyurethane sponge, soaked with the proper amount of electrolyte solution (in most assays $5 \cdot 10^{-3}$ M methylamine and $5 \cdot 10^{-2}$ M KCl, plus wetting agent), was placed at the middle of the perspex electrode holder. (Note: This same solution was used as the internal filling solution for the glass reference combination electrode.) The electrode was renewed by placing the air-gap sensor on top of the electrode holder and allowing the electrode surface to contact the sponge slightly with several rotations of the teflon body of the electrode. In this way a reproducible base line could always be achieved. "Buffer" solution pH 12 (1 ml; NaOH + 0.2 M KCl) was placed in the polyethylene cell, followed by 1 ml of the methylamine

sample solution. Instantly, the electrode was placed on top of the cell holder for measuring the evolution of methylamine. Teflon-coated magnetic stirring bars were used to stir all solutions. Readings of the equilibrium pH (pH_e) were taken 12 and 24 min after the mixing and stirring of the buffer and substrate. The results were compared to determine the optimal time of reaction. The amount of methylamine was determined from a calibration plot of pH_e vs. methylamine concentration. The polyethylene cells were washed and dried thoroughly after each measurement.

RESULTS

Effect of electrolyte composition

The padding electrolyte (i.e. on the surface of the air-gap electrode) was studied first to decide at which electrolyte composition the electrode responses would be the most sensitive, the fastest, and least prone to interferences from possible contaminants commonly encountered, e.g. ammonium ion and dimethylamine. From the data obtained (Table 1), two conclusions were drawn: (1) the lower the salt concentration, i.e. potassium chloride, the better the selectivities, and (2) the lower the substrate (i.e. methylamine) concentrations, the better the sensitivities. Therefore, a compromise electrolyte composition, $5 \cdot 10^{-2}$ M potassium chloride and $5 \cdot 10^{-3}$ M methylamine, was used for all further experiments.

TABLE 1

The effect of electrolyte composition

Reagents[a]		Equilibrium pH observed at 10^{-3} M substrate concentration		
KCl	CH_3NH_2	NH_4Cl	Methylamine	Dimethylamine
$1 \cdot 10^{-1}$	$1 \cdot 10^{-3}$	7.22	8.03	7.91
	$5 \cdot 10^{-3}$	7.30	7.98	7.87
	$1 \cdot 10^{-2}$	7.22	7.96	7.87
$5 \cdot 10^{-2}$	$1 \cdot 10^{-3}$	7.22	7.70	7.15
	$5 \cdot 10^{-3}$	7.25	7.96	7.86
	$1 \cdot 10^{-2}$	7.12	7.72	7.60
$1 \cdot 10^{-2}$	$1 \cdot 10^{-3}$	7.40	8.31	8.23
	$5 \cdot 10^{-3}$	7.18	7.85	7.74
	$1 \cdot 10^{-2}$	7.10	7.66	7.55

[a]Placed on surface of air-gap glass electrode.

Studies of optimum pH for the methylamine air-gap electrode

The influence of carbon dioxide desorption. Air-gap electrodes operated at the basic pH values used in the sample solution show an effect of carbon dioxide desorption from the electrolyte layer (which is coated on the flat bottom of the Radiometer glass electrode) superimposed on the signals from the absorption and hydration of gaseous methylamine onto the electrolyte layer during the analysis. Since the desorption of carbon dioxide from the electrolyte layer causes a decrease in acidity (increase in pH values), the electrode response shifts in the same direction as for the absorption and hydration of methylamine. Therefore, this desorption of carbon dioxide from the electrolyte layer causes a drift in the characteristic response curve, which limits the sensitivity obtained. The magnitude of this desorption interference was studied at different pH values (Fig. 1). The results obtained indicate that the desorption of carbon dioxide from the electrolyte layer starts around a pH of the sample solution of 6.0, steadily increases until pH 11.0, then tends to level off beyond pH 13.0. This proves that, in general, the higher the pH of the sample solution, the greater the interference from carbon dioxide desorption.

The evolution of methylamine. Methylamine is a weak acid which exists in equilibrium with its dissolved gas in aqueous solution, and is, in turn, in equilibrium with the same gas above the sample solution. As the pH of the sample solution is changed, the equilibrium will finally be in favor of the gaseous component above the sample solution; therefore, a total conversion of methylamine to the gaseous state above the sample solution can be achieved. The effect of the pH of the sample solution on the methylamine gas evolution was studied, and the result (Fig. 2) was compared with the study of carbon dioxide desorption.

A buffer of pH 12.0 was decided to be optimum for good methylamine evolution, with a reasonably low amount of drifting due to carbon dioxide desorption.

Interference studies

The influence of ammonium ion and dimethylamine on the response characteristics of a methylamine air-gap electrode are shown in Figs. 3 and 4. The mixed solution method was used to calculate the selectivity coefficient, k_{ij}: the methylamine concentration was varied while that of interferent was present at concentrations of $1.0 \cdot 10^{-4}$, $1.0 \cdot 10^{-3}$, and $1.0 \cdot 10^{-2}$ M [19]. The results obtained (Table 2) indicate that the dimethylamine interfered more strongly than the ammonium ion.

Effect of temperature

The temperature effect on the response characteristics of the methylamine air-gap electrode was studied at three different temperatures. As shown in

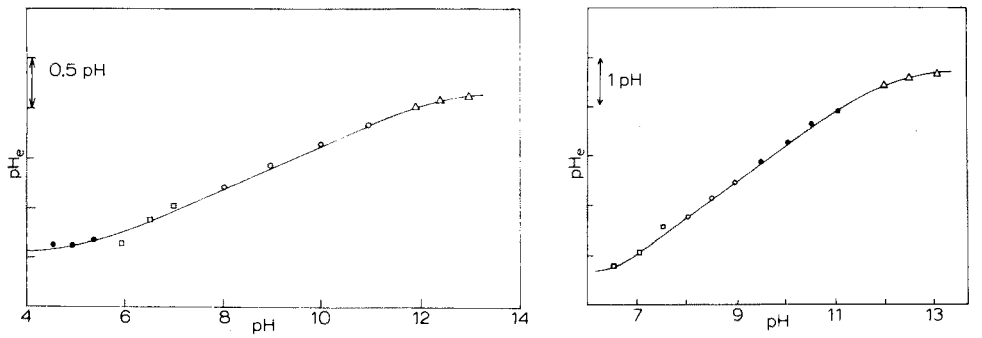

Fig. 1. The effect of pH of the sample solution on the CO_2 desorption from the electrode "surface-coated" electrolyte layer. pH_e is the equilibrium pH recorded at the electrode surface. •, phosphate buffer, 0.1 M; □, phosphate buffer, 0.1 M; ○, tris buffer, 0.1 M; △, KCl—NaOH "buffer", 0.2 M.

Fig. 2. Effect of pH of the sample solution on the evolution of gaseous methylamine. △, KCl—NaOH buffer, 0.2 M; •, borax buffer, 0.025 M; ○, tris buffer, 0.1 M; □, phosphate buffer, 0.1 M.

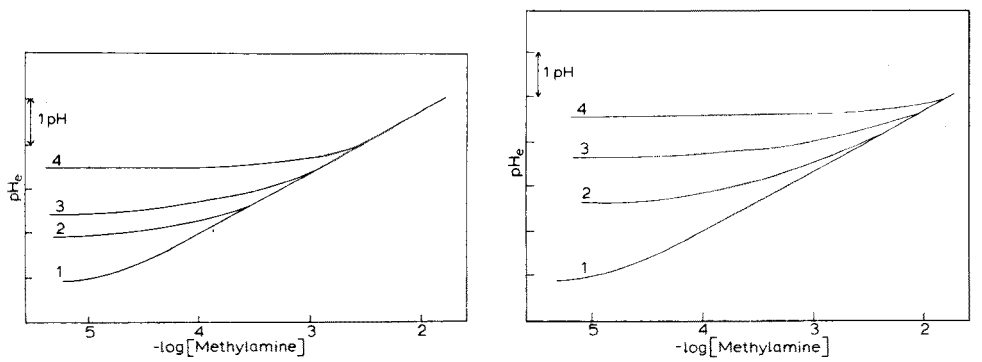

Fig. 3. Influence of ammonium chloride on response characteristics of methylamine air-gap electrode. 1, $1.0 \cdot 10^{-3}$ M methylamine; 2, $1.0 \cdot 10^{-3}$ M methylamine + $1.0 \cdot 10^{-4}$ M ammonium chloride; 3, $1.0 \cdot 10^{-3}$ M methyl amine + $1.0 \cdot 10^{-3}$ M ammonium chloride; 4, $1.0 \cdot 10^{-2}$ M methylamine + $1.0 \cdot 10^{-2}$ M ammonium chloride.

Fig. 4. Influence of dimethylamine on response characteristics of methylamine air-gap electrode. 1, $1.0 \cdot 10^{-3}$ M methylamine; 2, $1.0 \cdot 10^{-3}$ M methylamine + $1.0 \cdot 10^{-4}$ M dimethylamine; 3, $1.0 \cdot 10^{-3}$ M methylamine + $1.0 \cdot 10^{-3}$ M dimethylamine; 4, $1.0 \cdot 10^{-3}$ M methylamine + $1.0 \cdot 10^{-2}$ M dimethylamine.

Fig. 5, the higher the temperature, the more methylamine gas evolved, and the wider the linear range at 35 °C, i.e. from $1.0 \cdot 10^{-5}$ to $1.0 \cdot 10^{-2}$ M with a detection limit of $6.7 \cdot 10^{-6}$ M. At room temperature (23 °C) the linear range was not as wide, yet the sensitivity, $8.5 \cdot 10^{-6}$ M, was not much different from that obtained at 35 °C. Hence, all further studies were performed at room temperature.

TABLE 2

Influence of ammonium chloride and dimethylamine on methylamine air-gap electrode response

Reagent	k_{ij} at reagent concentration of:		
	$1.0 \cdot 10^{-4}$ M	$1.0 \cdot 10^{-3}$ M	$1.0 \cdot 10^{-2}$ M
Dimethylamine	2.2	1.2	1.2
Ammonium chloride	$9.1 \cdot 10^{-1}$	$4.5 \cdot 10^{-1}$	$1.6 \cdot 10^{-1}$

Calibration curves by the equilibrium method and the kinetic method

Figure 6 is the calibration curve obtained by measuring the equilibrium pH of a sample solution of methylamine whose original pH was adjusted to 12.0. For each standard concentration, at least ten determinations were performed. The slopes of the straight-line portion of the calibration curve obtained from the data collected, after incubation for 12 min and 24 min, are 1.35 and 1.38 ΔpH_e units/decade, respectively, calculated by the least-squares fitting method. The same set of data was analyzed by the kinetic method i.e. measuring the constant initial velocities vs. methylamine concentrations (Fig. 7). The results indicate that the calibration curve by the kinetic method has a slope of 0.74 ΔpH_e/decade. Also, a lower concentration of methylamine can be detected, $1.45 \cdot 10^{-6}$ M, compared to the equilibrium method, $8.5 \cdot 10^{-6}$ M (for the data collected after 24 min). The readings taken after mixing for 12 min show that the evolution process is 97—99 % complete, compared with the readings taken after 24-min mixing at different concentrations where an equilibrium pH_e is reached.

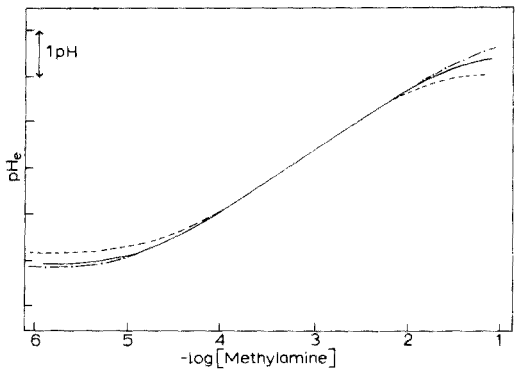

Fig. 5. Influence of temperature on the response characteristics of methylamine air-gap electrode. (- - - -) 15 °C; (——) 23 °C; (— · —) 35 °C.

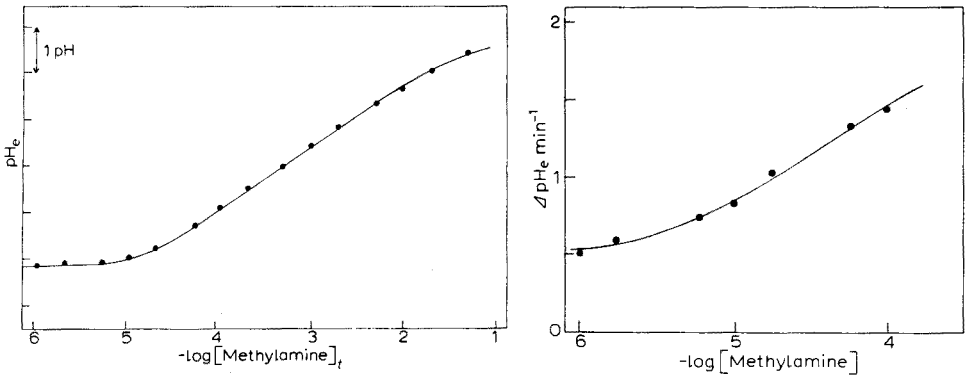

Fig. 6. Calibration curve by the equilibrium method. Electrolyte = $5 \cdot 10^{-3}$ M methylamine + $5 \cdot 10^{-2}$ M KCl; solution pH = 12.0; T = 23 °C. The data collected after 24-min incubation present a calibration curve with a linear region given by the equation, $Y = -1.35\,x + 12.49$ (r.s.d. 1.48 %). Data collected after 12-min incubation show a linear region given by: $Y = -1.38\,x + 12.48$ (r.s.d. 5.35 %).

Fig. 7. Calibration curve by the kinetic method. Conditions as for Fig. 6. The linear portion of this calibration curve is given by: $Y = -0.74\,x + 4.49$ (r.s.d. 13.7 %).

DISCUSSION AND CONCLUSIONS

The complete removal of salt, i.e. potassium chloride, from the electrolyte solution caused bad reproducibility, possibly because of fluctuations in ionic strength before and after each measurement. The optimum pH for minimizing carbon dioxide desorption in the presence of methylamine — for the least problems with desorption, the highest methylamine responses and a "total conversion" mode of methylamine evolution — should be above pH 13.0. But, practically, it is not always reliable to measure pH at values above 12.0, with a regular type of glass electrode. Hence, at pH 13, neither the equilibrium method nor the kinetic method gave a Nernstian type of response.

The curvature observed in the calibration plots of Figs. 6 and 7 at high and low concentrations of methylamine can be explained by: (1) incomplete transport of methylamine to the electrode sensing surface at high sample concentrations; (2) the long times required for low concentrations of gaseous methylamine to reach equilibrium at the electrode surface; (3) at low sample concentrations, the water transport and desorption of carbon dioxide may provide the major contributions to the electrode responses, so that the signal from the sample becomes less prominent. The standard deviation around the linear part of the calibration curve obtained from the data taken 24 min after mixing is 0.0062 pH_e (corresponding to a relative standard deviation of 1.48 %), that from the data taken 12 min after mixing is 0.0223 pH_e (corresponding to a relative standard deviation of 5.35 %), and that from the kinetic method is 0.0571 $\Delta pH_e/\Delta t$ (corresponding to a relative standard deviation of 13.70 %). Therefore, parameters such as small variations in room temperature,

the freshness of the electrolyte solution, the internal filling solution level, etc., which are not important in the long incubation time method, become important for reproducibility in the short incubation time method and in the kinetic method. Especially in the case of the kinetic method, up to 30 % of the data used would have to be discarded because of wild scattering if strict experimental conditions were not followed. As can be seen, the applicable range of the kinetic method is much narrower than that obtained from the equilibrium method; this limits the future use of this mode of analysis.

Ammonium ion and dimethylamine were selected for the interference studies because they are commonly encountered in the environment, as the original forms of fertilizers and the degradation products of some N,N'-dimethylcarbamate pesticide residues, i.e. Dimetilan, Isolan, pyrolan, etc. The procedure described herein for the assay of methylamine and dimethylamine could be applied to the assay of carbamate pesticides after hydrolysis.

The financial assistance of the National Institutes of Health, Environmental Sciences (Grant No. ES 00426), is gratefully acknowledged. The authors wish to thank Dr. J. Růžička and Dr. E. Hansen of the Technical University of Denmark, for their kind help and assistance with the air-gap electrode.

REFERENCES

1 D. T. Dubin, J. Biol. Chem., 237 (1960) 783.
2 P. J. Large, R. R. Endy, and D. J. Murden, Anal. Biochem., 32 (1969) 402.
3 K. Harada, T. Anan, T. Kii and K. Yamada, Suisan Daigakko Kenkyu Hokoku, 16 (1967) 11.
4 M. Yoshioka, A. Ohara, H. Kondo and H. Kanazawa, Chem. Pharm. Bull., 17 (1969) 1276.
5 S. Holder and H. Bremer, J. Chromatogr., 25 (1966) 48.
6 H. Hirokuki, S. Hoichiro, R. Soji, M. Fumiko and O. Fumiko, Anal. Biochem., 35 (1970) 377.
7 Y. Kaburaki, Y. Mikami, Y. Okabayashi, and Y. Saida, Bunseki Kagaku, 18 (1969) 1100.
8 A. DiCorcia, D. Fritz and F. Bruner, Anal. Chem., 42 (1970) 1500.
9 A. DiCorcia, and R. Samperi, Anal. Chem., 46 (1970) 977.
10 W. Grabowicz, Chem. Anal., 14 (1969) 271.
11 D. N. Kramer, U.S. Clearing House Fed. Sci. Tech. Inform., (1969) No. 713556.
12 D. N. Kramer and J. M. Sech, Anal. Chem., 44 (1972) 395.
13 J. Růžička and E. H. Hansen, Anal. Chim. Acta, 69 (1974) 129.
14 J. Růžička, E. H. Hansen, P. Birgarrd and E. Reymann, Anal. Chim. Acta, 72 (1974) 215.
15 E. H. Hansen, H. B. Filho and J. Růžička, Anal. Chim. Acta, 71 (1974) 225.
16 E. H. Hansen and J. Růžička, Anal. Chim. Acta, 72 (1974) 353.
17 G. G. Guilbault and M. Tarp, Anal. Chim. Acta, 73 (1974) 355.
18 W. Fiedler, E. H. Hansen and J. Růžička, Anal. Chim. Acta, 74 (1975) 423.
19 G. J. Moody and J. D. R. Thomas, Talanta, 19 (1972) 623.

Analytica Chimica Acta, 84 (1976) 23—29

AN ENZYME REACTOR ELECTRODE FOR UREA DETERMINATIONS

GILLIS JOHANSSON and LARS ÖGREN
Department of Analytical Chemistry, University of Umeå, S-901 87 Umeå (Sweden)
(Received 19th December 1975)

SUMMARY

An enzyme reactor electrode system for the determination of urea is described. A buffer is pumped through an enzyme reactor (0.4 ml) containing urease immobilized with glutaraldehyde to glass. The effluent is mixed with sodium hydroxide pumped through a second channel and fed through an ammonia gas electrode. Samples are introduced via a third flow channel and mixed with the buffer. The conversion of urea to ammonia is quantitative for sample concentrations of less than 0.03 M for a flow rate of 40 ml h^{-1}. The reactor electrode shows a Nernstian slope of 57 mV/decade for $5 \cdot 10^{-5}$—$3 \cdot 10^{-2}$ M urea. The response is independent of variations in the flow rate, enzyme activity or temperature of the reactor.

During recent years considerable interest has been focused on enzyme electrodes. Much of the work reported on successive improvements of the technique has been based on the determination of urea as an example. At first, urease was immobilized in a gelatinous layer wrapped round a cation-selective glass electrode [1—3]; the electrode responded to the ammonium ions produced in the enzymatic reaction. The selectivity of the glass electrodc was not very high and therefore other approaches were studied. The nonactin electrode [4] provided better selectivity for ammonium over the alkali metals [5]. Further refinements reduced the interferences [6] to a level where blood serum measurements became feasible, despite some remaining interferences [7, 8]. Other approaches for urea determinations have included sensing of the pH-changes of a polyacrylamide gel containing entrapped urease and wrapped around a pH-electrode [9]. The carbon dioxide level has also been monitored [10] and ion exchangers have been used to improve the selectivity [11]. The ammonia gas electrode [12] can provide an unlimited selectivity for ammonia over ions in the solution. This electrode has been covered with a layer of enzyme on the surface [13] and used for urea determinations. It has also been used in a flow system containing soluble urease [14]. The air-gap electrode [15] also provides excellent selectivity [16] and has been used for urea determinations in blood and serum [17, 18]. A metal sulphide gas electrode can also be used for ammonia determinations above $10^{-3.5}$ M ammonia [19]. A double-membrane urea electrode was recently described [20]. Several reviews have summed up the work on enzyme electrodes [21—23].

Substantial improvements have resulted from the work mentioned above but still several problems remain to be solved, the most notable being the variation of the signal with stirring and the change of the calibration with time. In the air-gap electrodes [16—18], the enzyme is separated by the air-gap from the sensing electrode surface, and this allows the enzyme reaction and the release of ammonia to be conducted at their optimal pH values [16].

In the present paper, a rather different approach is described. The enzyme is separated entirely from the electrode so that both the enzyme and the electrode are operated at their optimum pH. The immobilized enzyme is contained in a small reactor in a flow system operated under such conditions that the substrate is converted to products with 100 % efficiency. The effluent from the reactor is made alkaline with a flow of sodium hydroxide and passed into a flow-through gas electrode.

An enzyme reactor has been used analytically in connection with flow microcalorimetry [24] as well as on a larger scale where fractions of the effluent were analyzed with a cation-selective electrode [25]. An arrangement utilizing similar ideas as the reactor electrode has been described by Sundaram [26], who immobilized urease on the inside of a plastic tubing.

EXPERIMENTAL

Apparatus

The flow system shown in Fig. 1 was used for the measurements. A three-channel peristaltic pump or an infusion pump with three all-glass syringes was used. The buffer was 0.2 M Tris-HCl (pH 7.0) and 2mM EDTA. The next channel contained water which could either flow directly to a mixer or be diverted through a sample loop. The samples were thus interspaced with water. The buffered sample was fed into the enzyme reactor and then mixed with 1.4 M sodium hydroxide. The effluent was passed through a heat-exchanger coil (650 mm long, i.d. 0.5 mm, volume 140 μl) which was immersed in water. The effluent was then passed through the flow chamber of an EIL ammonia probe (Electronic Instruments Ltd., England, Model 8002-2). This gas electrode for ammonia contains a membrane permeable

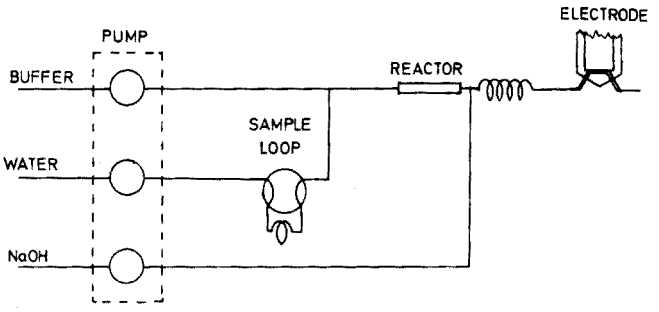

Fig. 1. Flow system for the enzyme reactor electrode.

to ammonia but impermeable for ions; its performance was recently evaluated [27]. The potential of the glass electrode in the ammonia probe was monitored by a pH-meter provided with a strip chart recorder and a printer in parallel. The tubings, connectors, heat exchangers and the sample loop were assembled from teflon components for liquid chromatography (Altex).

Two enzyme reactors, A and B, were used. Reactor A was 35 mm long, (i.d. 6 mm, volume 1 ml) and contained polyacrylamide gel with immobilized urease (Sigma Chemical Co., U-5376). Reactor B was 45 mm long (i.d. 3.4 mm, volume 400 μl) and contained urease immobilized on glass beads (see below). Filter discs were inserted at the ends and the connections were made so that the dead volume was very small.

Immobilization of urease

The urease was covalently bound to glass via glutaraldehyde coupling, by methods pioneered by Weetall and Hersch [25]. This is one of the simplest and gentlest coupling methods [28]. The technique has also been used with the enzyme thermistor [29].

CPG-10 controlled pore glass (10 ml; diameter 70—150 μm, pore diameter 70 nm; Corning Glass Works, N.Y.) was boiled in 150 ml of 5 % nitric acid for 45 min. The glass beads were washed with about 1 l of water on a glass filter G3 and dried in an oven at 95 °C.

3-Aminopropyltriethoxysilane (5 g) was added to 45 ml of water and the pH was carefully adjusted to 3.45 with 5 M HCl. The dried glass was added, the pH checked and then the mixture was kept at 75 °C on a water bath for 2 h 45 min. The flask was swirled every 15 min. The mixture was filtered, washed and dried as described above. The alkylamino glass can be stored in this condition until batches are needed.

A buffer containing 0.1 M sodium phosphate (pH 7.0) and 2.5 % glutaraldehyde was prepared by adding the aldehyde (BDH Chemicals) from a 25 % stock solution just before use. Alkylamino glass (1 g) was added to 5 g of the glutaraldehyde buffer. The reaction was allowed to proceed for 1 h at room temperature, the first 30 min at reduced pressure to decrease the oxygen partial pressure. The activated glass was washed well with distilled water.

Urease (100 mg; Sigma U-1500, 1500-3000 U g^{-1}) was dissolved in 3 ml of cold (+4 °C) 0.1 M sodium phosphate (pH 6.0) and the activated glass was added. The solution was kept at +4 °C for 2.5 h, the first 30 min at reduced pressure. The glass beads were washed with 250 ml of cold buffer and 500 ml of cold water and stored moist at +4 °C.

RESULTS

The ammonia probe was calibrated with ammonium chloride solutions introduced via the sample loop, the enzyme reactor being removed during this operation. The response was strictly linear between 0.2 and 10^{-5} M NH_4^+

in the sample. The slope was 57.3 mV/decade, compared to a Nernstian value of 58.4 mV/decade.

Next the column with polyacrylamide immobilized enzyme, reactor A, was inserted and samples of urea in water were passed through. For a total flow rate of 22 ml h^{-1} a linear response was obtained between 10^{-2} and 10^{-4} M urea in the samples. For a total flow rate of 7.8 ml h^{-1}, the upper limit of linearity was extended to $5 \cdot 10^{-2}$ M urea. If a slightly curved calibration curve was acceptable the arrangement could be used for measurements down to 10^{-5} M urea. The gel could not be tightly packed as then the flow would be hindered. Therefore a loose suspension, 60 mg in 1 ml, had to be used and the reactor thus had a considerable dead volume. At lower flow rate, 10—35 min were required before a steady-state was attained.

The column containing urease immobilized on glass, reactor B, proved to be much more efficient and to have a low dead volume. A calibration curve is shown in Fig. 2; it can be seen that for a flow rate of 40 ml h^{-1} the response is linear between $5 \cdot 10^{-5}$ and $3 \cdot 10^{-2}$ M urea with a slope of 56.9 mV/decade. The urea is thus converted to ammonia with 100 % efficiency over the linear range. Figure 3 shows the recordings from successive samples of urea; the samples were introduced before the base line had been reached. In fact there were some pockets in the flow system so that the time to return to the base line after a concentrated sample was rather long. If the samples have about the same concentration equilibrium is reached within 2.5—3.5 min. As can be seen in Fig. 3 there will be a flat portion and the length of this depends

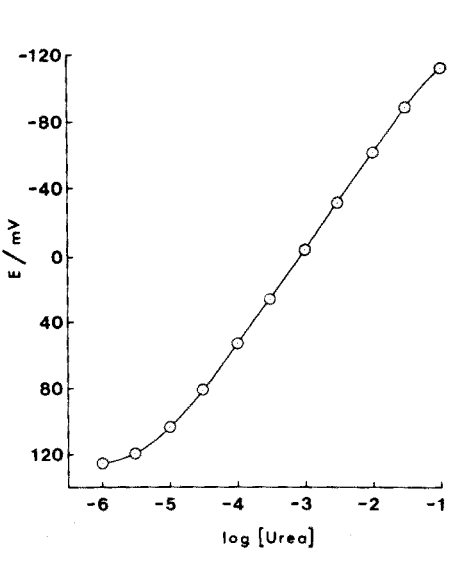

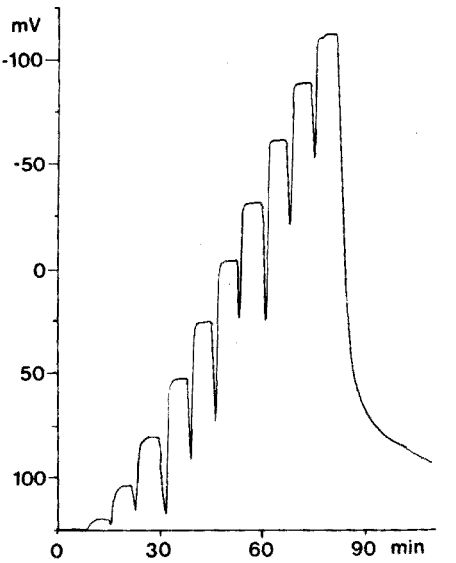

Fig. 2. Response curve for the enzyme reactor electrode with reactor B (urea immobilized to glass). Concentration of urea relates to the sample concentrations. Flow rate 40 ml h^{-1}.

Fig. 3. Recorder trace for 1.9-ml samples of $3 \cdot 10^{-6}$, 10^{-5}, $3 \cdot 10^{-5}$, 10^{-4}, $3 \cdot 10^{-4}$, 10^{-3}, $3 \cdot 10^{-3}$, 10^{-2}, $3 \cdot 10^{-2}$ and 10^{-1} M urea.

on the sample size; 1.9-ml samples were used for the recordings shown in Fig. 3. Under these conditions up to 8 samples could be run per hour. The response time is limited by the ammonia probe, because it takes some time before a diffusion equilibrium is set up over the membrane. To indicate the overall stability, the voltage recordings printed every 30 s are shown in Table 1; it can be seen that the potential is extremely stable except for the highest concentration where the conversion efficiency is less than 100 %.

Eleven samples containing accurately known urea concentrations evenly spaced between 10^{-3} and 10^{-2} M were analyzed. A line was calculated with a least-squares procedure and the standard deviation amounted to 0.23 mV at 40 ml h^{-1} and 0.15 mV at 23 ml h^{-1}. The results are thus better than the stated reproducibility of the ammonia sensor, 2 %.

A diluted urine sample was analyzed with the enzyme reactor electrode. A direct determination gave a value of 2.08 mM urea and with standard addition a value of 2.09 mM urea.

The two most important sources of error are related to the operation of the ammonia sensor. Variations of the temperature of the flowing sample cause uneven temperature distribution within the probe. Differences in temperature between an external reference electrode and the reference electrode inside a glass electrode are known to produce very large e.m.f. errors. The time constant for thermal equilibrium is of the order of 30 min. In the flow system described, heat will be evolved by the enzymatic reaction and during the addition of sodium hydroxide. To reduce the temperature fluctuations a thermal buffer consisting of a coil immersed in a beaker with water was added. The other source of error for the sensor is the disturbance caused by gas bubbles in the flow chamber. As the solubility of air in sodium hydroxide is less than in water, the solution may be super-saturated with oxygen after the mixing "T". The heat exchanger had a beneficial effect as it also cooled the flowing solution. In some cases the buffer was also deaerated somewhat.

Exactly the same calibration curve was obtained at a flow rate of 23 ml h^{-1} as at 40 ml h^{-1}, except that the range was increased somewhat at the upper end. An enzyme column only 22 mm long, thus containing only half as much enzyme, was also used and gave identical results except that the upper limit

TABLE 1

Voltage recordings in mV of the urea measuring system as a function of time and concentration

Urea concn.	Time (min)					
	2.5	3.0	3.5	4.0	4.5	5.0
$3 \cdot 10^{-6}$	120.0	119.5	119.4	119.4	119.4	119.5
$1 \cdot 10^{-4}$	53.4	53.2	53.1	53.1	53.1	53.4
$1 \cdot 10^{-3}$	−3.3	−3.5	−3.5	−3.5	−3.5	−3.6
$1 \cdot 10^{-2}$	−60.5	−60.5	−60.5	−60.4	−60.3	−60.4
$1 \cdot 10^{-1}$	−109.0	−109.6	−109.9	−109.8	−110.0	−110.2

for linear response decreased somewhat. The enzyme columns were stored in a refrigerator during the night and could be used for about one month without any appreciable loss of activity. Heavy metals are known to inhibit the enzyme, but it was found that if samples containing 1 mM lead(II) or 1 mM cadmium(II) were run through the activity returned to normal as fast as the metal ions were washed away with the buffer.

Ammonium ions in the solution can be differentiated from urea by inserting a column of ion exchanger. A column (70 mm long, i.d. 2 mm) was filled with Dowex AG50W-X8, (100—200 mesh, sodium form) and inserted in the flow system after the sample loop and before the mixing T-tube (Fig. 1). When samples containing up to 10^{-2} M ammonium chloride were introduced, the ammonium ions were completely removed. The capacity of the small column was estimated to be sufficient for removal of the ammonium ions from several hundred serum or urine samples. The ion exchanger is sensitive to increases in the electrolyte concentration, so that 1 M NaCl elutes the ammonium ions. When samples of urea were also run through the system with the ion-exchange column in place, no absorption of urea occurred. In clinical chemistry, ion exchangers for removal of ammonium ions have been suspected of urea absorption. The results presented here show that this is not the case for aqueous solutions of urea.

DISCUSSION

The enzyme reactor electrode operates with complete conversion of the substrate to the required products. Over the linear range, there is excess of enzyme activity and variations in flow rate, in the temperature of the reactor or in the enzyme activity do not affect the response. Most earlier types of enzyme electrode depend on a diffusion equilibrium over a thin layer. The diffusion rate depends on temperature and the diffusion layer is affected by stirring. The enzyme reactor electrode, however, gives a response curve with the same slopes as that of the glass electrode. The reactor electrode can be calibrated with ammonium chloride solutions as well as with urea solutions. Another advantage of the enzyme reactor electrode concept is that both the enzyme reactor and the ammonia probe can be operated at their optimum pH values. This is in contrast to covered enzyme electrodes where a compromise is necessary; changes in pH may then result in errors because of variations in the NH_3/NH_4^+-ratio.

The working conditions can be strictly controlled for the enzyme reactor electrode so that a very precise result can be obtained. The weakest part of the system is the ammonia sensor, which has a rather long time constant. The calibration curve is displaced when the ionic strength of the solution changes, probably because of variations in the activity coefficient of ammonia in the flowing solution.

The authors thank Professor K. Mosbach, Lund, for providing a first batch of immobilized urease and giving advice on the immobilization. They also thank Miss B. Bylund for making the experiments with the ion exchanger.

REFERENCES

1 G. G. Guilbault and J. G. Montalvo, Jr., J. Amer. Chem. Soc., 91 (1969) 2164.
2 G. G. Guilbault and J. G. Montalvo, Jr., Anal. Lett., 2 (1969) 283.
3 G. G. Guilbault and J. G. Montalvo, Jr., J. Amer. Chem. Soc., 92 (1970) 2533.
4 R. P. Scholer and W. Simon, Chimia, 24 (1970) 372.
5 T. A. Neubecker and G.A. Rechnitz, Anal. Lett., 5 (1972) 653.
6 J. G. Montalvo, Jr., Anal. Chim. Acta, 65 (1973) 189.
7 G. G. Guilbault and G. Nagy, Anal. Chem., 45 (1973) 417.
8 G. G. Guilbault, G. Nagy and S. S. Kuan, Anal. Chim. Acta, 67 (1973) 195.
9 H. Nilsson, A-C Åkerlund and K. Mosbach, Biochim. Biophys. Acta, 320 (1973) 529.
10 G. G. Guilbault and F. R. Shu, Anal. Chem., 44 (1972) 2161.
11 G. G. Guilbault and E. Hrabankova, Anal. Chim. Acta, 52 (1970) 287.
12 J. W. Ross, J. H. Riseman and J. A. Krueger, Pure Appl. Chem., 36 (1973) 473.
13 T. Anfält, A. Graneli and D. Jagner, Anal. Lett. 6 (1973) 969.
14 R. A. Llenado and G. A. Rechnitz, Anal. Chem., 46 (1974) 1109.
15 J. Růžička and E. H. Hansen, Anal. Chim. Acta, 69 (1974) 129.
16 E. H. Hansen and J. Růžička, Anal. Chim. Acta, 72 (1974) 353.
17 G. G. Guilbault and M. Tarp, Anal. Chim. Acta, 73 (1974) 355.
18 G. G. Guilbault and W. Stokbro, Anal. Chim. Acta, 76 (1975) 237.
19 T. Anfält, A. Graneli and D. Jagner, Anal. Chim. Acta, 76 (1975) 253.
20 D. S. Papastathopoulos and G. A. Rechnitz, Anal. Chim. Acta, 79 (1975) 17.
21 G. A. Rechnitz, Chem. Eng. News, 53 (1975) 35.
22 G. G. Guilbault and T. J. Rohm, Int. J. Environ. Anal. Chem., 4 (1975) 51.
23 G. J. Moody and J. D. R. Thomas, Analyst (London) 100 (1975) 609.
24 A. Johansson, J. Lundberg, B. Mattiasson and K. Mosbach, Biochim. Biophys. Acta, 304 (1973) 217.
25 H. H. Weetall and L. S. Hersch, Biochim. Biophys. Acta, 185 (1969) 464.
26 P. V. Sundaram, Max-Planck-Institute für Exp. Medizin, Göttingen, personal communications, 1974 and 1975.
27 P. L. Bailey and M. Riley, Analyst (London) 100 (1975) 145.
28 H. H. Weetall, Anal. Chem., 46 (1974) 602A.
29 K. Mosbach and B. Danielsson, Biochim. Biophys. Acta, 364 (1974) 140.

Analytica Chimica Acta, 84 (1976) 31–36

A GENERAL STANDARD ADDITION METHOD FOR KINETIC SUBSTRATE DETERMINATIONS IN ENZYMATIC ANALYSIS

NIELS RHOD LARSEN and ELO HARALD HANSEN

Chemistry Department A, Technical University of Denmark, Building 207, DK-2800 Lyngby (Denmark)

(Received 22nd December 1975)

SUMMARY

A standard addition method for kinetic substrate determination in enzymatic analysis is described; the only prerequisite of the method is that the Michaelis—Menten rate expression is fulfilled for the pertinent reaction. The advantages of the method compared to conventional enzyme kinetic procedures are discussed. The method has been used in determining urea in aqueous samples and in sera by means of the ammonia air-gap electrode.

In analytical procedures based on equilibrium measurements in thermodynamically stable systems, standard addition methods are frequently employed. In these procedures the analytical concentration of a certain species is determined on the basis of an observed change in a signal, e.g., potential, between the original sample solution and a sample aliquot to which a known concentration of the species in question has been added. Standard addition methods are, however, not common in kinetic procedures of analysis; to the best knowledge of the authors, such methods have not previously been described for kinetic enzymatic analysis.

For most enzymatic reactions, the Michaelis—Menten rate expressions will apply, i.e. at fixed enzyme activities

$$V = \frac{V_{max}\,[S]}{K_m + [S]} \qquad (1)$$

where V is the initial rate of the reaction, K_m is the Michaelis constant, [S] is the initial substrate concentration, and V_{max} is the maximum initial rate, i.e., $V_{max} = V$ for $[S] \gg K_m$. In kinetic substrate determinations, the initial rate measurements are generally evaluated at substrate concentrations which are an order of magnitude or more smaller than K_m since these conditions will lead to direct proportionality between V and [S]. This does imply, however, that V_{max} and K_m maintain their values whether a calibration procedure is performed or an analysis is done with the actual sample medium. The application of this procedure therefore involves two very significant limitations.

(1) The presence of certain species (e.g., metal ions), even in trace amounts only, may have a large influence on the activity of the enzyme and thus on V_{max} and K_m. If a calibration curve is to be relied on, it must, therefore, be possible to control fully the content of any such activators or inhibitors in a given sample, even if pH, the ionic strength and the temperature are secured at constant levels.

(2) It is essential to have access to a highly sensitive method of measurement, partly because it is appropriate to operate at low substrate concentrations, i.e. at $[S] \ll 0.1\ K_m$, where K_m typically is of the order of 10^{-3} M, and partly because the initial rate ought to be determined within the first 5 % of the reaction.

The limitations imposed by point 1 may be eliminated by using a standard addition procedure, because the analytical content of the measured species is then calculated on the basis of reaction rates in media in which only the concentration of this particular species varies. Provided that the initial rates are measurable at low substrate concentrations (point 2), the simple standard addition method described by Yatsimirskii [1] for general kinetic analysis can be implemented, i.e., the method based on the first part of the rate-substrate curve where it can be assumed linear. But often this is not feasible because the available methods of measurements are not sufficiently sensitive. Operating at substrate concentrations significantly above $0.1\ K_m$ may easily lead to very complex computations, although these may be greatly simplified if the conditions under which the standard addition procedure is implemented are selected appropriately.

The aim of this paper is to describe a generally applicable standard addition method for kinetic substrate determinations where the only prerequisite is that the Michaelis–Menten rate expression is satisfied for the pertinent enzymatic reaction. The applicability of the procedure described has been checked for determinations of urea in serum at a constant activity of the enzyme urease, by monitoring the liberated ammonia, and thus the initial rate values, with the air-gap electrode [2, 3].

THEORY

If the substrate concentration [S] in eqn. (1) is replaced by $X + C_i$, where X is the unknown concentration and C_i is the known added concentration of the species to be measured, eqn (1) may be rearranged to read

$$V_i = \frac{V_{max}\ (X + C_i)}{K_m + (X + C_i)} \tag{2}$$

where V_i signifies the initial rate for the i'th reaction. Since this equation contains three unknowns (V_{max}, K_m and X), the calculation of X requires individual determinations of V_i at three different C_i values. The solution of this set of three equations with respect to X then yields

$$X = \frac{V_1V_2C_3(C_1 - C_2) + V_1V_3C_2(C_3 - C_1) + V_2V_3C_1(C_2 - C_3)}{V_1V_2(C_2 - C_1) + V_1V_3(C_1 - C_3) + V_2V_3(C_3 - C_2)} \tag{3}$$

where the indices correspond to $i = 1$, 2 and 3, respectively. This voluminous expression may be reduced considerably by fixing $C_1 = 0$ and $C_3 = aC_2$, the only restriction being that $C_2 > C_1$ and $a \neq 1$, i.e.

$$X = \frac{aC_2V_1(V_3 - V_2)}{V_1(V_2 - aV_3) + (a-1)V_2V_3} \quad (4)$$

In these equations, X and C_i signify the concentrations present in the reaction mixtures; thus, if the additions of the known concentrations are accompanied by simultaneous dilutions it is necessary to make due allowance for this in the calculations.

As with other standard addition procedures, the one described here requires high precision of the individual measurements. Generally, the highest accuracy of the method is obtained when the rate differences are as large as possible, that is, when $(V_2 - V_1) \simeq (V_3 - V_2) \simeq 1/2V_{max}$, since any error in the determinations of V_i then will have the least significance. In practice, the method will presumably find application mainly at $X > 0.1\ K_m$, yet at high substrate concentrations, eqn. (1) may not be valid because of substrate inhibition. It is, therefore reasonable to choose C_2 of the same order of magnitude as K_m and then to operate with an a-value preferably as high as possible, yet low enough to avoid substrate inhibition; thus, the upper limit of a should be fixed with due allowance for any such potential substrate inhibition.

In order to illustrate these points, a series of calculated examples with varying X and C_2 values were computed on the basis of eqn. (4) where $C_1 = 0$. The results are reproduced in Table 1 where $a = 4$, which for $C_2 = K_m$ implies that $V_3 > 0.8\ V_{max}$. The calculations were made on the assumption that the error in V_i is +3 % (↑) or −3 % (↓); the ±3 % limit was chosen as a realistic value for the accuracy with which most methods allow the initial rates to be determined. The calculations in Table 1 show that, as outlined previously, V_i must be determined very precisely if reasonably good results are to be achieved. It should be pointed out, however, that the three calculated combinations of the arrows are those where the results become most unfavourable. Thus, combinations such as ↓↓↓ and ↑↑↑ (systematic errors) do not lead to any errors in the final results. The calculations shown also indicate that the best results should be obtained for $X < K_m$ (which in these examples was fixed at 10^{-3} M) and for C_2 of the same order of magnitude as K_m.

EXPERIMENTAL

Equipment

The apparatus and the air-gap electrode assembly as used for rate measurements have been described earlier [2].

Chemicals and reagents

The chemicals and urease used were identical to those specified previously [2].

TABLE 1

Calculated examples of the analytical concentration X, assuming an error of ± 3 % in V_i

X ($\cdot 10^{-4}$ M)	C_2 ($\cdot 10^{-4}$ M)	X calculated[a] ($\cdot 10^{-4}$ M)			
		Control	↑↓↓	↑↓↑	↓↑↓
1.00	1.00	1.00	1.18	1.27	0.79
	5.00	1.00	1.08	1.17	0.85
	10.00	1.00	1.08	1.20	0.82
	50.00	1.00	1.07	1.52	0.55
3.00	1.00	3.00	6.58	9.57	1.56
	5.00	3.00	3.50	3.56	2.29
	10.00	3.00	3.37	3.87	2.30
	50.00	3.00	3.29	4.75	1.47
10.00	1.00	10.00	−2.86	−3.17	0.67
	5.00	10.00	21.1	13.1	4.50
	10.00	10.00	14.0	18.8	5.45
	50.00	10.00	11.8	18.3	3.86

[a] $K_m = 1.00 \cdot 10^{-3}$ M, and $a = 4.00$. The first column is a control for the V_i values used in the computations. The symbols ↑ and ↓ indicate rate values of $V_i = +3$ % and $V_i = -3$ %, respectively. The sequence of the arrows is V_1, V_2 and V_3.

All stock solutions of urease and of urea used in the standard addition experiments were prepared by dissolution in 1.0 M Tris buffer of pH 9.00 (HCl). The concentration of the urease solution was $1.0 \cdot 10^{-2}$ mg ml^{-1}, while the concentrations of the urea solutions (C_i) were: $C_1 = 0$ (Tris buffer only); $C_2 = 2.00 \cdot 10^{-3}$ M; and $C_3 = 7.99 \cdot 10^{-3}$ M.

The aqueous urea sample-standards were prepared by dissolution in distilled water, the concentration of urea being such that the samples covered the physiological range of serum ($2 \cdot 10^{-3}$ M—$8 \cdot 10^{-3}$ M). The freeze-dried serum used was Auto-Ref. (DADE Division, Americal Hospital Supply Co., Miami, Fla.) dissolved in distilled water. The urea concentrations designated here as "true values" are those reported by the manufacturer (as determined by the monoxime reaction). These values were checked by the urea method [3] based on end-point determination of ammoniacal nitrogen with the air-gap electrode.

Procedure

The urea sample solution (50 µl) was pipetted into the thermostated measuring chamber (20.0 ± 0.1 °C) of the air-gap electrode assembly, and 200 µl of urease solution and 200 µl of urea stock solution were added (C_i). The initial rate V_i was then measured. Each series of analysis comprised three rate determinations (V_1, V_2 and V_3 for C_1, C_2 and C_3, respectively). The urea concentrations of the samples were then computed from eqn. (4).

RESULTS AND DISCUSSION

The mathematical procedure described herein was applied to the determination of urea. In a previous paper on reaction-kinetic determinations with the air-gap electrode used as an ammonia gas sensor [2] it was shown that this sensor is well suited for measurements of the activity of urease by monitoring the initial rate of the conversion of urea

$$\text{Urea} \xrightarrow{\text{Urease}} CO_2 + 2\ NH_3 \qquad (5)$$

Thus, in order to determine urea, the enzyme activity was kept constant while the urea concentration was varied. Table 2 shows the results of such a series of experiments; in the computations due allowance was made for the fact that the 50-μl pipette was found by calibration to contain only 49 μl. Except for the lowest urea concentration, the values determined for the aqueous samples show reasonably good accuracy, while the results for the freeze-dried serum samples show the poorest agreement at the highest concentration of urea.

Although the experimental conditions were fixed in accordance with the theory of the method, it may — on the basis of the urea experiments alone — be too presumptuous to draw conclusions about the practical accuracy of the method with respect to K_m and the concentration of the substrate measured. From a Lineweaver and Burk plot [4], K_m was determined to be $2.0 \cdot 10^{-3}$ M under the conditions for which the aqueous urea samples were determined. Furthermore, this plot showed that the Michaelis-Menten expression was obeyed for the range of urea concentrations present in the samples.

TABLE 2

Determinations of urea by means of the standard addition method with the air-gap electrode

Sample	V_i relative			Urea ($\cdot 10^{-3}$ M)	
	V_1	V_2	V_3	True	Found[a]
Aqueous urea solns.	0.21	0.77	1.26	2.02	1.7
	0.39	0.86	1.46	4.04	4.2
	0.52	0.89	1.34	6.06	6.1
	0.70	1.04	1.45	8.08	7.9
Freeze-dried sera[b]	0.37	0.83	1.22	2.86	3.1
	0.73	1.05	1.44	7.16	8.4

[a]The concentrations of the added urea standards in the reaction mixtures were $C_1 = 0$, $C_2 = 8.90 \cdot 10^{-4}$ M, and $C_3 = 3.56 \cdot 10^{-3}$ M, i.e., $a = 4.00$.
[b]Auto-Ref. dissolved in distilled water.

The calculations in Table 1 and the results in Table 2 indicate that the method should be used with care. But in some cases standard addition may prove to be the only potentially applicable method if the activity of the enzyme is greatly influenced by the general constitution of the sample. The significance of this may be realized from the analyses of the freeze-dried sera. When these were analyzed on the basis of V_1 and a calibration plot prepared from all the measured V_i values and the concentrations of the aqueous urea samples, the urea concentrations obtained were $3.8 \cdot 10^{-3}$ M and $9.5 \cdot 10^{-3}$ M compared to the correct values of $2.86 \cdot 10^{-3}$ M and $7.16 \cdot 10^{-3}$ M, respectively. In fact, the freeze-dried sera had an activating effect on the urease which led to considerable errors. When the standard addition procedure described here is applied, the result is normally independent of possible activating or inhibiting effects of other species present, because the reaction rates (V_i) used in the computations are determined in reaction media where only the concentration of the measured substrate varies. Such effects on the enzyme activity will generally lead to a change in V_{max} and K_m only, while the Michaelis–Menten expression will still be fulfilled [4].

It may often be advantageous, though not essential, to use a standard addition procedure in enzyme–kinetic substrate determinations. The sole inconvenience of the proposed method compared to the simple standard addition procedure which can normally be used at $[S] < 0.1\ K_m$, is that three determinations of V_i are required whereas the simple procedure calls for only two determinations of the initial rates. This disadvantage may, however, be compensated for by the fact that the initial rates cannot be determined at low substrate concentrations. Thus, it would not have been feasible to apply simple standard addition to these urea samples when the air-gap electrode was used under the conditions described.

REFERENCES

1 K. B. Yatsimirskii, Kinetic Methods of Analysis, Pergamon, Oxford, 1966, p. 48.
2 N. R. Larsen, E. H. Hansen and G. G. Guilbault, Anal. Chim. Acta, 79 (1975) 9.
3 E. H. Hansen and J. Růžička, Anal. Chim. Acta, 72 (1974) 353.
4 G. Michal, in H. U. Bergmeyer (Ed.), Methods of Enzymatic Analysis, Vol. 1, 2nd English edn., Academic Press, New York, 1974, p. 144.

Analytica Chimica Acta, 84 (1976) 37–46

IDENTIFICATION AND DETERMINATION OF XANTHATE, DIXANTHOGEN AND SULFUR XANTHATE BY FAST-SWEEP DIFFERENTIAL PULSE POLAROGRAPHY, A.C. POLAROGRAPHY AND CYCLIC VOLTAMMETRY

A. M. BOND and Z. SZTAJER

Department of Inorganic Chemistry, University of Melbourne, Parkville 3052, Victoria (Australia)

G. WINTER

Division of Mineral Chemistry, C.S.I.R.O., Port Melbourne 3207, Victoria (Australia)

(Received 29th September 1975)

SUMMARY

The chemical reactions occurring in the treatment of sulfide ores by flotation are still a matter of controversy when xanthates (I) are used as collectors. Either the metal xanthate and/or dixanthogen (II) or sulfur xanthates (III) could provide the required hydrophobicity for successful selective flotation. Because of the present difficulties in distinguishing between the various xanthate species by physical measurements, and electrochemical investigation in acetone was undertaken to see if rapid and reliable analytical methods could be developed for the simultaneous identification and determination of (I), (II), and (III). At platinum electrodes, (I), (II), and (III) give characteristic voltammetric waves at well separated potentials and cyclic voltammetry provides a simple means for their identification. At mercury electrodes all species give polarographic waves: (I) gives two extremely well defined oxidation waves with the one at more positive potentials being well removed from the waves for (II) and (III). The determination of (I) by fast-sweep differential pulse polarography is therefore possible over the concentration range 10^{-6}—10^{-2} M. (II) and (III) show less suitable d.c. polarographic behaviour and their reduction processes are complicated by adsorption. However, under a.c. polarographic conditions, (III) gives a well defined wave enabling its determination down to 10^{-6} M. For (II), no wave was found at mercury electrodes at potentials separated from the waves arising from (I) and (III). The determination of (II) can therefore only be undertaken over the concentration range 10^{-4}—10^{-2} M at platinum electrodes.

The chemical reactions leading to the beneficiation of sulfide ores by flotation when xanthates are used as collectors is still a matter of controversy. A critical review of the subject has been presented by Grenville et al. [1]. It appears probable that the metal xanthate and/or the oxidation product of the xanthate ion (I), viz. dixanthogen (II), imparts the hydrophobicity required for successful flotation. More recently, it was pointed out [2] that the formation of sulfur xanthates (III) cannot be ignored as an additional likely possibility.

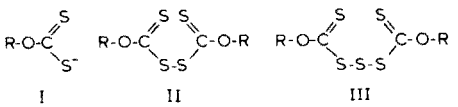

I II III

Both (II) and (III) are stable oily liquids capable of providing a hydrophobic surface as shown by contact angle measurements [2]. Because of their similarity in chemical composition and molecular structure [3, 4], only minor differences are observed in their infra-red spectra, so that unambiguous differentiation is difficult by this technique, especially if both compounds are present.

Although sulfur xanthates exhibit a characteristic u.v. spectrum (G. Winter, unpublished work), the bands are broad and overlap with absorption bands displayed by dixanthogens, most of the metal xanthates or the free xanthate ion. U.v. spectroscopy is, therefore, unsuitable for the analysis of solutions likely to contain mixtures of the three compounds.

Clearly an alternative method of identification is required. In the hope of achieving this, polarographic and voltammetric studies of xanthate ions, dixanthogens and sulfur xanthates in acetone solutions were undertaken. Acetone was chosen as the medium for this investigation because of the excellent solubility of all three species and because the use of an organic solvent was considered likely to provide simpler electrode processes than those found in aqueous media [5—8]. Both platinum and mercury electrodes were investigated since interaction with the electrode surface might occur with sulfur ligands, and the electrode processes could vary substantially at the different electrode materials. Several polarographic and voltammetric methods were examined to provide optimum conditions for both the identification and determination of each species.

EXPERIMENTAL

All measurements were performed at 20 ± 0.1 °C in acetone. The supporting electrolyte was either 0.1 M Et_4NClO_4 or 0.01 M $LiClO_4$, and all solutions were thoroughly degassed with acetone-saturated argon before the electrochemical measurements. Compounds (I) were prepared as their potassium salts by reaction of an alcoholic solution of potassium hydroxide with carbon disulfide. Compounds (II) were prepared by oxidation of an aqueous solution of (I) with potassium persulfate. Compounds (III) were prepared as described previously [2]. Elemental analyses (Australian Microanalytical Services) gave satisfactory results.

All polarograms and voltammograms were recorded with a Princeton Applied Research Corporation (PAR) Model 174 Polarographic Analyzer. A three-electrode format was used with platinum as the auxiliary electrode and Ag/AgCl (0.1 M LiCl; acetone) as the reference electrode. The platinum working electrode was a disc electrode and the dropping mercury electrode was used with controlled drop-time.

Fast-sweep differential pulse polarography was done by interfacing a PAR linear-sweep module accessory 174/51 and the digital timer circuitry [9] to the Polarographic Analyzer. Full details of this new variety of polarographic methodology have been given recently [9].

A.c. polarograms were obtained with the PAR AC Polarographic Interface Model 174/50, PAR Lock-in-Amplifier Model 129A and Optimation Sine Wave Oscillator RCD-10 in conjunction with the 174 Polarograph. Other electrochemical measurements were performed directly with commercially available instrumentation.

RESULTS AND DISCUSSION

Platinum electrodes

Oxidation of xanthate occurs at platinum to give dixanthogen under conditions of controlled potential electrolysis:

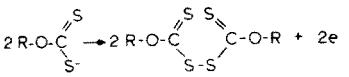

(1)

Figure 1(a) shows a cyclic voltammogram for the butyl derivative and a well defined wave is obtained in the forward scan at about +0.40 V vs. Ag/AgCl. Presumably the oxidation occurs via the formation of a radical which subsequently dimerizes,

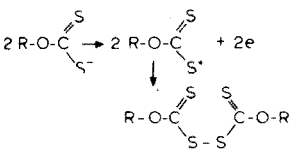

(2)

although the mechanistic details in acetone are not known.

The reduction of dixanthogen to xanthate gives a voltammetric wave at about −1.35 V vs. Ag/AgCl at the platinum electrode. Figure 1(b) shows the cyclic voltammogram for the dixanthogen. On the reverse scan the oxidation of xanthate at +0.40 V vs. Ag/AgCl identifies the product of the reduction as the xanthate ion and defines the overall electrode process as

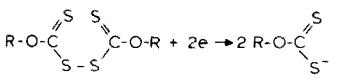

(3)

The mechanism of the reduction process is not known but chemically the xanthate/dixanthogen couple is reversible. Since the reduction of dixanthogen and oxidation of xanthate occur at vastly different potentials they are readily distinguished by voltammetric methods at platinum electrodes.

A cyclic voltammogram of a sulfur xanthate is shown in Fig. 1(c). On the forward scan two reduction waves are seen at about −0.65 and −1.05 V vs. Ag/AgCl. On the reverse scan three well-defined reduction waves occur at about −1.00, −0.30 and +0.45 V vs. Ag/AgCl. Thus the more negative

reduction wave forms part of a reversible couple and the less negative process gives xanthate and another species as a product of this reduction. At this stage no convincing mechanism can be suggested for the electrode process; the important aspect of this work is that sulfur xanthate gives a characteristic cyclic voltammogram at potentials well removed from the other two species of interest. Thus, by using appropriate methodology, the three species (I), (II) and (III) are readily distinguished and identified by voltammetry at a platinum electrode.

For determining dixanthogen and sulfur xanthates, the initial potential should be set at a suitable potential, e.g. 0.0 V vs. Ag/AgCl and the scan

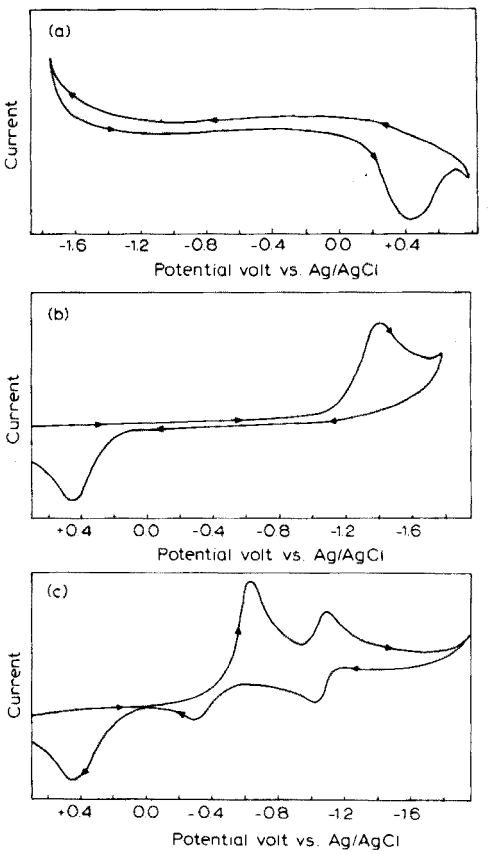

Fig. 1. (left) Cyclic voltammograms of (a) xanthate, (b) dixanthogen and (c) sulfur xanthate at platinum in acetone (0.1 M Et_4NClO_4). In each case the butyl derivative is shown and the concentration is 10^{-3} M. Scan rate = 200 m V s^{-1}.

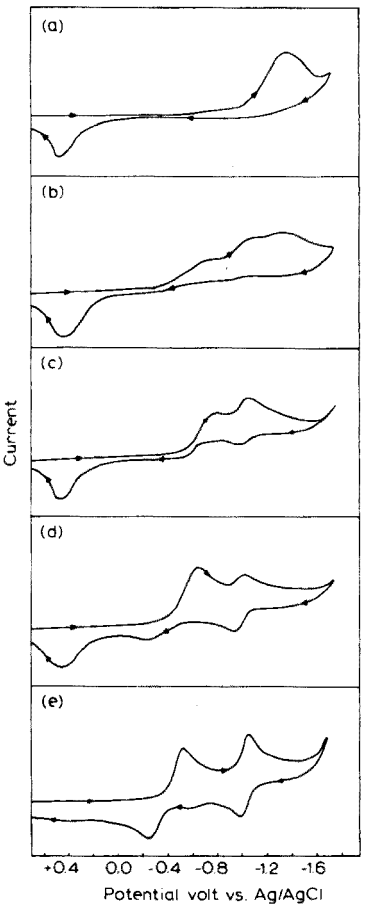

Fig. 2. (right) Decomposition of methyl dixanthogen in acetone (0.1 M Et_4NClO_4) as a function of time. Scan rate = 200 mV s^{-1}. (a) 0 h; (b) 3 h; (c) 6 h; (d) 9 h; (e) 48 h. (d) is identical to a solution of methyl sulfur xanthate.

commenced in the negative direction. To determine the presence of xanthate, a voltammogram, commencing at say 0.0 V vs. Ag/AgCl and scanning in the positive direction must be recorded. A clean electrode and the first scan must be used. A wave appearing at about +0.4 V vs. Ag/AgCl on the first scan verifies the presence of xanthate. Absence of this wave indicates that no xanthate is present. Table 1 summarizes the data obtained at platinum electrodes.

The ability to distinguish between the various species led to an interesting observation concerning the stability of dixanthogen in acetone (0.1 M Et_4NClO_4) solution. On standing dixanthogen in acetone, the voltammograms gradually changed to provide waves identical to those for sulfur xanthate, as shown in Fig. 2(a—d). Methyl dixanthogen takes about 10 h to decompose completely to methyl sulfur xanthate. Decomposition occurs to a third and unknown product on further standing in solution. Methyl sulfur xanthate is also unstable in acetone and decomposes in an identical fashion, as indicated by cyclic voltammograms. Figure 2(e) shows the cyclic voltammogram obtained by leaving either dixanthogen or sulfur xanthate in acetone. The rate of decomposition decreases drastically for the ethyl, propyl and butyl dixanthogens. After one week, the ethyl dixanthogen decomposed completely to ethyl sulfur xanthate, whilst the butyl dixanthogen had decomposed only by about 50 % after 3 weeks. Further decomposition, as noted for the methyl derivative, was not observed. Therefore, the stability for dixanthogens in 0.1 M perchlorate—acetone media is Me << Et < Prop < Bu.

The above study shows that voltammetry at platinum electrodes in acetone provides a rapid method for identifying each of the species under investigation. The conversion of dixanthogen to sulfur xanthate (electrochemical identification) suggests that further work in the field of flotation can be greatly facilitated by the development of methods for distinguishing the various species.

Polarography

Data obtained at the dropping mercury electrode are summarized in Table 2. Specific comments on each system are given below:

Xanthate. Bond et al. [8] have shown that in acetone, xanthate gives two reversible oxidation waves involving the formation of mercury complexes (the reduction wave for the potassium ion is not included in the discussion).

$$3Xan^- + Hg \rightleftarrows Hg(Xan)_3^- + 2e^-; E_{\frac{1}{2}} = -0.365 \text{ V} \quad (4)$$

$$2Hg(Xan)_3^- + Hg \rightleftarrows 3\,Hg(Xan)_2 + 2e^-; E_{\frac{1}{2}} = -0.093 \text{ V} \quad (5)$$

For d.c. polarography, a linear limiting current versus concentration plot was obtained over the range $5 \cdot 10^{-4}$—10^{-2} M for both waves, the detection limit being governed by the charging current. A.c. techniques also gave well defined waves, but differential pulse polarograms were substantially superior. Figure 3

TABLE 1

Summary of cyclic voltammetric behaviour at platinum electrodes
(Concentration = 10^{-3} M. Scan rate = 200 mV s^{-1}. Supporting electrolyte is 0.1 M Et_4NClO_4)

Compound	Peak potentials for reduction waves (V vs. Ag/AgCl)			Peak potentials for oxidation waves (V vs. Ag/AgCl)		
Potassium methyl xanthate				+0.38		
Potassium ethyl xanthate				+0.43		
Potassium propyl xanthate				+0.44		
Potassium butyl xanthate				+0.44		
Methyl dixanthogen[a]			−1.34	+0.38		
Ethyl dixanthogen[a]			−1.36	+0.42		
Propyl dixanthogen[a]			−1.38	+0.44		
Butyl dixanthogen[a]			−1.40	+0.45		
Methyl sulfur xanthate[a]	−0.62	−1.07		+0.40	−0.28	−1.04
Ethyl sulfur xanthate[a]	−0.60	−1.06		+0.43	−0.28	−1.02
Propyl sulfur xanthate[a]	−0.64	−1.04		+0.45	−0.32	−0.98
Butyl sulfur xanthate[a]	−0.62	−1.06		+0.45	−0.28	−1.02

[a]Xanthate generated as a product of reduction.

shows examples of a series of polarograms obtained in the present work and includes (Fig.3(a)) a differential pulse polarogram for the two waves. Linear plots of peak current, i_p, versus concentration were obtained over the range $6 \cdot 10^{-7}$—10^{-2} M with this method (Fig. 4(a)). The use of fast-sweep differential pulse polarography, in which a scan rate of 200 mV s^{-1} was used, and the entire differential pulse current—potential curve recorded on a single drop of mercury, allows substantial time-saving and gives equivalent performance. It is therefore the preferred method. The i—E curve with this method is essentially the same as for differential pulse polarography.

Dixanthogen. Dixanthogen gives a well defined reduction wave (Fig. 3(b)). With fast-sweep differential pulse polarography, the wave with an $E_{\frac{1}{2}}$-value of −0.40 V vs. Ag/AgCl was dependent (non-linearly) on concentration over the range $7 \cdot 10^{-7}$—10^{-3} M. Above this concentration the peak current decreased slightly with increasing concentration. At concentrations above 10^{-4} M, a more negative wave with an $E_{\frac{1}{2}}$-value of −0.90 V vs. Ag/AgCl

TABLE 2

Summary of polarographic data obtained in acetone (0.1 M Et_4NClO_4)[a]

Compound	D.c.p.	A.c.p.	D.p.p.	F.s.d.p.p.	Preferred technique (limit of detection)
Xanthate (I)	Two well-defined oxidation waves; $E_{1/2}$ = +0.08 and −0.35 V at 10^{-3} M. i_d is a linear function of concn. for $5 \cdot 10^{-4}$—10^{-2} M.	Two well-defined oxidation waves; E_p = +0.07 and −0.36 V at 10^{-3} M.	Two well-defined oxidation waves; E_p = +0.06 and −0.36 V at 10^{-3} M. i_p is a linear function of concn. for 10^{-6}—10^{-2} M.	As for d.p.p.	F.s.d.p.p. with the more positive wave (10^{-6} M).
Dixanthogen (II)	One well-defined reduction wave; $E_{1/2}$ = −0.40 V at 10^{-3} M. At higher concns. maxima etc. occur.	One well-defined reduction wave; with E_p = −0.40 V at 10^{-3} M.	One well-defined reduction wave; E_p = −0.40 V at 10^{-3} M. i_p is a non-linear function of concn for 10^{-6}—$5 \cdot 10^{-3}$ M.	As for d.p.p. up to $5 \cdot 10^{-3}$ M. Above 10^{-4} M wave with E_p = −0.90 V appears; i_p is a linear function of concn. for 10^{-4} — 10^{-2} M.	F.s.d.p.p., but only in the absence of I and III. (10^{-6} M).
Sulfur xanthate (III)	Two main reduction waves; $E_{\frac{1}{2}}$ = −0.36 and −1.06 V at 10^{-3} M. Process complicated by adsorption. Polarograms very complex at high concns.	Two very well-defined reduction waves; E_p = −0.37 and −1.07 V at 10^{-3} M. i_p at −1.07 V is a non-linear function of concn. for 10^{-6}—10^{-3} M. Other waves appear at high concns.		Two well-defined reduction waves; E_p = −0.40 and −0.89 V at 10^{-4} M. i_p is a non-linear function of concn. for $5 \cdot 10^{-7}$—$5 \cdot 10^{-4}$ M. Above $5 \cdot 10^{-4}$ M very complex behaviour appears.	A.c.p. with wave at −1.07 V (10^{-6} M).

[a]D.c.p. = d.c. polarography; a.c.p. = a.c. polarography; d.p.p. = differential pulse polarography; f.s.d.p.p. = fast sweep differential pulse polarography. All potentials are given versus the Ag/AgCl electrode.

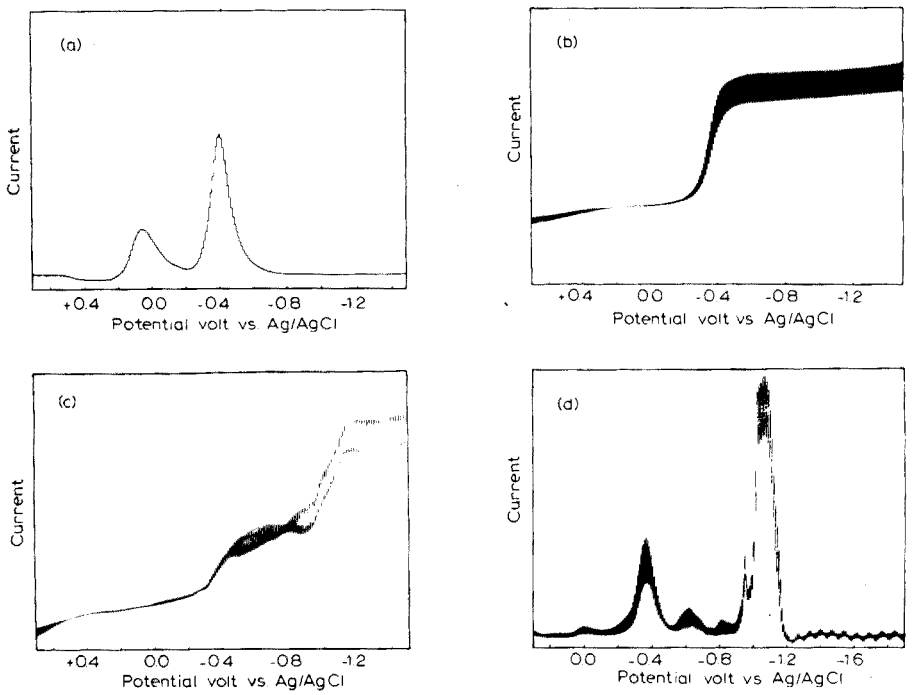

Fig. 3. A selection of polarograms obtained in acetone (0.1 M Et_4NClO_4). (a) Differential pulse polarogram of potassium propyl xanthate. Amplitude = 25 mV, drop time = 2 s, scan rate = 5 mV s^{-1}, concentration = 10^{-4} M. (b) D.c. polarogram of a 10^{-3} M solution of propyl dixanthogen. (c) D.c. polarogram of a 10^{-3} M solution of propyl sulfur xanthate. (d) A.c. polarogram of a 10^{-3} M solution of propyl sulfur xanthate. Amplitude = 30 m V (p–p). Frequency = 400 Hz. In-phase component. Drop time = 0.2 s.

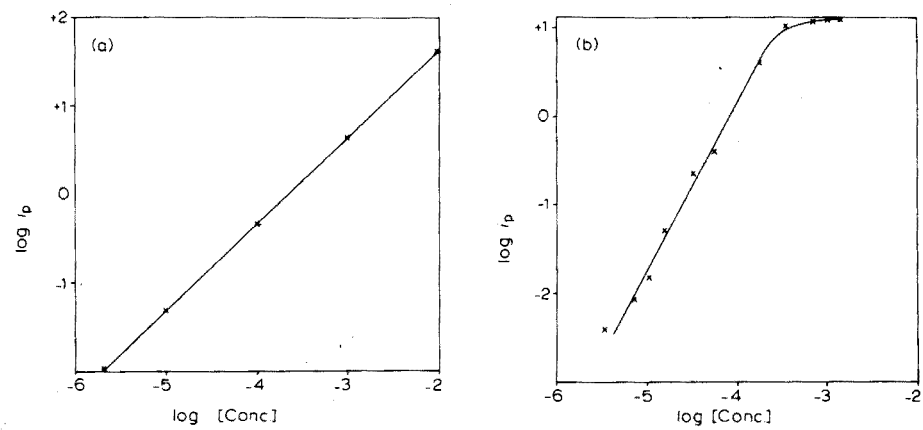

Fig. 4. Calibration curves for (a) potassium butyl xanthate in acetone (0.01 M $LiClO_4$) by fast-sweep differential pulse polarography and (b) butyl sulfur xanthate in acetone (0.1 M Et_4NClO_4) by a.c. polarography. Current is in μA and concentration in mol l^{-1}.

grew. This wave was linearly dependent on concentration over the range 10^{-4}—10^{-2} M. Similar phenomena were found with differential pulse and d.c. polarography. At high concentrations, maxima and erratic behaviour were found in d.c. polarography. Figure 5 shows an electrocapillary curve for this compound and obviously considerable adsorption is involved in the electrode process.

Sulfur xanthate. Figure 3(c) shows a d.c. polarogram of a sulfur xanthate. An extremely complex electrode process(es) is found. The electrocapillary curve (Fig. 5) shows that as for xanthate and dixanthogen, considerable

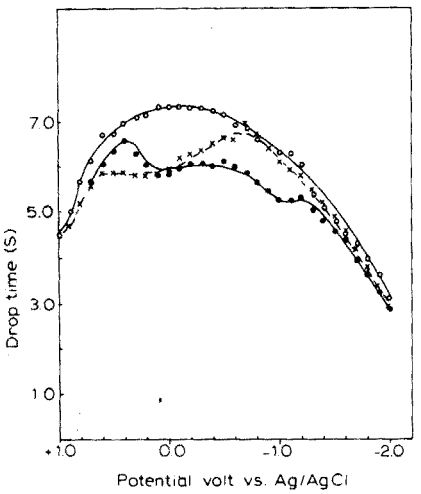

Fig. 5. Electrocapillary curves in acetone. ○, 0.1 M Et_4NClO_4; ●, 10^{-3} M butyl dixanthogen in 0.1 M Et_4NClO_4; ×, 10^{-3} M sulfur butyl xanthate in 0.1 M Et_4NClO_4.

adsorption occurs. At low concentrations (10^{-6}—$5 \cdot 10^{-4}$ M) a well defined fast-sweep differential pulse peak appeared at about —0.40 V vs. Ag/AgCl, but at higher concentrations, the polarogram became too complex for analytical use. The best polarographic technique for determining sulfur xanthates was a.c. polarography in 0.1 M Et_4NClO_4; the well defined wave (Fig. 3(d)) at —1.10 V vs. Ag/AgCl depended on concentration (non-linearly, Fig. 4(b)) over the range 10^{-6}—$5 \cdot 10^{-3}$ M. The wave at —0.4 V vs. Ag/AgCl seen at low concentrations in the differential pulse polarograms was also observed under a.c. conditions, but this and other waves had low peak current per unit concentration values. Thus the a.c. polarographic technique provides a distinctive wave which can be used for the determination of sulfur xanthates.

Optimal analytical methods

For rapid identification of the three species, (I), (II) and (III), linear-sweep or cyclic voltammetry at platinum electrodes in the acetone solvent system provides a useful technique. The detection limit is about 10^{-4} M. In any

work requiring the identification of the species present, studies at platinum electrodes would appear to be an essential first stage of the procedure. For xanthate and sulfur xanthate, polarographic methods provide markedly lower limits of detection. Fast-sweep differential pulse polarography enables the determination of xanthate down to 10^{-6} M when the more positive of the two oxidation waves present at mercury electrodes is used. This wave occurs at potentials well removed from those of (II) or (III). For sulfur xanthate, a.c. polarography gives a well defined wave at considerably more negative potentials than (I) or (II) and the technique can be used to determine this species down to 10^{-6} M. Unfortunately, with dixanthogen, the polarographic wave occurs at a potential too close to waves observed for the other two species. Thus, despite the high sensitivity of the fast-sweep differential pulse method towards this species, the determination of dixanthogen in the presence of (I) and (III) is not possible via polarography in acetone. Quantitative analysis for this species can therefore only be undertaken at platinum electrodes over the concentration range 10^{-4}—10^{-2} M.

Validation and limitations of methods

At platinum electrodes, each of the waves from (I), (II), and (III) were monitored individually at the 10^{-3} M level and then in the presence of at least a 10-fold excess of the other two species. No difficulties arose in detecting the sulfur xanthate or xanthate under the above conditions. However, dixanthogen could only be detected in the presence of about a 2-fold excess of the sulfur xanthate; above this limit the waves of the dixanthogen were masked by that of the sulfur xanthate.

At mercury electrodes the most positive of the xanthate waves was shown to be completely independent of the concentration of either (II) or (III) under differential pulse conditions at a concentration of 10^{-4} M. Similarly, the recommended a.c. method for determining sulfur xanthate was shown to be interference-free with respect to both (I) and (II).

REFERENCES

1 A. Grenville, N. P. Finkelstein and S. A. Allison, I.M.M. Trans., 81 (1971) C1.
2 G. Winter, Inorg. Nucl. Chem. Lett., 11 (1975) 113.
3 Y. Watanabe, Acta Crystallogr., Sect. B, 27 (1971) 644.
4 N. J. Broendmo, S. Esperas, H. Guaveu and S. Husebye, Acta Chem. Scand., 27 (1973) 731.
5 S. G. Salamy and J. C. Nixon, Aust. J. Chem., 7 (1954) 146.
6 R. Woods, J. Phys. Chem., 75 (1971) 354; and refs. therein.
7 R. Woods, Aust. J. Chem., 25 (1972) 2329.
8 A. M. Bond, A. T. Casey and J. R. Thackeray, J. Electroanal. Chem., 48 (1973) 71.
9 H. Blutstein and A. M. Bond, Anal. Chem., 48 (1976) 248.

Analytica Chimica Acta, 84 (1976) 47—52

CONTRIBUTION A L'ÉLECTROCHIMIE DES THIOLS ET DISULFURES PARTIE IV. POLAROGRAPHIES D.C., A.C., IMPULSIONNELLE DIFFÉRENTIELLE ET VOLTAMÉTRIE CYCLIQUE DU DISULFIRAM

C. A. MAIRESSE-DUCARMOIS, G. J. PATRIARCHE et J. L. VANDENBALCK

Université Libre de Bruxelles, Institut de Pharmacie, Bd du Triomphe (Campus Plaine) 1050 Bruxelles (Belgique)

(Reçu le 19 décembre 1975)

RÉSUMÉ

L'étude des caractéristiques électrochimiques du disulfiram est réalisée par les polarographies conventionnelle, alternative, différentielle à impulsions et par voltamétrie cyclique. Ce composé présente des phénomènes d'adsorption très importants et des caractéristiques très différentes des autres disulfures étudiés précédemment. L'étude est réalisée en fonction du pH et de la concentration. La limite de détection du composé est atteinte vers $5 \cdot 10^{-7}$ M en utilisant la méthode impulsionnelle différentielle.

SUMMARY

D.c., a.c. and differential pulse polarography and cyclic voltammetry are used to elucidate the electrochemical behaviour of disulfiram. Very strong adsorption phenomena occur, and the electrochemical characteristics of disulfiram are quite different from those of the disulphides studied previously. Changes in the behaviour of the compound as functions of pH and concentration are described. With the differential pulse method, the limit of detection is $5 \cdot 10^{-7}$ M (0.16 mg l^{-1}).

Lors d'études antérieures consacrées à l'électrochimie des thiols et disulfures d'intérêt pharmacologique[1, 2] nous avons été en mesure d'élucider divers mécanismes présidant aux processus rédox de ces substances. Etant donné l'importance accordée dans la littérature à l'étude des dérivés soufrés [3, 4] nos travaux se poursuivent ici par l'étude du disulfiram (bis(diéthylthiocarbamyl)disulfure) composé très couramment utilisé lors du traitement de l'alcoolisme. Il nous est donc apparu intéressant d'étudier en détails la réactivité électrochimique de celui-ci, d'autant plus que son comportement diffère fortement des autres disulfures étudiés antérieurement.

Plusieurs auteurs ont proposé des méthodes de dosages spectrophotométriques [5] et électrochimiques [6, 7]. Brand et Fleet, ont étudiés l'électrochimie d'un homologue très voisin, à action antifongique le disulfure de tétraméthylthiuram [8].

PARTIE EXPERIMENTALE

L'appareillage et les réactifs utilisés en ce qui concerne les polarographies d.c., a.c. et impulsionnelle différentielle (p.p.) sont identiques à ceux décrit antérieurement [1]. En ce qui concerne la voltamétrie cyclique, l'instrumentation est constituée pour les vitesses rapides d'un générateur de signaux Tacussel GSTP, d'un oscilloscope Telequipement type DM 64 couplés à l'ensemble PRG 34 qui restitue pour chaque goutte les informations sur enrégistreur. Pour les vitesses lentes, nous avons utilisé un générateur de signaux triangulaires construit dans nos laboratoires couplé à un enrégistreur Hewlett-Packard type 7004 B.

Le disulfiram étant très peu soluble dans l'eau, les solutions mères sont préparées dans l'alcool absolu et les solutions destinées à l'expérimentation contiennent 40 % (v/v) d'alcool absolu.

RÉSULTATS ET DISCUSSION

Étude en fonction du pH

L'étude est réalisée à l'aide d'une solution $3 \cdot 10^{-4}$ M par litre en disulfiram dans toute l'échelle des pH apparents envisagés allant de pH 1,10 à 11,55.

La polarographie conventionnelle montre deux vagues cathodiques bien définies dont les potentiels de demi-palier varient linéairement avec le pH jusqu'à une valeur de 4. Au delà de pH 6, ces potentiels de demi-vague restent inchangés même si le pH croît. A tous les pH l'écart de potentiel entre les deux vagues reste constant (± 220 mV) de même que l'intensité totale qui a une valeur d'environ 410 nA.

La Figure 1 montre que si l'on porte les valeurs du pH en fonction des $E_{1/2}$, on observe deux portions de droite dont l'intersection se situe entre pH 4 et 5. La pente de la première partie de la droite est de 55 mV, valeur fort proche de celle déterminée par Gregg et Tyler [7] qui utilisaient des electrolytes de support et des solvants très différents de ceux employés lors de nos expérience: Le point d'intersection des droites qui correspond à la variation du potentiel de demi-palier avec le pH donne pour valeur de pK_a: 4,43; le K_a du disulfiram déterminé à 25 °C ± 0,02 est donc dans ce cas égal à $3{,}71 \cdot 10^{-5}$.

En milieu alcalin la stabilité du disulfiram est fortement altérée par la rupture du point disulfure ce qui donne naissance à des ions diéthyldithiocarbamates. Nous observons d'ailleurs à pH 11,5 l'apparition d'une vague polarographique chevauchant les domaines anodique et cathodique, qui remplace une des deux vagues cathodiques et dont le potentiel de demi-palier se situe au même endroit qui celui des disulfures dans le même milieu.

En ce qui concerne les valeurs des courants, ceux-ci sont pratiquement égaux pour les deux vagues cathodiques si la mesure est réalisée par la méthode d.c. Par contre, si l'on utilise la méthode à tension sinusoïdale surimposée (a.c.), l'intensité du pic situé au potentiel de pic le plus négatif est beaucoup plus élevée que l'autre (Fig. 2) la différence dans la réversibilité des deux

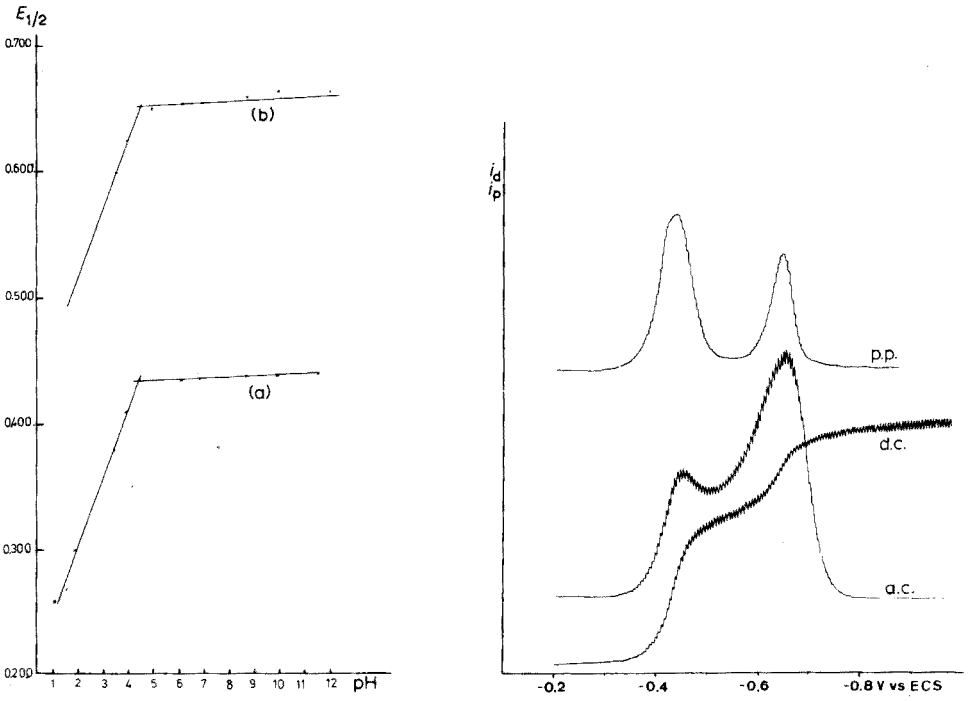

Fig. 1. Courbes $E_{1/2}$ (V vs. ECS) en fonction du pH (a) vague anodique (b) vague d'adsorption. ($3 \cdot 10^{-4}$ M disulfiram, 40 % éthanol.)

Fig. 2. Polarogrammes d.c., a.c. et p.p. d'une solution $5 \cdot 10^{-4}$ M de disulfiram à pH 8,8. D.c.: sensibilité 2,5 μA, temps de chute de gouttes 0,9 s. A.c.: sensibilité 5 μA, temps de chute de gouttes 0,9 s, amplitude 10 mV. P.p.: sensibilité 2,5 μA. temps de chute de gouttes 2 s, retard 1.8 s, durée de l'impulsion 40 ms, amplitude 20 mV, vitesse de déroulement 2mV s^{-1}.

réactions d'électrodes étant responsable de cet état de fait. La polarographie impulsionnelle est tout à l'opposé de ce que l'on observe en a.c.; la valeur de l'intensité du deuxième pic est plus petite que celle du premier et en milieu acide (pH 1,10) une inversion dans l'allure des pics se manifeste ce qui complique l'interprètation des phénomènes observés.

Nous pouvons cependant attribuer la réduction du pont disulfure à la première vague cathodique tandis que la seconde relève de phénomènes d'adsorption. En effet, l'intensité totale de la vague varie proportionnellement avec la concentration pour des teneurs comprises entre $3 \cdot 10^{-4}$ M et $8 \cdot 10^{-4}$ M, tandis que la hauteur de la vague que nous attribuons à l'adsorption garde son intensité constante quel que soit le changement effectué sur les concentrations. La première vague répond aussi au critère $if(h_{Hg})^{\frac{1}{2}}$ tandis que la seconde pas. Un tracé des courbes électrocapillaires nous révèle une phénomène d'adsorption très significatif (Fig. 3).

Nous pouvons donc assimiler la réduction du disulfiram à un processus

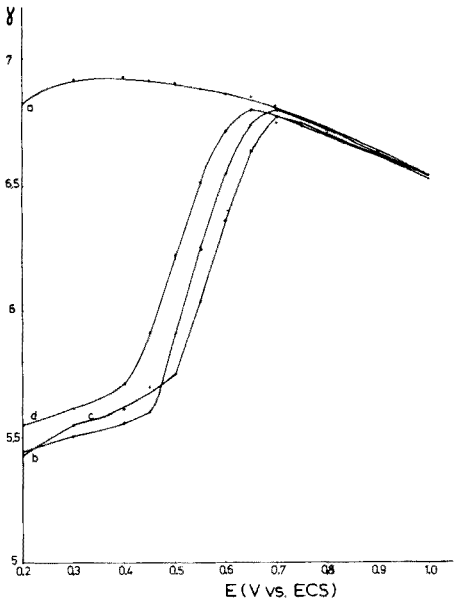

Fig. 3. Courbes électrocapillaires à pH 7. (a) Solution tampon pH 7, 40 % éthanol. (b) Solution de disulfiram $8 \cdot 10^{-4}$ M (c) Solution de disulfiram $3 \cdot 10^{-4}$ M (d) Solution de disulfiram $1 \cdot 10^{-4}$ M.

mettant en jeu deux électrons suivant le schéma réactionnel:

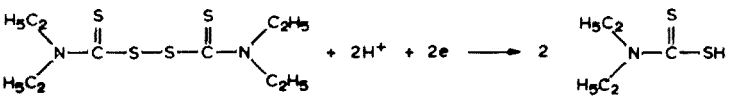

avec probablement formation d'un composé intermercuriel du type suivant:

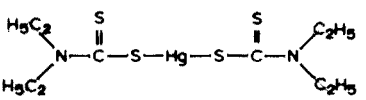

Étude en fonction de la concentration

L'étude réalisée à pH 7,0 permet de montrer que la concentration en disulfiram exerce une influence sur les tracés polarographiques obtenus (Tableau 1). À des concentrations assez élevées ($5 \cdot 10^{-3}$ M), la vague d'adsorption en d.c. se dessine sous forme d'un maximum du premier ordre, tandis qu'er p.p. on observe jusqu'à $1 \cdot 10^{-3}$ M un pic inversé dont le potentiel de sommet coincide avec le potentiel de l'onde développée en d.c. Cette inversion de pic est à notre avis due à des phénomènes d'adsorption et de désorption brutales au niveau de l'électrode. Si l'on diminue la concentration jusqu'à $3 \cdot 10^{-4}$ M, les deux vagues sont toujours présentes avec un déplacement des potentiels vers des valeurs plus positives. En dessous de ces teneurs seule la

TABLEAU 1

Comportement polarographique du disulfiram en fonction de la concentration (Tampon pH 7, 40 % éthanol)

Concentration (M)	D.c.				A.c.		P.p.	
	$E_{\frac{1}{2}}$[a]	$E_{\frac{3}{4}} - E_{\frac{1}{4}}$ (mV)	$E_{\frac{1}{2}}$[a]	$E_{\frac{3}{4}} - E_{\frac{1}{4}}$ (mV)	E_{p_1}[a]	E_{p_2}[a]	E_{p_1}[a]	E_{p_2}[a]
$5 \cdot 10^{-3}$	−0,495	35	max. adsorpt.		−0,515	−0,770	−0,500	−0,760[b]
$1 \cdot 10^{-3}$	−0,495	45	−0,685	20	−0,500	−0,685	−0,485	−0,745[b]
$5 \cdot 10^{-4}$	−0,475	40	−0,675	35	−0,490	−0,695	−0,475	−0,675
$1 \cdot 10^{-4}$	−0,630	45	—	—	−0,655	—	−0,630	—
$5 \cdot 10^{-5}$	−0,630	45	—	—	−0,655	—	−0,625	—

[a] V vs. E.C.S. [b] inversé.

vague de réduction subsiste. Celle-ci est alors proportionnelle à la concentration en d.c., a.c. et p.p. Elle peut donc très aisément servir à la détermination quantitative du dérivé étudié.

La limite de détection atteinte est particulièrement basse en utilisant la méthode p.p. Elle est de l'ordre de $5 \cdot 10^{-7}$ M ce qui correspond à une teneur en produit de 0,158 mg l^{-1}. Cette méthode peut donc servir à l'analyse de traces de disulfiram d'autant plus que ce dérivé se différencie électrochimiquement assez fortement des autres disulfures étudiés [1].

Voltamétrie cyclique

La voltamétrie cyclique montre que les phénomènes d'adsorption sont particulièrement intenses à vitesses de balayage lent (25—200 mV s^{-1}). En milieu alcalin, sur goutte pendante, ceux-ci perturbent tellement le tracé que le pic de réduction est englobé dans le pic d'adsorption, la désorption du disulfiram se marque par une chute brutale de l'intensité (Fig. 4). Par contre, lors de la réoxydation, les deux pics anodiques sont nettement différenciés.

A vitesse de balayage plus rapide (400 mV s^{-1}) sur gouttes renouvelées toutes les 3 s, il est intéressant de constater que les deux pics cathodiques et anodiques sont nettement séparés et particulièrement bien développés (Fig. 5a). À 2 V s^{-1} (gouttes renouvelées toutes les 2 s), les deux pics de réoxydation fusionnent (Fig. 5b).

En milieu acide, à vitesse lente, les tracés sont profondément perturbés; plusieurs pics et épaulement se manifestent et se confondent ce qui ne permet pas une interprètation valable des phénomènes observés. Ceci peut être dû à une saturation et un blocage de la goutte par formation de plusieurs couches de dérivés intermercuriels qui s'adsorberaient et se désorberaient très rapidement. Lors d'un balayage rapide sur oscilloscope (de 400 mV s^{-1} à 2 V s^{-1}) le milieu acide diffère du milieu alcalin par le fait que les deux pics cathodiques se séparent de plus en plus au fur et à mesure que la vitesse croît mais la réoxydation ne montre qu'une seule intensité de pic, les deux réactions d'oxydation se confondant par suite de la vitesse élevée du balayage.

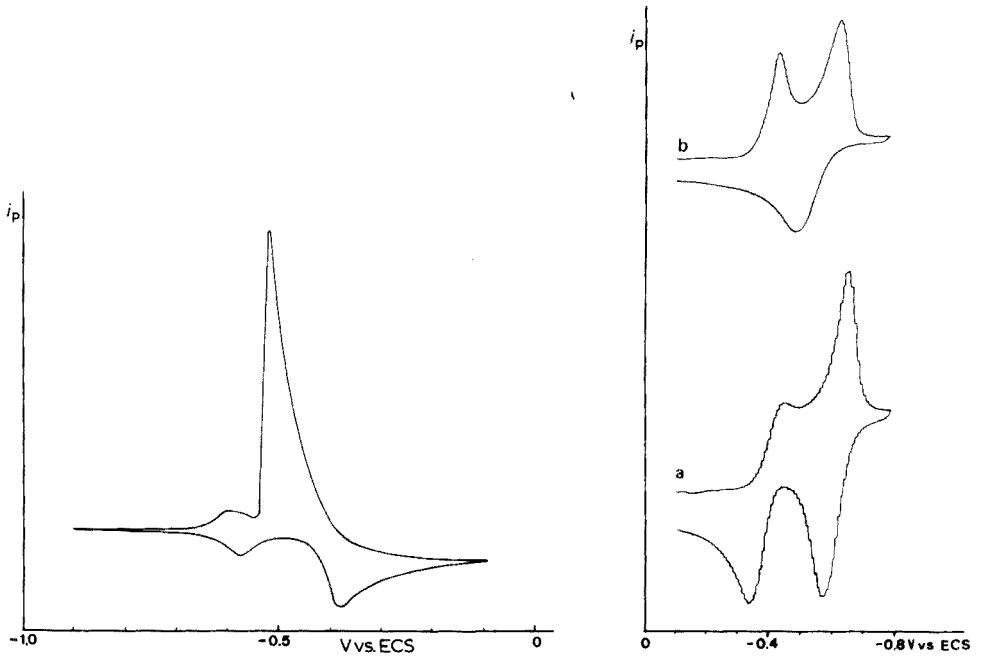

Fig. 4. Voltammétrie cyclique sur goutte pendante, d'une solution $3 \cdot 10^{-4}$ M de disulfiram à pH 9,9; vitesse de balayage 50 mV s^{-1}.

Fig. 5. Voltammetries cycliques sur goutte renouvelée après chaque cycle, d'une solution $3 \cdot 10^{-4}$ M de disulfiram à pH 9,9. (a) Sensibilité 5 μA, vitesse de balayage 400 mV s^{-1}, temps de chute de gouttes 3,7 s, retard 0,2 s, durée des impulsions 3,5 s, amplitude 20 mV, vitesse de déroulement 2 mV s^{-1}. (b) Sensibilité 25 μA, vitesse de balayage 2 V s^{-1}, temps de chute de gouttes 2 s, retard 1,2 s, durée des impulsions 0,8 s, amplitude 20 mV, vitesse de déroulement 2 mV s^{-1}.

Nos remerciements vont au Professeur W. Kemula pour les conseils qu'il nous prodiqué lors de son séjour dans nos laboratoires. Nos remerciements vont aussi au Fonds National de la Recherche Scientifique (F.N.R.S.) pour l'aide précieuse qu'il apporte à (G. J. P.).

BIBLIOGRAPHIE

1 C. A. Mairesse-Ducarmois, G. J. Patriarche et J. L. Vandenbalck, Anal. Chim. Acta, 71 (1974) 165; 76 (1975) 299; 79 (1975) 69.
2 C. A. Mairesse-Ducarmois, J. L. Vandenbalck et G. J. Patriarche, J. Pharm. Belg., 28 (1973) 300.
3 J. H. Karchmer, The Analytical Chemistry of Sulfur and its Compounds, Vols. 1 et 2, Wiley-Interscience, New York, 1973.
4 M. Baizer, Organic Electrochemistry, Dekker, New York, 1973, Chap. 16.
5 R. Fried, A. N. Masoud et F. M. Klein, J. Pharm. Sci., 62 (1973) 1368.
6 D. G. Prue, C. R. Warner et B. T. Kho, Drug standards, 61 (1972) 249.
7 E. C. Gregg et W. P. Tyler, J. Amer. Chem. Soc., 72 (1950) 4561.
8 M. J. D. Brand et B. Fleet, Analyst (London) 95 (1970) 1023.

Analytica Chimica Acta, 84 (1976) 53—59

THE COULOMETRIC GENERATION OF CHROMATE ION FROM THE SILVER—SILVER CHROMATE ELECTRODE: TITRATION OF LEAD(II)

G. S. KELSEY* and H. W. SAFFORD

Department of Chemistry, University of Pittsburgh, Pittsburgh, Pennsylvania 15260 (U.S.A.)

(Received 2nd October 1975)

SUMMARY

The electrochemical behavior of the Ag/Ag_2CrO_4 electrode is described. The efficiency of the cathodic generation of chromate ion as a function of current density, supporting electrolyte and pH, and the optimal conditions for preparation of the electrodes are discussed. The electrode is useful for the coulometric titration of lead(II) in aqueous and in 50 % (v/v) acetone solutions. At the microequivalent level of lead, the titration error is 1—2 %.

The electrogeneration of chromium(VI) from a chromium metal anode has been described [1]; the species in aqueous solution — chromate ion and dichromate ion — are produced at current efficiencies of 98 % and 95.5 % in basic and acidic solutions, respectively. Applications of this method have been primarily to redox titrations [2—4].

Much attention has been given to the determination of lead(II) in recent years. Since the precipitation of lead by chromate has been carefully studied by volumetric titration [5], it was deemed worthwhile to develop a coulometric method based on in situ titrant generation. Monnier and Zwahlen [1] showed that there is a fairly broad pH range over which the current efficiency changes by about 2.5 %. Unfortunately, this region encompasses the pH range necessary for successful titration of lead. Thus, an alternative source of chromate was sought.

Electrodes of the second kind, with silver as base metal and cation for the adhering sparingly soluble salt have been developed for coulometric generation of iodide [6], sulfide [7] thiocyanate [7], hexacyanoferrate(II) [8], and sulfhydryl reagents [9]. The present paper describes a study of the anodic formation of a silver—silver chromate electrode and the subsequent cathodic production of chromate ion for the titration of lead(II).

---

*Present Address: Department of Chemistry, University of Missouri, Columbia, Missouri 65201. (U.S.A.)

EXPERIMENTAL

Materials

All chemicals were reagent grade (Baker analyzed). Deionized water was used for the preparation of aqueous solutions. Standard lead solutions were prepared by dissolving pure lead shot (99.999 %, A. D. Mackay, Inc., New York) in nitric acid, evaporating to dryness and subsequently dissolving the residue in acidified water. The silver used to fabricate electrodes was 0.5-in. ribbon, 0.005-in. thick (99.6 ± 0.1 % Ag).

Apparatus

Current sources used in the galvanostatic generation of chromate ion were a Sargent Model IV coulometric current source standardized against a Leeds-Northrup 10-ohm high-precision resistor and a 0—15-mA continuously variable current source of non-commercial origin.

Coulometric experiments were carried out in Metrohm Model EA880 universal titration vessels. Two types of platinum electrode were used as counter electrodes. Platinum flag electrodes of about 1-cm^2 area were used for coulometric titrations. During deposition of silver chromate on silver anodes, a cylindrical platinum gauze cathode (25 mm diam., 40 mm high) was used. For this deposition, a rectangular silver foil electrode of about 5-cm^2 area was employed. Silver chromate coating was deposited by anodic polarization of this electrode in a 0.1 M potassium chromate solution at a current density of about 1mA cm^{-2} for a total charge of 5 coulombs. Subsequent generation of chromate ions was effected by reduction of this silver chromate surface.

Current—potential curves were obtained with the variable current source and a Sargent Model NX pH/mV meter as a digital millivoltmeter.

Determination of chromium(VI)

The amount of chromate ion generated coulometrically was determined by utilizing the intense magenta-colored complex with s-diphenylcarbazone [10]. The method adopted was that of Saltzman [11] with the omission of the permanganate oxidation step. Because of the observed deterioration of the chromogenic reagent, a differential spectrophotometric method was employed; the absorbance of the sample solution was measured against a number of standard solutions prepared at the same time from stock potassium chromate. The concentrations of the standard solutions were selected so that they were within ± 20 % of the sample concentration. Sample and standard solutions were then placed in the appropriate beams of the spectrophotometer and the absorbances at 543 nm recorded.

Coulometric efficiency

The current efficiency for the process

$$Ag_2CrO_4 + 2e^- \rightarrow 2\,Ag + CrO_4^{2-} \qquad (1)$$

was calculated as the ratio of the quantity of chromate ion determined spectrophotometrically to the quantity liberated theoretically from the electrode, calculated from Faraday's Law. A differential error analysis of the measured parameters (current, time, absorbance, etc.) involved in the calculation yielded a total error of between 0.5 % and 1.0 %, depending on the amount of scatter in the data points of the differential spectrophotometric analysis.

RESULTS AND DISCUSSION

Current efficiency

Electrodepositions were carried out in 0.1 M potassium chromate solutions at pH 8, where the equilibrium of the reaction $HCrO_4^- \rightleftharpoons H^+ + CrO_4^{2-}$ lies far to the right. Subsequent studies of current efficiency for the reverse stripping process proved that Ag_2CrO_4 and not $AgHCrO_4$ or $Ag_2Cr_2O_7$ was indeed deposited on the silver anodes. The silver chromate coating adhered to the surface of the electrode when deposited under the above condition of pH and at current densities between 0.1 and 10 mA cm^{-2}.

Figure 1 shows the current—potential behavior of silver anodes in 0.1 M sodium perchlorate and 0.1 M potassium chromate. To aid in the selection of conditions for deposition of silver chromate, chronopotentiograms were manually recorded at three different constant currents in 0.1 M potassium

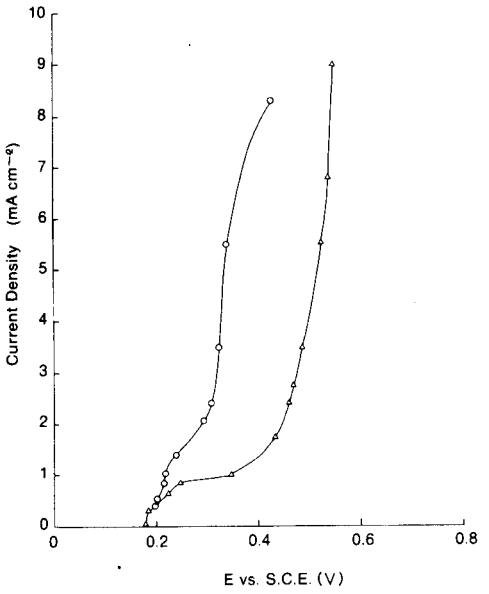

Fig. 1. Anodic current—potential curves for silver electrodes. ○, 0.1 M K_2CrO_4 ; △, 0.1 M $NaClO_4$.

chromate solution (Fig. 2). When slight differences in electrode area are taken into account, the three curves pass through a common point on the ramp between the silver oxidation and solvent oxidation plateaux. Since, on average, the two electrode processes compete equally in the ramped region, the effective total coulombs consumed by the process of interest (coating formation) is about 5. In order to verify this conclusion, the pH of the potassium chromate solution was monitored during electrodeposition to obtain a measure of the efficiency of the process. The three reactions of interest are

cathode: $2e^- + 2H_2O \rightarrow H_2 + 2OH^-$

anode: $Ag \rightarrow Ag^+ + e^-$

anode: $2H_2O \rightarrow 4H^+ + O_2 + 4e^-$

Since the anode and cathode were not isolated during deposition, the hydrogen ion formed at the silver—silver chromate electrode when the potential shifts to oxidation of solvent will react with hydroxide ion generated at the platinum cathode. If the cathodic reaction proceeds at 100 % current efficiency, the final concentration of hydroxide ion will be attained when oxidation of silver ceases. Thus, the amount of silver chromate which can be deposited on a given surface can be calculated. pH data showed that the maximum amount of silver chromate which could be plated onto the silver foil electrode of 5-cm^2 area consumed ca. 5 coulombs of charge, which is in good agreement with Fig. 2.

Photomicrographs of silver foil and electrodes electrocoated under various conditions of current density and pretreatment aided in the selection of optimal deposition conditions. Immersion of the silver in 6 M nitric acid for several seconds created a uniformly roughened surface and was chosen as the final pretreatment before electrodeposition. The surfaces of electrodes

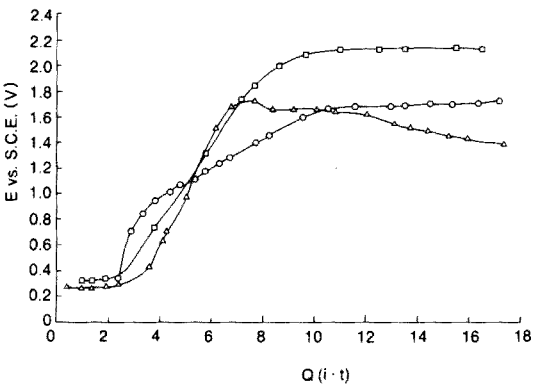

Fig. 2. Potential of silver anode as a function of charge passed at three applied currents in 0.1 M K_2CrO_4. □, 1.93 mA cm^{-2}; ○, 0.965 mA cm^{-2}; △, 0.482 mA cm^{-2}.

deposited at 1 mA cm^{-2} were characterized by smooth and regular coatings. These observations, together with those of the $E = f(Q)$ curves, led to the choice of the following conditions for electrodeposition: a current density of 1 mA cm^{-2} and a total consumption of 5 coulombs.

Current efficiency studies included a variety of media at mildly acidic and basic pH values. Chromate was generated under two separate sets of conditions. Firstly, total coulombs passed were held constant as the current density was varied. These experiments were designed to show the effect of current density on current efficiency while theoretically stripping the same amount of electroactive substance from the electrode. Secondly, generation time was held constant as current density was varied. These experiments were designed to keep the level of spontaneous (non-Faradaic) dissolution constant.

Figure 3 shows the behavior of the silver—silver chromate electrode in sodium nitrate solutions. The curves are qualitatively identical to those obtained in sodium perchlorate supporting electrolyte, and so the latter are not reproduced here. Current efficiencies greater than 1.0 at low current densities are due to the natural dissolution of the electrode coating, which was a significant source of error only at extended residence times in solution. This effect was more pronounced in the sodium perchlorate solutions tested. The fall-off in current efficiency (Fig. 3(b)) at highest current density was due to exhaustion of the silver chromate coating in spots and the consequent competing solvent reduction there. The nitrate data were closer to the ideal current efficiency of 1.0, and this fact, together with the requirements of solution pH (lead hydroxide precipitates in basic solution) and fairly constant

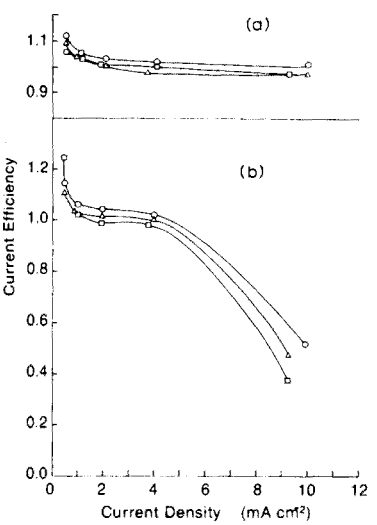

Fig. 3. Current efficiency as a function of current density in $NaNO_3$ solutions at pH 6.2. (a) At constant Q. (b) At constant generation time. △, 0.1 M $NaNO_3$; □, 0.5 M $NaNO_3$; ○, 1.0 M $NaNO_3$.

current efficiency over a range of current densities, led to the choice of 0.1 M sodium nitrate as the medium for the titration of lead. Current densities between 2 and 8 mA cm^{-2} were chosen, which corresponds to the flattest portion of the curve in Fig. 3(a).

End-point detection

Several end-point detection techniques were found to be suitable in the titration of lead with coulometrically generated chromate. Potentiometric methods were successful when a period of equilibration was allowed between titrant increments; Table 1 summarizes the results obtained with silver wire, chromium metal and silver—silver chromate indicating electrodes. In all these experiments, the cathodic generating current was switched on for a specified number of seconds, and then turned off for an equilibration period, at the end of which the potential of the indicating electrode was recorded. Direct plots of potentials against accumulated generation times or the first derivative curves were used for end-point location. For the first two entries of Table 1, the indicating electrode was a silver billet plated with silver chromate, as was the generator cathode; during series of titrations with this sensing electrode, the inflection at the end-point became poorer on successive runs, and eventually bare silver metal areas became exposed, necessitating replating of the electrode. Since intermittent current application was necessary (for equilibration purposes), it was thought that the generating electrode itself could be used as end-point indicator, thus eliminating one source of non-Faradaic chromate. The data reported in Table 2 show that sufficient accuracy can be achieved without the use of the intermittent generation technique, at a slight sacrifice in precision, but a substantial savings in analysis time. The precision could probably be improved with the use of 50 % acetone medium as in Table 1. The data in Table 2 were obtained in totally aqueous solution and represent the averages of five experiments each.

This work was taken from the thesis of G.S.K., who wishes to thank the Chemistry Department of the University of Pittsburgh for financial support.

TABLE 1

Coulometric titration of lead(II) with chromate (0.1 M $NaNO_3$ in 50 % (v/v) acetone at an applied current density of 19.58 mA)

No. runs	Lead concn. (M)	Indicator electrode	Gen. Time/ Equil. Time (s)	Error %	s_r
7	$2.70 \cdot 10^{-4}$	Ag/Ag_2CrO_4	20/40	−2.3	±2.5
2	$6.76 \cdot 10^{-5}$	Ag/Ag_2CrO_4	5/55	+1.0	±1.0
4	$2.70 \cdot 10^{-4}$	Cr	20/40	+0.7	±1.3
2	$6.76 \cdot 10^{-5}$	Cr	5/55	+0.03	±0.25
2	$6.76 \cdot 10^{-5}$	Ag	5/55	+0.22	±3.8

TABLE 2

Coulometric titration of lead(II) with chromate (Potential of the indicator electrode recorded continuously during uninterrupted titration)

Pb(II) taken, mmol	0.01351 ± 0.00007	0.00337 ± 0.00005	0.000673 ± 0.00001
Time to end-point	135.5 ± 4.5	33.48 ± 2.66	26.32 ± 1.92
Pb(II) found, mmol	0.01374 ± 4.2[a]	0.00339 ± 7.4[a]	0.000658 ± 0.0[a]
Current, mA	19.58	19.58	4.824
Error (%)	+1.7	+1.6	−2.2

[a]Relative standard deviation (s_r).

REFERENCES

1 D. Monnier and P. Zwahlen, Helv. Chim. Acta, 39 (1956) 1865.
2 A. I. Kostromin and A. A. Akhmetov, Zh. Anal. Khim., 24 (1969) 503.
3 A. I. Kostromin, A. A. Akhmetov and L. N. Orlova, Zh. Anal. Khim., 25 (1970) 195.
4 A. I. Kostromin, A. A. Akhmetov and L. N. Burygina, Zh. Anal. Khim., 27 (1972) 315.
5 I. M. Kolthoff and Yu-Djai Pan, J. Amer. Chem. Soc., 61 (1939) 3402.
6 F. Magno, Anal. Chim. Acta, 40 (1968) 431.
7 M. Fiorani and F. Magno, Anal. Chim. Acta, 39 (1967) 285.
8 F. Magno and G. Pilloni, Anal. Chim. Acta, 41 (1968) 413.
9 F. Magno and V. Peruzzo, Anal. Chim. Acta, 50 (1970) 491.
10 J. H. Yoe and L. A. Sarver, Organic Analytical Reagents, Wiley, New York, 1941, p. 156.
11 B. E. Saltzman, Anal. Chem., 24 (1952) 1016.

Analytica Chimica Acta, 84 (1976) 61—65

CARBON FIBRES AS WORKING ELECTRODES IN THE COULOMETRIC TITRATION OF POTASSIUM HYDROGENPHTHALATE AND HYDROCHLORIC ACID

V. J. JENNINGS and T. D. BAILEY

Department of Chemistry and Metallurgy, Lanchester Polytechnic, Coventry CV1 5FB (England)

(Received 26th November 1975)

SUMMARY

The use of a carbon fibre tow as a working electrode for the coulometric titration of potassium hydrogenphthalate and hydrochloric acid is described. Quantities of about 10^{-4} mole can be determined with an accuracy and precision of about 0.5 %. A single carbon fibre can be used as working electrode in coulometric titrations of about 2 μg of hydrochloric acid with a relative standard deviation of 1.4 %.

It has been shown previously [1] that a 10,000-filament carbon fibre working electrode may be used for coulometric iodine titrations. The present work describes the use of such an electrode for two acidimetric titrations. The advantages of such an electrode lie in its relatively low cost and large surface area for its volume. There is also the possibility of using a single fibre for microcoulometric titrations; some preliminary results for such titrations are presented here. Microcoulometric titrations have been previously reported [2] where titrand volumes of 10 μl of acids have been used. Generating currents as low as 0.12 μA have been used [3] for the determination of nanogram quantities of halides. The small volumes and generating currents used in the present work are thus not unique. However, it is shown that microcoulometric titrations can be done conveniently with carbon fibre working electrodes; further, the end-point of such micro-titrations can be established with a carbon fibre indicator electrode as a micro pH electrode [4].

EXPERIMENTAL

Chemicals and glassware

All chemicals used were of analytical grade. The volumetric glassware was of Grade A standard.

Titration of 25 ml of 0.01 M potassium hydrogenphthalate

The 100-ml titration cell used was similar to that described previously [1]. A Thorn coulometric titrator (TE110) provided the current of 24.12 mA to the working electrode which was a 3.1-cm long tow of carbon fibre sealed into a glass tube with an epoxy resin. The calculated active surface area was about 73 cm^2. The counter electrode was a coil made from a 1.5-m length of 28-s.w.g. silver wire. The supporting electrolyte was 25 ml 0.01 M potassium chloride, which was pretitrated to a phenolphthalein pink end-point to determine the "blank" value. Then 25 ml of 0.1 M potassium hydrogenphthalate was pipetted into the cell and the titration commenced by passage of current. Pure nitrogen gas was bubbled through the solution before titration and an atmosphere of nitrogen maintained over the surface of the solution during the titration.

The "blank" times and titration times were about 2 s and 1000 s, respectively. For seven titrations, the mean charge was 24.21 C (theor. 24.26), the error of the mean being −0.2 % and the relative standard deviation 0.4 %.

Titration of 1 ml of 0.1 M hydrochloric acid

The cell and electrodes used were identical to those mentioned above. The supporting electrolyte (25 ml of 0.1 M potassium chloride and 20 ml of distilled water) was titrated to a methyl red end-point; two drops of 0.1 % methyl red were used. The blank titration time for a current of 24 mA was about 2 s. A 1-ml aliquot of 0.1 M hydrochloric acid was added and titrated to the end-point; the titration time was about 400 s. Further 1-ml aliquots of the acid were added and titrated sequentially. The indicator colour faded during each titration so that a further drop of indicator had to be added for each individual titration and titrated to the desired colour change before the next 1-ml aliquot of acid was added.

For six successive 1-ml aliquots, the average charge required was 9.68 C (theor. 9.645), the error of the mean being +0.4 % and the relative standard deviation 0.2 %.

Microtitration of 0.01 M hydrochloric acid with a single carbon fibre as generating electrode

The titration cell used, requiring a microscopic slide, was modelled on that first reported by Wigglesworth [5] and described in Korenman's book [6].

Preliminary experiments were carried out with a glass slide on which the electrodes — a single carbon fibre and a 0.17-mm diameter silver wire — were mounted longitudinally. An epoxy resin ring was made round the electrodes in the centre of the slide to take 15 μl of 0.1 M potassium chloride, methyl red indicator and μl-amounts of 0.01 M hydrochloric acid. It was just possible to see the indicator colour change marking the end-point for 1—5 μl of 0.01 M hydrochloric acid, but the precision and accuracy were poor. A generating current of 12 μA was used, because a current of 24 μA produced gas evolution at the silver electrode.

After these tests, it was decided to construct a titration cell in which the end-point could be detected by other means. Since the potential of a carbon fibre responds to pH changes [4], a 4-electrode cell was constructed in which the coulometric generating current was passed between a carbon fibre and a silver electrode, and the pH change was followed from the potential of a carbon fibre electrode against an Ag/AgCl wire electrode. The potassium chloride content of the supporting electrolyte sufficed to maintain a constant potential of the reference electrode.

The actual titration cell consisted of four parallel electrodes mounted with a polystyrene resin (Isopon) on a 3 × 1-in. glass microscope slide. The two outer electrodes, about 6 mm apart, were of silver wire approximately 0.17 mm in diameter; one of these was coated electrochemically with silver chloride. The two inner electrodes were low-temperature carbon fibres (7—8 μm diameter) about 2 mm apart. The resin was allowed to set around the electrodes leaving an oval depression about 9 × 4 mm. Into this depression were added 15 μl of 0.1 M potassium chloride solution as the supporting electrolyte, and the sample (5 μl of 0.01 M hydrochloric acid, prepared by dilution of standard 0.1 M solution) from 10-μl microsyringes (S.G.E. Pty. Ltd). A generating current of about 12 μA from the Thorn Coulometric Titrator was passed between the silver electrode and the furthest carbon fibre. The current was calculated from the potential drop across a Vishay Welwyn 1000-ohm (±0.01 %) precision resistor (No. 4805, 75-03); the potential was measured to 0.1 mV with a Beckman Research pH meter, to obtain a precision in current measurement of 1 %.

The potential across the indicating carbon fibre electrode and the Ag/AgCl wire was measured with a Pye pH meter, model 290, in the millivolt mode.

During the titration the microscope slide was vibrated after each period of current generation to assist mixing of generated titrant and titrand. A difficulty encountered was the loss of sample by evaporation, but this could be minimized by surrounding the titration cell with filter paper soaked in distilled water and covering the cell with a watch glass.

Table 1 shows the results obtained for a set of 5 titrations and Fig. 1 shows the potentiometric titration curves for two of these titrations.

DISCUSSION

Titrations with the carbon fibre tow electrode

The mean error of −0.2 % obtained for the titration of 0.01 M potassium hydrogenphthalate is within the acceptable limits for titrimetric determinations, but the relative standard deviation of 0.4 % is high. A further series of 5 titrations with a different carbon fibre electrode gave a mean error of −0.3 % but an even higher relative standard deviation of 0.6 %. There are several possible reasons for this: (1) inefficient mixing of the generated titrant with titrand because of individual fibres matting when wet; (2) variable current efficiency because of the carbon fibres being slightly attacked chemically;

TABLE 1

Coulometric titration of 5 μl of 0.01 M ($182 \cdot 10^{-8}$ g) hydrochloric acid with a single carbon fibre generating electrode (Generation current 12 μA)

Titration number	1	2	3	4	5
Time to end-point, s	408	422	420	416	418
μg HCl found	1.85	1.91	1.90	1.88	1.90

Mean weight hydrochloric acid : 1.89 μg
Mean error : +3.7 %
Relative standard deviation : 1.4 %

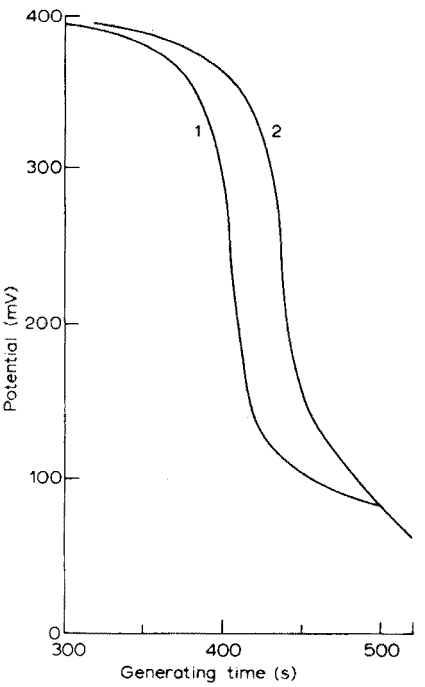

Fig. 1. Potentiometric titration of 5 μl of 0.01 M hydrochloric acid with coulometrically generated hydroxyl ion. Generating current 12 μA. Curves 1 and 2 correspond to titrations 1 and 2 in Table 1. For curve 2 the time axis has been reset 20 s to the right.

(3) leakage of solution through the mounting resin. This carbon fibre tow electrode is therefore useful only if precisions and accuracies of around 0.5 % are acceptable.

The titration results for 1-ml aliquots of 0.1 M hydrochloric acid confirmed these conclusions.

Coulometric microtitration of 0.01 M hydrochloric acid

Table 1 shows that the titration of 5 μl of 0.01 M (about 2 μg) hydrochloric acid is possible with an error of +4 % and a relative standard deviation of 1.4 %. Figure 1 proves that the use of the carbon fibre indicating electrode is successful and that this electrode is capable of following pH changes accurately in μl-volumes of solutions.

The maximum rate of potential change at the end-point was about 50 mV per 10 s of current generation. Previous work [4] indicates that 50 mV is equivalent to a change in pH of about 1 unit. Potentials before the end-point were relatively reproducible; for the five titrations given in Table 1, the potentials at the 75 % titration stage (300 s) were within 5 mV of each other, However, the potentials after the end-point at 125 % titration time (500 s) were less reproducible and showed variations of up to 40 mV. This may be due to carbon dioxide absorption from the atmosphere.

REFERENCES

1 V. J. Jennings, A. Dodson and R. J. Eastman, Anal. Chim. Acta, 76 (1975) 143.
2 R. Schreiber and W. D. Cooke, Anal. Chem., 27 (1955) 1475.
3 E. Bishop and R. G. Dhaneshwar, Anal. Chem., 36 (1964) 726.
4 V. J. Jennings and P. J. Pearson, Nature (London), 256 (1975) 31.
5 V. B. Wigglesworth, Biochem. J., 31 (1937) 1719.
6 I. M. Korenman, Introduction to Quantitative Ultramicroanalysis, Academic Press, New York, (1965), p. 63.

Analytica Chimica Acta, 84 (1976) 67—78

NEBULIZATION EFFECTS WITH ACID SOLUTIONS IN I.C.P. SPECTROMETRY

S. GREENFIELD, H. McD. McGEACHIN and P. B. SMITH

Albright and Wilson Limited, Industrial Chemicals Division, P.O. Box 80, Oldbury, Warley, West Midlands B69 4LN (England)

(Received 7th January 1976)

SUMMARY

The effect of high acid concentrations in the sample solution on signal intensity has been investigated with a high-power plasma as the excitation source. With mineral acids the intensity is reduced by a factor which correlates well with the expected reduction in sample uptake caused by increased viscosity. With organic acids such an expected reduction is outweighed by other enhancements which can be represented as a function of the viscosity, surface tension and density of the solution. Such a dependence of all the effects on solution properties suggests that they should be attributed to the aspiration and nebulization system rather than to the plasma source.

As part of a continuing programme of research on the inductively coupled plasma torch we have investigated the effect of mineral and organic acid concentrations on the intensity of spectra emitted by transition metals when they are excited by a high-power inductively coupled plasma torch.

Koirtyohann and Lichte [1] gave an added stimulus to the work by their report that the intensity of the cadmium radiation, excited by a low-power inductively coupled plasma torch, could change by a factor of three depending on the concentration of nitric acid.

Although comparatively little has been published on interference effects in spectrometry with a plasma source, such effects have been extensively studied in flame photometry. These include:

(a) spectral interference, where the line of interest cannot easily be resolved from a line of another element or from a molecular band;
(b) chemical interference, where the presence of another element depresses the intensity of a line by a reduction in the population of free atoms, because of the formation of molecules or radicals;
(c) ionization effects, where the presence of another element (usually of low ionization potential) makes a dramatic change in the electron density in the source, thereby shifting the ionization equilibrium and perhaps changing the spatial distribution of the excited particles;
(d) contamination from the construction materials of the source;

(e) physical interferences, where changes in aspiration rate, in nebulization, in the transport of aerosol to the source and in the subsequent evaporation of the solvent and vaporization of solute occur, because of changes in viscosity, surface tension or density of solutions.

In a conventional flame the interferences caused by mineral acids are of several types. Chemical interferences can occur by formation of stable compounds, spectral interference can be caused by molecular banding, and physical interferences can arise because the addition of acids influences the aspiration rate and the nebulization process and thus alters the nebulizer yield. Reviews of these phenomena have been given by Rubeska [2] and Koirtyohann [3].

With the high-temperature inductively coupled plasma torch, the absence of the traditional chemical interferences on calcium and aluminium in the presence of phosphate has been confirmed by Greenfield et al. [4] and Fassell et al. [5]. Of the others, it seems reasonable to examine first the physical interferences which occur when mineral acids are injected into the plasma; of these, aspiration rate and nebulizer performance are probably the most important factors in the analysis of solutions with the plasma torch. Certainly with our high-power plasma it seems unlikely that the presence of different acid concentrations would cause a marked change in the evaporation of the aerosol. This is inferred from the observation that refractory powders such as zirconia and tungsten carbide are rapidly vaporized if introduced in similar conditions, so that the evaporation of a solution would be expected to be practically instantaneous, regardless of its composition or droplet size. This inference might not be valid with plasmas of lower power; for example, when a power of 0.8 kW was used, not only was instability apparent when powders were introduced, but in addition some of the powder passed through without being vaporized. When there is adequate power in the source, however, it seems likely that the major effects of mineral acids stem not from the source but from the nebulizer.

Winefordner and Latz [6] have investigated the parameters influencing sample flow rate in flame photometry but restricted their investigation to organic and aqueous organic solutions. Similarly, Bukreev et al. [7] have applied statistical methods for the solution of some flame photometric problems. They considered the effect of different concentrations of mineral acids (up to 4 N) on the intensity of 25—1000 p.p.m. sodium and found agreement between theory and experiment. No information is available for acid concentrations as high as 60 % (w/w), perhaps because of the difficulty in sustaining a flame at these high solute levels. However, there is no difficulty with these high concentrations with a high-power (6 kW) plasma, although, as when powders are introduced, a low-power (0.8 kW) plasma becomes unstable.

THEORETICAL BACKGROUND

The sample solution is introduced into the plasma by surrounding a capillary with a high-velocity argon gas stream parallel to it. The pressure differential created draws the sample solution through the capillary. The Poiseuille equation may be applied

$$Q = \frac{\pi R^4 P}{8\eta L} \tag{1}$$

where Q is the rate of flow, R the capillary radius, P the pressure differential, η the viscosity and L the capillary length.

A correction of this formula replaces the R^4 term by $(R^4 + 4\eta R^3/B)$ where B is the coefficient of sliding friction of the liquid on the wall. The correction [8] takes account of the fact that the velocity of the liquid is not zero at the wall, as assumed in Poiseuille's equation, but that it slips over it. The volume flowing at high viscosities is thus greater than that predicted by the Poiseuille equation. Turbulent flow commences [9] when the Reynolds number exceeds 2000. The Reynolds number R_e is defined as $R_e = V\rho D/\eta$, where V is the fluid velocity, ρ the density and D the capillary diameter.

The mechanism of droplet formation following the aspiration of the sample is an extensive subject and is covered elsewhere [10—14]. Nukiyama and Tanasawa [15] produced an empirical relationship between the droplet diameter and solution properties in conjunction with nebulizer parameters

$$d_0 = \frac{585}{v}\left(\frac{\sigma}{\rho}\right)^{\frac{1}{2}} + 597\left(\frac{\eta}{(\sigma\rho)^{\frac{1}{2}}}\right)^{0.45}\left(1000\,\frac{Q_{liq}}{Q_{gas}}\right)^{1.5} \tag{2}$$

where d_0 is the mean droplet diameter in μm, v is the velocity of gas in m s^{-1} (or more strictly the difference between gas and liquid velocities), σ is the surface tension in dyne cm^{-1}, ρ is the density of the liquid in g ml^{-1}, η is the viscosity in poises, and Q_{liq} and Q_{gas} are the volume flows of the liquid and gas. This empirical formula was derived from experiments where the solution properties were within the following limits: $30 < \sigma < 73$; $0.01 < \eta < 0.3$; $0.8 < \rho < 1.2$. Extrapolation outside these ranges may be dangerous.

The droplet size may affect the emission in two ways: when the size is large, more material is lost to the drain in transporting the aerosol to the plasma whenever indirect nebulization is used. In addition, with lower-power plasmas, large droplets may not be completely evaporated in their passage through the high-temperature zone.

In the case of mineral acids, the change of surface tension with increasing concentration is not large compared to the changes in density and viscosity. This is not, however, the case with organic solvents. Considerable work has been carried out on organic solvents and their effects on flame photometry (see refs. 1, 12 and 13, for example). Avni and Alkemade [16] examined the effects of acetone, methanol and n-propanol on the sodium emission

excited in an air-acetylene flame supplied by indirect atomization. Ascribing the enhancement of radiation principally to improved functioning of the nebulizer with organic solvents, these authors state that the enhancement effect cannot be related to a single factor but is a function of changes in surface tension, viscosity, volatility, heat of evaporation, etc.

EXPERIMENTAL

Equipment

The equipment has been fully described [17]. In all the present experiments the power in the plasma was 6.0 kW.*

Solutions

The solutions prepared contained a mixture of 50 p.p.m. ($\mu g\ ml^{-1}$) each of nickel, iron, cobalt, chromium, and copper in the following strengths of acids or methanol (expressed as % w/w).

Nitric acid	9.5 %,	22.5 %,	41.0 %
Hydrochloric acid	4.2 %,	10.2 %,	19.0 %
Perchloric acid	8.8 %,	20.4 %,	36.4 %
Sulphuric acid	16.7 %,	37.3 %,	63.5 %
Phosphoric acid	17.4 %,	33.0 %,	57.2 %
Acetic acid	10.4 %,	23.8 %,	51.2 %
Propionic acid	9.9 %,	24.9 %,	49.8 %
Formic acid	12.2 %,	29.6 %,	55.8 %
Methanol	17.4 %,	33.0 %,	57.2 %

Temperature

All work was carried out in a room kept at 21 ± 0.5 °C, thereby eliminating the need to thermostat the solutions before or during nebulization.

RESULTS

Aspiration rate

The validity of Poiseuille's equation was tested when applied to the SP 900 nebulizer operated under normal plasma conditions with a variety

*The power dissipated in the plasma was 6 kW, measured calorimetrically according to B.S. 1799 and not by using a "Reflected Power Meter". When the impedance of the coil surrounding the plasma is not exactly matched to the transmission line the power fed along the line cannot all be absorbed and some of it is reflected in the form of a second travelling wave, which must return along the line. The forward and reflected waves interact all along the line to set up a standing wave. "Reflected Power Meters" are designed for convenient switching between the forward and reflected waves and are calibrated to read power in the load. The net power transmission is equal to the forward power minus the reflected power. The efficiency of transfer of the power in the load to the plasma is not 100 % and it is essential that the power values measured by the "Reflected Power Meter" be calibrated in terms of the power dissipated in the plasma.

of solutions of different acid concentrations. Poiseuille's law (eqn. 1) states that for a nebulizer operated under fixed conditions, ηQ is a constant. Thus the relation

$$\frac{Q_{\text{soln.}}}{Q_{\text{water}}} = \frac{\eta_{\text{water}}}{\eta_{\text{soln.}}} \tag{3}$$

is expected so that a straight line passing through the points (0,0) and (1,1) is predicted when these ratios are plotted as in Fig. 1. However, the straight line obtained does not pass through the origin. This is in agreement with the modification of Kundt and Warburg previously mentioned; for the Poiseuille equation is modified to

$$Q = \frac{a}{\eta} + b$$

so that

$$\frac{Q_{\text{soln.}}}{Q_{\text{water}}} = \frac{\dfrac{a\eta_{\text{water}}}{\eta_{\text{soln.}}} + b\eta_{\text{water}}}{a + b\eta_{\text{water}}} \tag{4}$$

which is a straight line passing through (1,1) but with a positive intercept.

The points were obtained by measuring the mass of each solution aspirated in 60 s. Density data [18] were used to convert these to volume flow rates; published values [19] of viscosity data were used.

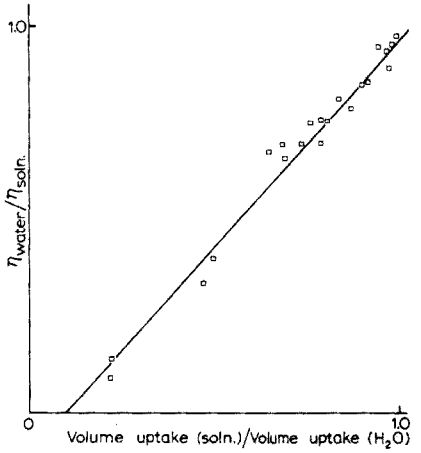

Fig. 1. Correlation between volume uptake and viscosity.

Effect of mineral acid concentration on signal intensity

The most obvious effect is likely to be the variation in sample uptake caused by different viscosities. There are other possible effects such as the formation of refractory species (which is unlikely if the temperature is high enough) or a fall in temperature because of the extra energy required to dissociate the acid (which is unlikely to be noticeable if there is adequate power in the plasma). The variations in signal produced by the latter two effects will depend on the element in question, while those produced by changes in sample uptake will have very similar effects on all elements.

A solution containing 50 p.p.m. of nickel, iron, cobalt, chromium and copper in water and in different concentrations of nitric, hydrochloric, perchloric, sulphuric and phosphoric acids was used as sample. The ratios of the line intensities in the acid solutions to those in water are shown in Table 1. It can be seen that the five elements behave very similarly, so much so that for a given acid concentration the relative standard deviation of the ratios (s_r) for the different elements is always well under 10 % and typically 1—2 %.

TABLE 1

Variation of signal intensities with acid concentration and solution uptake volume to the nebulizer

(The wavelengths used for measurement were 361.9 nm (Ni), 259.9 nm (Fe), 345.3 nm (Co), 425.4 nm (Cr) and 324.7 nm (Cu).)

	Concn. (Wt %)	$\text{Intensity}_{(\text{soln.})}/\text{Intensity}_{(H_2O)}$						Uptake Ratio[a]	s_r[b]
		Ni	Fe	Co	Cr	Cu	Av.		
H_2O	—	1.00	1.00	1.00	1.00	1.00	1.00		
HNO_3	9.5	0.92	0.93	0.90	0.92	0.91	0.92	0.955	1.45
	22.5	0.81	0.82	0.79	0.79	0.80	0.80	0.88	1.47
	41.0	0.63	0.64	0.64	0.63	0.61	0.63	0.685	1.80
HCl	4.2	0.90	0.92	0.90	0.90	0.91	0.90	0.953	1.30
	10.2	0.80	0.81	0.83	0.80	0.81	0.81	0.89	1.30
	19.0	0.76	0.77	0.77	0.74	0.76	0.76	0.77	1.20
$HClO_4$	8.8	0.86	0.86	0.86	0.90	0.87	0.87	0.96	1.9
	20.4	0.80	0.80	0.80	0.83	0.79	0.80	0.915	1.8
	36.4	0.69	0.69	0.67	0.68	0.67	0.68	0.77	1.5
H_2SO_4	16.7	0.66	0.59	0.69	0.67	0.68	0.66	0.67	6.9
	37.3	0.42	0.39	0.43	0.40	0.43	0.41	0.49	4.4
	63.5	0.16	0.16	0.17	0.19	0.17	0.17	0.17	7.9
H_3PO_4	17.4	0.78	0.72	0.76	0.84	0.76	0.76	0.74	3.7
	33.0	0.49	0.45	0.50	0.50	0.47	0.48	0.47	4.3
	57.2	0.19	0.18	0.19	0.19	0.19	0.19	0.22	3.1

[a] Ratio of the uptake rate of the acid solution to that of water.
[b] Relative standard deviation on the intensity ratio.

Table 1 also shows the ratio of the uptake rate of a given acid solution to that of water, obtained from Fig. 1, the viscosities being obtained from graphs based on values in the literature. There is a very marked correlation between this ratio and the net signal intensity ratios for the same acid solution (Fig. 2).

To prove conclusively that the signal reduction can be largely explained in terms of changing viscosity for acid solutions of different concentration, each solution was pumped through the nebulizer in such a way that a constant volume should flow irrespective of viscosity. This was accomplished by the use of a Sage Pump pumping at 1 ml min^{-1} ; this pump operates by driving a syringe, loaded with solution, at a constant rate, irrespective of viscosity. Comparison of the results for hydrochloric acid solutions given in Tables 1 and 2 indicates that the change in signal intensity is considerably reduced when the forced-feed system is used instead of the conventional non-forced feed system (cf. Fig. 3).

Jones [20] has used a somewhat similar variable-flow, forced-feed aspiration system for atomic absorption spectrometry with good results, though his purpose was not to take account of varying viscosities of sample solution.

If the volume flow rate for individual solutions is measured, the intensity of the signal obtained can be corrected by the ratio of the volume flow rate to that for water. The results shown in Fig. 3, again for hydrochloric acid, are obtained.

On the basis of this evidence it is possible to feed solutions of high acid content, for example, up to 60 % sulphuric acid or phosphoric acid, into the induction-coupled plasma torch without producing significant inter-

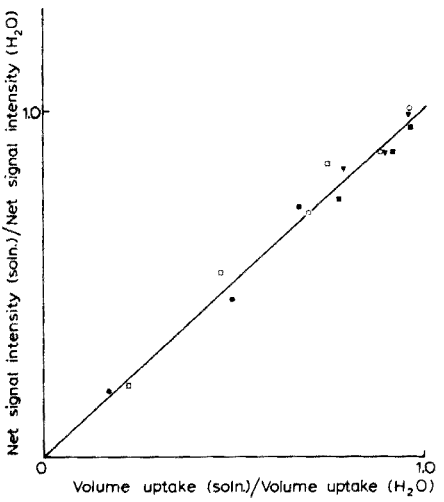

Fig. 2. Correlation between signal intensity ratios and volume uptake ▾ HCl, ○ HNO_3, □ H_3PO_4, • H_2SO_4, ▪ $HClO_4$.

TABLE 2

Effect of a forced-feed nebulizer system

	Concn. (Wt. %)	Intensity (soln.)/Intensity (H_2O)					
		Ni	Fe	Co	Cr	Cu	Av.
H_2O	—	1.00	1.00	1.00	1.00	1.00	1.00
HCl	4.2	0.95	0.98	0.96	1.02	1.08	1.00
	10.2	0.88	0.86	0.86	0.93	0.96	0.90
	19.0	0.87	0.84	0.84	1.03	0.94	0.90

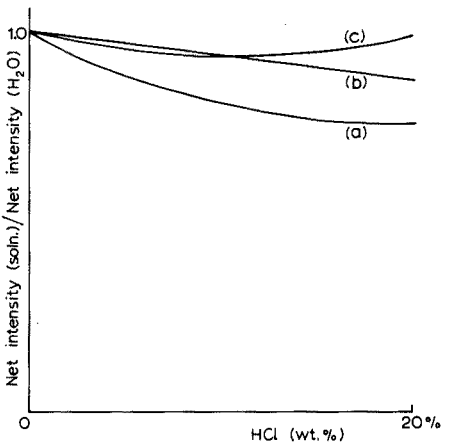

Fig. 3. Effect of forced feed and volume uptake correction (a) Normal feed. (b) Forced feed. (c) Volume correction.

ference effects, other than that ascribable to a nebulizer effect arising from viscosity. It must be emphasized, however, that this work was carried out at a high input power to the plasma and that these conclusions may not be valid at lower powers.

Organic acids and solvents

Injection of organic acids or solvents into a flame or inductively coupled plasma torch enhances the signal intensity. With low-power plasmas and flames, there are complex molecular spectra from carbon species; they are diminished in plasmas of higher powers. For instance, raising the power in the plasma from 3 kW to 6 kW changes its colour from green (C_2 Swan Bands) to purple (cyanogen banding). By suitable choice of coolant gas, usually oxygen, which in turn requires higher powers, both the C_2 and CN bands can be removed.

A further complication arises if the geometry of the injector and plasma

cell are not carefully designed. If the injector is too low or shaped as in Fig. 4(a) the organic vapour "fans out" and enters the plasma fire-ball. When this occurs the conditions in the plasma change, as evidenced by a large change in frequency, and this leads to complicated changes in signal intensity, a considerable reduction in sensitivity and a tendency to unstable operation. A correctly shaped injector (Fig. 4 (b)) correctly positioned in relation to the plasma, maintains the toroidal-shaped plasma, the organic vapour passing largely through the centre of the toroid with little change in frequency or deterioration in sensitivity and stability. The results and discussion which follow refer only to a correctly positioned injector of the type shown in Fig.4(b).

The first observations made concerned the background at the wavelengths of the spectral lines of the elements under consideration. On all lines the background showed some enhancement when organic solvents were introduced, presumably because of some molecular banding from the carbon species. This enhancement was always small and represented less than 10 % of the enhancement observed for the net signal intensity of the element itself. It would appear, therefore, that the enhancement of the net signal intensities for the various elements is due to changes in the physical parameters of the solution rather than changes in background. The enhancements can be large; a factor of two is not uncommon.

It has already been demonstrated that changes in viscosity of solutions give different volume uptake rates into the nebulizer. It is possible to calculate the increase or decrease in signal intensity, compared to an aqueous solution, caused by these changes in volume uptake. In all the organic acid solutions studied, the viscosity increases with concentration. This should lead to a decrease in signal intensity, contrary to observation. Thus there must be an increase in signal intensity which outweighs the decrease caused by viscosity and this must be due to the large changes in the physical properties of organic solutions for different concentrations. Changes of surface tension, which are small in the case of the mineral acids, are likely to play a major role.

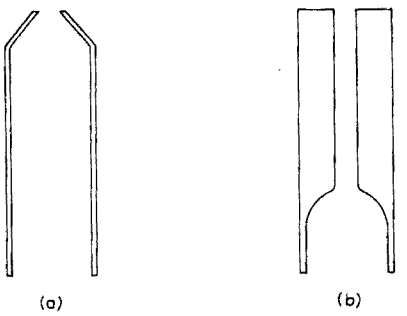

Fig. 4. Injector geometry.

The signal (I) is expected to depend on viscosity (because of the effect on sample uptake) according to the relation

$$I = I_w \left(\frac{c\eta_w}{\eta} + d \right) \tag{5}$$

where I_w is the signal obtained from an aqueous solution and where $c + d = 1$. The viscosity, in conjunction with the surface tension and density, also influences the size of the droplets produced by the nebulizer. The droplet size, as already mentioned, will influence the quantity of solution which is aspirated from the sample cup but which does not reach the plasma, for the larger the droplet, the greater the proportion falling, hitting the wall and going to the drain; another effect which may occur in low-power sources is the possibility of large droplets not being completely vaporized in their passage through the high-temperature zone. The signal is thus expected to depend on droplet size which in turn depends on the viscosity η, the surface tension σ and the density ρ. Thus

$$I = I_w \left(\frac{c\eta_w}{\eta} + d \right) f(\eta, \sigma, \rho) \tag{6}$$

where f is an unknown function to account for the effects of drop size. Trial and error established that relatively smooth curves could be obtained when the experimental data were plotted as a function of a variable t defined by $t = (\sigma\rho)^{1/2}/\eta$. It was encouraging to note that this variable occurs in Nukiyama and Tanawawa's expression for droplet size [15]. These smooth curves could be approximated by rectangular hyperbolae $tf(\eta, \sigma, \rho) =$ constant, and it was thus possible to derive the equation

$$I = I_w \frac{\eta}{(\sigma\rho)^{\frac{1}{2}}} \left(\frac{7.055}{\eta} + 1.245 \right) \tag{7}$$

Values calculated from this formula are plotted against the values observed for the organic acids and methanol in Fig. 5, together with the line y = x on which they should lie. There are some wild points but the correlation is good, the correlation coefficient being 0.86.

While the data were being examined it was noticed that the observed signals could also be approximated by a linear function of the variable t:

$$I = I_w \ (1.84 - 0.105 \ (\sigma\rho)^{\frac{1}{2}}/\eta) \tag{8}$$

No explicit provision is made in this case for the change in uptake with viscosity, which is known to occur, and so this would be expected to be a fundamentally poorer, if simpler, approximation. There is, however, little to choose between the overall representation of the data by this formula (Fig. 6) and the previous one, which has a little more theoretical backing, and the correlation coefficient of the simpler linear model is only marginally smaller at 0.84. When Fisher's z-transformation was applied, it was found that the difference was not significant.

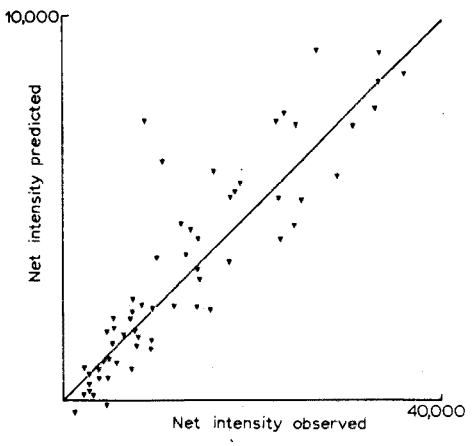

Fig. 5. Correlation between predicted and observed signal intensities.

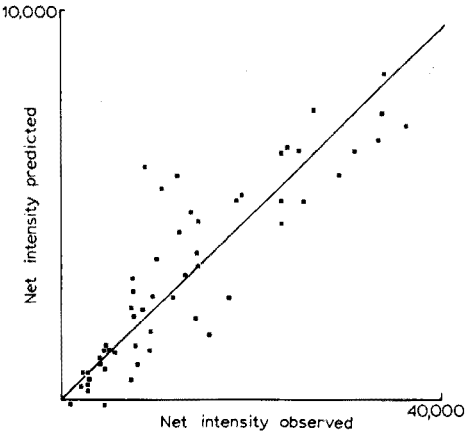

Fig. 6. Correlation between predicted and observed signal intensities (linear model).

Some of the discrepancies between predicted and observed values may be due to poor values for the viscosity, surface tension and density, all of which were interpolated or extrapolated from the sparse values reported in the literature. It is also possible that some are due to an inappropriate choice of relation to give the predicted values. The fact that discrepancies exist does not seem to be of very great importance, since standards whose liquid properties match those of the sample are normally preferred to the application of a correction factor of as yet somewhat uncertain magnitude and dubious range of validity.

The important conclusion is that what may seem at first glance to be interference effects in the plasma source can to a very large extent be attributed, by a satisfactory correlation between the signal and the solution properties, to the aspiration and nebulizing system. If the magnitude of these effects seems surprisingly large, it should be remembered that the concentrations of mineral acids and organic solvents that can be tolerated in a high-power plasma are also unusually high.

REFERENCES

1 S. R. Koirtyohann and F. E. Lichte, Summary of paper presented at the 5th International Conference of Atomic Spectroscopy, Melbourne, Australia, 1975.
2 I. Rubeska, in J. A. Dean and T. C. Rain (Eds.), Flame Emission and Atomic Absorption Spectrometry, Vol. 1, Dekker, New York, 1969, p. 332.
3 S. R. Koirtyohann in J. A. Dean and T. C. Rain (Eds.), Flame Emission and Atomic Absorption Spectrometry, Vol. 1, Dekker, New York, 1969, p. 296.
4 S. Greenfield, I. Ll. Jones and C. T. Berry, Analyst (London), 89 (1964) 713.
5 G. F. Larson, V. A. Fassel, R. H. Scott and R. N. Kniseley, Anal. Chem., 47 (1975) 238.

6 J. D. Winefordner and H. W. Latz, Anal. Chem., 33 (1961) 1727.
7 Yu. F. Bukreev, V. F. Grigor'ev and V. I. Bassukov, Tr. Mosk. Inst. Khim. Mashinostr., 44 (1972) 87.
8 Kundt and Warburg, Ann. Phys., 155 (1875) 337.
9 N.A. Lange (Ed), Handbook of Chemistry, 9th edn, Handbook publishers, Sandersby, Ohio, 1949.
10 W. R. Lane, Ind. Eng. Chem., 43 (1951) 1312.
11 W. R. Marshall, Chem. Eng. Progr. Monogr. Symp. Ser. 50 No. 2 (1954).
12 Kirk-Othmer, Encyclopedia of Chemical Technology, 2nd edn., Vol. 18, Interscience, New York, 1968, p. 634.
13 J. A. Dean, Flame Photometry, McGraw-Hill, New York, 1960.
14 R. Mavrodineanu and H. Boiteux, Flame Spectroscopy, Wiley, New York, 1965.
15 S. Nukiyama and Y. Tanasawa, Trans. Soc. Mech. Eng. Jpn., 4, 5, 6 (1938—1940). Translated by E. Hope, Defence Research Board, Ottawa, Canada.
16 R. Avni and C. T. J. Alkemade, Mikrochim. Acta, (1960) 460.
17 S. Greenfield, I. Ll. Jones, H. McD. McGeachin and P. B. Smith, Anal. Chim. Acta, 24 (1975) 224.
18 L. J. Gillespie, International Critical Tables, Vol. III, McGraw-Hill, 1929, p. 51.
19 S. J. Bates and W. P. Baxter, International Critical Tables, Vol. V, McGraw-Hill, 1929, p. 21.
20 A. H. Jones, At. Absorption Newslett., 9 (1970) 1.

Analytica Chimica Acta, 84 (1976) 79—88

THE APPLICATION OF OPTICAL PYROMETRIC AND TWO-LINE ATOMIC ABSORPTION TECHNIQUES TO THE DETERMINATION OF TEMPERATURES IN A GRAPHITE FURNACE ATOMIZER

M. J. ADAMS and G. F. KIRKBRIGHT

Department of Chemistry, Imperial College, London SW7 2AY (England)

(Received 11th December 1975)

SUMMARY

Optical pyrometric measurements of the final temperatures and temperature—time profiles at the centre of a commercial graphite furnace atomizer have been made. These are discussed and compared with the maximum electronic excitation temperatures and temperature—time profiles obtained for gallium and indium in the furnace.

The use of graphite furnace atomizers for analytical atomic absorption spectrometry (a.a.s.) has become widespread and the advantage of these atom cells for provision of high absolute sensitivity is well-known. The principal types of graphite furnace used routinely are those in which samples are vaporized by electrothermal heating of a hollow cylindrical graphite cell; these systems are based on the furnaces first described by L'Vov [1] and Massman [2]. Although these devices have found extensive application in a.a.s., few measurements have been reported of the temperature attained by the atomic vapour produced within the furnace.

Bratzel and Chakrabarti [3] have reported temperatures for the atomic vapour produced from gallium and indium above a carbon filament atomizer and within a small transverse aperture (1.5 mm diameter) in the filament. Findlay et al. [4] have described a method by which graphite furnace temperatures as high as 1700 °C can be monitored by a thermocouple placed inside the tube. For thermodynamic and kinetic studies of atomization in graphite furnaces a knowledge of the heating rate and final temperature of the cell is required; in early studies of this type the manufacturer's calibration of the furnace temperature has been accepted. Cresser and Mullins [5] have investigated the theoretical temperature– time curves expected for electrically heated atom cells but little information is available concerning the effect of aging of the graphite tube on the furnace temperature or on the variation with time of the atomic vapour temperature of elements introduced into the tube. This paper describes the determination with an optical pyrometer of the final temperatures obtaining in the graphite tubes in the widely used HGA 2000 furnace. The heating rates of the atomizer have been evaluated by

means of the spectral emission characteristics of the heated tube as discussed by Johnson et al. [6]. The application of the "two-line" atomic absorption method of Browner and Winefordner [7] to the determination of the electronic excitation temperature of gallium and indium in the furnace and the variation with time of this temperature for indium are also reported.

EXPERIMENTAL

Apparatus and reagents

A Perkin-Elmer model 305B atomic absorption spectrometer fitted with an HGA 2000 graphite furnace atomizer was employed for all absorption and emission measurements. Argon, at flow rate no. 4 and automatic stopped-flow conditions, was used as the furnace purge gas. The output from the spectrometer was fed to a potentiometric chart recorder (Servoscribe type RE511). The power to the graphite tube was supplied from a Perkin-Elmer transformer system, and the applied voltage (or temperature) was selected by the meter provided with this unit. A Leeds—Northrup disappearing-filament optical pyrometer was employed for the furnace temperature measurements. The atomic vapour temperatures were measured with a 150-W tungsten/iodine continuum radiation source fitted to a hollow-cathode lamp holder and positioned in the lamp housing so that the radiation was focussed at the centre of the graphite tube of the furnace atomizer. To select absorption wavelengths of interest (Ga 403.29 nm and 417.20 nm; In 410.18 nm and 451.13 nm) the continuum source was replaced by conventional hollow-cathode lamps for these elements.

Stock solutions (10,000 μg ml^{-1}) of gallium and indium were prepared from the pure metals by dissolution in ca. 30 % (v/v) analytical-grade nitric acid. The solutions were diluted as necessary with distilled water.

Procedure for optical pyrometer temperature measurements

Removal of the observation tube from the HGA 2000 furnace housing enables the inside surface of the graphite tube, directly opposite the sample introduction port, to be viewed. The temperature of this part of the graphite tube was determined at various applied voltages, corresponding to 200 °C steps from 1000 °C to 2200 °C, by focussing the radiation from the inner wall of the tube at the viewing lens of the optical pyrometer. These measurements were repeated many times during the useful lifetime of several graphite tubes.

The static temperature measurements made with the pyrometer were used to evaluate the heating rates of the graphite tubes at various applied voltages. The spectrometer was operated in the emission mode with slit-setting 3, and constant gain was applied to the photomultiplier tube. The emission from the furnace was monitored at 600 nm with respect to elapsed time from the commencement of the start of the heating cycle and at voltages of 3.0, 4.25, 5.50, 6.75 and 8.0 V applied across the graphite tube. The emission intensity vs. time curves were recorded on the potentiometric chart recorder, the scale

of which was set so that no signal damping by the recorder time-constant was observed. The final temperature attained by the furnace was determined at each applied voltage with the optical pyrometer, as described above.

Procedure for two-line a.a.s. temperature measurements

A commercial indium hollow-cathode lamp was employed to select the In 410.18-nm line and the monochromator was set at this wavelength. The hollow-cathode lamp was replaced by the uncalibrated tungsten continuum lamp and the absorption from an indium solution was determined from two samples of equal indium concentration. Aliquots (10 μl) of the required sample were transferred to the graphite tube with an Eppendorf micropipette; each solution was dried at 100 °C for ca. 30 s before atomization with a voltage of 5.5 V applied across the furnace. The 451.13-nm indium line was then selected, again with the hollow-cathode lamp, and the absorption by the same concentration of indium solution determined. The 410.18-nm line was reselected and a second concentration of indium solution examined. By this procedure of constant checking and reselecting the wavelength with the aid of the indium hollow-cathode lamp, problems with wavelength drift were minimized. Alternate measurements of the absorption at the 410.18-nm resonance line and 451.13-nm non-resonance line ensured that changes in the heating rate of the furnace associated with its use were smoothed out. Because of the changes in furnace properties with use, the absorption measurements were repeated many times over a period of several weeks and the mean absorption peak heights were recorded for various indium solution concentrations. An identical procedure was employed for the gallium absorption studies.

The temperature—time profiles of an atomic vapour produced in the HGA 2000 graphite furnace were investigated with a standard indium solution (2 μg ml^{-1}). A 10-μl aliquot of the indium solution was pipetted into the graphite tube and after the drying stage (30 s at 100 °C), the chart recorder and atomization programme were activated simultaneously. In this manner absorption vs. time profiles were recorded for the indium 410.18-nm and 451.13-nm lines at various applied voltages across the graphite tube. Temperature—time curves were determined from the absorption—time profiles.

RESULTS AND DISCUSSION

Final temperatures attained by the HGA 2000 atomizer

The power supply for the HGA 2000 unit used is provided with a calibrated meter by means of which the applied power to the furnace can be adjusted to select the furnace temperature. This set temperature then indicates the approximate final temperature attained by the furnace during its heating cycle. Because of the change in electrical resistance of a graphite tube throughout its useful lifetime, and because the open nature of this furnace gives rise to a temperature gradient along the tube, it was decided to determine

the final furnace temperature independently and compare the observed values with the nominal temperatures.

The final temperature achieved by the graphite furnace varies throughout its length, being hottest at the centre, so that a reproducible viewing point must be selected. As the sample for a.a.s. is placed centrally in the furnace and remains there until volatilized, the central point was selected for viewing, as described under Experimental.

A comparison of the nominal and observed furnace temperatures is presented in Fig. 1. It is apparent that the observed temperature of the furnace deviated from the set temperature by as much as ±10 % depending on the age of the graphite tube and the temperature selected. The mean observed temperature, throughout the useful lifetime of the furnace, was between 3 % and 7 % greater than the nominal temperature and the deviation increased with increasing temperature.

Because of this difference in observed and nominal temperatures, the term "furnace temperature" used later in this paper refers to the optical pyrometer temperature and not to the temperature indicated by the meter on the power supply. Where reference to the power settings is necessary, the voltage applied across the graphite tube is given as this is independent of the condition of the furnace.

Temperature—time profiles in the HGA 2000 furnace

Findlay et al. [4] monitored the furnace temperature with respect to time, using thermocouples placed inside the graphite tube; temperatures up to 1700 °C were measured and considerable temperature gradients were observed to exist, both radially and axially, in the HGA 2000 furnace. Most atomic absorption studies, however, are undertaken at furnace temperatures above 1800 °C, and a means of monitoring the temperature—time characteristics of

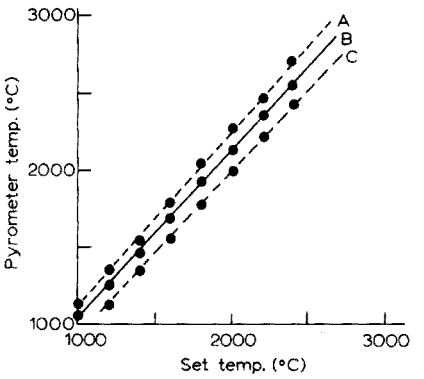

Fig. 1. Comparison of optical pyrometer temperature measurements and nominal temperatures for graphite furnace. A. Towards the end of the tube lifetime. B. Mean, throughout lifetime. C. New tube.

the graphite furnace at these higher temperatures was sought. Johnson et al. [6] have recently studied the temperature—time profiles of a carbon filament atomizer using the Planck's Law relationship between the emission intensity of a hot body and its temperature. The application of this method to the HGA 2000 graphite furnace is described here. For any particular instrumental arrangement and measuring the emission intensity at wavelength λ from the black body at temperature T as a voltage (V_λ) produced by a photomultiplier tube, it can be shown that a plot of log V_λ vs. $1/T$ is linear. This allows the temperature of the emitter to be determined from the emission intensity measured as a voltage; the procedure applied for monitoring the emission at 600 nm for applied voltages of 3.0—8.0 V is described under Experimental.

A graph of log (peak emission intensity) vs. the reciprocal of the temperature ($1/T$) in degrees Kelvin (shown in Fig. 2) is a straight line. With this linear relationship, the emission intensity—time curves could be converted to the corresponding temperature—time curves (Fig. 3). Temperatures below ca. 1000 °C were difficult to measure with acceptable precision by the optical pyrometer, and linear extrapolation to room temperature was assumed. As the heating rate is proportional to the square of the applied voltage, this assumption was tested by determining the heating rate for the linear portion of each curve in Fig. 3 and examining its variation with applied voltage; the plot of heating rate vs. (voltage)^2 was found to be linear for heating rates of 200—700 °C s^{-1} and applied voltages of 3.0—8.0 V. The extrapolation is therefore valid.

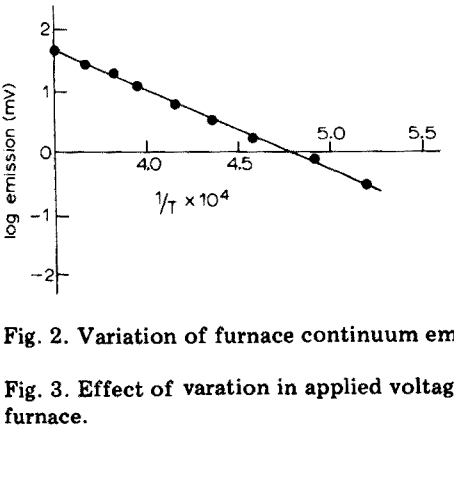

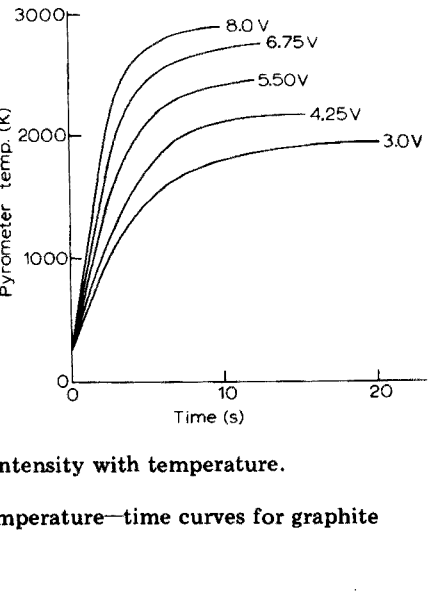

Fig. 2. Variation of furnace continuum emission intensity with temperature.

Fig. 3. Effect of varation in applied voltage on temperature—time curves for graphite furnace.

Electronic excitation temperatures by a two-line atomic absorption method

Browner and Winefordner [7] have described a two-line atomic absorption method for the measurement of flame temperatures which is applicable to non-flame atomization devices. This method uses an uncalibrated continuum light source and is relatively simple, rapid and accurate. For an atomic species having one or more electronic levels close to the ground state, it is possible to relate the relative absorption at the resonance line α_0 and at a non-resonance line α_1 to the relative populations of these levels. This may be accomplished using the appropriate expressions relating the relative absorption of the radiation from a continuum source for low and high absorbances to the atomic population in each state. At low and high absorbances, equations for the electronic excitation temperature of the atomic vapour may then be obtained [7]. Browner and Winefordner [7] have shown that if the growth curves (log absorption vs. log concentration) for the two wavelengths employed for each element are parallel, and if the intersection point of the low (slope = 1) and the high (slope = 1/2) absorption asymptotes occurs at the same concentration, then the equations for high and low absorbance are identical and knowledge of the absorption line profiles is not necessary.

The two-line atomic absorption method was applied to the determination of the atomic vapour temperatures for gallium and indium in the HGA 2000 graphite furnace with the 150-W continuum source as described under Experimental. Growth curves of log α vs. log (metal concentration) were constructed for both metals at each line employed (Figs. 4 and 5). The inflec-

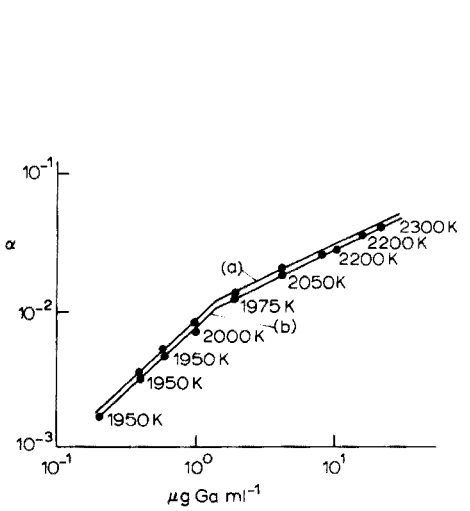

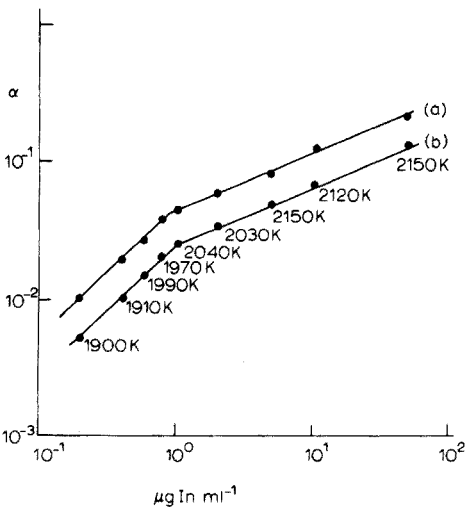

Fig. 4. Growth curves for relative absorption signals of gallium. (a) Gallium 403.29 nm. (b) Gallium 417.20 nm.

Fig. 5. Growth curves for relative absorption signals of indium. (a) Indium 410.18 nm. (b) Indium 451.13 nm.

tion points of these curves (Table 1) occurred at the same concentrations for the resonance and non-resonance lines for both elements; therefore the approximation to reduce the high absorbance equation to the form of the low absorbance equation was applicable. The data used to obtain these growth curves were employed to calculate atomic vapour temperatures for each element. At each concentration of gallium and indium employed, the relative absorption factors were determined repetitively (at least 6 times), and the mean of each of these factors was employed to calculate individual temperature values. The range of values obtained is shown in Figs. 4 and 5. Table 2 shows the mean electronic excitation temperature obtained and the relative standard deviation in these values. The individual values for the electronic excitation temperature for both gallium and indium increase as the concentration increases (Figs. 4 and 5); this effect may be attributed to increasing deviation obtained at high absorbance values by the use of the above-mentioned approximation.

Whether gallium or indium was used as the sensing element, the atomic vapour temperatures were similar and were ca. 15 % lower than the furnace wall temperature. As mentioned above, the working temperature range for gallium is 650—2200 K, hence the poorer precision of the results obtained with this metal is understandable. The two-line absorption temperature measurements in Table 2 were determined by recording the absorption peak heights. Thus, no information about the variation in temperature of the

TABLE 1

Inflection points for growth curves with continuum source

Element	Wavelength (nm)	Inflection point (μg ml^{-1})
Gallium	403.30	1.5
	417.20	1.5
Indium	410.18	1.0
	451.13	1.1

TABLE 2

Atomic vapour and furnace temperature measurements with an applied voltage of 5.5 V

Metal	Set temp.[a]	Furnace temp.[b]	Atom temp.[c]	s_r (%)
Ga	2273	2413	2047	6.06
In	2273	2413	2030	4.72

[a]Temperature (K) indicated on instrument meter.
[b]Temperature (K) determined by means of optical pyrometer measurements.
[c]Temperature (K) determined by means of two-line a.a.s. measurements.

atomic vapour produced in the graphite furnace with respect to time was obtained. From these results it cannot be said that the temperatures recorded were the maximum atomic vapour temperatures but merely the electronic excitation temperatures observed at the peak absorption. An experimental method for the determination of the temperature—time profiles of an atomic vapour produced in a graphite furnace is clearly required. Because of its usefu temperature working range (1220—3500 K), indium was selected as appropriate for study in the development of such a method. Absorption—time profiles were obtained, as described under Experimental, for the indium resonance line (451.13 nm) at various applied voltages; α_0/α_1 was measured at various times from the absorption—time profile and hence atomic vapour temperature—time profiles were determined.

The temperature—time profile curves of the indium atomic vapour in the HGA 2000 at applied voltages of 4.25 V, 5.50 V, 6.75 V and 8.00 V are shown in Fig. 6; also included are the furnace temperature—time curves determined with the optical pyrometer, and the absorbance—time profiles for

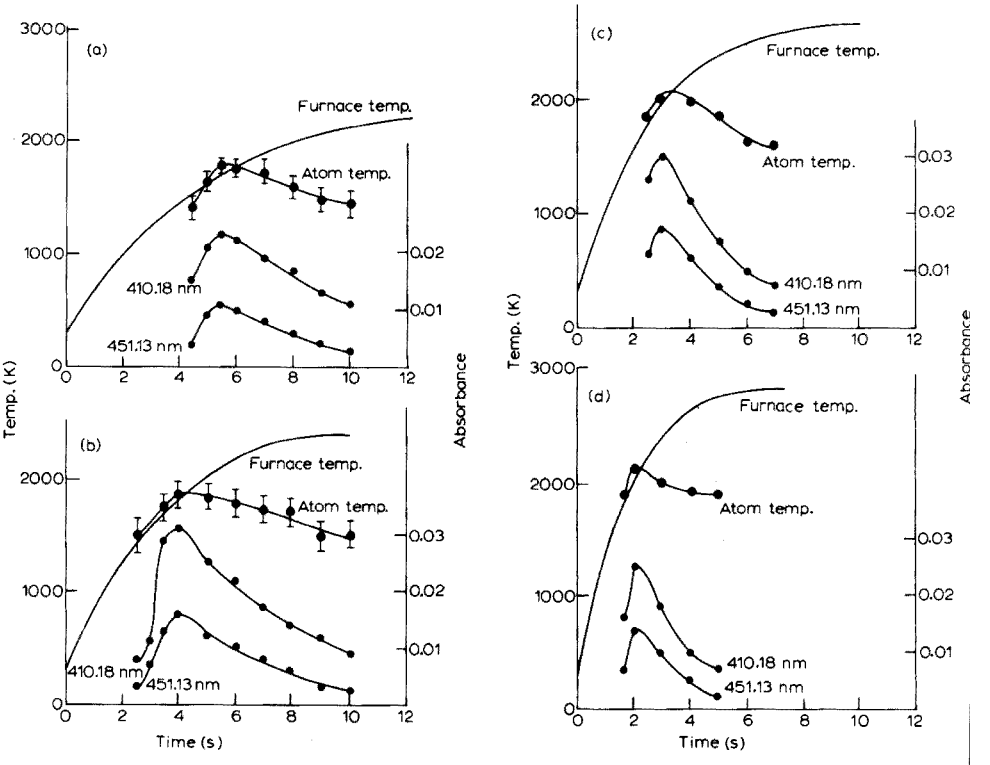

Fig. 6. Variation of electronic excitation temperature and absorbance with time for indium in graphite furnace, at different applied voltages. (a) 4.25 V; (b) 5.5 V; (c) 6.75 V; (d) 8.0 V. Variation of observed furnace temperature with time is shown for comparison.

the resonance and non-resonance absorption lines. Some significant results obtained from those curves are presented in Table 3.

The atomic vapour temperature—time profiles were of similar distribution to the absorption—time curves, i.e. rising rapidly to a maximum value, and then falling to lower absorption or temperature values more gradually with increasing time. This decay, however, was less pronounced for the temperature—time curves than for the absorption—time profiles.

CONCLUSION

The temperature—time characteristics of a resistively heated graphite electrode (such as a rod or tube furnace) depend on the applied voltage, electrode length and cross-sectional area, and the density, specific heat, thermal conductivity, resistivity and emissivity of the electrode material [5]. Cresser and Mullins [5] applied a simplified theoretical approach to calculate these profiles for graphite and tungsten filaments. The temperature—time curves (Fig. 3) for the HGA 2000 graphite tube atomizer were similar to those observed by Cresser and Mullins, i.e. a linear relationship exists between furnace temperature and time until temperatures are reached at which power losses from radiation and thermal conduction become significant.

The two-line atomic absorption method of temperature determination has been applied to the study of the atomization of gallium and indium in the HGA 2000 graphite furnace. Bratzel and Chakrabarti [3] applied this method from peak-absorption measurements to the determination of the temperatures of atomic vapours produced by graphite filament and graphite rod atomizers. Their studies indicated that gallium gave higher atomic vapour temperatures than indium. For indium the concentrational locations of the inflection points between the low and the high absorption portions of the growth curves were not the same for the resonance and non-resonance lines and low absorption figures only could be used. The higher temperature achieved for gallium was

TABLE 3

Some temperature measurements with the HGA 2000 furnace

Applied voltage (V)	Set temp.[a] (K)	Furnace temp.[b] (K)	Max. atom temp.[c] (K)
4.25	2073	2173	1830
5.50	2273	2413	1950
6.75	2473	2633	2070
8.00	2673	2853	2100

[a]Final meter temperature corresponding to the applied voltage.
[b]Furnace final temperature determined with the optical pyrometer.
[c]Maximum indium atom temperature by two-line a.a.s. method.

attributed by these workers to the greater boiling point (2676 K) of this metal than of indium (2353 K), implying that because gallium is in direct contact with the surface of the rod for a longer time, the temperature attained was greater.

The temperature studies reported here with the HGA 2000 graphite tube show similar temperatures for both gallium and indium (Table 2), and both species fulfilled the equilibrium condition of similar concentrational inflection points between the resonance and non-resonance transitions in their growth curves. These findings are probably related to the increased atom residence time associated with the large tube furnace and the way in which this influences the attainment of thermal equilibrium within the atomic vapour.

Temperature measurements derived solely from peak absorption methods provide no information concerning the change in atom temperature with time during the heating cycle of a furnace. Temperature—time profiles of the atomic vapour of indium showed that in all cases the mean temperature of the atomic vapour in the furnace increased with increase in furnace wall temperatures, achieved a maximum temperature at the same time as the absorption maximum occurred and finally decreased in a manner similar to, but less rapidly than, the atomic absorption—time curves. L'Vov [8] has shown that the duration of the atomic absorption signal in a tube furnace is controlled mainly by the rate of atom-loss by diffusion from the furnace. Because of the open nature of the HGA 2000 tube furnace, a severe temperature gradient exists along the length of the hot tube, and the rate of decrease of the atomic vapour temperature, after the maximum, can probably be attributed to the diffusion process controlling the absorption curve. That this rate of decrease is less severe than that observed for the absorption process may be due to collisions with the hot furnace walls or purge-gas molecules.

We wish to thank Perkin-Elmer Corp. for the loan of the Model 305B atomic absorption spectrometer employed in this work.

REFERENCES

1 B. V. L'Vov, J. Eng. Phys., 2 (1959) 44.
2 H. Massman, Spectrochim. Acta, Part B, 23 (1968) 215.
3 M. P. Bratzel, Jr. and C. L. Chakrabarti, Anal. Chim. Acta, 63 (1973) 1.
4 W. J. Findlay, A. Zdrojewski and N. Quickerd, Spectrosc. Lett., 7 (1974) 63.
5 M. S. Cresser and E. Mullins, Anal. Chim. Acta, 68 (1974) 377.
6 D. J. Johnson, B. L. Sharp, T. S. West and R. M. Dagnall, Anal. Chem., 47 (1975) 1234.
7 R. F. Browner and J. D. Winefordner, Anal. Chem., 44 (1972) 247.
8 B. V. L'Vov, Atomic Absorption Spectrochemical Analysis, Adam Hilger, London, 1970.

Analytica Chimica Acta, 84 (1976) 89—96

SOME APPLICATIONS OF RAPID SEPARATION OF MERCURY ON METALLIC COPPER TO ENVIRONMENTAL SAMPLES WITH DETERMINATION BY FLAMELESS ATOMIC ABSORPTION SPECTROMETRY

S. DOGAN and W. HAERDI

Department of Inorganic and Analytical Chemistry, University of Geneva, Sciences II, CH-1211 Geneva 4 (Switzerland)

(Received 17th December 1975)

SUMMARY

Preconcentration of mercury on a copper micro-column is particularly suitable for determination of mercury in various environmental samples. The micro-column is coupled to the cell for mercury determination by f.a.a.s. To avoid possible interferences by volatile organic compounds adsorbed on the copper together with mercury, an alumina column is placed just before the f.a.a.s. cell. With this method 1 ng of mercury can be determined with a precision of ±13 %. The time required for determinations is 15—120 min for 50—500-ml water samples (several preconcentrations can be done simultaneously), about 2.5 h for liquid biological samples, and 15—20 min for solid samples.

For relatively high mercury concentrations in aqueous media the tin(II) reduction—aeration method is often preferred because of its simplicity [1, 2]. For lower mercury concentrations a preconcentration step seems to be necessary [1, 3, 4]. Another approach, which is rather lengthy, is based on the electrodeposition of mercury on Au, Pt, Ag or Cu, and is particularly convenient for samples of small volume [5—7]. For solid samples such as sediments, rocks and bio-organics, a preliminary mineralization by combustion is necessary to preconcentrate the mercury vapour on gold metal [7—10]. This method is very much faster than wet mineralization and possible contaminations by the reagents are avoided.

In the present paper, first the preconcentration technique described recently [11] is applied to the determination of mercury in natural waters and waste-waters. Secondly, a very rapid and efficient mineralization technique by combustion or acid digestion is applied to mercury determinations, respectively, in solid samples or liquid biological materials from various sources.

EXPERIMENTAL

In a preliminary study, water samples (10—500 ml) from various sources were labelled with ^{203}Hg ($t_{\frac{1}{2}}$ = 47 days; C.E.A. France). After centrifugation or filtration on millipore membranes, the pH values of the samples were adjusted to 1.5—2.0 with nitric acid and the mercury was separated on micro-columns of copper powder as described previously [11]. For total added mercury concentrations in the 10^{-6}—10^{-8} M range, the separation efficiency was greater than 98 %; the efficiency was lower (75—80 %) for lower concentrations such as 10^{-11} M (1 ng/500 ml) owing to the adsorption of mercury on the walls of the vessel. The adsorbed mercury could be released by 1 M HCl [12]. No apparent interference by the other constituents of water was observed. The copper column on which mercury was retained was used directly for flameless atomic absorption spectrometry (f.a.a.s.).

Procedure for aqueous samples

The water sample (10—1000 ml) is passed through a millipore membrane (diameter 47 mm, porosity 0.45 μm) and immediately acidified with nitric acid (Merck G.R.) to pH 1.5—2.0. The ionic mercury is then separated by passage of the sample through a copper micro-column at a flow rate of about 4—5 ml min^{-1}.

It is possible to determine the total mercury content by oxidizing the filtrate in order to free the "bound mercury". This is done by treating the filtrate with ozone produced by passing oxygen over a high-voltage discharge lamp [13]. At a flow rate of oxygen of 100 ml min^{-1}, the oxidation is complete in about 10 min; even with relatively highly polluted samples oxidation is complete in about 30 min. The excess of ozone which accumulate in the solution is removed by passing a stream of nitrogen. This method of oxidation is unsuitable for samples containing, or which on oxidation liberate, highly volatile organo-mercurials such as $(CH_3)_2Hg$ and $(C_2H_5)_2Hg$, since the loss of mercury becomes significant.

Blank determination. Separation on copper micro-columns for a given sample is repeated by successive passages until a constant absorbance is reached. This value is taken as blank and subtracted from the absorbance of analytical samples.

It should be noted that it is indispensable to add traces of gold ($[Au]_t \approx 10^{-8}$ M) as $AuCl_3$ to the filtrate, to prevent mercury from being adsorbed on the walls of the vessel [12].

Procedure for solid samples

The dried solid sample (10—100 mg) in a quartz crucible is introduced into a quartz tube placed in a tubular furnace (see Fig. 1). The sample is burnt at 900—950 °C in an oxygen stream (flow rate 45 ml min^{-1}) which carries the volatile combustion products including mercury to and through

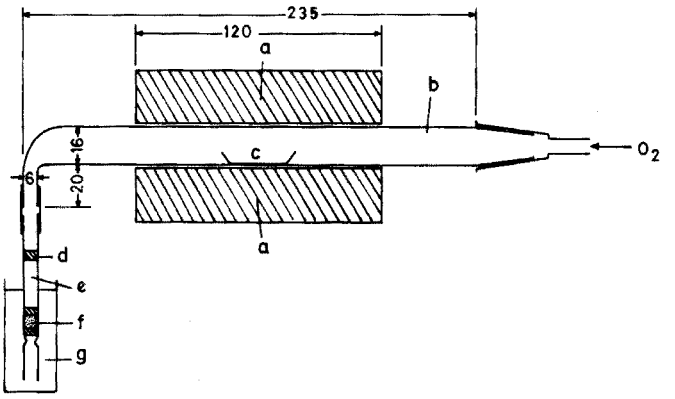

Fig. 1. Combustion and separation apparatus. a, tubular furnace; b, combustion tube (quartz); c, quartz crucible; d, quartz wool; e, copper powder micro-column; f, copper powder; g, ice bath. Dimensions in mm.

the copper micro-column, which is cooled in an ice bath, to ensure a quantitative separation of mercury. (This combustion can also be done with a Bunsen burner.) The micro-column is joined to the combustion tube by means of a length of short PVC tubing.

A little quartz wool (d) acts as a filter for any particulate matter that may be carried along. It should be removed before f.a.a.s.

For this procedure, the blank is similarly prepared, but without the sample.

In order to prevent possible clogging, the micro-column must be loosely filled with copper.

Procedure for liquid biological samples

Wet mineralization under pressure is well suited for mercury determinations in biological liquids such as blood and milk. For this purpose a slightly modified decomposition vessel (Uni-Seal decomposition vessels, Israel) was used (Fig. 2). It was necessary to make some modifications to the original vessel, to make it airtight and avoid deformation of the teflon crucible (b). The teflon disk (e) and viton "O" ring (d) must be renewed before each mineralization.

About 1 g of blood and 2 ml of concentrated nitric acid (Merck suprapur) are introduced into the vessel which is sealed and left at 150 °C for 2 h. The sealed vessel is cooled in liquid nitrogen or dry ice before it is opened. Its contents are transferred to a beaker and the pH is adjusted to 1.5—2.0 with solid sodium hydroxide (Merck suprapur). The mercury in solution is then separated on a copper micro-column as described previously [11].

F.a.a.s. analysis

Once the mercury has been separated, the micro-column is rinsed two or three times with methanol (Merck G.R.) and is incorporated in the analytical apparatus as shown in Fig. 3 (see also ref. 11).

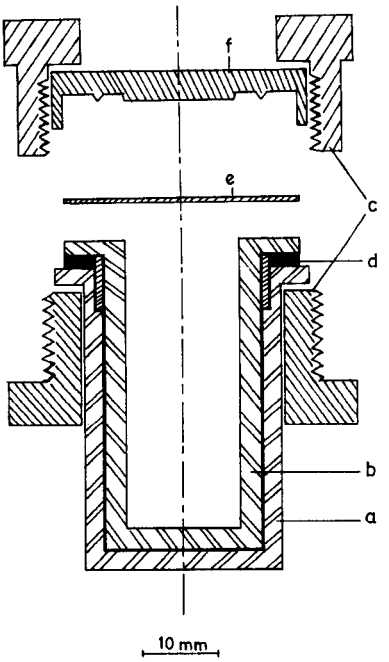

Fig. 2. Mineralization vessel. a, stainless steel container; b, teflon crucible (total volume, 5 ml); c, stainless steel retaining screws; d, viton "O" ring; e, teflon disk (0.6 mm); f, stainless steel cap.

RESULTS AND DISCUSSION

Determination of mercury in water

The described method proved to be very satisfactory for determinations of mercury in environmental water samples of various origins (lake, river, sea and tap-water) as well as in industrial waste-waters which do not contain a large amount of organic compounds and especially chlorinated organic or mineral compounds. Significant interference by volatile species absorbing in the 253.7-nm region was eliminated by passing the effluent gas over a 0.5—3-cm alumina column before its entrance into the f.a.a.s. cell (Fig. 3).

The detection limit was 1 ng absolute as can be seen from the results in Table 1 (in a sample of the Rhône river at Geneva).

Table 2 shows the results obtained for lake, river and sea-water samples. It is important to note that during the ozonization of sea water to liberate "bound mercury", some chlorine is also produced and causes very serious interference with the analysis. This oxidation procedure is therefore not recommended for sea-water samples.

Determination of mercury in blood samples

By labelling blood samples with ^{203}Hg, efficiencies of 98 % in the combined

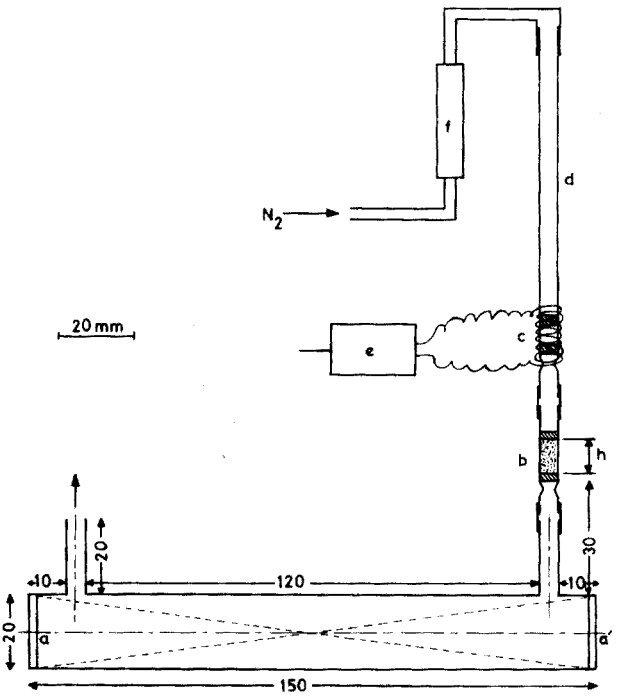

Fig. 3. F.a.a.s. measuring system. a, a', quartz windows (2 mm); b, alumina micro-column (h = 0.5—3.0 cm; Al_2O_3 standardized for chromatographic adsorption analysis acc. to Brockman); c, heating coil; d, copper micro-column; e, e.m.f. cell (0—5 A); f, flowmeter. Dimensions in mm.

TABLE 1

Analysis of river water and recovery of added mercury

Total volume (ml)	Hg added (ng)	Absorbance	Hg found (ng)[a]
100	0.0	0.005 (blank)	—
	1.0	0.011	1.2
	2.0	0.017	2.4
	4.0	0.026	4.2
	10.0	0.058	10.4
500	0.0	0.010	1.0
	3.0	0.024	3.8
	5.0	0.035	6.0
	100.0	0.101 (on 100 ml)	98.0

[a]After blank subtraction.

TABLE 2

Mercury in natural water samples[a]

Origin	Ionic Hg ($ng\ l^{-1}$)	Total Hg ($ng\ l^{-1}$)
Rhône river (at Geneva)	3.1 ± 0.8	11.3 ± 1.2
Arve river[b] (at Geneva)	1.8 ± 1.0	2.8 ± 1.0
Lake of Geneva (surface)	2.5 ± 1.2	8.9 ± 1.5
Lake of Geneva[c]	4.3 ± 1.0	11.6 ± 1.6
Lake of Geneva[d]	5.3 ± 1.2	15.4 ± 2.5
Adriatic Sea (at Rovinj/YU)	4.6 ± 1.1	—

[a]Experiments done on one sample only.
[b]Sandy water.
[c]Water pumped at about 30 m depth before sand filtration.
[d]Same water filtered over sand for domestic use.

TABLE 3

Mercury in a blood sample

Sample weight (g)	Hg added (ng)	Absorbance	Hg found (p.p.b.)[a]
Blank	—	0.007	—
0.968	—	0.036	5.8
1.007	—	0.030	4.4
0.981	10	0.081	4.5
—	10	0.058	10.0

[a]After subtracting blank and added mercury. Mean: 4.9 ± 0.9.

mineralization and separation steps were found for 1—2 ng of added mercury. The results for a blood sample are presented in Table 3.

Determination of mercury in plants

The accuracy of the method as applied to samples of vegetable origin was checked by analyzing the mercury content of standard orchard leaves (NBS reference material 1571) alone and mixed with flour to obtain lower amounts. As shown in Table 4, the results are in very good agreement with certified values and with those obtained by other workers [14].

In the analysis of such samples, the regularity of combustion and the flow

TABLE 4

Mercury content in standard orchard leaves (NBS 1571)

	Hg found (p.p.b.)	Hg certified (p.p.b.)
Orchard leaves	154.0 ± 13.0	155 ± 15
Flour (pure)	7.2 ± 2.2	—
Mixture 1	40.5 ± 4.5[a]	40.2[b]
Mixture 2	55.9 ± 4.3[a]	56.7[b]

[a] After blank subtraction (flour).
[b] Values calculated from the certified value.

TABLE 5

Mercury in some vegetation samples

Sample	Origin[a]	Hg (p.p.b.)[b]
Apple tree leaves	A	96—164[c]
	B	275—724[c]
Pine leaves	A	54.2 ± 2.0
	B	252.6 ± 4.5
Larch leaves	B	730—860[c]
Ripe wheat	A	10.6 ± 0.6
	B	13.6 ± 0.4
Zooplankton	C	268.2 ± 12.0
Phytoplankton	C	87.3 ± 4.0
Mixed plankton	C	301.7 ± 34.3

[a] A, Urban region; B, industrial region; C, Lake of Geneva.
[b] Values for dried weight.
[c] Values obtained at different periods of the year.

of oxygen are important factors in obtaining good precision. The limit of detection is 1 ng of mercury for 10—100-mg samples. Results for various vegetation samples are given in Table 5.

REFERENCES

1 See, e.g. A. M. Ure, Anal. Chim. Acta, 76 (1975) 1.
2 R. J. Baltisberger and C. L. Knudson, Anal. Chim. Acta, 73 (1974) 265.
3 J. Olafsson, Anal. Chim. Acta, 68 (1974) 207.
4 D. Voyce and H. Zeitlin, Anal. Chim. Acta, 69 (1974) 27.
5 M. J. Fishman, Anal. Chem., 42 (1970) 1462.
6 H. Brandenberger and H. Bader, At. Absorpt. Newsl., 6 (1967) 101; 7 (1968) 53.
7 H. Heinrichs, Z. Anal. Chem., 273 (1975) 197.

8 P. C. Leong and H. P. Ong, Anal. Chem., 43 (1971) 940.
9 D. H. Anderson, J. H. Evans, J. J. Murphy and W. W. White, Anal. Chem., 43 (1971) 1511.
10 J. W. Wimberley, Anal. Chim. Acta, 76 (1975) 337.
11 S. Dogan and W. Haerdi, Anal. Chim. Acta, 76 (1975) 345.
12 S. Dogan, Thesis, University of Geneva, 1976.
13 L. Lopez-Escobar and D. N. Hume, Anal. Lett., 6 (1973) 343.
14 W. F. Fitzerald, W. B. Lyons and C. D. Hunt, Anal. Chem., 46 (1974) 1882.

Analytica Chimica Acta, 84 (1976) 97—108

CHARACTERIZATION AND APPLICATION OF SILYLATED SUBSTRATES FOR THE PRECONCENTRATION OF CATIONS

DONALD E. LEYDEN* and G. HOWARD LUTTRELL**
Department of Chemistry, University of Georgia, Athens, Georgia 30602 (U.S.A.)
A. E. SLOAN and N. J. DeANGELIS
Wyeth Laboratories, Philadelphia, Pennsylvania 19101 (U.S.A.)
(Received 21st November 1975)

SUMMARY

Chelating functional groups immobilized on silica and controlled pore glass beads are used to preconcentrate cations from aqueous solution in the concentration region of ng ml^{-1}. The functional groups are chemically bonded to the substrates by silylation reagents which may be employed as received or further modified. For example, commercially available 1,2-diamines may be used or converted to the dithiocarbamate after immobilization. This report includes studies of ionic strength and sodium chloride effects on the recovery of transition metal ions. Batch extraction of transition metal ions is accomplished with silica as the substrate for solutions containing transition metal ions at μg ml^{-1} concentrations. Column extraction of solutions pumped at 50 ml min^{-1} is accomplished at concentrations of 25 ng ml^{-1}. Recovery is good in both cases. The cations were determined directly on pelletized substrates by x-ray fluorescence. However, the ions may be eluted from the substrate and determined by other methods. Examples of determinations of several cations in lake water and high-purity industrial water are given.

In previous reports [1, 2] the use of silylation reactions to prepare effective immobilized functional groups on silica or porous glass beads for the preconcentration of ions before determination by x-ray fluorescence was reported. Other preconcentration methods were summarized in those reports. This report presents a detailed study of an efficient and easily prepared series of amines, diamines and dithiocarbamates in relation to their ability to recover metal cations from solution. As a demonstration of the potential of these materials, several elements were determined in natural lake water and in high purity water.

EXPERIMENTAL

Reagents

Stock metal ion solutions (10^{-3} M) were made from perchlorate salts

*Author to whom correspondence should be addressed.
**Present address: Alcon Labs., Humaco, Puerto Rico 00661.

(G. F. Smith Co.) or from the nitrate salts (J. T. Baker Co.). The alkoxysilanes immobilized on the silica gel (E. M. Reagents Type G) and the controlled pore glass beads (Electro-Nucleonics CPG-10,200/400 mesh) were obtained from Dow-Corning. These were β-aminoethyl-γ-aminopropyltrimethoxysilane (Z-6020) and γ-aminopropyltrimethoxysilane (XZ-2024). All other chemicals used were of reagent-grade quality. The immobilization of the silanes and the synthesis of the dithiocarbamates have been previously described [1].

Apparatus

All x-ray fluorescence research data were obtained with a Philips model PW-1410 x-ray fluorescence spectrometer equipped with a sine-theta potentiometer. In all cases a LiF-200 analyzing crystal was used with gas flow and scintillation detectors in tandem. P-10 gas (Selox, Inc.) was used in the flow detector. Either a Mo or W x-ray tube was used as a source of x-radiation and was operated at 50 kV and 50 mA. The counting times varied but were less than 40 s in all cases. Spectrometer parameters were optimized by the usual procedures of step scanning to locate the peaks and background 2θ angles, and a PHA scope was used to determine the pulse-height energy win All spectrometer operations were under control of a Nova 1220 computer. For the industrial application, a Philips 50 kV vacuum x-ray spectrometer was used with a LiF-200 analyzing crystal and a scintillation counter detecto The radiation source was a W x-ray tube operated at 45 kV and 40 mA, and the counting times were 40 s.

Pellet preparation

The silica gel was pelletized for use in the x-ray spectrometer. Because of the mechanical instability of pressed silica gel and controlled pore glass pellet a binder of powdered cellulose was mixed with the samples before pressing. Equal weights of cellulose and substrate were used.

Studies of the extractive processes

Effect of ionic strength. Studies were undertaken to determine the behavio of the immobilized complexing materials as a function of ionic strength. Copper(II), cobalt(II) and nickel(II) were chosen as representative cations, while the Z-6020 diamine and Z-6020 N-alkyldithiocarbamate were used on the silica gel substrate. The cations (30 μg each) were placed in a beaker containing 100 mg of the substrate. The desired ionic strength was obtained by mixing different ratios of deionized water and 2 M $NaClO_4$ for a constant volume. Constant pH was maintained at 8.5 ± 0.2 (the substrate is self-buffering in this region). The mixture was stirred for 10 min and prepared for x-ray analysis.

Effect of NaCl. This experiment was performed under constant conditions of pH and ionic strength with Cu^{2+}, Co^{2+}, Ni^{2+} and Fe^{3+}. Different NaCl

concentrations were obtained by mixing various ratios of 2 M NaCl and 2 M $NaClO_4$ so that the total volume in each case was 25 ml. The solutions were stirred for 10 min, pellets were made from the filtered silica, and the ions of interest were determined by x-ray fluorescence.

Effect of calcium(II) and magnesium(II). An experiment was performed at constant ionic strength and pH to determine any effects of these cations on the extractive process. The N,N-dialkyldithiocarbamate of XZ-2024 (100 mg) was used along with 30 μg each of Ni^{2+} and Co^{2+}. A solution containing 100 μg ml^{-1} of each of Ca^{2+} and Mg^{2+} was prepared by dissolving appropriate amounts of calcium carbonate and magnesium metal in dilute perchloric acid and then diluting to volume. Various amounts of this solution were mixed with the substrate, the Ni^{2+} and Co^{2+} solution, and 10 ml of 2 M $NaClO_4$ (for ionic strength control) so that the total volume in each case was 25 ml. After stirring for 10 min, the solid extractant was filtered and pelletized for analysis by x-ray fluorescence.

Linear dynamic range. Studies were undertaken to investigate the range of concentrations to which this technique (immobilized chelates on silica gel) may be conveniently applied. To this end, solutions were prepared containing 100 mg of the immobilized Z-6020 diamine and varying amounts of zinc(II). The pH was kept constant with a borate buffer. All the solutions had a final volume of 25 ml and were stirred for 15 min. Finally the solid extractant was filtered and pelletized so that the zinc might be determined by x-ray fluorescence. An experiment similar to the one above was also performed with copper(II) and the N,N-dialkyldithiocarbamate of XZ-2024.

Reproducibility studies. These studies were divided into two parts; the first utilized Zn^{2+}, Cu^{2+} and Co^{2+} at a concentration of 10 μg ml^{-1} along with the immobilized Z-6020 diamine (100 mg). In this case, 2 ml of the 10 μg ml^{-1} sample was mixed with 5 ml of 0.1 M $NaClO_4$ and diluted to a total volume of 25 ml with deionized water. In the second part of the study, Cu^{2+}, Ni^{2+} and Co^{2+} in a more diluted form (0.25 μg ml^{-1}) were used with the N-alkyldithiocarbamate of Z-6020. For these more dilute solutions, a 50-ml sample was used to which 5 ml of 0.1 M $NaClO_4$ was added.

In each of the above cases, the substrate served to buffer the solution to a constant pH. Quadruplicate samples were analyzed in the usual manner by x-ray fluorescence.

Standard curves and recovery. This experiment sought to duplicate the way in which an actual analysis of natural waters would be performed. Standards were prepared that contained respectively 1, 2, 3, 4 and 5 μg ml^{-1} of each of the following cations in the same solution, Pb^{2+}, Co^{2+}, Hg^{2+}, Zn^{2+}, Cu^{2+}, Ni^{2+} and Mn^{2+}. A test solution was prepared that contained 4.5 μg Pb ml^{-1}, 5.0 μg Hg ml^{-1}, 3.0 μg Zn ml^{-1}, 2.0 μg Cu ml^{-1}, 1.0 μg Ni ml^{-1}, 0.5 μg Co ml^{-1}

and 4.0 μg Mn ml^{-1}. To 15 ml of each standard and the test solution, 15 ml of an ammonia—ammonium perchlorate buffer (pH 10.2 ± 0.2) were added, followed by 100 mg of the N,N-dialkyldithiocarbamate immobilized on silica gel. The mixture was stirred for 10 min, and the solid extractant prepared for analysis by x-ray fluorescence. The standard curves were plotted for each cation, and the percent recovery from the test solution was obtained from these curves.

Column recovery studies

For preconcentration work in the p.p.b. (ng ml^{-1}) range, batch extractions are not particularly convenient, and so recovèry studies were made for small columns packed with 100 mg of the N,N-dialkyldithiocarbamate immobilized on controlled pore glass. The glass columns were 6 cm long and 0.5 cm i.d. The height of the extractant in the column was about 1 cm. The sample solutions and the column were connected with tygon tubing (i.d. 3/8 in.), which passed through a variable speed peristaltic pump (Harvard Co.) to maintain a constant flow rate. Standard solutions (1 l) containing 10, 20, 30 and 50 ng ml^{-1} each of Cu^{2+}, Ni^{2+} and Co^{2+} were prepared. An additional test solution containing 25 ng ml^{-1} of the above ions was also made. All of these were passed through the column at a flow rate of 50 ml min^{-1}. After analysis, the standard curves were plotted and the percentage recovery on the test solution determined from these curves.

Analysis of lake water and water for pharmaceutical preparation

In order to determine if the column method could be employed in real analytical situations, lake water samples and bacteriostatic distilled water for pharmaceutical formulations were investigated. The fresh water lake, Lake Hartwell, is situated in northern Georgia at the South Carolina border. Samples (1 l) were taken, beginning at buoy number 13/2, and at 0.5, 1 and 2-mile intervals proceeding west from buoy 13/2 on a channel of the lake called "Lightwood Log Creek". A sample was taken also at a cove off the eastern shore of Hartwell State Park to see if there were any gross differences in metal ion concentrations between deep channel water and the shallow, placid water of a cove. The last sample was taken at the Hartwell Marina. Each of the samples was pumped through the previously described columns containing 100 mg of the N,N-dialkyldithiocarbamate immobilized on CPG-10 glass beads. Before the samples were pumped through the column, 25 ml of the ammonia—ammonium perchlorate buffer was added to control the pH and ionic strength. The pumping of the sample (50 ml min^{-1}) was done at the marina in order to avoid losses by adsorption onto the container surface. The columns with the extracted ions were then transported back to the laboratory for x.r.f. analysis. The pellets were scanned to determine the presence of various ions of interest, and ultimately, standards were prepared containing these ions in concentrations ranging from 1 to 50 ng ml^{-1}. Standard curves were plotted, and the concentrations of the lake water samples determined from these curves.

As an application of this preconcentration method in an industrial situation, the analysis of water to be used in pharmaceutical preparations was undertaken. This application was selected because water used in drug products, especially injectable formulations, characteristically contains metals only in the sub-p.p.m. range. Distilled, bacteriostatic water was therefore analyzed for the metals of interest (Fe^{3+}, Cu^{3+} and Pb^{2+}) at four different stages in the preparation of this water. The four locations monitored were: (1) entrance into the still (note: this is city water after it has been passed through a cation-exchange column), (2) the output of the still, (3) the output of the holding tank used to sterilize the water and store it before use, and (4) the output of the piping used to carry the water to the formulations area. Sampling was carried out on site, as described above in the analysis of lake water, with a 1-l water sample and 100 mg of the CPG-10 immobilized bisdithiocarbamate of Z-6020. Pellets were prepared as previously described for x.r.f. analysis for the metals of interest. Quantification was achieved by comparing the counts obtained on the water samples to those of a set of standards.

RESULTS AND DISCUSSION

The purpose of this investigation was to determine the applicability of immobilized complexing and chelating groups as preconcentration aids for multielement analysis by x-ray fluorescence. To be effective, these aids had to be inexpensive, readily available or easily synthesized, have a form suitable for x-ray analysis, and finally have a high distribution constant for the metal ions of interest. These conditions are met by using silanes containing appropriate functional groups immobilized on either a silica gel or a controlled pore glass matrix. The immobilized chelates used in this study are shown below

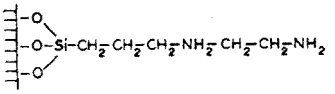

Z-6020 diamine (I)

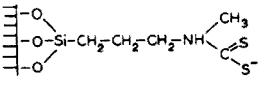

N, N-Dialkyldithiocarbamate of XZ-2024 secondary amine (II)

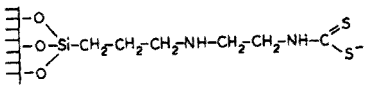

N-Alkyldithiocarbamate of Z-6020 diamine (III)

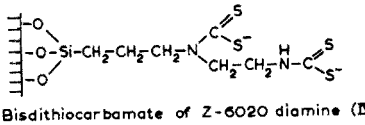

Bisdithiocarbamate of Z-6020 diamine (IV)

Other studies involving the above immobilized groups including the immobilized reaction, dithiocarbamate synthesis, effects of time and pH on the extraction, stability, capacity and distribution studies have already been described [1]. The studies presented in this paper are a continuation of the previous work.

Effect of ionic strength

Since natural waters vary greatly with respect to ionic strength, the extractive ability of two of the immobilized ligands (Z-6020 diamine and Z-6020 N-alkyldithiocarbamate) was investigated with respect to this parameter. The value of the ionic strength was varied by the use of different amounts of sodium perchlorate. The ionic strength values varied from about 0.07 to nearly 2, and the results of the experiment are illustrated in Fig. 1 for extraction of Cu(II), Ni(II) and Co(II). At low ionic strengths, the extraction curves go through a maximum. The maximum would be predicted from the fact that the pK_a of the ligands is lowered, so that it becomes a stronger acid and thus the dissociated form is more available for complexatio [3]. In the case of the dithiocarbamate, there is then a region of nearly constant extraction of nickel(II) and cobalt(II) with a small depression for copper(II). Then at ionic strengths of about 1.4, there is an increase in extractive efficiency, probably caused by lowering of the activity of the solvent water. The diamine does not show the increase in extraction at higher ionic strengths, but rather the efficiency of the system continues to decrease.

It is evident from the curves that for an actual analysis, care should be taken for work at low ionic strength values. Probably the ionic strength should be adjusted in the analyte so that it falls within the flatter portions of the curves.

Effects of other salts

Because chloride ion is found to some extent in almost all natural waters and has the ability to complex many metal ions, its effect on the extractive efficiency was investigated at constant pH and ionic strength. The immobilized Z-6020 diamine and monodithiocarbamate were used as the substrate

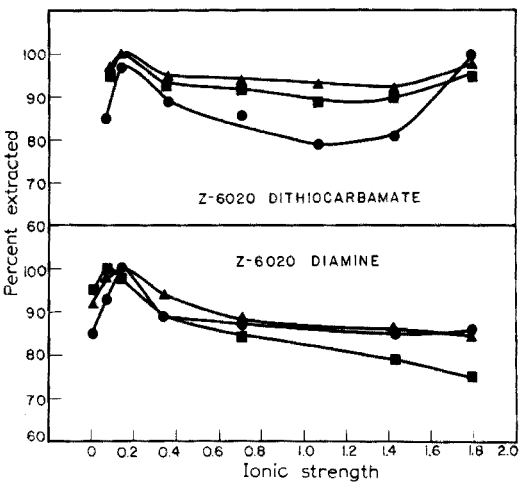

Fig. 1. Percentage extraction of cobalt, nickel and copper as a function of ionic strength at constant pH for Z-6020 diamine and Z-6020 monodithiocarbamate. •Cu(II). ▲Ni(II). ■Co(II).

The chloride can form complexes of the type MCl^+, MCl_2, MCl_3^-, etc. with many cations and thus compete with the immobilized ligand reducing the overall extraction. Extractions of Cu(II), Co(II), Ni(II) and Fe(III) were carried out in the presence of different amounts of sodium chloride. The results are shown in Fig. 2. For the dithiocarbamate there is little change in extraction of cobalt(II) and copper(II) up to about 1 M NaCl and a slightly larger effect at higher concentrations. For nickel(II), the initial effect was a reduction of about 5 % which remained about constant. However, the largest effect was for iron(III); this was expected since it, of all the ions tested, has the greatest affinity for chloride. For the diamine there is a slight decrease in extractive efficiency for Co(II), Ni(II) and Cu(II) with increasing sodium chloride concentration. At a little over 1 M NaCl, the extraction is about 90 % complete. The diamine is less efficient in competing with the chloride than is the dithiocarbamate because of the larger formation constants of the dithiocarbamate.

In areas where natural waters are found near limestone formations, concentrations of calcium(II) and magnesium(II) may be relatively large. For this reason, a trace metal analysis technique for these waters should not be affected by the presence of calcium and magnesium ions. To investigate their effects, nickel(II) and cobalt(II) were extracted by the N-alkyldithiocarbamate in the presence of varying amounts of both calcium and magnesium. This study indicated that there was no effect when 50—400 μg of the alkaline earth cation was added.

Linear dynamic range

Generally in extractions of this type (solid/liquid), the extractive efficiency begins to decrease as the amount of extracted cation begins to approach the overall capacity of the extractant. When this happens, the extraction curves as a function of cation concentration become non-linear. To determine when this happened, experiments were performed with copper(II) XZ-2024 dithiocarbamate and zinc(II) Z-6020 diamine; a constant amount of substrate was used with increasing amounts of cation, the total volume of solution was the same in each case, and the pH was kept constant (borate buffer). The results are shown in Fig. 3. The linear dynamic range for the diamine is about 1000 and about 500 for the dithiocarbamate. The curves begin to become non-linear at a loading corresponding to about 60 % capacity. The range is more than adequate for many applications and of course, may be extended by simply changing the sample size.

Precision, standard curves and recovery

To establish the precision of the method, two sets of experiments were carried out. In the first, a 2-ml sample of a solution containing 10 $\mu g\ ml^{-1}$ of each Zn(II), Co(II) and Cu(II) was extracted with the Z-6020 diamine. In the second study, a more dilute sample solution was used (50 ml of 0.25 $\mu g\ ml^{-1}$ of Co(II), Cu(II), and Ni(II)) with the Z-6020 monodithiocarbamate.

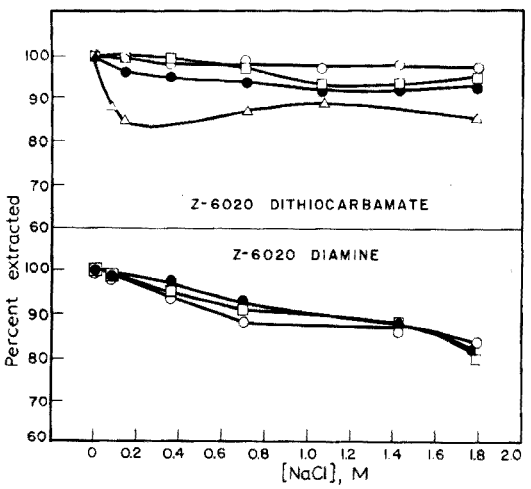

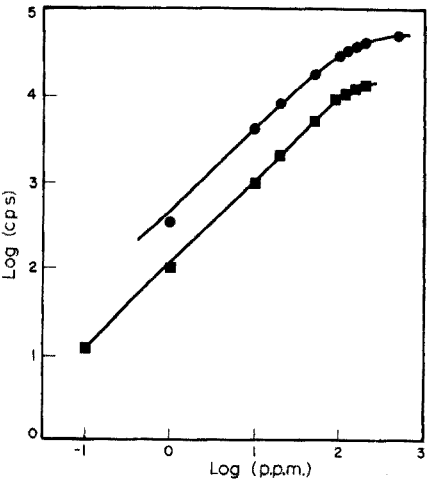

Fig. 2. Percent extraction at constant ionic strength and pH as a function of [NaCl]. ○Co(II). □Cu(II). ●Ni(II). △ Fe(III).

Fig. 3. Examples of linear dynamic range studies. ●Cu(II) — XZ-2024 dithiocarbamate ■Zn(II)—Z-6020 diamine.

In this way two different immobilized substrates were used at very different cation concentrations. In both cases, quadruplicate samples were determined by x-ray fluorescence. The results are shown in Table 1. In both cases, the precision is certainly adequate for work in this concentration range. The statistics given include both the imprecision in the extraction itself and statistical nature of the x-ray photon counting procedure; thus they reflect the reproducibility of the complete procedure.

Standard curves and recoveries were studied for the conditions under which an actual multielement trace analysis might be performed. Standards containing seven cations were prepared and extracted along with a synthetic test sample, by the silica-immobilized N,N-dialkyldithiocarbamate. After

TABLE 1

Results of precision studies

	Z-6020 Diamine			Z-6020 Monodithiocarbamate		
	Zn	Cu	Ni	Cu	Ni	Co
Mean (net c.p.s.)[a]	345	416	503	827	983	764
s	9	11	2	37	12	12
s_r	2.6	2.8	0.5	4.4	1.2	1.6

[a]Mean of 4 results. s is the standard deviation and s_r the relative standard deviation.

x-ray analysis, the standard curves were plotted (Fig. 4), and from them the percentage recovery of the test sample was determined. The recovery results are given in Table 2. The percentage recoveries are, in general, very good except for the high values for the manganese and lead.

Column studies

Up to this point, all the work described was the result of batch extraction procedures. Such procedures are adequate for samples containing cations in the p.p.m. range. However, often the analyst is concerned with pollutants occurring at the p.p.b. level. This means that for x-ray analysis, large volumes of solution will be needed for the preconcentration step. Preconcentration in this case would be more efficient by using a column procedure.

Small glass columns were used containing 100 mg of the silylated controlled pore glass beads. Silica gel could not be used because of channeling problems and the large pressure drop across the column. The effect of flow rate on the recoveries was established by passing 1 l of copper(II) solution (1 ng ml^{-1}) through two columns in tandem containing the N,N-dialkyldithiocarbamate immobilized on the CPG-10 glass beads. The flow rate was varied by changing the speed of the peristaltic pump. The color of the copper dithiocarbamate

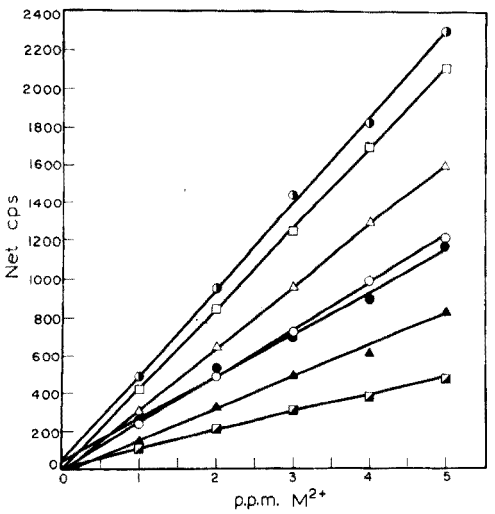

Fig. 4. Standard curves for multielement recovery studies. • Zn, □ Cu, △ Ni, ○ Co, • Pb, ▲ Hg, ▪ Mn.

TABLE 2

Batch extraction recovery studies with N,N-dialkyldithiocarbamate (IV) on silica

Cation	Pb^{2+}	Hg^{2+}	Zn^{2+}	Cu^{2+}	Ni^{2+}	Co^{2+}	Mn^{2+}
$\mu g\ ml^{-1}$ present	4.5	5.0	3.0	2.0	1.0	0.5	4.0
Mean recovery %	107±1.5	100±1.5	103±2.6	100±4.4	100±1.2	100±1.6	110±1.5

complex is so intense that the presence of less than 1 μg of copper is easily detected visually. After 1 l of solution had passed through the two columns, only about the upper 10 % of the first column was colored, and there was no colored complex on the second column. The results were essentially the same for flow rates of 10, 25, 50 and 70 ml min^{-1} through the column. It is probable that even faster flow rates would have been successful with a faster pump. These flow rates are from 5 to 10 times faster than can be tolerated by columns containing conventional ion-exchange resins, and serve to illustrate the applicability of this type of method for processing large volumes of water in reasonable periods of time.

Another more quantitative experiment was performed with 1-l standard solutions containing 10, 20, 30 and 50 ng ml^{-1} of each Co(II), Cu(II) and Ni(II) along with a synthetic test solution containing 25 ng ml^{-1} of each of these cations. These solutions were passed through different columns at a flow rate of 50 ml min^{-1}, and the extracted metal was determined by x-ray fluorescence. The results are contained in Table 3.

Analysis of lake water and water for pharmaceutical preparations

These experiments were performed to determine if the method could really be applied to natural waters and industrial situations where very low concentrations of various cations are often encountered. It should be emphasized that these results should be considered as being only semi-quantit since no multiple samples were taken in the same place nor were the samples checked by another independent analytical method.

The results are shown in Tables 4 and 5 for Zn(II), Cu(II), Ni(II) and Mn(II in the lake water, and Pb(II), Cu(II) and Fe(III) for pharmaceutical water. In the analysis of the lake water, except for manganese(II), the ions became more concentrated as the marina was approached from the center of the channel. The concentrations range from less than 0.5 ng ml^{-1} to nearly 10 ng ml^{-1}, which are reasonable levels for this type of water. The manganese data are different from those for the other three cations. The concentration was unexpectedly high, ranging from almost 300 ng ml^{-1} in the lake channel to about 50 ng ml^{-1} at the marina. Manganese is very abundant in the earth's crust, and the presence of a manganese-containing geological formation along Lightwood Log Creek could explain the high values found. The samples were also analyzed for Hg, Pb, As and Cr, but these metals, if present, were below the limit of detection (about 0.5 μg), though they could probably be determi if 3—10 l of lake water were passed through the column.

TABLE 3

Column extraction recovery study with bisdithiocarbamate on CPG-10 (50 ml min^{-1})

Cation	Cu^{2+}	Ni^{2+}	Co^{2+}
ng ml^{-1} present	25.0	25.0	25.0
ng ml^{-1} found	26.0	26.5	28.0
Mean % recovery	104 ± 2.8	106 ± 1.5	112 ± 1.6

TABLE 4

Lake water samples[a]
(1-l Samples. Concentrations in ng ml^{-1}.)

Element	Sample				
	1	2	3	4	5
Zn	0.5	0.5	2.1	2.0	0.6
Cu	0.5	0.5	1.0	1.0	0.5
Ni	0.5	0.5	6.0	8.4	1.5
Mn	287	151	96	44	59

[a]Sample 1: buoy 13/2. Sample 2: 1/2 mile from buoy 13/2. Sample 3: 1 mile from buoy 13/2. Sample 4: 2 miles from buoy 13/2 at Hartwell Marina. Sample 5: Hartwell State Park Cove.

TABLE 5

Distilled and redistilled water
(1-l Samples. Concentrations in ng ml^{-1}.)

Element	Sample[a]			
	1	2	3	4
Pb	2	2	2	2
Cu	2	2	2	2
Fe	25	<2	8	10

[a]1: Tap water after treatment with cation exchanger before distillation. 2: Output at still. 3: Output of holding tank. 4: Output of plumbing used to transport water to formulation area.

In the analysis of water for pharmaceutical formulations, the only trend is seen in the case of iron(III). Before distillation, the iron(III) concentration was 25 ng ml^{-1}. After distillation the iron content fell below the limit of detection and then rose again as the water stayed in contact with the stainless steel holding tank and pipes. However, the final level was still extremely low, only 10 ng ml^{-1}. The lead(II) and copper(II) contents were at all stations below the limit of detection. Again the detection limits could have been lowered by simply increasing the sample size. In any case, these semiquantitative experiments indicate that the method shows promise for analyses of this type, in which "screening" of many samples for cation contamination rather than precise analysis is important.

This work was supported in part by Research Grant GP-3839X from the National Science Foundation and by Wyeth Laboratories.

REFERENCES

1 D. E. Leyden and G. H. Luttrell, Anal. Chem., 47 (1975) 1612.
2 D. E. Leyden, G. H. Luttrell, W. K. Nonidez and D.B. Werho, Anal. Chem., 48 (1976) 67.
3 K. I. Aspila, C. L. Chakrabarti and U. S. Sastri, Anal. Chem., 45 (1973) 363.

Analytica Chimica Acta, 84 (1976) 109–118

THE EXTRACTION OF MERCURY(II), SILVER(I), COBALT(II) AND CADMIUM(II) BY DIOCTYLARSINIC ACID IN CHLOROFORM

R. J. G. DOMINGUEZ and K. J. IRGOLIC*

Department of Chemistry, Texas A & M University, College Station, Texas 77843 (U.S.A.)

(Received 11th July 1975)

SUMMARY

Dioctylarsinic acid (HDOAA) in chloroform solution has been investigated as a reagent for the extraction of Hg(II), Ag(I), Co(II), and Cd(II). Silver, cobalt and cadmium are not extracted below pH 7. An extraction coefficient of 1.1, constant over the pH range 1—6.5, was observed for Hg(II). With HCl concentrations of 1—8 M the extractability of mercury decreased slowly, reaching $E_a^0 = 0.05$ at 8 M HCl. Silver formed a silver dioctylarsinate precipitate which collected at the interface. The extraction coefficients for Hg(II), Co(II) and Cd(II) increased above pH 7 to values of 20 (pH 9.1), 30 (pH 8.0), and 23 (pH 10), respectively. Reagent- and pH-dependence studies indicated that Co(II) and Cd(II) are extracted as $M(DOAA)_2$ or M(DOAA)Cl through interaction of HDOAA with $M(OH)_2$ or $M(OH)^+$. Mercury was extracted from solutions of pH 1—6.5 as $HgCl_2(HDOAA)_{2.5}$.

Various arsinic acids, R_2AsOOH, and arsonic acids, $RAsO(OH)_2$, with organic groups of low mass have been investigated as precipitants or extractants for various metal ions, and a brief summary of this work has been published [1]. Since the long-chain, water-insoluble dioctylarsinic acid (HDOAA) has become available, the extraction of lanthanide ions with this reagent has been investigated in detail [1, 2]. The study of HDOAA in chloroform solution as an extractant has now been extended to Hg(II), Ag(I), Co(II) and Cd(II).

EXPERIMENTAL

Reagents

The γ-emitters 55-h ^{115}Cd, 5.29-y ^{60}Co, 46.5-d ^{203}Hg and 243-d ^{110}Ag were produced at the Texas A & M University Nuclear Science Center by irradiating 99.9 % pure $CdCl_2 \cdot 2.5H_2O$, $CoCl_2 \cdot 6H_2O$, $HgCl_2$ and $AgNO_3$ in sealed Vycor glass vials, for appropriate periods of time.

HDOAA was prepared as described previously [3]. All other chemicals were of reagent grade.

*To whom correspondence should be addressed.

HDOAA solutions were prepared with ethanol-free chloroform, pre-equilibrated with water. A Hewlett-Packard Single Channel Analyzer, Model 5201-L Scaler, and a well-type Na(Tl)I scintillation crystal were used to determine the γ-activities of Ag(I), Co(II), and Hg(II). The γ-activities of samples of Cd(II) were determined with a Victoreen Multi-Channel Analyzer, Model PIP 400, and a well-type Na(Tl)I scintillation crystal, in order to avoid interferences from ^{115m}In, the γ-active daughter of ^{115}Cd.

The irradiated samples of salt had been pre-weighed to produce aqueous $1.0 \cdot 10^{-4}$ M metal ion solutions for Hg(II), Ag(I) and Cd(II) and $1.0 \cdot 10^{-3}$ M for Co(II) after appropriate dilution. Aliquots (2 ml) of these solutions registered at least 10^4 counts in times ranging from 10 to 600 s. Sodium chloride was used to adjust the ionic strength of the solutions.

Procedures

Equal volumes (5 ml) of the aqueous metal ion solutions and 0.1 M HDOAA solutions in chloroform were shaken in 30-ml plastic centrifuge tubes at room temperature for times ranging from 20 min to 3 h, depending on the particular metal ion studied. After centrifugation, 2-ml aliquots of the aqueous and organic phase were transferred to 1-dram glass vials, which were stoppered and then inserted into the crystal well for counting. The extraction coefficient, E_a^0, was calculated as the ratio of the γ-activities in the organic and aqueous phases at equilibrium.

The aqueous pH was measured with a glass combination electrode before and after equilibration. The pH values of the mercury, cobalt and cadmium solutions were adjusted with hydrochloric acid or sodium hydroxide; the silver solutions were adjusted with nitric acid or sodium hydroxide.

The chloride ion concentration in the organic phase was determined by potentiometric titration with silver nitrate and an Orion silver sulfide electrode. Other experimental procedures and the pertinent calculations have been discussed earlier [1, 8].

RESULTS AND DISCUSSION

Since all the metal ions studied do not behave in the same manner in extractions with HDOAA, each will be discussed separately.

Mercury(II)

The extraction of mercury(II) was studied with aqueous $1.0 \cdot 10^{-4}$ M $HgCl_2$ solutions. The equilibrium in the system $HgCl_2$, 1.0 M NaCl, H_2O, pH = 7—0.1 M HDOAA in $CHCl_3$, was established rapidly. The extraction coefficient remained constant for shaking times of 10—90 min. A shaking time of 20 min was, therefore, employed in all subsequent experiments.

Practically no mercury was extracted from aqueous solutions which

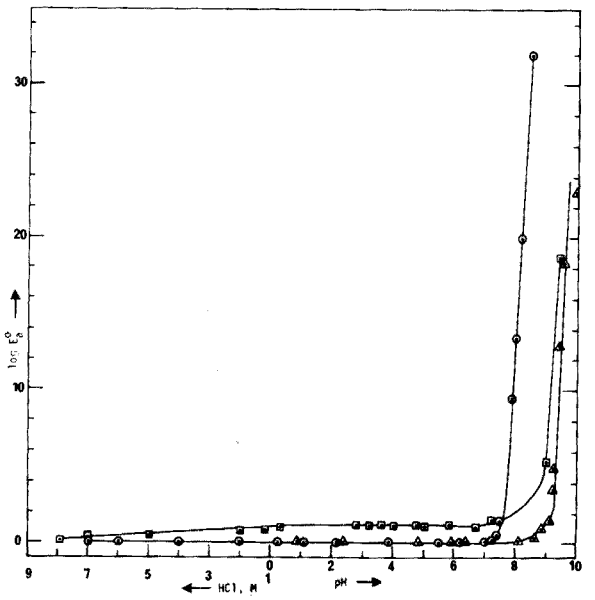

Fig. 1. pH Profile of the extraction of Hg(II), Cd(II) and Co(II) by dioctylarsinic acid in chloroform. △ $1.0 \cdot 10^{-4}$ M Cd(II); extraction time, 1 h. □ $1.0 \cdot 10^{-4}$ M Hg(II); extraction time, 20 min. ○ $1.0 \cdot 10^{-3}$ M Co; extraction time, 3 h. [HCl] + [NaCl] = 1.0 M.

contained 8 M HCl or more. The extraction coefficient, E_a^0, increased slowly from less than 0.05 at 8 M HCl to about 1.1 at 0.1 M HCl, and then remained constant in the pH region 1—6.5 (Fig. 1). Above pH 7 the extraction coefficient increased sharply with increasing pH, reaching at pH 9.1 a value of about 20, which corresponds to 95 % extraction of the mercury.

Two reagent-dependence studies were performed, one with aqueous 1.0 M HCl solutions and the other with solutions that were 1.0 M with respect to NaCl at pH 2.9. Plots of log E_a^0 versus the logarithm of the uncomplexed HDOAA monomer concentrations (Fig. 2) gave straight lines for which least-squares slopes of 2.6 were calculated.

E_a^0 was constant in the pH range 1—6.5 (Fig. 1). Experiments showed that E_a^0 increased when the HCl concentration decreased from 2.88 M to 1.90 M. A least-squares slope [log E_a^0 versus p(HCl)] of 0.26 was obtained; this value is not interpretable on the basis of substitution of $DOAA^-$ for Cl^-.

A loading experiment, intended to complex all the available HDOAA with Hg(II) and thus determine the HDOAA/Hg(II) ratio in the extracted complex, was unsuccessful because of the limited solubility of $HgCl_2$ in water.

The extraction efficiency does not vary over a wide pH range and this suggests that the chloride ions are transferred with the Hg(II) to the chloroform phase. Chloride determinations on the equilibrated organic phases did not give really significant results because of the low concentration of the mercury complex, but the results obtained were consistently larger than

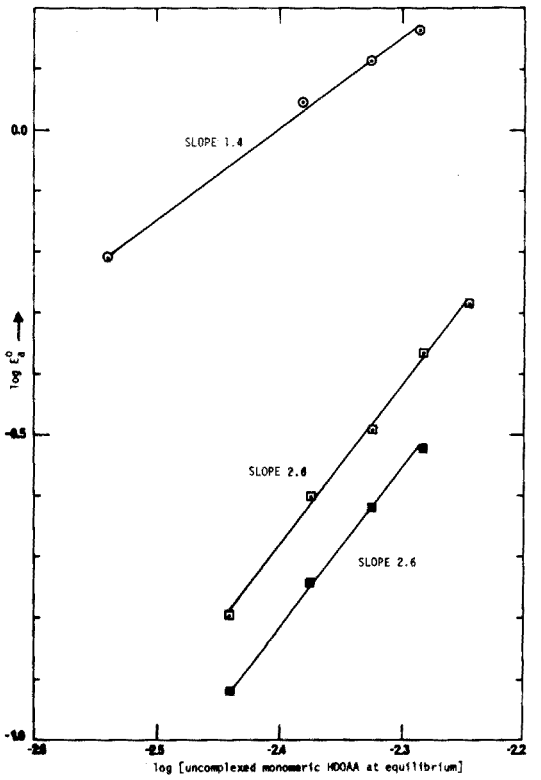

Fig. 2. The reagent-dependence of the extraction coefficient of Hg(II) and Co(II). ○ $1.0 \cdot 10^{-3}$ M Co(II); extraction time, 3 h. □ $1.0 \cdot 10^{-4}$ M Hg(II); pH 2.9; extraction time, 20 min. ■ $1.0 \cdot 10^{-4}$ M Hg(II); 1.0 M HCl; extraction time, 20 min. [HCl] + [NaCl] = 1.0 M. HDOAA, 0.02—0.07 M in $CHCl_3$ (5 ml).

those obtained in the absence of $HgCl_2$. If the chloride ions had been replaced by DOAA anions during the extraction process, a slope of 2.0 should have been found in the pH-dependence study.

The reagent-dependence studies produced lines of slope 2.6, and support the coordination of HDOAA to $HgCl_2$. Since E_a^0 is pH-independent, the HDOAA molecules must coordinate to the mercury atom via their arsenyl oxygen atoms. The stoichiometry of the extraction can be described by:

$$HgCl_{2(a)} + 2.5\ HDOAA_{(o)} \rightleftharpoons (HgCl_2 \cdot 2.5\ HDOAA)_{(o)} \qquad (1)$$

The extraction of Hg(II) as an HDOAA complex of $HgCl_2$, instead of as mercury(II) dioctylarsinate, $Hg(DOAA)_2$, is not unexpected, since the mercury—chlorine bonds are largely covalent and therefore compatible with the chloroform phase. The complexation of $HgCl_2$ with HDOAA increases the solubility of the salt in chloroform. Solutions of $HgCl_2$ of various hydrogen ion concentrations were also equilibrated with chloroform in

the absence of HDOAA. The amounts of $HgCl_2$ transferred into pure chloroform were negligible.

Mercury(II) prefers tetrahedral coordination in its complexes, although pentacoordinated and hexacoordinated octahedral compounds have also been reported [4]. The tentative structure given below for the extracted complex can be formulated by considering, in addition to the preferred tetrahedral coordination of mercury(II), the tendency of dioctylarsinic acid to form hydrogen-bonded dimers [5] in the solid, in the melt, and in organic solvents. The incorporation of a fifth HDOAA molecule into the complex probably increases the non-polar nature of the complex and enhances its extractability.

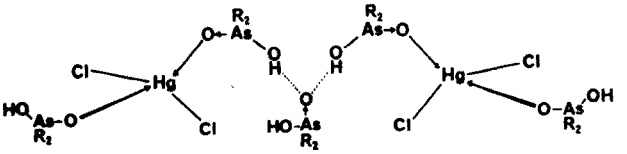

Since the extraction coefficient is not zero for 3—8 M HCl solutions, which in the absence of $HgCl_2$ convert all the HDOAA in the organic phase to the adduct HDOAA · HCl [6], but only decreases gradually with increasing acid concentration, $HgCl_2$ must be capable of replacing HCl in the HDOAA · HCl adduct. The extraction of an appreciable amount of $HgCl_2$ from a very dilute $1.0 \cdot 10^{-4}$ M solution in the presence of 100,000-fold excess of hydrochloric acid indicates that the mercury adduct is much more stable than the HCl adduct. Concentration equilibrium quotients are available [6] for the formation of the $(HDOAA \cdot HCl)_2$ adduct. These data together with the results obtained for the mercury system, were used to calculate concentration equilibrium quotients for the mercury complex extracted from $\geqslant$3 M HCl solutions. By combining the equations

$$K_{HCl} = \frac{[(HDOAA \cdot HCl)_2]_{(o)}}{[(HDOAA)_2]_{(o)}[HCl]^2_{(a)}} \text{ and } K_{Hg} = \frac{[HgCl_2 \cdot 2.5\ HDOAA]_{(o)}}{[HgCl_2]_{(a)}[HDOAA]^{2.5}_{(o)}}$$

and employing the dimerization constant [6] of HDOAA, $K_D = [(HDOAA_2]/[HDOAA]^2$, the concentration equilibrium quotient of the extracted mercury complex can be derived. Average values of 0.84 and $1.0 \cdot 10^3$ were used for K_{HCl} and K_D, respectively. The concentration equilibrium quotient for the mercury complex was of the order of 10^{12}. The pH-dependence slope of 0.26 found in this region is probably caused by the competition between $HgCl_2$ and HCl for the reagent.

Reagent- and pH-dependence studies were not carried out above pH 7, because a yellow—orange precipitate, reported to consist of a mixture of mercury(II) chloride oxides of the type $HgCl_2 \cdot nHgO$ (n = 3, 4) [7], was formed. These precipitates made it impossible to determine the extraction coefficients accurately because it was difficult to withdraw representative

aliquots from the inhomogeneous aqueous phase. However, it seems probable that HDOAA reacts with the HgO, forming $Hg(DOAA)_2$, which is extracted more efficiently into the chloroform phase than $HgCl_2(HDOAA)_{2.5}$

Silver(I)

When $1.0 \cdot 10^{-4}$ M silver nitrate solutions, adjusted to 0.1 M—$1 \cdot 10^{-8}$ M in HNO_3, were shaken with 0.1 M HDOAA in chloroform, almost no activity was found in the chloroform phase. On careful observation of the equilibrated systems, a precipitate, probably silver(I) dioctylarsinate, $(C_8H_{17})_2As(O)OAg$, was observed at the interface. Insufficient amounts of this purplish-brown solid were isolated for its analysis, but the material was soluble in 4 M HNO_3, although it did not dissolve in 10^{-3}, 10^{-2} or 10^{-1} M HNO_3, or in chloroform. Since salts of metal ions with two DOAA anions, e.g. those formed by cadmium(II) and cobalt(II), are soluble in chloroform, it seems that the dioctylarsinate group associated with the silver ion does not shield the polar parts of this salt sufficiently to make it soluble in the rather non-polar chloroform phase.

Cobalt(II)

The time-dependence study performed with $1.0 \cdot 10^{-3}$ M $CoCl_2$ solutions at pH 7.5 showed that shaking for 3 h is necessary for equilibrium to be reached. The extractability of cobalt(II) by a chloroform solution of HDOAA was checked with HCl solutions in the concentration range 1—9 M and in the range pH 0—8. The pH profile (Fig. 1) shows that cobalt(II) is not extracted below pH 7. Above pH 7 the extraction coefficient, E_a^0, increases sharply, from a value of 0.1 at pH 7, to 32 at pH 8.5. At about pH 8.6, a $Co(OH)_2$ precipitate appeared in the aqueous phase; after reaction with HDOAA, this was easily extracted into the chloroform layer. The presence of the precipitate in the aqueous phase made it impossible to determine the extraction coefficient accurately.

A pH-dependence study was carried out in the range pH 7.1—7.7 with aqueous cobalt(II) solutions, which were 1 M in NaCl. Plots of the logarithms of E_a^0 versus the equilibrium pH produced straight lines with a slope of 1.95. A reagent-dependence study at pH 8.2 and 1.0 M NaCl gave a straight line with a least-squares slope of 1.4 (Fig. 2). The pH values, which should remain constant in all the reagent-dependence experiments, varied, however, from 8.13 8.23 although all the aqueous phases were at pH 9 before equilibration. This variation makes the pH-dependence results unreliable.

It is evident from the pH-profile that HDOAA does not extract species, such as $H_2[CoCl_4]$, which have been claimed to exist in aqueous media at high HCl concentrations. Since HDOAA reacts with other complex acids containing platinum, rhenium, tungsten, molybdenum, iron, niobium and tantalum [8] as central atoms, it is concluded that either $H_2[CoCl_4]$ is not

present in these solutions or that HCl is preferentially extracted, converting all HDOAA to HDOAA · HCl, which might not be capable of exchanging chloride ions for tetrachlorocobaltate(II) ions. It has been shown that HDOAA will be converted quantitatively to HDOAA · HCl upon equilibration with hydrochloric acid solutions varying in concentration from 3 M to 7 M. At higher hydrochloric acid concentrations, at which considerable amounts of $H_2[CoCl_4]$ could be present, HDOAA · HCl reacts with additional hydrogen chloride molecules to form species of the type $R_2As(OH)_mCl_n$ ($m + n = 3$) [6]. These dioctylchloro(hydroxy)arsanes are not capable of serving as extracting agents.

In the pH range 0—7, in which the cobalt ion exists as an aquated cation, there is again no extraction. Cobalt(II) can only be extracted efficiently from aqueous solutions above pH 7.8.

When the non-integral slopes obtained from the pH- and reagent-dependence studies, which were carried out above pH 7.2, are employed to elucidate the nature of the complex extracted, the cobalt species possibly present in solution, or as a precipitate above pH 7, must be considered carefully. The large amount of work on the aqueous chemistry of cobalt(II) [9] shows that the major species of cobalt(II) in the pH range 7—9 are $Co(OH)^+$ and $Co(OH)_2$.

Pietsch and Pichler [10] observed that cobalt(II) was not extracted, from solutions of pH below 7, by chloroform solutions of dibutylarsinic acid; 30 % of the cobalt was extracted at pH 8. At pH 8, HDOAA extracted 90 % of the metal ion; the extraction efficiency of HDOAA is greater than that of dibutylarsinic acid because of the longer alkyl chain length. In the pH region 7—8, the aquated $[Co(H_2O)_n]^{2+}$ cannot react with HDOAA to form, for example, $Co(DOAA)_2$. If such an interaction occurred at pH 8, where $1.0 \cdot 10^{-3}$ M solutions of cobalt(II) gave almost quantitative extraction into the organic phase, $2.0 \cdot 10^{-3}$ moles of hydrogen ions would migrate into the aqueous phase to produce an aqueous equilibrium pH of about 3; the experimental value found was pH 7.

It is possible that $DOAA^-$ anions react with $[Co(H_2O)_n]^{2+}$ to form the $Co(DOAA)_2$, which should be soluble in chloroform. Aqueous solutions of initial pH 4—9.5 without cobalt(II) were equilibrated with chloroform solutions of HDOAA (0.1 M) in order to determine whether or not $DOAA^-$ anions are formed. An aqueous solution of initial pH 9.5 possessed a pH of about 6 after this equilibration. Such a pH drop could not produce more than ca. $5 \cdot 10^{-5}$ moles of $DOAA^-$ anions per liter. Since, under similar conditions, almost all the cobalt(II) is extracted from aqueous $1.0 \cdot 10^{-3}$ M cobalt(II) solutions, $DOAA^-$ anions cannot be responsible for more than 5 % of the extraction.

Since the interaction of $[Co(H_2O)_n]^{2+}$ with either HDOAA or $DOAA^-$ anions can be ruled out, the $Co(OH)^+$ ion and/or the $Co(OH)_2$ precipitate must be the reactive species. The cobalt hydroxide precipitate in representative solutions employed in this study dissolved to rather a large extent.

Formation constants for the $Co(OH)^+$ ($K = 2.51 \cdot 10^4$) and $Co(OH)_2$

($K = 6.29 \cdot 10^4$) species have been reported [9]. With these constants the concentration of $Co(OH)^+$ and the amount of cobalt present as $Co(OH)_2$ can be calculated as a function of pH and metal ion concentration.

A cobalt(II) solution initially containing $1.0 \cdot 10^{-3}$ M Co(II) adjusted to an initial aqueous pH of 8.6 gave an extraction coefficient of 0.37, corresponding to a cobalt concentration of $2.7 \cdot 10^{-4}$ M in the organic phase. The solution before equilibrium was calculated to contain $9 \cdot 10^{-5}$ moles of $Co(OH)^+$ and $2.2 \cdot 10^{-5}$ moles of $Co(OH)_2$ per liter. The total quantity of cobalt-hydroxy compounds is, therefore, $11.2 \cdot 10^{-5}$ moles per liter. If these hydroxy species are extracted, the calculated cobalt concentration in the organic phase ($1.1 \cdot 10^{-4}$ M) agrees reasonably with the experimental value ($2.7 \cdot 10^{-4}$ M) considering the rather large uncertainties in the formation constants. It therefore appears that the extraction of cobalt(II) proceeds as follows:

$$Co(OH)_{2(a)} + 2HDOAA_{(o)} \rightleftharpoons Co(DOAA)_{2(o)} + 2H_2O_{(a)} \quad (2)$$

$$Co(OH)^+_{(a)} + HDOAA_{(o)} + DOAA^-_{(o)} \rightleftharpoons Co(DOAA)_{2(o)} + H_2O_{(a)} \quad (3)$$

Approximate calculations given earlier indicate that $DOAA^-$ anions might be present in a concentration about equal to the $Co(OH)^+$ concentration.

Another possibility is the extraction of Co(DOAA)Cl formed from $Co(OH)^+$, HDOAA and chloride ion:

$$Co(OH)^+ + HDOAA_{(o)} + Cl^-_{(a)} \rightleftharpoons Co(DOAA)Cl_{(o)} + H_2O_{(a)} \quad (4)$$

The extraction processes described by eqns. (2)—(4) do not generate hydrogen ions and do not consume hydroxide ions except those bonded to the cobalt atoms. Therefore, the extraction coefficient should be pH-independent as far as the interaction between HDOAA, $DOAA^-$ anions and cobalt is concerned. The concentration of the cobalt-hydroxy species, however, is pH-dependent thus influencing E^0_a. Experimentally the pH-dependence studies produced straight lines with slopes varying between 1.9 and 1.7. This dependence can thus be viewed as resulting from the formation of more of the extractable hydroxy species as the aqueous phase pH is increased. It does not indicate a transfer of protons into the aqueous phase during extraction. The reagent-dependence slope (Fig. 2) of 1.4 can now also be explained as resulting possibly from the extraction of a mixture of the $Co(DOAA)_2$ and Co(DOAA)Cl compounds. These results are, however, not conclusive since the experiments had to be performed in unbuffered systems, in which the equilibrium pH values varied by 0.1 units in a region where E^0_a was strongly dependent on pH.

Cadmium(II)

Upon neutron irradiation of cadmium(II) chloride, containing the natural distribution of cadmium isotopes, the two radioactive isotopes ^{115}Cd and ^{115m}Cd are produced predominantly; ^{115}Cd decays to ^{115m}In which emits

0.335-MeV γ-radiation. The γ-ray peaks of ^{115}Cd and ^{115m}Cd appear at 0.52 and 0.485 MeV, respectively. The extremely low concentration of indium would not affect the chemical parameters of the cadmium extraction system, even if all the indium were extracted. Only the Cd γ-activities were determined by setting the lower level discriminator on the analyzer appropriately.

The extraction coefficient in the system $1.0 \cdot 10^{-4}$ M $CdCl_2$, H_2O, pH 8.8, 1.0 M NaCl—0.1 M HDOAA in $CHCl_3$, was time-independent for shaking times of 50—95 min. In all subsequent experiments a shaking time of 60 min was employed.

As the pH profile (Fig. 1) shows, cadmium(II) is not extracted appreciably from solutions of pH 1—8. Between pH 8 and 9 the extraction coefficient increases slowly. Above pH 9, extraction increased very sharply. At about pH 10, a viscous white foam of the surfactant sodium dioctylarsinate was formed on shaking.

A pH-dependence study was carried out in the range pH 7—9.2. The plot of log E_a^0 versus equilibrium pH is a straight line with a least-squares slope of 0.5. Such a slope cannot be interpreted as any reasonable interaction of HDOAA with cadmium(II) ion to yield a cadmium dioctylarsinate with concomitant transfer of hydrogen ions into the aqueous phase.

Several attempts were made to perform a reagent-dependence study. The only pH region available for these experiments was pH 8—9.3, because the extraction coefficient was too small in the more acidic region. All the buffers available to keep the pH constant in this region such as phosphate, sodium borate/boric acid and tris(hydroxymethyl)amine/HCl buffer, form insoluble precipitates with cadmium(II). With unbuffered solutions the equilibrium pH values varied considerably and randomly, making the reagent-dependence study useless.

Before attempting to explain the extraction process for the cadmium(II) system, some observations should be mentioned. In the presence of 1 M NaCl, cadmium hydroxide is a fine silky precipitate; without NaCl, it is flocculent. The precipitate from $1.0 \cdot 10^{-4}$ M cadmium(II) solution at pH 10.5 in the presence of 1.0 M NaCl remains suspended in solution; at the same pH and cadmium concentration, but without NaCl, the precipitate settles very quickly.

A hydroxide precipitate, present before extraction at above pH 8, disappeared once these solutions were equilibrated with HDOAA in chloroform. Thus the extraction of cadmium(II) appears to be similar to that of cobalt(II). The Cd^{2+} ion, which is the predominant species in the pH range 0—8, does not extract. Consequently, the most likely cadmium species involved in the extraction are $Cd(OH)^+$ and $Cd(OH)_2$.

These observations can be put on a more quantitative basis, as in the cobalt(II) case. The typical difference between "before" and "after" equilibration pH values for cadmium(II) is about 1 pH unit, the same as is observed when chloroform is equilibrated with water or when HDOAA in chloroform is equilibrated with aqueous cobalt(II) solutions. Calculations of

the total quantity of cadmium hydroxide species can be made from the $Cd(OH)^+$ ($K = 2 \cdot 10^4$) and $Cd(OH)_2$ ($K = 2.5 \cdot 10^3$) formation constants available [11]. For an initial aqueous pH of 10 (equilibrium pH 8.98), the total quantity of cadmium hydroxide compounds, at a total cadmium content of $1.0 \cdot 10^{-4}$ mol l^{-1}, is $7.1 \cdot 10^{-5}$ mol l^{-1}. If all these hydroxy species were extracted, an E_a^0 value of 2 should be observed. A value for E_a^0 of approximately unity was obtained experimentally. This corresponds to a cadmium(II) concentration of $5.1 \cdot 10^{-5}$ M in the organic phase at equilibrium This result is strong evidence that an acid–base interaction between HDOAA, cadmium hydroxide, $DOAA^-$ and $Cd(OH)^+$ is the most probable process by which the extraction of cadmium by HDOAA proceeds.

The pH-dependence slope of 0.5 cannot be interpreted as being related to the transfer of protons into the aqueous phase as a result of the extraction of cadmium(II). It simply reflects the increase in the production of cadmium hydroxide species in the pre-equilibrium solutions concomitant with increase in the pH of these solutions. It is therefore likely that the extracted species have the formulae Cd(DOAA)Cl and $Cd(DOAA)_2$.

Financial support by the Robert A. Welch Foundation of Houston, Texas, is gratefully acknowledged.

REFERENCES

1 K.J. Irgolic and A.M. Olivares, Mikrochim. Acta, (1974) 369 and references cited therein.
2 M. I. El Seoud and K. J. Irgolic, Anal. Chim. Acta, 75 (1975) 377.
3 K. J. Irgolic, R. A. Zingaro and M. R. Smith, J. Organometal. Chem., 6 (1966) 17.
4 F. A. Cotton and G. Wilkinson, Advanced Inorganic Chemistry, 2nd edn., Wiley-Interscience, New York 1966, p. 611.
5 M. R. Smith, K. J. Irgolic, E. A. Meyers and R. A. Zingaro, Thermochim. Acta, (1970) 51.
6 A. M. Olivares and K. J. Irgolic, J. Inorg. Nucl. Chem., 34 (1972) 1399.
7 J. Lamme, Bull. Soc. Chim. France, (1948) 1019.
8 A. M. Olivares, Ph.D. Dissertation, Texas A & M University, 1972.
9 L. G. Sillen and A. E. Martell, Stability Constants of Metal–Ion Complexes, Chemical Society, London, 1964, p. 54.
10 R. Pietsch and E. Pichler, Mikrochim. Acta, (1961) 860.
11 L. G. Sillen and A. E. Martell, Stability Constants of Metal–Ion Complexes, Chemical Society, London, 1964, p. 63.

Analytical Chimica Acta, 84 (1976) 119—126

THE EXTRACTION OF NIOBIUM (V) AND TANTALUM (V) BY OCTYLARSINIC ACID IN CHLOROFORM

K. J. IRGOLIC* and R. J. G. DOMINGUEZ

Department of Chemistry, Texas A. and M. University, College Station, Texas 77843 (U.S.A.)

(Received 11th July 1975)

SUMMARY

Dioctylarsinic acid (HDOAA) in chloroform solution extracts Nb(V) and Ta(V) efficiently from solutions containing oxalate and oxalic acid at hydrochloric acid concentrations greater than 1*M*. The extraction coefficients are 92.5 at 7*M* hydrochloric acid and 251 at 6*M* hydrochloric acid for niobium and tantalum, respectively. These metals can be extracted even more efficiently from sulfuric acid solutions. The results of the reagent- and pH-dependence studies suggested that a trimeric, monobasic oxoacid of niobium, associated with ten HDOAA molecules, is extracted. Tantalum appears to be present in the organic phase as $(H_2DOAA)^+$ $[Ta(C_2O_4)_3 (HDOAA_n]$ (n=1 or 2).

Dioctylarsinic acid (HDOAA) extracts lanthanide [1, 2] and transition [3, 4] metal ions into chloroform, and preliminary studies [5] have shown that HDOAA is a good extractant for transition metals capable of forming oxo-acids. As representative examples of such metals, niobium (V) and tantalum (V) have now been studied.

EXPERIMENTAL

Reagents

The γ- active isotope 35-d $^{95}Nb(V)$ in 0.5 M oxalic acid was obtained from Nuclear Environmental Engineering Inc. The γ- active isotope 115-d ^{182}Ta was produced by irradiating tantalum oxalate at the Texas A&M Nuclear Science Center. Dioctylarsinic acid was prepared as described previously [6]. Niobium oxalate (Kawecki-Berylco Industries Inc; assay 21.4 % Nb) was found to contain 48.4 % oxalate (permanganate titration); its approximate composition is, therefore, $NbO(C_2O_4)OH \cdot K_2C_2O_2$. It was used as purchased. $TaO(C_2O_4)OH$ (99.8 %) was obtained from Research Organic/

* To whom all correspondence should be addressed.

Inorganic Chemical Corp. All the other substances employed were of reagent grade. A niobium (V) stock solution ($2.5 \cdot 10^{-3}$ M) was prepared by dissolving 0.1086 g of the niobium oxalate in the required volume of 0.10 M oxalic acid to make 100 ml of solution — 1:25 dilution with water gave $1.0 \cdot 10^{-4}$ M Nb(V) $4.0 \cdot 10^{-3}$ M oxalic acid solutions. Tantalum(V) stock solutions were prepared similarly with 0.5 M oxalic acid; dilution gave solutions containing $1.0 \cdot 10^{-4}$ M Ta(V) and $2.0 \cdot 10^{-2}$M oxalic acid. These diluted aqueous solutions were spiked with the radioactive isotope to register at least 10^4 counts in 10 s per 2 - ml aliquot. Sodium chloride was employed to adjust the ionic strength, and hydrochloric acid, sulfuric acid or sodium hydroxide was used to adjust the pH.

Procedure

Equal volumes (5 ml) of the aqueous metal ion solutions and 0.1 M HDOAA in $CHCl_3$ solution were shaken for 3.5 h (Nb) or 1 and 36 h (Ta) in 30-ml plastic or glass centrifuge tubes. To prevent evaporation of the chloroform in the 36-h experiments, the glass centrifuge tubes were sealed with Teflon-sleeved stoppers. Details of the procedure and calculations have been described earlier [1, 5]. Most of the extraction coefficients required for the pH- and reagent-dependence studies are averages of several values which did not differ by more than 5 %.

RESULTS AND DISCUSSION

Niobium (V)

The study of the extraction of niobium (V) is complicated by the insolubil or instability of most niobium compounds under conditions which allow equilibration of their solutions with chloroform solutions of HDOAA. Alkali metal niobates of the general formula $MNbO_3$ (M = alkali metal) are soluble in neutral and basic solutions, but precipitate as hydrated Nb_2O_5 (commonly known as "niobic acid") on acidification. Niobium pentachloride hydrolyzes in aqueous medium and is stable only in 10—12 M HCl.

Niobium oxides dissolve in solutions containing oxalic acid and alkali meta oxalates. The 1.0×10^{-4} M niobium solutions for all these experiments, prep as described above, remained homogeneous in the presence of 0.01—12 M HCl, but a precipitate began to form at ca. pH 3. Niobium oxalate—HCl systems were therefore amenable to extraction studies over a wide range of acidity, and sulfuric acid media could also be used. The equilibrium in the system niobium oxalate, aqueous HCl—0.1 M HDOAA in chloroform was reached rather slowly. Shaking for at least 3 h was necessary to obtain time-independent extraction coefficients, and 3.5 h was used in all extraction experiments.

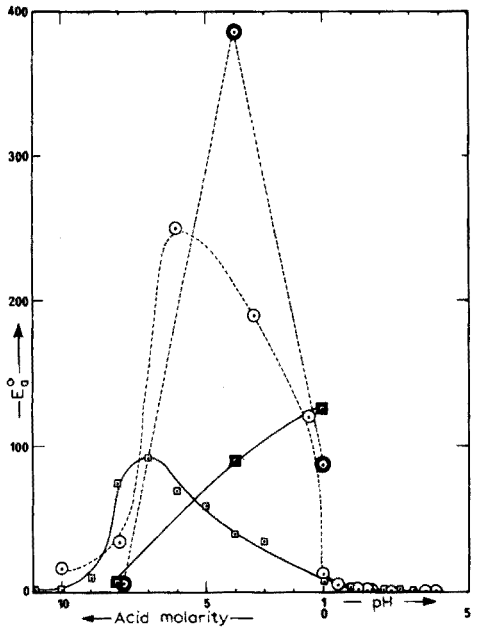

Fig. 1: pH profile of the extraction of $1 \cdot 10^{-4}$ M niobium(V) and $1 \cdot 10^{-4}$ M tantalum(V) by dioctylarsinic acid in $CHCl_3$ (5 ml, 0.1 M). Phase ratio, 1. [HCl]+[NaCl]=1.0 M in the pH region. Tantalum in HCl (⊙) and H_2SO_4 (●); extraction times are 1 h for the pH region, and 1 h for the acid region. Niobium in HCl (⊡) and H_2SO_4 (■); extraction time, 3.5 h.

The pH profile (Fig. 1) obtained with "niobium oxalate" solutions, in the pH range 0—3 and in 1—12 M HCl, shows that appreciable extraction occurs over almost the entire range. The extraction coefficient increased from 0.5 at pH 2.6 to ca. 6.5 at pH 0. Above pH 2.6 a niobium-containing precipitate collected at the interface on shaking, and accurate determinations of extraction coefficients were impossible. The extraction efficiency increased markedly as the initial HCl concentration was changed from 1 M to 7 M. At the latter concentration the extraction coefficient was 92.5, corresponding to almost 99 % extraction of niobium in one equilibration. Above 7 M HCl the extraction efficiency decreased, and niobium was not extracted from 12 M solutions.

The extraction of niobium(V) as a function of sulfuric acid concentration was also studied. Niobium was extracted even more efficiently from H_2SO_4 than from HCl solutions (Fig. 1); $E_a^\circ = 125$ was achieved at 1 M H_2SO_4 whereas the maximum value attained in HCl solutions was 92.5.

A pH-dependence study in the pH range 0.3 — 2.6 with solutions 1.0 M in chloride ion showed that the extraction coefficient increased with decreasing

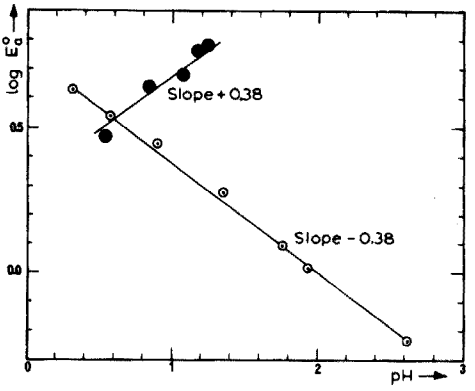

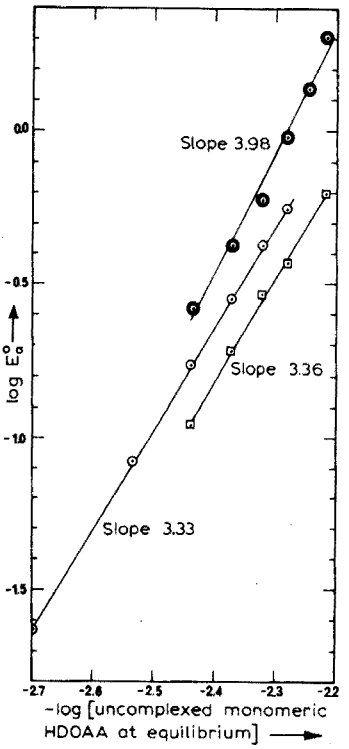

Fig. 2: pH-dependence of the extraction of $1 \cdot 10^{-4}$ M niobium(V) with HDOOA in $CHCl_3$ (5ml,0.1 M). Phase ratio, 1. Extraction time, 3.5 h. ⊙ HCl solutions [HCl] + [NaCl] = 1.0 M ⊙ $H_2C_2O_4$. solutions.

Fig. 3: Reagent-dependence of the extraction of $1 \cdot 10^{-4}$ M niobium(V) with 0.01—0.08 M. HDOAA $CHCl_3$ (5 ml). Phase ratio, 1. Extraction time 3.5 h. ⊙ pH 7.0, $[Cl^-] = 0$, $H_2C_2O_4$ media. ▫ pH 1.70, [HCl] + [NaCl] = 1.0 M. ⊙ pH 2.40, [HCl] + [NaCl] = 1.0 M.

equilibrium pH (Fig. 2). The slope of the straight line obtained by plotting log E_a^o v. the equilibrium pH was −0.38. A similar experiment in the pH range 0.5 — 1.2 in the absence of chloride ion, with solutions whose pH had been adjusted with oxalic acid, gave a straight line of slope +0.38 (Fig. 2).

The reagent-dependence studies produced straight lines of slopes 3.33, 3.36, and 3.98, for different conditions (Fig. 3). The extraction coefficient is also influenced by the chloride ion concentration. A chloride-dependence study was carried out for 0—1.0 M chloride concentrations at pH 1.12. The value of E_a^o increased markedly with decreasing chloride ion concentration, from a value of 0.6 at 1.0 M chloride to 11 in the chloride-free solutions. No niobium was found in the organic phase when extraction with chloroform alone was attempted.

Attempts to explain the results of the above studies are seriously impaired by the almost total lack of knowledge of the species present in solutions

containing niobium(V), oxalate ions, oxalic acid, HCl, and chloride ions. The results of the pH-dependence study with solutions containing 1 M chloride ion suggest the extraction of an acidic niobium species. With increasing acidity, "niobic acid" would be produced and this would enhance the extraction, as observed. The slope of -0.38 of the pH-dependence plot (Fig. 2) indicates that one acidic hydrogen atom interacts with HDOAA per three niobium atoms. Polymeric niobium species in oxalic acid exist, although their composition is uncertain [7, 8]. One study [8] reports the existence of approximate trimers in "niobium oxalate" solutions made from dried Nb_2O_5. Freshly precipitated Nb_2O_5 is highly hydrated and mononuclear species predominate [8] in such oxalic acid solutions. The supplier of "niobium oxalate" would not detail the preparative procedure, but stated that freshly precipitated, hydrated Nb_2O_5 was not used. The presence of a trimer in the solutions used for the extraction experiments therefore seems possible. The dependence, to the power of 3.3, of the extraction coefficient on the reagent concentration at aqueous equilibrium pH values of 0.70 and 1.70 indicates the association of ten HDOAA molecules with each trimer. The stoichiometry of the extraction process can be represented by:

$$(\text{Nb trimer})^{-}H^{+}_{(a)} + 10\ \text{HDOAA}_{(o)} \rightleftarrows \{[\text{HDOAA}]_9\text{Nb trimer}]^{-}\,H_2\,\text{DOAA}^{+}\}_{(o)}$$

The actual structures of the niobium polymers present, presumably, in solution are not known, but the formula suggested for the trimeric "niobic

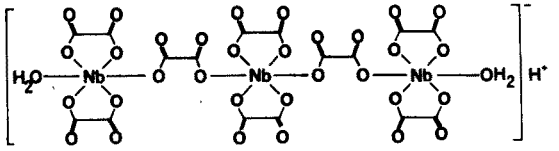

acid" is monobasic, and should be capable of forming adducts with HDOAA similar to those observed for mineral acids [9]. The ion pair thus generated could then be extracted into the chloroform phase as an overall neutral species. The solubility of the extracted species in the organic medium is certainly enhanced by the coordination of an additional nine HDOAA molecules to each niobium trimer. Since the structure and stoichiometric composition of the proposed trimer are uncertain, it is difficult to discern how the HDOAA molecules interact with the niobium complex. An attempt to analyze the organic phase of representative extractions for oxalate content was unsuccessful because of the low concentrations of oxalate, although oxalate was detected in the organic phase. The presence in the extracted species of other ligands such as OH^{-} and O^{2-} in place of some of the oxalate groups can, therefore, not be excluded.

The pH profile and the pH-dependence study both show that the extraction coefficient increases with increasing aqueous acidity. One of the ten HDOAA molecules may serve as the acceptor of a proton from the "niobic acid", forming the $[R_2\,As(OH)_2\,]^{+}$ cation. The remaining nine HDOAA molecules might

then replace the terminal water molecules, expand the coordination sphere of niobium through interaction of the arsenyl oxygen atom with the central metal atom, replace one or more carboxylate group by HDOAA-arsenyl groups, but retain the oxalate molecules by hydrogen bonding with the hydroxyl group of HDOAA and the oxalate ion, and/or hydrogen bond to the oxalate groups without direct interaction with the niobium atom.

Niobium(V) appears to prefer a coordination number of 6, though 7 and 8 are also known [10]. These complexes possess octahedral geometry, preserved in the postulated structure for the trimeric "niobic acid". The coordination sphere of niobium in the extracted complex may therefore be expanded beyond six ligands by coordination of the arsenyl group of HDOAA. Another reagent-dependence study carried out at pH 2.4 produced a slope of almost 4. The number of HDOAA molecules coordinated to niobium may change with pH, but attempts to explain this result cannot be made until the nature of the niobium complexes in aqueous solutions are better understood.

A slope of +0.38 was obtained from a pH-dependence study in oxalic acid solutions of niobium(V) in the absence of chloride ions. The transfer of one proton to the aqueous phase for every three niobium ions extracted appears unlikely. The oxalic acid concentration had to be varied from 1 M to less than 0.1 M in order to prepare solutions in the pH range 0.05—1.3. Since oxalate ions are almost certainly involved in the formation of the extracted species, the observed change in E_a^o values is probably not due to pH alone. In the chloride dependence study, the extraction coefficient increased considerably with decreasing chloride ion concentration; the reason for this change is not known at present. A detailed explanation will not be possible until the chemistry of the aqueous niobium(V)/oxalic acid/oxalate system has been elucidated to a much greater extent.

Tantalum(V)

The extraction of tantalum(V) by chloroform solutions of HDOAA was studied with aqueous $1.0 \cdot 10^{-4}$ M solutions prepared from tantalum(V) oxalate. The equilibrium in the aqueous Ta(V), 1.0 M Cl^-, pH 1.63—0.1 M HDOAA in $CHCl_3$ system was established very slowly. The extraction coefficient increased rapidly during the first hour of extraction and then continued to increase gradually for 96 h.

The extraction coefficient, E_a^o is pH-dependent (Fig. 1). Practically no tantalum was extracted above pH 2.3. E_a^o increased rather abruptly as the aqueous pH was lowered, and increased even further in the region 1—6 M HCl, reaching a maximum E_a^o value of 251 at 6 M HCl. Above 6 M HCl, the extraction efficiency decreased, because under these conditions HDOAA begins to form [9] compounds of the type $R_2As(OH)_m Cl_n$ (m = 1,0, n = 2,3) which do not coordinate to the metal ion. In order to elucidate the extraction stoichiometry prevalent at various shaking times, pH and reagent-dependence studies with a shaking time of 1 h, and another with a shaking

time of 36 h were performed. Plots of log E_a^o vs. the aqueous equilibrium pH (Fig. 4) gave straight lines for which least-squares slopes of −0.97 and −1.09 were calculated, respectively. Two reagent-dependence studies were also carried out with a shaking time of 1 h at pH = 0.8 and a shaking time of 36 h at pH 1.6 (Fig. 5). In all of these studies, the solutions contained 1 M chloride ions. By plotting log E_a^o vs. the logarithm of the uncomplexed HDOAA monomer concentrations, straight lines with least-squares slopes of 3.1 and 2.1, respectively, were obtained. A chloride-dependence study was performed at pH 1.9 with different chloride ion concentrations from 0 to 1.0 M. The extraction coefficient rose drastically, from a value of 0.24 at 1.0 M chloride, to 20 in the absence of chloride ion.

The pH-dependence studies with shaking times of 1 h and 36 h were identical within the limits of experimental error. The slopes of about −1 indicate that one proton is co-extracted with each tantalum(V) ion. It has been suggested that tantalum(V) oxalate complexes with an oxalate: Ta ratio of 3:1 exist in solutions prepared from freshly precipitated Ta_2O_5 in aqueous oxalic acid [11]. Accordingly, the species $HTa(C_2O_4)_3$ may exist in acidic solution, increasing in concentration with increasing acidity. Such a species would account reasonably for the results of the pH-dependence studies.

The integral values for all slopes of the pH- and reagent-dependence studies support the idea that a discrete, mononuclear species of tantalum is extracted. Because of the low concentration of oxalate in the organic phase after extraction (since tantalum was present at a concentration of only about 10^{-5} M) oxalate could not be determined, although it was detected.

Tantalum(V) forms complexes with coordination numbers of 6, 7 and 8 [10]. Thus, the other HDOAA molecules involved in the extraction, as shown by the reagent-dependence studies, could be accommodated within the tantalum coordination sphere by presuming a direct interaction of the HDOAA—arsenyl group with tantalum. The extracted species can thus be formulated as the ion

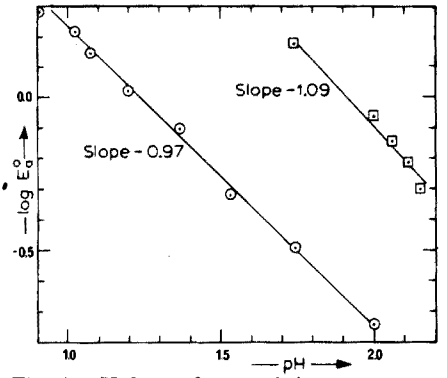

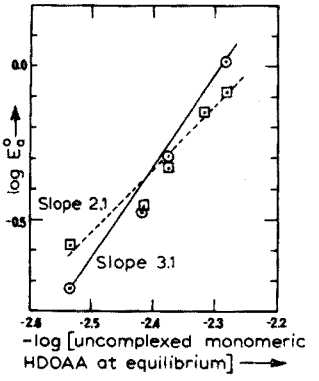

Fig. 4: pH-dependence of the extraction of $1 \cdot 10^{-4}$ M tantalum(V) with 0.1M HDOAA in $CHCl_3$. Phase ratio, 1. [HCl]+[NaCl]=1.0M. Extraction times, 1h (⊙) and 36 (⊡).

Fig. 5: Reagent-dependence of the extraction of 1.10^{-4}M tantalum(V) with 0.02-0.06M HDOAA in $CHCl_3$. [HCl]+[NaCl]=1.0M. ⊡ pH, 1.6; time, 36h. ⊙ pH 0.8; time 1h.

pair $[H_2DOAA]^+[Ta(C_2O_4)_3(HDOAA)_n]^-$ (n=2 for 1 h extraction and n=1 for 36 h extraction). As for niobium(V), the above formula does not imply that one or more of the oxalate groups might not be replaced of O^{2-} or OH^-. Alternatively, the neutral HDOAA molecules could be involved in hydrogen bonding to the oxalate groups coordinated to tantalum.

The extracted species in the 1-h extraction system has more HDOAA molecules associated with tantalum than the species in the 36-h system. The formation of the $(H_2\ DOAA)^+[Ta(HDOAA)_2(C_2O_4)_3]$ species may be kinetically favored over the $(H_2DOAA)^+[Ta(HDOAA)\ (C_2O_4)_3]$ compound. Upon further equilibration, the 2:1 species replaces the 3:1 species in the 36-h system, possibly because of its higher thermodynamic stability.

The dependence of E_a^o on sulfuric acid concentration was studied with aqueous solutions of tantalum (Fig. 1). The value of E_a^o increased drastically from 86.5 at 1 M H_2SO_4 to 386 at 4 M H_2SO_4, then plunged to 4.6 at 8 M H_2SO_4. As for niobium(V), E_a^o was generally higher for the H_2SO_4 system than for the HCl system. In the niobium(V) system, E_a^o increased from 8 M H_2SO_4 to a maximum of 125 at 1 M H_2SO_4; in contrast, in the tantalum system E_a^o decreased from a maximum of 386 at 4 M H_2SO_4 to 86.5 at 1 M H_2SO_4. These trends in the extraction coefficients indicate the possibility of separating these two metals with HDOAA.

Financial support by the Robert A. Welch Foundation of Houston, Texas, is gratefully acknowledged.

REFERENCES

1 K. J. Irgolic and A. M. Olivares, Mikrochim. Acta, (1974) 369.
2 M. J. El Seoud and K. J. Irgolic, Anal. Chim. Acta, 75 (1975) 377.
3 R. J. G. Dominguez and K. J. Irgolic, Anal. Chim. Acta, 00 (1976) 00.
4 K. J. Irgolic and R. J. G. Dominguez, Anal. Chim. Acta, 00 (1976) 00.
5 A. M. Olivares, Ph. D. Dissertation, Texas A&M University, 1972.
6 K. J. Irgolic, R. A. Zingaro and M. R. Smith, J. Organometal. Chem., 6 (1966) 17.
7 A. N. Nevzorov and N. S. Onoprienko, Russ. J. Inorg. Chem., 13 (1968) 1102.
8 R. W. Conrad and J. E. Lard, J. Less-Common Metals, 7 (1964) 316.
9 A. M. Olivares and K. J. Irgolic, J. Inorg. Nucl. Chem., 34 (1972) 1399.
10 F. A. Cotton and G. Wilkinson, Advanced Inorganic Chemistry, Wiley-Interscience, New York, 1966, pp.919—926.
11 V. P. Shvedov and E. M. Zhurenkov, Russ. J. Inorg. Chem., 11 (1966) 886.

Analytica Chimica Acta, 84 (1976) 127—134

THERMOMETRIC DETERMINATION AND ANALYTICAL APPLICATION OF THE LANDOLT EFFECT

F. F. GAÁL

Institute of Chemistry, Faculty of Sciences, University of Novi Sad (Yugoslavia)

V. I. SÖRÖS

Institute of Chemistry, Faculty of Technology, University of Novi Sad (Yugoslavia)

V. J. VAJGAND

Institute of Chemistry, Faculty of Sciences, University of Belgrade (Yugoslavia)

(Received 10th October 1975)

SUMMARY

The thermometric determination of the Landolt effect applied to the hydrogen peroxide—iodide—ascorbic acid reaction is described. The appropriate kinetic equations are used to interpret the thermometric curve and the calibration curve of the indicator reaction catalysed by molybdenum. The effects of the iodide, hydrogen peroxide, and hydrogen ion concentrations on the shape of the thermometric curves are discussed. This thermometric method can be used to determine micro amounts of iron, zirconium, thorium, vanadium, molybdenum and tungsten, with satisfactory accuracy and precision.

Landolt-type reactions are of considerable importance in kinetic analysis. Their analytical application is based on the correlation between the length of the incubation period and the amounts of catalysts and inhibitors present. Erdey and Svehla [1] converted the hydrogen peroxide—iodide reaction to a Landolt-type reaction by addition of ascorbic acid. They were the first to apply a Landolt reaction to the kinetic determination of micro amounts of molybdenum. Bognár and Svehla et al. [2—5] developed and applied a number of Landolt reactions based on evolution of iodine, bromine and chlorine.

Because the Landolt effect in these reactions can easily be detected not only visually but also by instrumental methods, these catalytic reactions have become used increasingly for the determination of micro amounts of metallic and non-metallic ions. The instrumental methods that have been used to determine the Landolt effect include polarography [6], spectrophotometry [7—9], potentiometry [9] and biamperometry [10, 11].

The most important contributions to the theoretical understanding of Landolt-type catalytic reactions have been made by Svehla [12], who proved that the hydrogen peroxide—iodide—ascorbic acid indicator reaction catalyzed by molybdenum until the Landolt effect intervenes, is of zero-order with respect to iodide concentration.

Many catalytic reactions are suitable indicator reactions for thermometric end-point determination of the titration [13]. The thermometric method is also convenient for the determination of the Landolt-type indicator reaction rate in kinetic determinations of small amounts of some metallic ions [14] as well as of fluorides and fluorosilicates [11].

In this paper the effects of various factors on the thermometric determination of the Landolt effect are described with reference to the hydrogen peroxide—iodide—ascorbic acid indicator reaction. The catalytic effect of metal ions on the reaction is utilized for the determination of micro amounts of iron, zirconium, thorium, vanadium, molybdenum and tungsten. In order to establish the optimal experimental conditions, the influence of some parameters on the shapes of the thermometric curves and the calibration curve has been studied.

EXPERIMENTAL

Apparatus

The temperature changes during the reaction were followed by means of a thermistor in the usual way. The inner resistance of the thermistor was 7 kiloh The temperature change was recorded on a "Servogor" RE 511 chart recorder (Goerz-Electro).

Solutions

Reducing solution I. Dissolve 17.4 g of potassium iodide, 3.1 g of ascorbic acid and 36.5 g of sodium acetate trihydrate in water, and mix with 25.5 ml of glacial acetic acid. Dilute to 1 l with distilled water.

Reducing solution II. Dissolve 17.4 g of potassium iodide and 6.2 g of ascorbic acid in water and dilute to 1 l with distilled water.

Reducing solution III. Dissolve 17.4 g of potassium iodide and 3.1 g of ascorbic acid and dilute to 1 l with buffer pH 3.6.

Buffer pH 3.6. Mix 75 ml of M sodium acetate with 925 ml of M acetic acid

Oxidizing solution I. Mix 21.0 ml of 30 % hydrogen peroxide and 50.0 ml of M H_2SO_4 and dilute to 100 ml with distilled water.

Oxidizing solution II. Mix 21.0 ml of 30 % hydrogen peroxide and 50.0 ml of M HCl and dilute to 100 ml with distilled water.

Stock solutions of metal ions were prepared from $FeCl_3 \cdot 6H_2O$, $Th(NO_3)_4 \cdot 5H_2O$, NH_4VO_3, $(NH_4)_6Mo_7O_{24} \cdot 4\ H_2O$ and $Na_2WO_4 \cdot 2H_2O$. The stock solution of zirconium was prepared by fusing zirconium nitrate with sodium hydrogen sulfate, dissolving the melt, and adding ammonia to precipitate zirconium hydroxide, which was then dissolved in hydrochloric acid.

Appropriate diluted solutions were prepared as required.

All solutions were made of reagent-grade chemicals in twice-distilled water.

Procedure

Mix 5 ml of the reducing solution containing potassium iodide and ascorbic acid in a Dewar vessel with 5 ml of the solution of catalyst (in the determination of thorium add 4.5 ml of the buffer solution pH 3.6). Place the Dewar vessel in a thermostat at 23 °C and leave it until the temperature has stabilized. Then add 0.5 ml of the hydrogen peroxide solution to start the indicator reaction.

In determinations of vanadium, molybdenum, and tungsten, use solutions I and V; in determinations of zirconium, use solutions II and VI; and in determinations of iron and thorium, use solutions III and VI.

RESULTS AND DISCUSSION

On the curves obtained by thermometric recording of the rate of the Landolt reaction, more or less sharp breaks indicate the end of the incubation period, i.e. the moment of intervention of the Landolt effect. The thermometric curves obtained in the determination of molybdenum are shown in Fig. 1. The Landolt effect on these curves is determined by graphic interpolation o

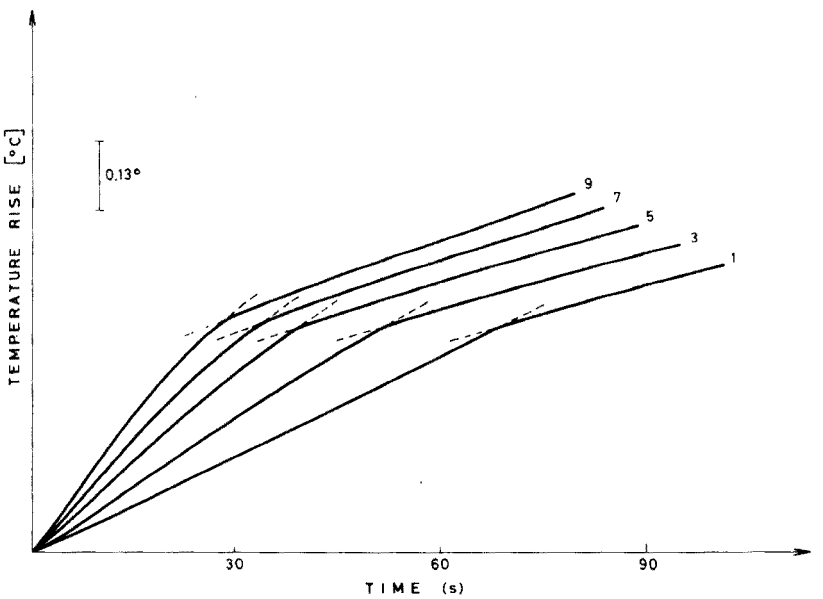

Fig. 1. Thermometric kinetic curves obtained in determinations of molybdenum by application of the hydrogen peroxide—iodide—ascorbic acid indicator reaction. Numbers on the curves show the amounts of molybdenum in $\mu g\ ml^{-1}$.

segments of the curves before and after the effect occurs. The concentration of the catalyst is determined from a calibration curve obtained by plotting $1 \cdot 10^{-2}/t$ (in s^{-1}) against concentration of metal ion (in $\mu g\ ml^{-1}$); in the case of molybdenum, a linear graph was obtained for 1—10 μg Mo ml^{-1} with $1 \cdot 10^{-2}/t$ values of about 1.4—3.4 s^{-1}. The results of such determinations of six metal ions are given in Table 1.

The change in concentration of hydrogen peroxide, i.e. the temperature change at different stages of the reaction, can be interpreted theoretically. The mechanism of the molybdenum-catalysed reaction is known [15]; if it is assumed that the iodide concentration during the incubation period is constant, then the reaction rate in this period can be written as

$$-\frac{d[H_2O_2]}{dt} = C[(k_1 + k_2\, 10^{-pH})\,[H_2O_2] + k_3[Mo]] \qquad (1)$$

where k_1 and k_2 are the corresponding rates of the uncatalysed reaction, k_3 is the rate constant of the catalysed reaction, C is the initial iodide concentration, and [Mo] is the molybdenum concentration.

Solution of eqn. (1) for the limiting conditions of the incubation period gives the hydrogen peroxide concentration:

$$[H_2O_2]_i = \frac{(k_1 + k_2\, 10^{-pH})\,[H_2O_2]_0 + k_3[Mo]}{(k_1 + k_2\, 10^{-pH})\, e^{C(k_1 + k_2\, 10^{-pH})\, t_i}} - \frac{k_3[Mo]}{(k_1 + k_2\, 10^{-pH})} \qquad (2)$$

The concentration of hydrogen peroxide consumed in this incubation period, i.e. the concentration of dehydroascorbic acid formed, can be calculated from

TABLE 1

Thermometric determinations of metal ions

Ions	pH	Useful range ($\mu g\ ml^{-1}$)	Taken ($\mu g\ ml^{-1}$)	Found[a] ($\mu g\ ml^{-1}$)	Error (%)	s_r (%)
Fe(III)	3.6	0.1—1.0	0.419	0.408	−2.6	2.2
			0.628	0.643	+2.4	3.8
Th(IV)	3.6	100—700	209.0	206.0	−1.4	0.2
			419.0	410.0	−2.2	2.1
Zr(IV)	1.6	10—100	42.0	42.7	+1.7	1.7
			69.9	71.3	+2.0	2.6
V(V)	4.5	4—44	19.0	19.4	+2.1	0.2
			28.6	29.1	+1.7	0.7
Mo(VI)	4.5	1—10	4.19	4.10	−2.2	0.9
			6.28	6.32	+0.6	1.0
W(VI)	4.5	10—100	41.9	40.7	−2.9	0.6
			62.9	64.5	+2.5	0.2

[a]Average of 4 results.

$$[H_2O_2]_1 = [H_2O_2]_0 - [H_2O_2]_i = [C_6H_6O_6]_i \quad (3)$$

In these equations, $[H_2O_2]_0$, $[H_2O_2]_i$ and $[H_2O_2]_1$ represent the initial concentration of hydrogen peroxide, the concentration at time t_i (a particular moment of the incubation period) and the concentration consumed during this period, respectively; $[C_6H_6O_6]_i$ is the concentration of dehydroascorbic acid formed during time t_i.

The decrease in iodide concentration in the post-incubation period can be represented by:

$$[I^-]_t = C - ([H_2O_2]_i - [H_2O_2]_t) \quad (4)$$

where the subscript t indicates a particular moment of the post-incubation period. Thus the reaction rate in this period can be expressed as:

$$-\frac{d[H_2O_2]}{dt} = k_1[H_2O_2]\,(C - [H_2O_2]_i + [H_2O_2]) + k_2 10^{-pH}\,[H_2O_2](C - [H_2O_2]_i + [H_2O_2]) + k_3\,[Mo](C - [H_2O_2]_i + [H_2O_2]) \quad (5)$$

Solution of eqn. (5) for the limiting conditions of the post-incubation period gives:

$$[H_2O_2]_t = \frac{A(B[H_2O_2]_i + k_3[Mo]) - k_3[Mo]\;C\,e^{-(k_3[Mo] - A \cdot B)(t - t_i)}}{B \cdot C\,e^{-(k_3[Mo] - A \cdot B)(t - t_i)} - B[H_2O_2]_i - k_3[Mo]} \quad (6)$$

where, for simplification, $(C - [H_2O_2]_i$ is designated by A, and $(k_1 + k_2\,10^{-pH})$ by B.

The hydrogen peroxide consumption at a particular moment of this period, i.e. the concentration of iodine evolved, can be represented by:

$$[H_2O_2]_2 = [H_2O_2]_i - [H_2O_2]_t = [I_2]_t \quad (7)$$

In eqns. (6) and (7), $[H_2O_2]_t$ is the concentration at time t of the post-incubation period and $[H_2O_2]_2$ is the corresponding consumption of hydrogen peroxide at that moment.

On the above basis, the temperature change ΔT during the reaction can be expressed by:

$$\Delta T = \frac{V_r}{q}(\Delta H_1[C_6H_6O_6]_i + \Delta H_2[I_2]_t) \quad (8)$$

where V_r is the volume of the reaction mixture (in litres), q is the heat capacity of the system (in kcal °C), ΔH_1 is the enthalpy of the incubation period and ΔH_2 is the enthalpy of the post-incubation period (in kcal/equivalent).

The enthalpy of the hydrogen peroxide—iodide reaction is 23.2 ± 0.6 kcal/equivalent of hydrogen peroxide [16]. The enthalpy of the iodine—ascorbic acid reaction, measured by direct thermometry, was found to be 3.1 ± 0.3 kcal/equivalent of ascorbic acid.

By means of eqns. (3, 7 and 8) and on the assumption that V_r/q is a constant, the enthalpy change during the reaction can be plotted (Fig. 2.). The calculations were done on a Varian 620-L-100 computer by BASIC programs. All the curves in Fig. 2 were obtained with initial concentrations of $1.67 \cdot 10^{-2}$ N ascorbic acid and $6.95 \cdot 10^{-5}$ M molybdenum. The effects of iodide, hydrogen peroxide and hydrogen ion concentrations on the shapes of the thermometric curves were examined. Curves 1, 3, and 5 (Fig. 2) show that at the same concentration of hydrogen peroxide the breaks become sharper as the iodide concentration decreases; this effect was confirmed by calculating and comparing the first derivatives of the curve segments before and after occurrence of the Landolt effect. Curves 2, 3 and 4 (Fig. 2) prove that at the same concentration of iodide the hydrogen peroxide concentration

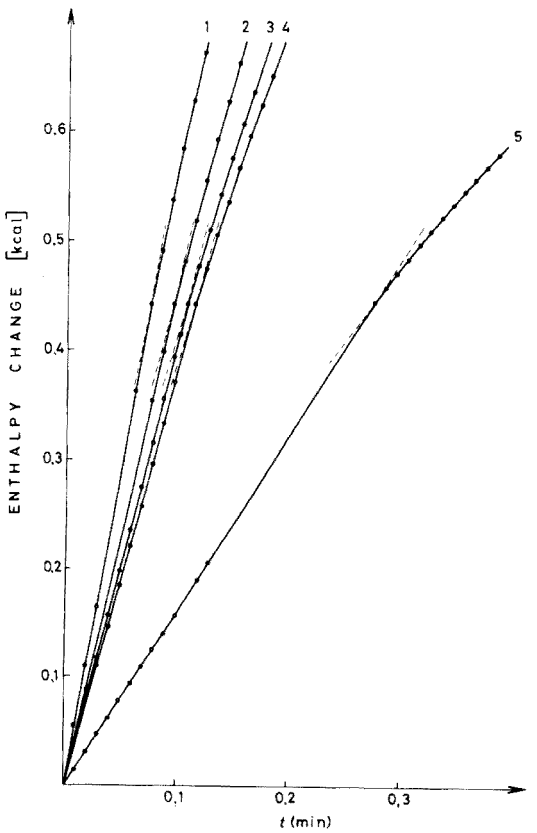

Fig. 2. Enthalpy change of the hydrogen peroxide—iodide—ascorbic acid system obtained by application of kinetic equations. Curves 1, 3 and 5 are given for $3.53 \cdot 10^{-1}$ N H_2O_2 and the following concentrations of iodide: 1—$7.00 \cdot 10^{-2}$ M; 3—$5.00 \cdot 10^{-2}$ M; 5—$2.00 \cdot 10^{-2}$ M. Curves 2, 3 and 4 are given for $5.00 \cdot 10^{-2}$ M KI and the following hydrogen peroxide concentrations: 2—$8.82 \cdot 10^{-1}$ N; 3—$3.53 \cdot 10^{-1}$ N; 4—$8.82 \cdot 10^{-2}$ N. All of these refer to initial concentrations.

has no essential influence on the shape of the thermometric curve. Changes in the hydrogen ion concentration over the range pH 3.0—4.5 under the given conditions had virtually no effect on the shape of the curves. Selection of the optimal chart speed allowed the breaks in the thermometric curves to be recorded more sharply.

On the basis of these investigations, the sharpness of the break in these thermometric curves is influenced mainly by the indicator reaction mechanism and by the difference in the reaction heat of the incubation and the post-incubation periods.

On the basis of the known reaction stoichiometry, and on the assumption that for the same initial concentration of ascorbic acid the hydrogen peroxide consumption until the Landolt effect intervenes is always the same, application of eqn. (3) shows that the duration of the incubation period depends on the concentration of the catalyst (Fig. 3, curves a). The curves in Fig. 3 show the effects of using different concentrations of iodide and hydrogen peroxide. In order to determine the lower concentrations of the catalyst, Fig. 3 shows

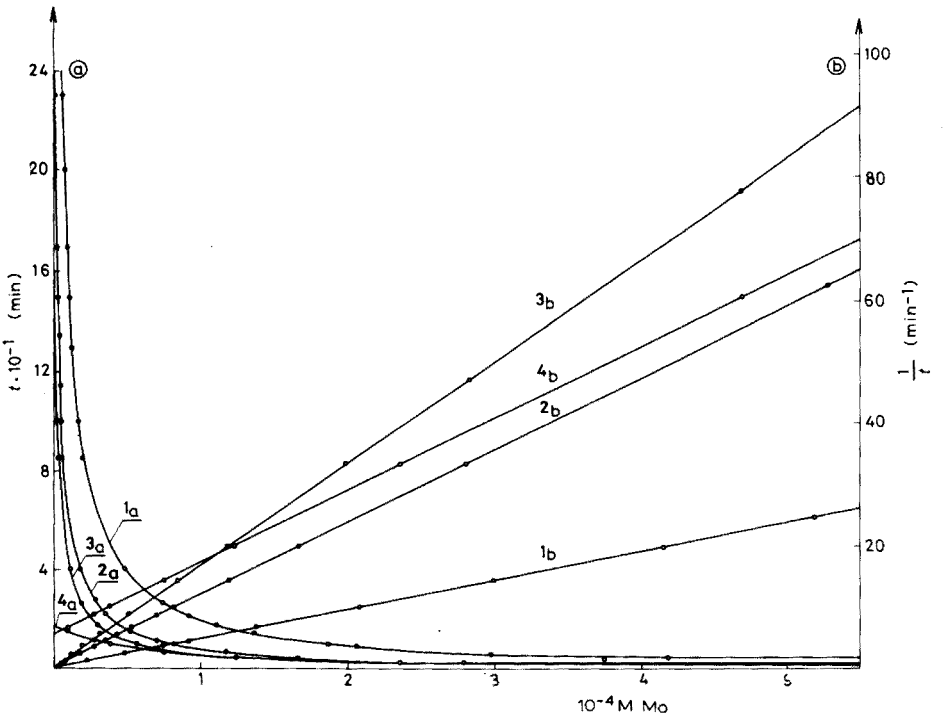

Fig. 3. Calibration curves obtained by application of kinetic equations. Curves 1, 2 and 3 are given for $1.76 \cdot 10^{-1}$ N H_2O_2 and for following iodide concentrations: 1—$2.00 \cdot 10^{-2}$ M; 2—$5.00 \cdot 10^{-2}$ M; 3—$7.00 \cdot 10^{-2}$ M. Curves 2 and 4 are given for $5.00 \cdot 10^{-2}$ M KI and for various hydrogen peroxide concentrations: 2—$1.76 \cdot 10^{-1}$ N; 4—$2.65 \cdot 10^{-1}$ N. For all curves, the ascorbic acid concentration is $1.67 \cdot 10^{-2}$ N.

that it is better to use the lower iodide and peroxide concentrations (curve 1a), so that the time differences obtained for particular concentrations of the catalyst are greater; the precision is then improved. Curves (b) in Fig. 3 show that the correlation between the concentration of the catalyst and the reciprocal time value when the Landolt effect intervenes is strictly linear.

In conclusion, the equations interpreting the rate of Landolt reactions can be applied not only to explain the experimental curves, but also to improve the experimental conditions in thermometric determinations based on the Landolt effect.

REFERENCES

1 L. Erdey and G. Svehla, Hung. Acta Chim., 26 (1961) 77.
2 J. Bognár, Mikrochim. Acta, (1968) 455.
3 J. Bognár and L. Sipos, Z. Phys. Chem., 242 (1969) 49.
4 H. Thompson and G. Svehla, Z. Anal. Chem., 247 (1969) 224.
5 A. Páll, G. Svehla and L. Erdey, Talanta, 17 (1970) 211.
6 V. Toporova and L. Tamarchenko, Zh. Anal. Khim., 22 (1967) 234.
7 M. Karayannis, S. Tzouwara-Karayanni and T. Hadjiioannou, Anal. Chim. Acta, 70 (1974) 351.
8 J. Bognár and O. Jellinek, Mikrochim. Acta, (1969) 366.
9 H. Weisz and K. Rothmaier, Anal. Chim. Acta, 68 (1974) 93.
10 H. Weisz and S. Pantel, Anal. Chim. Acta, 76 (1975) 487.
11 F. Gaál, V. Sörös and V. Canić, Mikrochim. Acta, II (1975) 689.
12 G. Svehla, Analyst (London), 94 (1969) 513.
13 See, e.g., V. Vajgand, F. Gaál, and S. Brusin, Talanta, 17 (1970) 415, and refs. therein.
14 V. Vajgand, F. Gaál, Lj. Zrnić-Zeremski and V. Sörös, Proceedings of the 3rd International Conference on Thermal Analysis, Davos, 2(1971) 437.
15 G. Svehla and L. Erdey, Microchem. J., 7 (1963) 206.
16 J. Brandštetr and P. Sapáková, Collect. Czech. Chem. Commun., 38 (1973) 2249.

Analytica Chimica Acta, 84 (1976) 135—141

THE MICRODETERMINATION OF CHLORIDE, SULPHATE, PHOSPHATE AND NITRITE BY REFLECTANCE SPECTROMETRY

R. REISFELD, S. LEVI and W. J. LEVENE*

Department of Inorganic and Analytical Chemistry, The Hebrew University of Jerusalem (Israel)

(Received 10th November 1975)

SUMMARY

Quantitative spot tests with a reflectance spectrometer have been developed for chloride (10—320 p.p.m.), sulphate (10—120 p.p.m.), phosphate (2—30 and 10—180 p.p.m.) and nitrite (1—35 and 10—100 p.p.m.). There are few interferences with these tests, and their effects can be overcome by standard techniques except for the interference from phosphate when it is present in the sulphate test, in large concentrations.

Previous papers [1—3] have described methods for the microdetermination of mercury(II), lead(II) and copper(II). The present work extends the spot test technique to the microdetermination of chloride, sulphate, phosphate and nitrite, which are determined by measuring the diffuse reflectance spectra of their appropriate complexes deposited as uniform coloured spots on filter paper.

Chloride is determined indirectly by measuring the silver(I) remaining after adding a drop of the chloride solution under test to a filter paper, to which a drop of silver nitrate solution, of concentration exceeding that of the chloride, had been applied and dried. A drop of chromate solution is added to precipitate reddish-brown silver chromate, the colour of which decreases with increasing chloride concentration. Chloride can thus be determined by measuring the diffuse reflectance at 530 nm.

The determination of sulphate is also an indirect determination, based on a reaction [4] in which the excess of barium after quantitative precipitation of $BaSO_4$ in the solution being tested, is measured by adding yellow sodium rhodizonate to the filter paper to produce a reddish-brown spot of barium rhodizonate, whose colour is best measured at 570 nm.

The determination of phosphate is based on the quantitative formation of yellow ammonium molybdophosphate [4], measured at 430 nm. The sensitivity can be improved by oxidizing benzidine with ammonium molybdophosphate to obtain benzidine blue and molybdenum blue, which are measured at 630 nm.

---

*Present address: The Israel Electro-Optical Industry, Ltd., Rehovot, Israel.

For the determination of nitrite, the test is based on the diazo-coupling reaction [4] which occurs in the presence of nitrous acid. Sulphanilic acid and an aromatic amine produce an intensely blue complex which is measured at 525 nm.

EXPERIMENTAL

The experimental procedure has been described [1]. All the chemicals used were reagent-grade and the water was triply-distilled. Drops of reactants were applied from microsyringes (7 μl). Diffuse reflectance measurements were made with the Fast Scanning Spectrocolorimeter Model SCF-1 (Israel Electro-Optical Industry Ltd.). The test specimens were prepared on Whatman 120 filter card strips, 18 spots per strip. Sufficient accuracy is generally obtained by taking the average reflectance of 2 spots for each measurement, so that 9 measurements can be made on each strip. The photographs reproduced here are multiple exposures on Polaroid film from a camera mounted on the oscilloscope of the instrument, which presents the spectral reflectance curve.

Chloride

Reagents. The aqueous 0.5 % silver nitrate solution may be stored in a darkened bottle for several weeks. The standard chloride solutions were prepared from NaCl.

Procedure. A spot of the $AgNO_3$ solution is applied to the filter card, which is dried for 10 min at 40—55 °C. A drop of the chloride solution is applied (its pH must be less than 7) and the card dried again. It is dried a third time after the application of a drop of aqueous 0.5 % (w/v) potassium chromate solution. The brown spots formed are chemically stable for at least several weeks, and can be used for calibration purposes. Reflectance is measured at 530 nm.

Sulphate

Reagents. The aqueous 0.3 % (w/v) sodium rhodizonate solution used must not be more than 2 d old. The sulphate solutions were prepared from $Na_2SO_4 \cdot 10H_2O$.

Procedure. Drops of aqueous 0.25 % (w/v) barium nitrate solution, of the sulphate solution under test, and of the sodium rhodizonate reagent are applied successively to the filter card, each being dried before the application of the next. The final test spot is reddish-brown, and is stable for 1—2 d. Reflectance is measured at 570 nm. The barium nitrate spots may be applied in advance to the filter strip cards, which may then be stored for at least several weeks without deterioration.

Phosphate

Reagents. (1) Nitric acid (35 ml, d. 1.2) is added to an aqueous 5 % solution of $(NH_4)_6Mo_7O_{24} \cdot 4\ H_2O$. (2) Benzidine (0.05 g) is dissolved in 10 ml of acetic acid, and poured into 100 ml of water. (3) Equal volumes of reagents 1 and 2 are mixed. This reagent may be freshly prepared and used from an ice bath, or it may be stored for up to a week in a refrigerator, and used cold.

The phosphate test solutions were prepared from standardized 88 % phosphoric acid.

Procedure. For relatively high concentrations of phosphate (10—180 p.p.m.), a drop of reagent (1) is applied to the filter card which is dried (prepared filter papers may be stored for several days). A drop of the phosphate solution under test is then applied, forming a yellow precipitate whose diffuse reflectance is measured at 430 nm: it is stable for several weeks and can be used for calibration purposes.

For lower concentrations of phosphate (1—35 p.p.m.), a drop of reagent (3) is applied to the filter card, which is dried for 10 min (prepared filter papers may be stored for several days). A drop of the phosphate solution under test is then applied. The spot is again dried for 10 min and the blue reaction products are developed by neutralizing the spot with a drop of aqueous 10 % (w/v) sodium acetate solution. The spot is dried in air (40—55 °C) for 5—6 min and measured at room temperature at 630 nm within 1 h.

Nitrite

Reagents. (1) N-1-Naphthyleneethylenediaminedihydrochloride (0.4 g) is dissolved in 100 ml of water, with 0.8 g of sulphanilic acid. (This order should be followed because of the difficulty in dissolving the amine in sulphanilic acid solutions.) (2) Reagent (1) is diluted (1 + 1). Both these solutions must be stored in dark bottles in darkness, and may be kept for a fortnight. Sodium nitrite solutions were used.

Procedure. Reagent (1) is used for 1—40 p.p.m. and reagent (2) for 5—100 p.p.m. of nitrite. A drop of the appropriate reagent is applied to the filter card and dried for 10 min. (Filter cards prepared in this way may be stored for 1—2 d.) A drop of the nitrite solution under test is applied, and the diazo blue dye is dried and measured at 525 nm within a few hours.

RESULTS

The techniques described provide filter paper spots with reproducible values of the diffuse spectral reflectance, R. In spite of the finite thickness of the filter paper (and of the concentration gradient of coloured deposits within this thickness), the function $F(R) = (1 - R)^2 / 2R$ is linearly dependent upon the concentration (C), within a specific range, for each of the anions

concerned. This range is limited by the stoichiometric amounts of the reagents used, and by the progress towards saturation of the uppermost layers of the cellulose medium in which the colourant is deposited.

Chloride

Figure 1A shows the spectral reflectance curves obtained for a series of chloride concentrations. The largest changes in reflectance occur at 530 nm and Fig. 2 shows the dependence of $F(R)$ on the concentration at this optimal wavelength. Each point on the graph is the average value from two spots. The curve has a negative slope because of the progressive decrease in the concentration of silver chromate and is linear up to 320 p.p.m. Cl^-. The standard deviation from linearity within this range is 6 p.p.m. The lower limit of the measurement is 10 p.p.m.

Hydrogencarbonate, nitrate, sulphate and fluoride do not interfere, but phosphate, bromide and iodide interfere; phosphate can be precipitated from the solution by ammonium molybdate before testing, and bromide and iodide can be removed by oxidation to bromine and iodine.

Sulphate

Figure 1B shows the spectral reflectance curves for sulphate spot tests. The optimum wavelength is 570 nm, and $F(R)$ depends linearly on C at this wavelength at concentrations up to 120 p.p.m. according to the equation $F(R) = 0.1348 - 3.34 \cdot 10^{-4}\, C$. The standard deviation of the points (each point is a mean of 3 results) from this line is 3 p.p.m. Measurements can be made down to 10 p.p.m.

Cyanide, sulphide, nitrate and chloride do not interfere, even at high concentrations, but phosphate interferes at concentrations greater than twenty times the sulphate concentration.

Phosphate

Figure 1C shows the reflectance curves for the spot tests with reagent (1). The mean of 2 results provides adequate precision. The curve of $F(R)$ as a function of C has a positive slope and is linear up to 180 p.p.m. with the equation $F(R) = 2.846 \cdot 10^{-4}\, C + 5.184 \cdot 10^{-3}$. The standard deviation is 3 p.p.m. and measurements can be made down to 10 p.p.m.

Figure 1D shows the reflectance curves for spot tests with reagent (3). It is again sufficient to use the mean of two measurements at 630 nm, and the relationship $F(R) = 1.076 \cdot 10^{-3}\, C + 2.105 \cdot 10^{-3}$ holds up to 30 p.p.m. within which range the standard deviation is 0.5 p.p.m. With this reagent, measurements can be made down to 2 p.p.m.

In qualitative spot tests for phosphate with benzidine and ammonium molybdate, saturated sodium acetate solutions are generally used [4]. This is not acceptable in a quantitative test because of the instability of the coloured reaction product in alkaline solutions. The recommended sodium acetate concentration must therefore be adjusted when this test is made on highly acid or alkaline specimens.

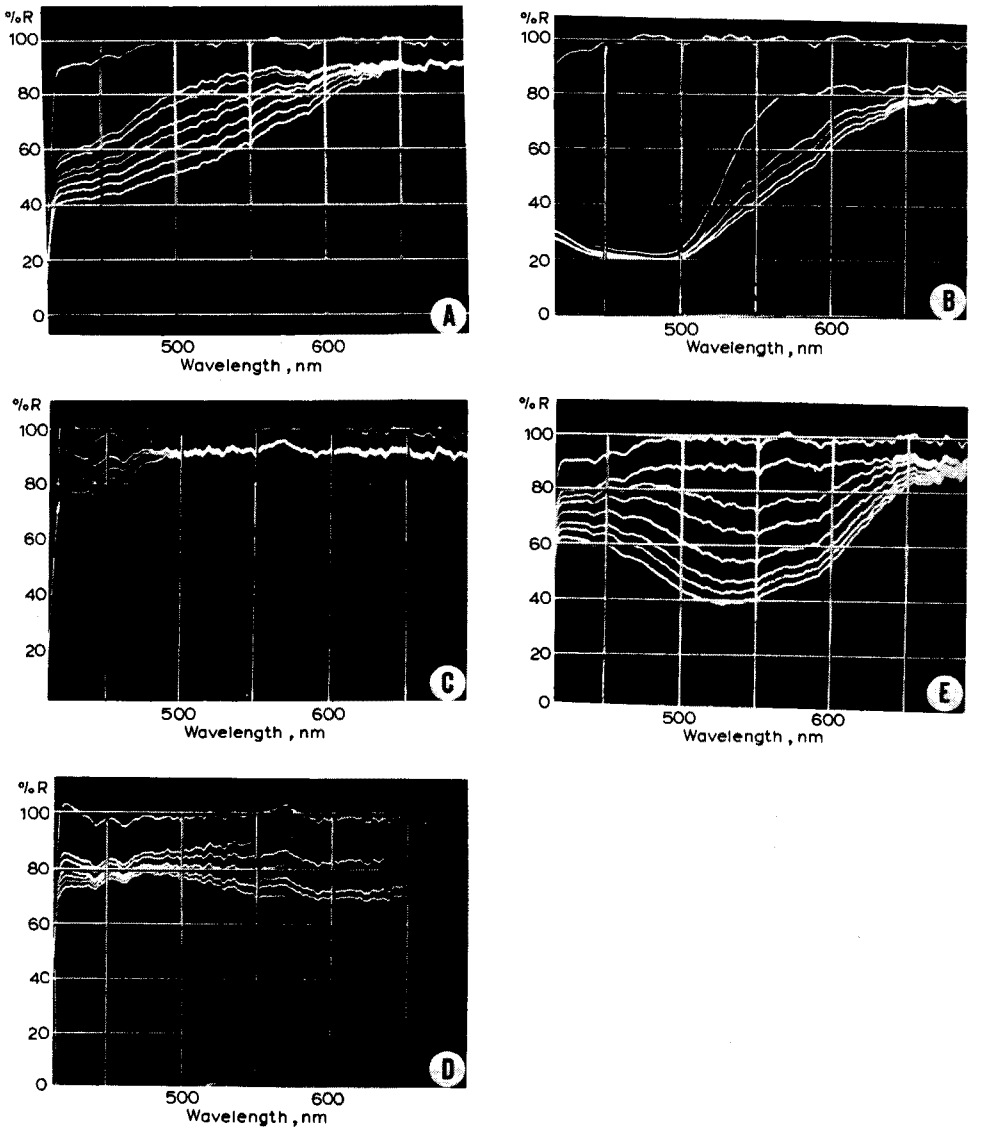

Fig. 1. Diffuse reflectance spectra for the different tests. The uppermost curve in each set is the instrument calibration ($MgCO_3$ block). A. Chloride: successive curves downward relate to tests on solutions containing 400, 350, 300, 250, 200, 100 and 0 p.p.m. Cl^-. B. Sulphate: successive curves downward relate to 400, 250, 200, 100 and 0 p.p.m. sulphate. C. Phosphate (reagent 1): successively lower curves relate to 0, 50, 100, 140 and 180 p.p.m. phosphate. D. Phosphate (reagent 3): successively lower curves relate to 0, 10, 30, 60, 100 and 180 p.p.m. phosphate. E. Nitrite: successively lower curves relate to 0, 10, 20, 40, 60, 80 and 100 p.p.m. nitrite.

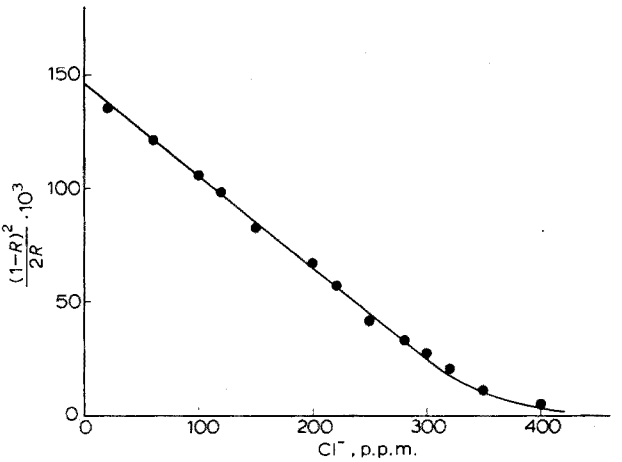

Fig. 2. F(R) as a function of [C] for the chloride test. Wavelength 530 nm.

The benzidine and ammonium molybdate solutions are added together as a single drop (despite the difficulty of storing the reagent) in order to achieve the required homogeneity of the spot, which otherwise comprises concentric rings of different colours.

Arsenate and silicate interfere, but their effects can be overcome by the addition of tartaric acid [4] to the acetate solution (1 g to each 50 ml of solution). It was further shown that the interference from fluoride can be overcome by adding a beryllium salt [4] to reagent (3). Oxalate interference could be overcome by ignition. No other interfering anions were found.

Nitrite

Figure 1E shows the spectral reflectance curves for the nitrite tests with reagent (1), and Fig. 3 shows the F(R)—concentration curve for 525 nm; each point is the mean of 2 results. The curve is not linear but is highly repeatable in the range 1—35 p.p.m. Linear results (Fig. 3, curve 2) are obtained with reagent (2) in the range 10—100 p.p.m. according to the equation $F(R) = 2.796 \cdot 10^{-3} C + 1.702 \cdot 10^{-3}$, with a standard deviation of 1.5 p.p.m. This test is specific for nitrite.

This work was supported by the Israel National Council of Research and Development.

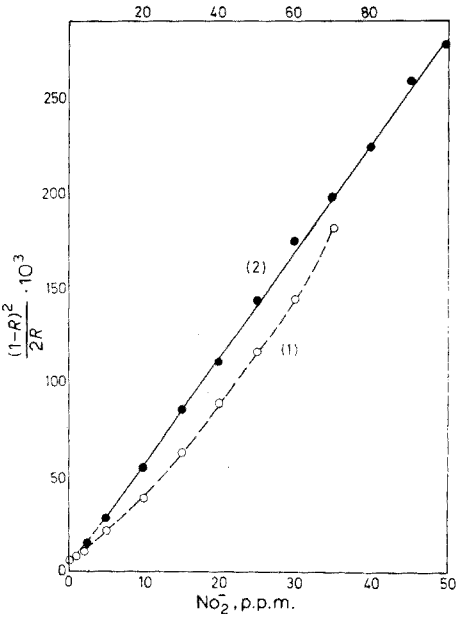

Fig. 3. F(R) as a function of [C] for the nitrite test at 525 nm. 1, reagent (1); 2, reagent (2).

REFERENCES

1 R. Reisfeld, E. Greenberg and W. J. Levene, Anal. Chim. Acta, 74 (1975) 253.
2 R. Reisfeld, S. Levi, E. Greenberg and W. J. Levene, Anal. Chim. Acta, 76 (1975) 477.
3 R. Reisfeld, S. Levi, E. Greenberg and W. J. Levene, Anal. Chim. Acta, 79 (1975) 326.
4 F. Feigl, Spot Tests in Inorganic Analysis, Elsevier, Amsterdam, 1958.

Analytica Chimica Acta, 84 (1976) 143—148

AN EXTRACTION—SPECTROPHOTOMETRIC METHOD FOR THE DETERMINATION OF TUNGSTEN IN GEOLOGICAL MATERIALS

N. COGGER

Geochemical Division, Institute of Geological Sciences, London WC1X 8NG (England)

(Received 24th November 1975)

SUMMARY

A method based on solvent extraction of the stable tetraphenylarsonium tungsten(V)—thiocyanate ion-association complex has been extended to the spectrophotometric determination of tungsten in geological materials. Decomposition with a mixed sodium peroxide and sodium carbonate sinter and fusion, followed by leaching with water, gives a filtrate free from iron and most of the niobium which may be present in the sample. Silica is removed from the solution by evaporation with hydrofluoric and orthophosphoric acids. The effect of molybdenum was investigated; up to approximately a 100-fold amount showed negligible interference. Results are presented for simulated samples and mineral concentrates.

Most methods for the colorimetric determination of small amounts of tungsten are based on the reaction of tungsten(V) with toluene-3, 4-dithiol [1, 2] or with the thiocyanate ion [1, 3—7]. The dithiol method is the more sensitive, but it is seriously affected by interference from molybdenum.

In a review and experimental assessment of procedures for the spectrophotometric determination of tungsten with thiocyanate, Fogg et al. [4], developed for the determination of tungsten in steel a method which is completely free from interference by vanadium, and in which the extent of the interference by molybdenum is determined by the concentration of iron in the sample solution. The method [4] employs the technique of Affsprung and Murphy [3] in which the stable, insoluble tetraphenylarsonium tungsten(V) —thiocyanate ion association complex is extracted into chloroform; in addition, Fogg et al. [4] also prevented the formation of a red coloration in the chloroform solution (caused by traces of oxidizing agents) by the addition of a small amount of hydroquinone to the solvent. This paper extends the method [4] to the determination of tungsten in geological materials.

The technique selected for taking samples into solution removes iron from the solution, and the interference of molybdenum under these conditions was studied.

As standard samples covering a suitable range of tungsten values were not available, simulated samples (GS1—12) were prepared from silt, ground to pass 200—300 mesh, to which were added weighed amounts of ignited

tungstic oxide, together with tin(IV) and molybdenum(VI) oxides, within the range 0.002—2 % of tungsten in the final prepared samples. The samples were mixed for ca. 8 h in a tumbler mixer. Sample homogeneity was ascertained by replicate determinations of tungsten by a rapid geochemical prospecting method based on dithiol.

EXPERIMENTAL

Apparatus

A Unicam SP 500 spectrophotometer (1 and 4 cm glass cells) was used.

Reagents

All chemicals used were of analytical-reagent grade, except where otherwise stated.

Tin(II) chloride solution. Dissolve 10 g of $SnCl_2 \cdot 2H_2O$ in 90 ml of hydrochloric acid (density 1.18). After 3 days prepare fresh.

Titanium(III) chloride solution. Dilute the technical grade (ca. 30 % (w/v) $TiCl_3$) with an equal volume of hydrochloric acid (density 1.18). Prepare fresh daily.

Tetraphenylarsonium chloride solution, 0.025 M. Dissolve 1.05 g of $C_{24}H_{20}AsCl \cdot HCl$ in 100 ml of water.

Chloroform containing 0.08 % of hydroquinone. Dissolve 0.2 g of hydroquinone in 20 ml of ethanol and mix with 230 ml of chloroform. Prepare fresh daily. Reject if a pink colour develops.

Standard sodium tungstate solution (2500 μg W ml^{-1}). Dissolve 2.2432 g of $Na_2WO_4 \cdot 2H_2O$ in distilled water and dilute to 500 ml. From this, prepare solutions containing 25 and 5 μg W ml^{-1} in hydrochloric acid (density 1.18). The more dilute solution should be prepared fresh daily.

Procedure

Decomposition of samples. Weigh 0.1—0.5 g of sample, ground to pass 200 mesh, into a 45-ml iron crucible. According to sample weight, add 1—3 g of sodium peroxide and 0.25—0.75 g of sodium carbonate and mix thoroughly Include a blank determination. Cover with a lid and sinter in a muffle furnace at 450—480 °C for ca. 45 min. Complete the attack by fusion over a Meker burner at full heat for ca. 45 s and allow to cool.

Add ca. 15 ml of water to the crucible, cover with the lid, and when the reaction subsides add a few drops of ethanol to reduce manganates. Complete the leaching by heating the mixture on a water bath for 5—10 min. Allow to

cool and filter the mixture through a Whatman 541 filter paper into a 50-ml or 100-ml graduated flask. Clean the crucible with a rubber policeman and wash the residue into the filter with small volumes of 0.5 % sodium hydroxide solution; wash the paper with the same solution. Dilute to volume with distilled water and mix thoroughly. Store the solution in a polythene bottle. When the tungsten content of the sample is expected to be low, the contents of the crucible may be washed directly into a graduated flask, diluted to volume, mixed thoroughly, and centrifuged. Store the centrifugate in a polythene bottle as before.

Removal of silica. Transfer an aliquot of the alkaline solution to a small platinum dish, add 2 ml of orthophosphoric acid (density 1.75), mix cautiously (add a few more drops of orthophosphoric acid if necessary to make the solution acidic, but avoid excess), add 1—2 ml of 40 % hydrofluoric acid, and evaporate to a small volume. Wash the sides of the dish with a small volume of distilled water, evaporate the solution until syrupy, and increase the temperature of the hot plate sufficiently to expel traces of hydrofluoric acid. This final removal of hydrofluoric acid may be expedited by heating the dish over a burner cautiously until fumes of phosphoric acid just appear; avoid prolonged heating since this would cause attack of the vessel and lead to the formation of a metaphosphoric acid glass which is soluble only with great difficulty. Allow to cool, add ca. 0.4 ml of water, warm gently until the contents of the dish are fluid (add a few more drops of water as necessary, but avoid excess), cool, and transfer to 100-ml conical flask with a total volume of 17 ml of hydrochloric acid (density 1.18).

Colour development. To the acidic solution obtained above add 3 ml of tin(II) chloride solution, and swirl; by syringe pipette, add 0.2 ml of titanium(III) chloride solution, and swirl; cover the flask with a small clock glass (or insert a small filter funnel), add a glass bead to prevent bumping and simmer at the boiling point for 5 min. Cool thoroughly in chilled water. With 20 ml of 6 M hydrochloric acid transfer the solution to a 100-ml separating funnel, fitted with a PTFE stopcock. The final volume should be ca. 40 ml. By syringe pipette, add 1 ml of tetraphenylarsonium chloride solution, swirl, add 3 ml of 2 M sodium thiocyanate solution (reject this reagent solution when it turns pink), and mix thoroughly. Extract the tetraphenylarsonium tungsten(V)—thiocyanate complex with 9 ml of hydroquinone-treated chloroform, shaking for 1 min, and transfer the chloroform layer to a 50-ml separating funnel fitted with a PTFE stopcock. Repeat the extraction twice by shaking for 30 s with 8- and 7-ml portions of the treated chloroform, adding 0.5 ml of tetraphenylarsonium chloride solution before each extraction.

To the combined chloroform extracts in the separating funnel, add 10 ml of distilled water and 1—1.5 g of ammonium hydrogen difluoride, and shake for 30 s to remove traces of titanium and niobium. Dry the funnel stem with a roll of filter paper and pass all the chloroform layer through a small

Whatman 41 filter paper directly into a 25-ml graduated flask. Rinse the aqueous layer with two 1-ml portions of the treated chloroform and run these through the filter; wash the paper with small volumes of the treated chloroform, dilute to volume with the solvent, and mix thoroughly. Measure the absorbance at 402 nm against pure chloroform in 1- or 4-cm glass cells. Correct for the blank if necessary. Calculate the percentage of tungsten in the sample by reference to a calibration curve.

Calibration curve. Transfer 1—10 ml of the standard solutions (to give final concentration ranges of 1—10 and 0.2—2 μg W ml^{-1}, respectively) to 100-ml conical flasks. Include a blank and dilute to 17 ml with hydrochloric acid (density 1.18) add 2 ml of orthophosphoric acid (density 1.75) and follow the procedure used for the tests, commencing at "colour development". Measure the absorbance in 1- or 4-cm cells according to tungsten content, with pure chloroform as the reference liquid.

RESULTS AND DISCUSSION

Analyses of the simulated samples (GS 1—12) and various mineral concentrates are given in Tables 1 and 2, which show that the method gives good precision within the range 0.003—3 % of tungsten and is in addition, potentially suitable for the determination of larger amounts. Orthophosphoric acid is used to retain tungsten in solution as a stable heteropoly acid during the removal of silica by hydrofluoric acid. Small amounts of silica are tolerated (up to ca. 40 μg ml^{-1} in the volume of hydrochloric acid solution before the addition of reducing agents), but because of the tendency of tungsten to

TABLE 1

Recovery of tungsten

Sample	% W added	% Sn added	% Mo added	% W found Range	Mean[a]	% W recovery
GS 1	0.002	0.007	—	0.002 — 0.003	0.003	150
GS 11	0.007	0.002	—	0.007 — 0.008	0.008	114
GS 9	0.010	0.12	—	0.011 — 0.012	0.012	120
GS 2	0.020	0.060	—	0.020 — 0.021	0.021	105
GS 4	0.050	0.30	—	0.050 — 0.051	0.051	102
GS 3	0.10	0.10	0.002	0.093 — 0.101	0.096	96
GS 10	0.20	0.020	0.003	0.185 — 0.202	0.196	98
GS 5	0.30	0.050	0.005	0.294 — 0.[illegible]	0.296	99
GS 6	0.50	0.20	0.010	0.489 — 0.504	0.498	100
GS 12	0.70	1.20	0.040	0.688 — 0.711	0.698[b]	100
GS 7	1.00	0.050	0.020	0.975 — 1.02	0.989	99
GS 8	2.00	0.80	0.050	1.95 — 2.07	2.01[b]	105

V.P. 18 Jan 77

[a] Mean of 4 or 5 determinations.
[b] Determination by a gravimetric method gave 0.75 % for GS 12 and 2.07 % W for GS 8.

TABLE 2

Tungsten in geological materials

Sample		% W found present method		% W grav. method[b]
		Range	Mean[a]	
Columbite concentrate, Sierra Leone	B1	1.39—1.42	1.41	1.36
	B2	1.01—1.06	1.04	0.94
Rock, Uganda		3.00—3.06	3.03	2.91
Wolfram concentrate, Uganda	No. 1	8.40—8.45	8.42	—
	No. 2	11.7—11.9	11.8	11.4
	No. 3	21.4—21.6	21.5	—

[a]Mean of 4—6 results. [b]Analysed independently.

co-precipitate with silicic acid, it is better practice to eliminate the silica completely, particularly when low tungsten values are expected.

The effect of molybdenum for molybdenum to tungsten ratios ranging from 1000:1 to 1:1 was investigated by taking pure solutions in hydrochloric acid (density 1.18) through the colour development procedure after adding orthophosphoric acid. The results (Tables 3 and 4) show that approximately a 100-fold excess of molybdenum can be tolerated before tungsten losses become significant. The low recoveries for tungsten at higher

TABLE 3

The effect of molybdenum
(All numbers represent μg element in chloroform extract)

Mo present	W present	Mo + W recovered	Mo blank	% W recovery[a]
200	10	9.8	0.2	96
1000	10	10.2	0.3	99
2000	10	10.5	1.1	94
4000	10	11.2	1.9	93
10,000	10	12.0	2.7	93
30	30	29.6	0.0	99
150	30	29.3	0.2	97
300	30	30.0	0.2	99
600	30	29.5	0.3	97
1500	30	29.9	0.7	97
160	160	160.8	0.0	101
320	160	161.8	0.5	101
800	160	160.5	0.5	100
2000	160	160.5	0.8	100

[a]Mean of three determinations.

TABLE 4

Relationship of tungsten recovery to molybdenum:tungsten ratio

Ratio Mo:W	1:1	5:1	10:1	20:1	100:1	200:1	1000:1
Mean % recovery	100	99	99	97	99	94	93

ratios may be caused by an inhibiting effect exerted on the tungsten by the large excess of molybdenum present at the thiocyanate extraction stage, but molybdenum to tungsten ratios greater than 50:1 are rarely encountered in geological samples.

The author wishes to thank the Director, Institute of Geological Sciences, for permission to publish this work.

REFERENCES

1 E. B. Sandell, Colorimetric Determination of Traces of Metals, 3rd edn., Interscience, New York, 1959.
2 B. F. Quin and R. R. Brooks, Anal. Chim. Acta, 58 (1972) 301.
3 H. E. Affsprung and J. W. Murphy, Anal. Chim. Acta, 30 (1964) 501.
4 A. G. Fogg, D. R. Marriott and D. T. Burns, Analyst (London), 95 (1970) 848, 854.
5 A. G. Fogg, T. J. Jarvis, D. R. Marriott and D. T. Burns, Analyst (London), 96 (1971) 475.
6 E. G, Lillie and L. P. Greenland, J. Res. U.S. Geol. Surv., 1(5) (1973) 555; Anal. Abstr., 27 (1974) 1340.
7 V. Yatirajam and S. Dhamija, Talanta, 22 (1975) 760.

Analytica Chimica Acta, 84 (1976) 149—155

COMPARISON OF STANDARDS IN THE KARL FISCHER METHOD FOR WATER DETERMINATION

WILLIAM P. BRYAN and P. BHASKARA RAO

Department of Biochemistry, Indiana University School of Medicine, Indianapolis, Indiana 46202 (U.S.A.)

(Received 17th November 1975)

SUMMARY

An accurate method for Karl Fischer titrations of water is presented. It involves continuous flushing of the titration cell with rigorously dried carbon dioxide and careful amperometric end-point determination. The water content of sodium tartrate dihydrate was determined, both by titration and drying at 150 °C, and is close to the theoretical value. This work does not support the contention that the dihydrate contains occluded water. Sodium tartrate dihydrate is a good primary standard for the Karl Fischer reagent.

In a critical study of the Karl Fischer method for water determination [1], Beasley et al. [2] evaluated sodium tartrate dihydrate and water as primary standards for the Karl Fischer reagent. Their results indicated that sodium tartrate dihydrate was not a suitable primary standard because of the occlusion of about 0.3 % by weight of water within the crystal structure. This would give rise to a 2 % error in the determination of the Karl Fischer reagent titer if the theoretical water content of the dihydrate was used.

A micro Karl Fischer titration has been developed for the determination of traces of water in freeze-dried proteins [3]; this development involved careful attention to sources of error, some of which had already been discussed [4]. In the work described here, this improved method was used on the macro scale to re-examine the reported discrepancy between water and sodium tartrate dihydrate standardization of the Fischer reagent. A simple macro method for accurate Karl Fischer titration of water is reported and it is shown that there is no detectable occluded water in sodium tartrate dihydrate. This material can be conveniently used for standardization of Karl Fischer reagent.

EXPERIMENTAL

Reagents

Reagent-grade methanol was dried by distillation from magnesium; a little water was added so that blank titration values could be read on the buret. The Karl Fischer reagent (Fisher Chemical Co.) was stored in a Kimble 10-ml

automatic buret (Cat. No. 17124F) and protected from light; a tube filled with Aquasorb (Mallinckrodt Chemical Works) protected the reagent from atmospheric moisture.

Titration cell

The titration cell (A. H. Thomas, Cat. No. 9388-R20) had two 5-mm square platinum electrodes and was used with 140-ml threaded glass jars. The reagent was delivered to the cell through a flexible polyethylene tube made by drawing out heated 1/8-in. tubing; the undrawn end of the tubing was sealed to the buret tip. The tube passed into the cell through a slightly larger glass buret inlet tube in a rubber stopper. The drop size was less than 0.01 ml. Purging gas passed out of the cell through the annular space between the glass tube and the polyethylene tube. Removal of the stopper allowed addition of methanol from a 50-ml pipet or a weighed amount of sodium tartrate dihydrate through a funnel. These substances were added to a completely purged titration cell.

The cell was continuously purged with Aquasorb dried carbon dioxide during titrations. The gas was passed through a flow meter (a simple acrylic rotameter with a range of 0—0.4 standard cubic feet of air per h) and then through a metal or glass drying tube, all connections being made of metal or glass (e.g. 1/8-in. stainless steel tubing). Serious leakage of water occurs through rubber or plastic tubing; a glass-lined filter trap (Chemical Research Services, Addison, Illinois) gave good results, but acrylic tubes used for gas drying in gas chromatography are not recommended. A Hoke packless miniature brass bellows valve was used between the drying tube and the titration cell, to protect the desiccant when not in use and to insure that no water leakage occurred through valve packing. A Cajon UltraTorr high-vacuum fitting and teflon-taped brass pipe fittings were used to attach the stainless steel tube to the valve and the valve to the drying tube.

Carbon dioxide is superior to nitrogen for cell purging since it is heavier and tends to displace any water vapor leaking into the cell through the buret entrance. A drop of Karl Fischer reagent on the buret tip was slowly decolorized when nitrogen was used, but not when carbon dioxide was used at the same flow rate.

The simple amperometric circuit used for end-point detection (Fig. 1) is very similar to that described by Beasley et al. [2]. Cell current was observed with a 50-μA microammeter of 2000-ohm internal resistance. Before the start of a titration, the variable resistance was adjusted to give a current of 30 μA through a 10000-ohm "dummy cell"; this insured that a potential of $(30 \cdot 10^{-6})$ (10000 + 2000) = 0.360 V existed across the electrodes when no current flowed in the titration cell. During the titration the voltage across the electrodes was [0.360—(nA) (2000)] V. The discussion pertaining to Fig. 8 in the paper of Beasley et al. [2] should be consulted in order to compare the present method with previous ones.

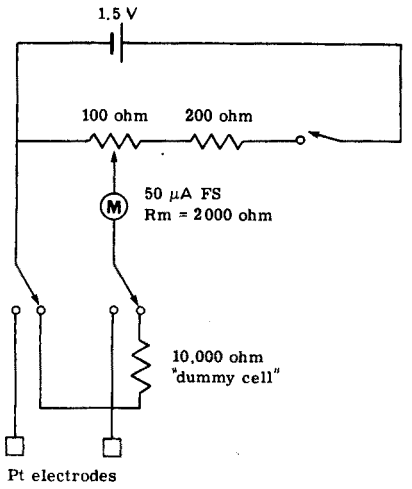

Fig. 1. Amperometric circuit for end-point detection in Karl Fischer titrations.

Procedures

In the direct Karl Fischer titration of water in methanol, negligible current flows until an excess of iodine is present. Current readings at several levels of excess of Karl Fischer reagent were plotted against volume of reagent added, and the linear plots were extrapolated to zero current to obtain end-points. When methanol was used as solvent, the meter readings were unstable if the solution was stirred; it was necessary to stop stirring after complete mixing and wait for several minutes until a stable non-stirred diffusion current was obtained. This current could be estimated to the nearest microampere; generally about 4 readings of current at different excesses of Karl Fischer reagent were taken. End-points were estimated to the nearest 0.01 ml.

Standardization of Karl Fischer reagent against distilled water. An oven-dried 140-ml jar was attached to the cell cover and electrodes, and a small teflon-coated magnetic stirring bar added. Dried carbon dioxide was then passed for at least 15 min at about 50 ml min^{-1}. The rubber stopper containing the buret inlet tube was then removed and 50 ml of dried methanol was added from a pipet which had been previously rinsed with methanol and dried with compressed air. A measured amount of distilled water was added from a calibrated Agla micrometer syringe [5] (Burroughs Wellcome Company) equipped with a flexible polyethylene delivery tube similar to that on the reagent buret. The delivery tube was passed through the buret inlet tube and a drop of water formed at its tip. The micrometer was read, the tip of the delivery tube was dipped into a small beaker of methanol, and the rubber stopper was attached to the titration cell. Gas flow was

momentarily stopped to minimize water evaporation during water addition. About 40 μl of water was delivered into the cell, after which the delivery tube tip was dipped into the methanol and removed from the titration cell. The micrometer was again read and the temperature noted. The weight of water was calculated from volume delivered and water density. It is estimated that known weights of water were delivered with an accuracy of about 2 parts per thousand. The buret tip was then inserted into the cell and the water-in-methanol solution was titrated with full-strength Karl Fischer reagent, while maintaining a carbon dioxide flow of about 50 ml min^{-1}.

Standardization of Karl Fischer reagent against sodium tartrate dihydrate. After addition of methanol to the titration cell as described above, 0.2—0.3 g of the dihydrate was quantitatively added through a funnel. All the tartrate usually dissolved during the titration, but some samples appeared to contain traces of material which were completely insoluble in methanol. A blank titration of 50.0 ml of dried methanol was included in each set of comparisons between distilled water and sodium tartrate dihydrate.

Weight losses on drying of sodium tartrate dihydrate were determined by heating empty weighing bottles to 150 °C for several hours, capping while still hot, and cooling each bottle in an individual desiccator. The bottles were quickly weighed after equalizing air pressures. About 3 g of the dihydrate was quickly added and weighed, followed by overnight heating at 150 °C. The bottles were then cooled and weighed as before. About 3 h is required for the bottles to come to constant weight when heated at 150 °C.

RESULTS

Results of a number of comparisons of distilled water with different samples of reagent-grade sodium tartrate dihydrate in the standardization of Karl Fischer reagent are given in Table 1. It can be seen that slightly higher values for Karl Fischer reagent titers are obtained with the dihydrate when the theoretical value of 15.66 % water is used. The average difference between tartrate and water titers for all the samples is +0.02 or about +0.3 %. A different result was obtained by Beasley et al. [2]. In a more limited series of comparisons, they obtained an average difference of —0.13 or about —2 %. Thus the present results can be taken to indicate that slightly less than the theoretical amount of water is present in the dihydrate samples, whereas their results indicated that the amount of water present is about 2 % greater than the theoretical value.

It should be possible to settle this discrepancy by measuring the weight loss of sodium tartrate dihydrate on drying to constant weight. In Table 2, drying results are compared with the water content of the dihydrate samples determined by Karl Fischer titration when the reagent is standardized against distilled water. The drying experiments do indicate that slightly less than the theoretical amount of water is present in the samples, and this is confirmed

TABLE 1

Comparison of various brands of sodium tartrate dihydrate with distilled water in standardization of Karl Fischer reagent

Source and lot	Titer (mg H_2O/ml reagent)			
	vs. Tartrate[a]	vs. Water	Difference	Av. difference
Harleco 4162P	6.57	6.55	+ 0.02	
Harleco 4162P	6.55	6.55	0.00	+ 0.01
Harleco 4162P	6.57	6.56	+ 0.01	
Fisher 731675	5.85	5.79	+ 0.06	
Fisher 731675	5.87	5.85	+ 0.02	+ 0.03
Fisher 731675	5.82	5.82	0.00	
Baker 30494	5.79	5.80	− 0.01	
Baker 30494	5.84	5.79	+ 0.05	+ 0.01
Baker 30494	5.80	5.80	0.00	
Mallinckrodt BDM	5.83	5.79	+ 0.04	
Mallinckrodt BDM	5.82	5.81	+ 0.01	+ 0.04
Mallinckrodt BDM	5.85	5.78	+ 0.07	
MCB 19	5.86	5.82	+ 0.04	
MCB 19	5.88	5.82	+ 0.06	+ 0.03
MCB 19	5.79	5.79	0.00	

[a]Calculated from the theoretical value of 15.66 % water in sodium tartrate dihydrate.

by Karl Fischer determinations of water content. Agreement between the two methods is good.

DISCUSSION

Both our work [3] and that of Bastin et al. [4] indicate that special precautions against atmospheric moisture must be taken for Karl Fischer determinations of water on the micro scale. It is also necessary to take similar precautions on the macro scale if accurate water determinations, devoid of systematic errors from atmospheric water, are required. For example, 100 ml of air (25 °C, 50 % relative humidity) contains about 1 mg of water which would be equivalent to about 0.2 ml of full-strength Karl Fischer reagent.

Continuous flushing with dry gas is an easy method of removing all atmospheric and adsorbed water from the titration cell. Special precautions must be observed if the gas is to be sufficiently dry; the drying tube and gas line must be of metal or glass. A simple flowmeter is useful and should be placed before the drying tube. Molecular Sieve 4A or phosphorus pentoxide has been recommended as drying agent [4]. Aquasorb, which is an indicating, phosphorus pentoxide-based desiccant, gives good results, but anhydrous magnesium perchlorate, anhydrous calcium sulfate, or silica gel should be avoided.

TABLE 2

Comparison of water contents of various brands of sodium tartrate dihydrate by Karl Fischer titration and drying to constant weight at 150 °C

Source and lot	% H_2O			
	Titration	Av.	Drying[a]	% Difference
Harleco 4162P	15.60			
Harleco 4162P	15.68	15.64	15.62	+ 0.1
Harleco 4162P	15.63			
Fisher 731675	15.50			
Fisher 731675	15.60	15.58	15.61	− 0.2
Fisher 731675	15.64			
Baker 30494	15.67			
Baker 30494	15.54	15.63	15.61	+ 0.1
Baker 30494	15.67			
Mallinckrodt BDM	15.55			
Mallinckrodt BDM	15.63	15.55	15.61	− 0.4
Mallinckrodt BDM	15.47			
MCB 19	15.54			
MCB 19	15.50	15.56	15.60	− 0.3
MCB 19	15.65			

[a]Average of duplicate or triplicate determinations.

Sodium tartrate dihydrate was recommended as a primary standard for the Karl Fischer reagent by Neuss et al. [6] because of its purity, theoretical water content, and stability. However, the work of Beasley et al [2] indicated a discrepancy between drying and Karl Fischer determination of the amount of water present in this material. These workers obtained the theoretical water content by drying at 150 °C but got a value about 2 % higher when the Fischer titration was used. They ascribed the extra 2 % to occluded water which could not be removed by drying at 150 °C, and published a photomicrograph of sodium tartrate dihydrate crystals purporting to show regions of occluded water.

The present results do not support those of Beasley et al. There is no significant discrepancy between drying and Fischer titration, and both methods give values close to the theoretical water content. It is difficult to see how drying at 150 °C could remove water of hydration causing a breakdown in crystal structure, yet not remove any of the water occluded in the structure. The photomicrograph shows streaks and spots within the crystals which are probably simple crystal habit imperfections. We conclude that the extra water observed by Beasley et al. in their Karl Fischer titrations probably resulted from atmospheric water vapor contamination.

Sodium tartrate dihydrate is a good primary standard for Karl Fischer titration in methanol. The titration should not be so rapid that there is

insufficient time for the salt to dissolve before the end-point is reached. The present results indicate water contents which are slightly below the theoretical, probably because of impurities. For the most accurate results, the water content of a uniform sample of the dihydrate should be determined by drying and used in preference to the theoretical value for calculating Karl Fischer reagent titers.

This work was supported by Grant GB40606 from the National Science Foundation and the Grace M. Showalter Residuary Trust.

REFERENCES

1 J. Mitchell and D. M. Smith, Aquametry, Interscience, New York, 1948.
2 T. H. Beasley, Sr., H. W. Ziegler, R. L. Charles and P. King, Anal. Chem., 44 (1972) 1833.
3. P. B. Rao and W. P. Bryan, J. Mol. Biol., 97 (1975) 119.
4. E. L. Bastin, H. Siegel and A. B. Bullock, Anal. Chem., 31 (1959) 467.
5. J. W. Trevan, Biochem. J., 19 (1925) 1111.
6. J. D. Neuss, M. G. O'Brien and H. A. Frediani, Anal. Chem., 23 (1951) 1332.

Analytica Chimica Acta, 84 (1976) 157—164

DETERMINATION OF THE STABILITY CONSTANTS OF SOME HYDROXO AND CARBONATO COMPLEXES OF Pb(II), Cu(II), Cd(II) AND Zn(II) IN DILUTE SOLUTIONS BY ANODIC STRIPPING VOLTAMMETRY AND DIFFERENTIAL PULSE POLAROGRAPHY

H. BILINSKI*, R. HUSTON and W. STUMM

Institute for Water Resources and Water Pollution Control, Swiss Federal Institute of Technology (EAWAG), CH-8600 Dübendorf (Switzerland)

(Received 8th October 1975)

SUMMARY

Anodic stripping voltammetry and differential pulse polarography are used to study complex formation between Cu(II), Pb(II), Zn(II) or Cd(II) and hydroxide or carbonate ions under concentration conditions which approximate those in natural waters, i.e. $[Me]_t < 10^{-7}$ M. Lead(II) and copper(II) form similarly stable carbonato complexes, which suggests that $PbCO_3.aq$ and $CuCO_3.aq$ are the preponderant lead and copper species in natural waters. Carbonato complexes of zinc(II) and cadmium(II) are less stable; hence these metals are present in natural waters — depending on solution variables — as aquo, hydroxo or chloro (sea water) complexes.

Anodic stripping voltammetry (a.s.v.) and differential pulse polarography (d.p.p.) have been used to determine, from the shift of peak potentials, the extent of hydroxo and carbonato complex formation for the metals Cu(II), Pb(II), Zn(II) and Cd(II) in dilute solutions, where the total metal concentration lies in the range 10^{-7}—10^{-5} M.

In natural waters, the pertinent chemical, physical and geochemical reactions of metals as well as their physiological or toxicological effects depend on the nature of the species present. Natural waters typically have a pH range of 7—9 and contain CO_2, HCO_3^- and CO_3^{2-} with a total concentration of carbonate between 10^{-2} and 10^{-4} M. Under these conditions the solubility of these metals

$$[Me]_t = [Me^{2+}] + \sum [Me(OH)_i] + \sum [MeH_j(CO_3)_k]$$

is in the range 10^{-5}—10^{-7} M. The complex formation of these metals with OH^-, HCO_3^- and CO_3^{2-} has been determined previously by different authors (see below) under conditions where the total concentration of metal was 10^{-4} M or higher. To avoid precipitation at neutral pH values, these deter-

*Present Address: Department of Physical Chemistry, Institute "Rudjer Bošković", Zagreb, Yugoslavia.

minations were made at low or high pH values. Thus, in order to account for the metal ion speciation in natural waters, the information gained from these equilibrium constants must be extrapolated to the more neutral pH-range; however, some species prevailing in this pH range may remain undetected.

Electrode kinetic measurements based on a.s.v. and d.p.p. can detect metal ion species at concentrations as low as 10^{-8} M. Although a.s.v. and d.p.p. are less precise than other methods suitable for higher concentrations in the acid range, they can be used to estimate stability constants in the neutral and alkaline pH-range at soluble concentration levels, provided that the depolarization reactions are electrochemically reversible [1, 2].

EXPERIMENTAL

Chemicals

Stock solutions, 0.1 M in metal, were prepared by dissolving the required amounts of $Pb(NO_3)_2$, $Cu(NO_3)_2.3H_2O$, $Cd(NO_3)_2.4H_2O$ (Merck p.a) or $Zn(NO_3)_2.6H_2O$ (Fisher Scientific) in twice-distilled water. These solutions were further diluted to 10^{-3} M, from which sample solutions could be made freshly. All samples were 0.1 M in KNO_3 (Merck 'suprapur'). For a.s.v. determinations of lead(II), alkalinities and pH were varied coulometrically at a current of 0.03 mA. In all other experiments, alkalinities were adjusted by adding appropriate amounts of sodium hydrogencarbonate solution (with Eppendorf micropipettes); the pH was then varied with CO_2/Ar mixtures.

Instrumentation

For a.s.v. experiments, a Metrohm Polarecord E261, in conjunction with an a.s.v. cell assembly BM 503 were used. The hanging mercury drop surface area was 0.054 cm^2 and a constant sweep voltage of 0.0167 V s^{-1} was used. The stirring time was 3 min and the stabilizing period 1 min; the plating potentials for lead and copper were −1 V and −0.5 V, respectively.

For d.p.p. experiments, a PAR polarographic Analyzer Model 174 equipped with a PAR drop-timer was employed. The experimental conditions were as follows: drop-time 5 s, scan rate 0.2 mV s^{-1}, pulse amplitude 25 m V and voltage range 0.75 V. The cathodic potentials for Cu, Pb, Cd and Zn were +200 mV, −200 mV, −400 mV and −800 mV, respectively.

The pH of the solutions was measured by a Metrohm Digital pH Meter E500 equipped with a combined glass electrode EA120. All experiments were done at 25 °C.

RESULTS AND DISCUSSION

In polarography the half-wave potential, $E_{\frac{1}{2}}$ for reversible reactions depends on the depolarizable species [3]. Complex formation with a ligand L^{m-}, e.g.

$$M^{2+} + pL^{m-} \rightleftarrows ML_p^{(2-pm)}$$

shifts $E_{\frac{1}{2}}$ to more negative values [3],

$$\Delta E_{\frac{1}{2}} = \frac{RT}{nF} \ln \beta_p - \left(p \frac{RT}{nF} \ln [L^{m-}] \right) \quad (1)$$

where β_p is the stability constant of the complex $ML_p^{(2-mp)}$ and n is the number of electrons involved in the redox process ($2.3\,RTF^{-1} = 0.059$ V eq^{-1}).

For reversible systems, the peak potential, E_p, obtained with a.s.v. and d.p.p. lies near the polarographic $E_{\frac{1}{2}}$ value; as in polarography, E_p is shifted to more negative values as a consequence of complex formation. In accordance with eqn. (1), a plot of E_p (in V) vs. log $[L^{m-}]$ gives a straight line with a slope of $-p\ 0.059/n$ and an intercept of $(-0.059/n) \log \beta_p$. A curve concave towards the ordinate axis may indicate stepwise complex formation.

Figure 1 presents a.s.v. data for the Pb(II)—OH^- system; ΔE_p is plotted vs. pOH(= $-\log K_w$ + pH) where $\log K_w = 13.96$ [4]. The experimental points lie on a concave curve, to which two tangents with theoretical slopes of 29.5 and 59.1 mV can be drawn. The constants thus obtained are compared with other literature data [5—8] in Table 1. The constants obtained in this work are in good agreement with the literature values except for the value reported by Schorsch and Ingri [7], where chloro lead complexes interfered with hydrolysis and were not taken into account.

Figure 2(A—D) shows plots of $-\Delta E_p$ vs. $-\log [CO_3^{2-}]$, for carbonato complexes of Pb(II), Cu(II), Cd(II) and Zn(II). The concentration of $[CO_3^{2-}]$ ion was calculated with the help of the acidity constants of CO_2.aq. The slopes of the curves obtained by a.s.v. and d.p.p. are identical, although the a.s.v. experimental points are consistently higher (more negative potentials) than those of d.p.p., resulting in slightly larger values of log β (see Fig. 2).

The stability constants of the metal carbonato complexes determined in this work are listed, with the literature values, in Tables 2—4. For carbonato lead complexes (Table 2), the present constants agree well with the existing

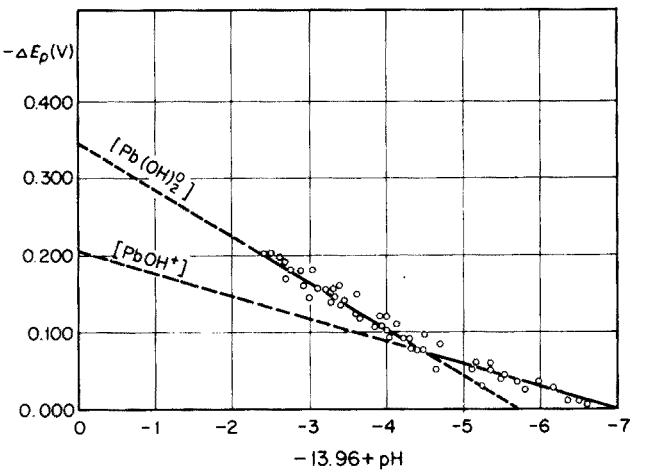

Fig. 1. A.s.v. data for the Pb(II)—OH^- system (0.1 M KNO_3, 25 °C).

TABLE 1

Comparison of stability constants of lead hydroxo complexes

Method	Medium	$[Pb]_T$	pH	$[PbOH^+]$ $\log^*\beta_1$	$[Pb(OH)_2]$ $\log^*\beta_2$	Ref.
E.m.f.	3.0 M $NaClO_4$	10^{-3}—$8 \cdot 10^{-2}$	5—8	—7.9	—	5
E.m.f.	0.3 M $NaClO_4$	10^{-3}—$8 \cdot 10^{-2}$	5—8	—7.8	—	5
E.m.f.	3.0 M $NaClO_4$	$>5 \cdot 10^{-4}$	>12	—	10.9	6
E.m.f.	0.3 M $NaClO_4$	$>5 \cdot 10^{-4}$	>12	—	10.34	6
E.m.f.	3.0 M NaCl	$>6 \cdot 10^{-4}$	>10	—	7.78	7
Pol.	1.0 M KNO_3			—6.9	10.8	8
ΔE_p, a.s.v.	0.1 M KNO_3	10^{-6}—10^{-5}	7—11	—7.0	11.5	This work

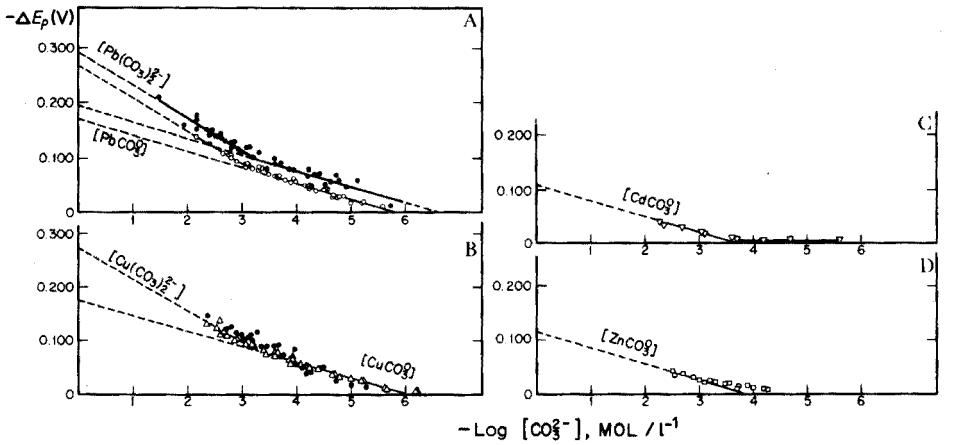

Fig. 2. Plots of $-\Delta E_p$ vs. $-\log [CO_3^{2-}]$ for carbonate complexes (0.1 M KNO_3, 25 °C). A, Pb by a.s.v. (•) and d.p.p. (○); B, Cu by a.s.v. (•) and d.p.p. (△); C, Cd by d.p.p.; D, Zn by d.p.p.

literature data. In the case of carbonato copper complexes, the log β_2 value reported by Ernst et al. [13] is lower than all the other values (Table 3). Table 4 gives the results for the cadmium and zinc carbonato complexes; clearly these metals form rather weak complexes with carbonates. The stability constant determined by d.p.p. for the cadmium carbonato complex agrees fairly well with that obtained by Gardiner [19] who used a cadmium-selective electrode. The values obtained for the Cd(II) and Zn(II) complexes in this work are lower than those reported by Zirino and Yamamoto [12] who estimated their constants by interpolations from correlations of dissociation constants vs. electronegativity.

The existence of bicarbonato complexes of Pb, Cu, Zn and Cd is still in doubt. Baranova and Barsukov [20] claimed the existence of $Pb(HCO_3)_2^0$ and $Pb(HCO_3)_3^-$ complexes from some polarographic data, as shown in Fig. 3(B). We have recalculated the same data as shown in Fig. 3(A) plotted

TABLE 2

Comparison of stability constants of lead carbonato complexes
(All results at 25 °C unless indicated otherwise)

Method	Medium	$[Pb]_T$ (M)	$[CO_3^{2-}]_T$(M)	pH	log β_1	log β_2	Ref.
A.s.v.	0.1 M KNO_3	10^{-5}—10^{-6}	$3 \cdot 10^{-2}$—$5 \cdot 10^{-4}$	7.3—10.3	6.4	9.8	This work
D.p.p.	0.1 M KNO_3	10^{-6}—$2 \cdot 10^{-7}$	10^{-4}—$3 \cdot 10^{-4}$	5— 9.1	6.1	9.1	This work
Sol.	0.3 M $NaClO_4$	10^{-4}—$5 \cdot 10^{-7}$	$3 \cdot 10^{-1}$—$1 \cdot 10^{-5}$	7.7— 9.8	5.75	9.15	9
Pol.[a]	1.7 M KNO_3	10^{-4}	$1 \cdot 10^{-2}$	10.9	—	8.2	10
Sol.	1.0 M $NaClO_4$	$2.2 \cdot 10^{-5}$ —10^{-6}	$3.2 \cdot 10^{-1}$ —$3 \cdot 10^{-2}$	10.1—11.3	7.0	9.0	11
—[b]	0			—	7.5	—	12
D.p.p. D.p.a.s.v.	0.1 M KNO_3	$2.5 \cdot 10^{-6}$		—	6.3	—	13
A.s.v. modif.[15]	0.7 M $NaClO_4$	$3 \cdot 10^{-9}$	10^{-1}—10^{-3}	6.5— 7.5	5.62	—	14

[a] At 18 °C.
[b] Estimated from dissociation constants vs. electronegativity curve.

TABLE 3

Comparison of stability constants of copper(II) carbonato complexes at 25 °C

Method	Medium	$[Cu]_T$(M)	$[CO_3^{2-}]_T$(M)	pH	log β_1	log β_2	Ref.
A.s.v.	0.1 M KNO_3	$4 \cdot 10^{-6}$—$1 \cdot 10^{-6}$	10^{-2}—$5 \cdot 10^{-4}$	9.5—6.5	6.0	10.0	This work
D.p.p.	0.1 M KNO_3	10^{-6}—$2 \cdot 10^{-7}$	10^{-4}—$3 \cdot 10^{-4}$	9.2—4.7	6.1	9.7	This work
Sol.	0 corr			—	6.34	—	16
Sol.	0 corr			—	6.77	10.01	17
D.p.p. D.p.a.s.v.	0.1 M KNO_3	$2.5 \cdot 10^{-6}$		—	5.7 6.1	8.1 8.2	13
I.s.e.	var.	$1.58 \cdot 10^{-5}$ —$7.5 \cdot 10^{-7}$		8.2—6	6.8	—	18

TABLE 4

Comparison of stability constants of cadmium(II) and zinc(II) carbonato complexes at 25 °C

Method	Medium	$[Me]_T$(M)	$[CO_3^{2-}]_T$(M)	pH	log β_1	Ref.
Cadmium						
D.p.p.	0.1 M KNO_3	10^{-6}—$4 \cdot 10^{-7}$	10^{-1}—$9 \cdot 10^{-4}$	8.7—4.7	≈3.5	This work
I.s.e.[a]	0.001 M KNO_3	$8.9 \cdot 10^{-6}$—$8.9 \cdot 10^{-7}$			4.02	19
—[b]	0				5.1	12
Zinc						
D.p.p.	0.1 M KNO_3	10^{-6}—$4 \cdot 10^{-7}$	$6.7 \cdot 10^{-2}$—$9 \cdot 10^{-4}$	9.1—4.8	≈3.9	This work
—[b]	0				5.3	12

[a] At 20 °C.
[b] Estimated from dissociation constants vs. electronegativity curve.

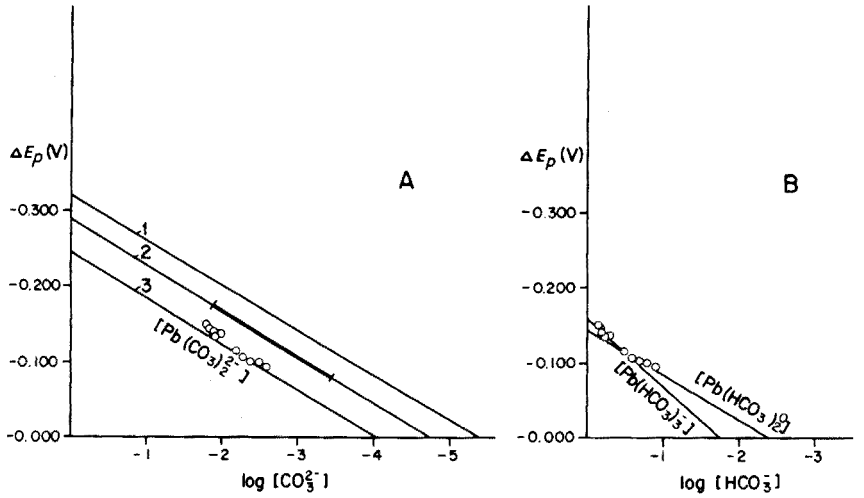

Fig. 3. Reinterpretation of the data of Baranova and Barsukov. The authors' data showing evidence for HCO_3^- complexes are replotted in (A), suggesting that their results may be explained equally well by the formation of a $Pb(CO_3)_2^{2-}$ complex. Line 2 is established from the present data in Fig. 2(A) by a.s.v. found for $I = 0.1$. From this line, corrected line 1 was drawn for $I = 0$ and then line 3, for $I = 1.0$ could be calculated. The data of Baranova and Barsukov fit the calculated line 3, for the $Pb(CO_3)_2^{2-}$ complex at $I = 1.0$. For A, (1) $I = 0$, calc. B—S (25 °C) → $\log \beta_2 = 10.8$; (2) $I = 0.1$, exp. B—S (25 °C) → $\log \beta_2 = 9.8$; (3) $I = 1.0$, calc. B—S (25 °C) → $\log \beta_2 = 8.2$. O, $I = 1.0$, exp. Ba (18 °C), recalc. B—S. For B, O $I = 1.0$, exp. Ba (18 °C); $\log \beta_2 = 4.77$; $\log \beta_3 = 5.19$.

as ΔE_p vs. $\log [CO_3^{2-}]$. This data can thus be also interpreted in terms of the carbonato lead complex, $Pb(CO_3)_2^{2-}$. Sipos et al. [14] have recently claimed that bicarbonato lead complexes do not exist, but they postulate the existence of a bicarbonato cadmium complex at lower pH values than those in the present work. Sipos et al. used the modified a.s.v. method of Bubić and Branica [15]; this modification gives a higher resolution of peak potentials than in the method used here.

From the results presented, it can be concluded that lead(II) and copper(II) form $MeCO_3^\circ$ and $Me(CO_3)_2^{2-}$ complexes of similar stability, while cadmium(II) and zinc(II) form only $MeCO_3^\circ$ complexes of much lower stability than that of lead and copper. Therefore, carbonato complexes of zinc and cadmium cannot be of any significance in natural waters.

REFERENCES

1 W. Stumm and H. Bilinski, in Advances in Water Poll. Res., Sixth Int. Conf., Jerusalem, June 8—23 (1972), Pergamon, Oxford and New York, 1973, p. 39.
2 W. L. Bradford, Limnol. Oceanogr. V 18(5), September (1973) 757.
3 J. Heyrovský and J. Kůta, Principles in Polarography, Acad. Sci., Prague (1966), p. 148.
4 L. G. Sillén and A. E. Martell, Stability Constants of Metal Complexes, Chem. Soc. Spec. Publ., 17 (1964 and 1971).

5 Å. Olin, Acta Chem. Scand., 14 (1960) 126.
6 B. Carell and Å. Olin, Acta Chem. Scand., 14 (1960) 1999.
7 G. Schorsch and N. Ingri, Acta Chem. Scand., 21 (1967) 2727.
8 G. W. Goward, Thesis, Princeton, 1954, quoted in ref. 4.
9 H. Bilinski and P. Schindler, to be published.
10 J. Faucherre and J. Bonnaire, Compt. Rend., 248(II) (1959) 3705.
11 N. N. Baranova, Russ. J. Inorg. Chem., 14 (1969) 1717.
12 A. Zirino and S. Yamamoto, Limnol. Oceanogr., 17 (1972) 661.
13 R. Ernst, H. E. Allen and K. H. Mancy, Water Res., 9 (1975) 969.
14 L. Sipos, private communication.
15 S. Bubić and M. Branica, Thalassia Jugosl., 9 (1/2) (1973) 47.
16 J. F. Scaife, Can. J. Chem., 35 (1957) 1332.
17 J. F. B. Silman, Thesis, Harvard Univ., 1958.
18 M. J. Stiff, Water Res., 5(5) (1971) 171.
19 H. Gardiner, Water Res., 8 (1) (1974) 23.
20 N. N. Baranova and V. L. Barsukov, Trans. from Geochim. No. 9 (1965) 1093.

Analytica Chimica Acta, 84 (1976) 165—171

AN ELECTROCHEMICAL STUDY OF REDOX INDICATORS PART I. SUBSTITUTED CHRYSOIDINES

U. J. LARSEN*, R. A. BOURNIQUE** and M. D. RYAN

Chemistry Department, Marquette University, Milwaukee, Wisconsin 53233 (U.S.A.)

(Received 29th September 1975)

SUMMARY

The electrochemical oxidation of various substituted chrysoidines was studied by cyclic voltammetry, to determine which have stable oxidation products. Only 4-hydroxychrysoidine has a stable product; the apparent oxidation potential is 0.779 V vs. NHE. 4-Methoxy- and 4-ethoxy-chrysoidine rapidly lose methanol or ethanol, respectively, so that the 4-hydroxychrysoidine wave appears on subsequent scans. All the other chrysoidines studied are irreversible. The results indicate that a hydroxy group in the 4-position is necessary for stability; the 4-alkoxychrysoidines can achieve the stable quinoidal structure by cleavage of the alkoxy group after nucleophilic attack.

Several substituted chrysoidines (chrysoidine is 2,4-diaminoazobenzene) have been suggested as redox indicators [1—3]. 4-Ethoxychrysoidine is an accepted indicator for titrations involving standard potassium bromate [1, 4], but there is little information about the redox properties of the other suggested substituted chrysoidines. Preliminary results on the formal potentials of such compounds, obtained mainly with commercially available 4-ethoxychrysoidine [5] suggested the preparation and study of eleven substituted chrysoidines.

Although there are numerous papers on the reduction of substituted azobenzenes, there are very few on their oxidation. Matrka et al. [6] have studied the oxidation of N,N-dimethyl-4-aminoazobenzene and some related compounds. Ladanyi et al. [7] have investigated the oxidation of 4-aminoazobenzene in more detail, using cyclic voltammetry. In the work described here, cyclic voltammetry was used to identify those compounds which have stable products, and may therefore serve as reversible indicators. For these compounds, the formal oxidation potentials can be determined from the voltammetric data.

---

*Present address: Chemistry Department, Wisconsin Lutheran College, Milwaukee, Wisconsin (U.S.A.).

**Author for correspondence.

EXPERIMENTAL

The preparation, purification and characterization of the chrysoidine derivatives have been described elsewhere [8]. Procedures for determining the formal potentials of the compounds, based on a modified potentiopoised technique, and on microtitrations, as well as other observations, have also been reported [8].

Cyclic voltammetry with a carbon paste or platinum electrode was done with a Beckman Electroscan 30, whereas a home-made potentiostat was used with a glassy carbon electrode (Pine Instrument Co., Grove City, Pa.). A saturated calomel reference electrode was used in all cases. The carbon paste electrode was prepared as described by Adams [9] after the chrysoidines had proved irreversible at the platinum electrode.

Solutions of the substituted chrysoidines were prepared by weighing an appropriate amount of the dye, dissolving it in the required amount of concentrated sulfuric acid, and diluting to the mark with water in a volumetric flask. In some cases, ethanol was added to increase solubility and reduce adsorption.

All solutions were prepared with distilled water and sparged with nitrogen for 15 min. The gas train included a vanadium chloride scrubber [10], and sulfuric acid of the same concentration as used in the sample. All compounds other than the chrysoidines were reagent-grade and used as received. Chrysoidine, the parent compound, was obtained from Aldrich Chemical Co., Milwaukee, Wis., and 4-ethoxychrysoidine from Eastman.

RESULTS AND DISCUSSION

All the dyes have irreversible waves at the platinum electrode; in most cases, no well-defined reduction peak could be obtained. Substitution of the carbon paste or glassy carbon electrode resulted in a quasi-reversible wave for 4-hydroxychrysoidine and a reducible secondary product for 4-methoxychrysoidine and 4-ethoxychrysoidine. The other compounds showed essentially irreversible waves, no reduction peak related to the oxidation peak being observed. In all cases, a reduction peak unrelated to the initial oxidation—reduction of the substituted chrysoidines was observed [11]. The anodic peak potentials of the various indicators are listed in Table 1.

These results are somewhat different from the data obtained by Ladanyi et al. [7] for 4-aminoazobenzene. Apparently the substituted chrysoidines are less subject to nucleophilic attack yielding electroactive products. No positive identification of the products was made by Ladanyi et al.

4-Hydroxychrysoidine

Figure 1 shows a cyclic voltammogram of 4-hydroxychrysoidine at the carbon paste electrode. This compound appeared to be the most reversible of the chrysoidines studied. The peak current function at slow scan rates is

TABLE 1

Anodic peak potentials of irreversible chrysoidine[a]

Indicator	E_p (v vs. SCE)	Indicator	E_p (v vs. SCE)
4-Nitrochrysoidine	No meaningful data	2-Methoxychrysoidine	0.780
4-Sulfochrysoidine	0.840	3-Methoxychrysoidine	0.902
4-Phenoxychrysoidine	0.790	Chrysoidine	0.800
2-Methylchrysoidine	0.860	4-Ethoxychrysoidine	0.730
3-Methylchrysoidine	0.960	4-Methoxychrysoidine	0.740
4-Methylchrysoidine	0.820	4-Hydroxychrysoidine	0.601

[a]Scan rate = 30 mV s^{-1}; carbon paste electrode. All indicator concentrations were 1.00 mM in 1 M H_2SO_4, except for the methylchrysoidines, where 3 M H_2SO_4 was used.

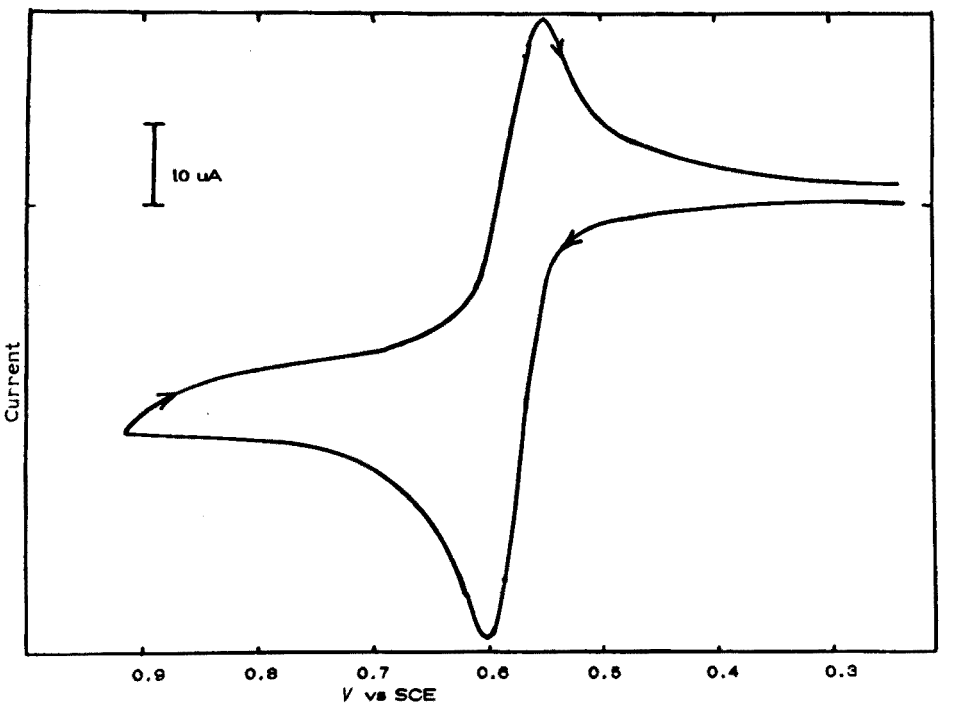

Fig. 1. Cyclic voltammogram showing related oxidation and reduction peaks for 4-hydroxychrysoidine, 1.0 mM in 3 M H_2SO_4. Scan rate, 30 mV s^{-1}.

similar to the peak current function measured for *o*-tolidine. It has been shown that the oxidation of *o*-tolidine is a two-electron oxidation process in strong acid solutions. [12]. The data in Table 2 indicate that the wave is much sharper than a one-electron oxidation, though not as sharp as a reversible two-electron oxidation. The broadness, as seen in the ΔE_p values, is probably due to a slow electron transfer. The theory of Nicholson [13] for

TABLE 2

Cyclic voltammetry of 4-hydroxychrysoidine
(1.05 mM indicator in 1.4 M H_2SO_4; glassy carbon electrode)

v ($V\,s^{-1}$)	E_p[a] (V vs. SCE)	ΔE_p (mV)	k_s ($\cdot 10^3 cm\,s^{-1}$, $\alpha = 0.45$)	E
0.01	0.552	40	1.9	0.532
0.02	0.556	53	1.1	0.530
0.05	0.559	51	1.9	0.534
0.1	0.563	56	2.2	0.534
0.2	0.570	75	1.6	0.533
		Av.	1.7 ± 0.4	

[a]Anodic peak potential, ΔE_p is the difference between the anodic and cathodic peak potentials, i.e. $E_{pa} - E_{pc}$.

a slow electron transfer was used to calculate the value of the heterogeneous rate constant, k_s, from the ΔE_p values (Table 2). From this information, the following mechanism can be proposed:

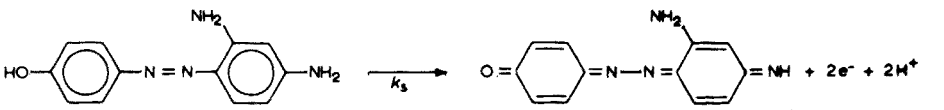

In addition, a two-electron oxidation of 4-hydroxychrysoidine is consistent with the results of chemical oxidation with cerium(IV) [8].

As the scan rate (v) was increased, the peak current function, $i_p\, v^{-\frac{1}{2}}\, C^{-1}$ (where C is the concentration of 4-hydroxychrysoidine), increased dramatically For $C = 0.74$ mM, the peak current function increases from 450 to 1740 $\mu A\, mM^{-1}\, (V/s)^{-\frac{1}{2}}$ for scan rates from 0.01 to 10 $V\,s^{-1}$. Thus it appears that 4-hydroxychrysoidine is adsorbed weakly on the electrode surface; in order to reduce adsorption, solutions were made up in 20 % ethanol. The variations in the peak current function for three different concentrations are shown in Fig. 2; the curves are consistent in shape with the theoretical derivations of Wopschall and Shain [14] for weak adsorption of reactant. The quasi-reversibility of the electron transfer makes it difficult to measure the degree of adsorption quantitatively; the addition of alcohol does reduce the degree of adsorption and increases the solubility.

In spite of adsorption, it is still possible to measure the apparent oxidation potential, $E^{\circ\prime}$, because the adsorption has a negligible effect on the wave at slow scan rates. The value of $E^{\circ\prime}$ can be calculated from the theory for quasi-reversible electron transfers [13]. A value of 0.533 V vs. SCE or 0.779 V vs. NHE was obtained for 4-hydroxychrysoidine. This compares with a value of 0.78 V vs. NHE determined from a titration with cerium(IV) [8].

4-Alkoxychrysoidine

The oxidation of 4-methoxychrysoidine and 4-ethoxychrysoidine is markedly different from that of the other substituted chrysoidines. Figure 3 shows a cyclic voltammogram of 4-ethoxychrysoidine. The most noticeable feature is the new couple at about 0.58 v vs. SCE. The peak current from the first oxidation still corresponds to two electrons, but adsorption is more severe than with 4-hydroxychrysoidine. The new couple which appears at 0.58 v is due to decomposition of the product of the two-electron oxidation of 4-ethoxychrysoidine. The peak potentials of the new couple are about the same as for 4-hydroxychrysoidine, though the wave is somewhat broader. This identification was further verified by obtaining a voltammogram with both 4-ethoxychrysoidine (EtOC) and 4-hydroxychrysoidine present. Where the new couple appears, only one wave was seen with no distortion of the peaks. The following mechanism is postulated:

$$EtOC \rightarrow [EtOC]^{2+} + 2e^-$$

$$[EtOC]^{2+} + H_2O \longrightarrow$$

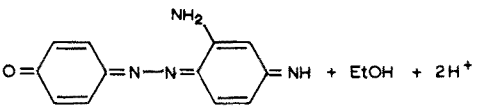

The actual sequence of the loss of electrons, protons and ethanol is unknown, but this reaction sequence has been suggested for 4-methoxyphenol [15]. No qualitative change in peaks were seen even at scan rates of 10 V s^{-1}, so that it was impossible to measure any of the rate constants involved. 4-Methoxychrysoidine gave results that were identical to the oxidation of 4-ethoxychrysoidine; again, a wave caused by 4-hydroxychrysoidine was seen, but no additional waves appeared at 10 V s^{-1}.

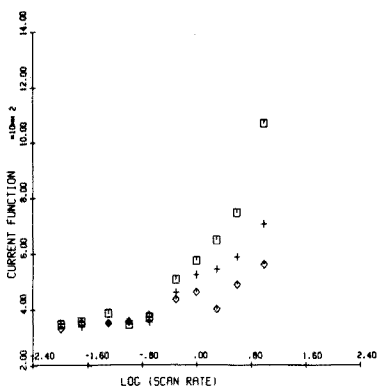

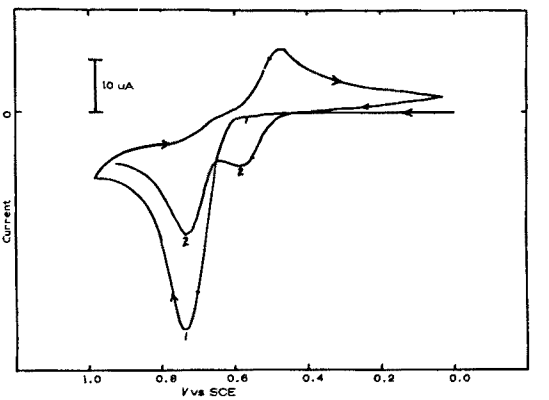

Fig. 2. Variation of peak current function for 4-hydroxychrysoidine with log v where v is the scan rate in V s^{-1}. 20 % ethanol, 1.4 M H_2SO_4. C: □ 0.35 mM; + 1.07 mM; ◇ 2.19 mM.

Fig. 3. Cyclic voltammogram for 4-ethoxychrysoidine in 1 M H_2SO_4, 1.0 mM in 3 M H_2SO_4. Scan rate, 30 mV s^{-1}.

The irreversibility of 4-ethoxychrysoidine is probably due to the short lifetime of the initial oxidation product. This irreversibility makes it impossible to measure the $E^{\circ\prime}$ value. The oxidation of 4-ethoxychrysoidine is probably not a reversible indicator reaction even though the color change, which is due to the 4-hydroxychrysoidine couple, is reversible. Thus the $E^{\circ\prime}$ value from the titration data is not a reversible, thermodynamic value.

4-Methylchrysoidine

4-Methylchrysoidine was studied as a typical substituted chrysoidine that gave an irreversible wave. It can be seen that adsorption still occurs, from the $i_p v^{-\frac{1}{2}} C^{-1}$ value in Table 3. No reduction of any oxidized product was seen at scan rates up to 20 V s^{-1}. The irreversibility may be due to a fast irreversible chemical reaction of the initial oxidation product, which would render the overall wave irreversible [7]. The ultimate product is probably not due to nucleophilic attack by water, for the compound formed should be reducible. There have been few previous studies of such compounds to provide any comparisons. On the basis of the voltammetric studies of the irreversible chrysoidines, it is easier to understand the titration data reported previously [8]. Because no reversible couple is formed, considerable drift in the potentials measured during the titration was observed. Finally, the color was not reversible because no easily oxidized stable product was formed in the oxidation of the substituted chrysoidines, except for the 4-hydroxy-, 4-ethoxy-, and 4-methoxy-chrysoidines.

Thus, cyclic voltammetry can be used to survey a series of related indicators to determine which form reversible couples that can give stable potentials. Secondly, for those indicators which are reduced reversibly, it is possible to measure the apparent oxidation potential of the indicator. This discussion assumes that the product of the electrochemical reaction is the same as the

TABLE 3

Cyclic voltammetry of 4-methylchrysoidine
(1.24 mM indicator; glassy carbon electrode)

v (V s^{-1})	$i_p v^{-\frac{1}{2}} C^{-1}$ (μA) mM^{-1} (Vs^{-1})$^{-\frac{1}{2}}$	E_p[a] (v vs. SCE)
0.01	323	0.835
0.03	358	0.858
0.1	357	0.880
0.3	361	0.895
1.0	411	0.930
4.0	407	0.933
10.	436	0.983

[a]Anodic peak potential.

product of the chemical oxidation. Matrka et al. [6, 17] have found that cerium(IV) oxidation of 4′-hydroxy-N,N-dimethyl-4-aminoazobenzene is the same as the electrochemical oxidation. That compound is very similar to 4-hydroxychrysoidine. The products of bromate oxidation are probably different from those of electrochemical oxidation because bromine can add to aromatic rings. In contrast, the initial products of chemical oxidation, e.g. with cerium(IV), will probably be the same as for the electrochemical oxidation; while potentials may be shifted because of complexation, very low pH values can be used to minimize that problem.

In conclusion, cyclic voltammetry can be used to establish which of the substituted chrysoidines give stable reversible products. In addition, the $E^{\circ\prime}$ value of 4-hydroxychrysoidine was found by cyclic voltammetry to agree well with the value calculated from the cerium(IV) titration [8].

We are grateful to the Marquette University Graduate School and Graduate School Committee on Research for support given to Ulrich J. Larsen in the form of research assistantships.

REFERENCES

1 E. Schulek and P. Rosza, Z. Anal. Chem., 115 (1939) 185.
2 E. Schulek and Z. Somogyi, Z. Anal. Chem., 128 (1948) 398.
3 E. Pungor and E. Schulek, Z. Anal. Chem., 150 (1956) 161.
4 R. Belcher and S. J. Clark, Anal. Chim. Acta, 4 (1950) 58.
5 R. W. Adler, M. S. Thesis, Marquette U., Milwaukee, Wis., 1966.
6 M. Matrka, J. Marhold and Z. Ságner, Collect. Czech. Chem. Commun., 34 (1969) 1615.
7 L. Ladanyi, M. Vajda and Gy. Vamos, Acta Chim (Budapest), 68 (1971) 47.
8 U. J. Larsen, R. A. Bournique, R. W. Adler and G. A. Klaus, Talanta, 21 (1974) 877.
9 R. N. Adams, Electrochemistry at Solid Electrodes, Dekker, New York, 1969, p. 281.
10 L. Meites, Polarographic Techniques, Interscience, New York, 2nd edn, 1965, p. 89.
11 L. Ladanyi, M. Vajda, A. Magi and Gy. Vamos, Acta Chim. (Budapest), 65 (1970) 245.
12 T. Kuwana and J. W. Strojek, Discuss. Faraday Soc., 45 (1968) 134.
13 R. S. Nicholson, Anal. Chem., 37 (1965) 1351.
14 R. Wopschall and J. Shain, Anal. Chem., 39 (1967) 1514.
15 D. W. Leedy, J. Electroanal. Chem., 45 (1973) 467.
16 D. H. Evans, J. Phys. Chem., 76 (1972) 1160.
17 M. Matrka and J. Marhold, Collect. Czech. Chem. Commun., 33 (1968) 4273.

Analytica Chimica Acta, 84 (1976) 173—177

ENZYMATIC DETERMINATION OF ACETAZOLAMIDE IN HUMAN PLASMA

GERALD J. YAKATAN, CAROL A. MARTIN and ROBERT V. SMITH

Drug Dynamics Institute, College of Pharmacy, University of Texas at Austin, Austin, Texas 78712 (U.S.A.)

(Received 24th October 1975)

SUMMARY

An enzymatic method utilizing carbonic anhydrase has been evaluated for the determination of acetazolamide in human plasma. A modified procedure, which is accurate, precise and rapid and is useful for bioavailability studies, is described.

Acetazolamide (5-acetamido-1,3,4-thiadiazole-2-sulfonamide,I) is employed for its diuretic effect and is used in the management of chronic simple and secondary glaucoma. Recent investigations in these laboratories of the bioavailability of acetazolamide from tablet dosage forms required a rapid, accurate and precise method for the determination of acetazolamide in plasma.

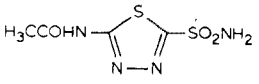

(I)

Bayne et al. [1] recently described a high-performance liquid chromatographic (h.p.l.c.) assay for acetazolamide, based on three liquid—liquid partition steps followed by h.p.l.c. on a reverse-phase column with aqueous methanol as the eluant, and Wallace et al. [2] have reported a gas chromatographic method for acetazolamide in plasma. Both these methods were too time-consuming for the large numbers of analyses that were expected in our bioavailability work. Attempts to devise colorimetric assays for acetazolamide in biological fluids have been reported to be only partially successful [1, 3].

Maren [4] devised an enzymatic method for acetazolamide, based on the inhibition of carbonic anhydrase which catalyzes the conversion of carbon dioxide to carbonic acid. The rate of formation of carbonic acid can be monitored through titration of a standard amount of base as measured with the indicator, phenol red. The "titration time", therefore, is directly proportional to the amount of acetazolamide added to a standard enzyme-alkali sample. Maren's method [4] has been investigated, validated, and modified for use in measuring therapeutically relevant levels of acetazolamide in human plasma.

EXPERIMENTAL

Apparatus

A reaction vessel was prepared according to Maren's specifications [4]. A cap for the exit tube was made from a disposable syringe plunger held in place during determinations by a sleeve of Tygon tubing. Reaction times were monitored with a bar-press timer calibrated in 0.1-s intervals (CGA Precision Scientific). Reagent and sample solutions were measured and dispensed with Eppendorf pipettes.

Reagents

Acetazolamide (a gift from Lederle Laboratories) showed λ_{max} at 265 nm in 0.1 M HCl, with a molar absorptivity of 10,500 l mol^{-1} cm^{-1} in agreement with the values published by Clark [5],(λ_{max} 265 nm, ϵ = 10,532). The reference acetazolamide revealed a single peak (retention time = 3.28 min) when chromatographed (2 ft × 2 mm Corasil/C18 column eluted with methanol—water (1:3) at 0.5 ml min^{-1}) on a high-performance liquid chromatograph equipped with a u.v.-photometric detector (Waters Associates ALC 202). All other solvents and reagents were of analytical reagent-grade quality.

Buffer and indicator solutions were prepared with deionized water as described by Maren [4]. Human heparinized blood, diluted 100-fold with deionized water, was used as a source of carbonic anhydrase.

Procedure

The reaction cell is purged constantly with CO_2 at 200—250 ml min^{-1} and immersed in an ice bath at 0 ± 0.5 °C; a 1-l beaker filled with ice and continuously stirred was employed. Before each determination, a glass rod (2 mm diam. × 15 cm) is dipped to a depth of about 2 mm in n-octanol, touched to the side of the octanol container, and then placed in the reaction cell.

Reagents, acetazolamide standard, and sample solutions are maintained at 0 °C. To evaluate the proper function of the cell, the uncatalyzed reaction rate is determined. The exit tube is stoppered, the octanol rod put in place, and 0.4 ml of phenol red solution, 0.3 ml of water, and 0.1 ml of carbonate buffer are added in that order. The timer is started simultaneously with the addition of the carbonate buffer. The uncatalyzed reaction occurs in approximately 60 s, as shown by the indicator color change from red to yellow.

Standard Curve. The catalyzed reaction rate is determined (for zero point on time vs. concentration of inhibitor curve) by treating 0.4 ml of phenol red solution with 0.05 ml of diluted human heparinized blood, 0.25 ml of water, and 0.1 ml of carbonate buffer. A typical catalyzed reaction occurs in 20 s.

The catalyzed reaction rate in the presence of varying amounts of inhibitor

(acetazolamide) is determined. The reaction cell (fitted with octanol rod) is treated with 0.4 ml of phenol red indicator solution, 0.05 ml of diluted human heparinized blood, 0.1 ml of acetazolamide solution, 0.15 ml of water and 0.1 ml of carbonate buffer. The reaction times are determined in triplicate for acetazolamide solutions containing 0.04, 0.12, 0.20, 0.28 μg ml^{-1}. Between each determination, the reaction cell is filled three times with cold water, twice with cold acetone and dried at reduced pressure. A standard curve (time vs. equivalent concentration of acetazolamide in plasma) is produced (Y coordinates, 0—20 s; reaction time minus catalyzed reaction time) by linear regression (Wang 600 programmable calculator); a correlation coefficient of 0.998 or greater was found.

Determinations in Plasma. Heparinized plasma is collected. Aliquots (0.1 ml) are diluted 25-fold with water and heated for 5 min at 100 °C on a water bath to destroy the native carbonic anhydrase. The diluted samples are assayed in triplicate, as described above for establishing the standard curve; values varying by less than ± 5 % should be produced. The average values are referred to the standard curve to assess the concentrations of acetazolamide in the samples.

If the reaction time for a sample exceeds the maximum value on the standard curve, the sample is diluted 2—4 times and the reaction time is redetermined.

RESULTS AND DISCUSSION

Maren's method [4] was evaluated for routine determinations of acetazolamide in plasma. Maren's cell was modified by placing a cap on the exit part, to prevent the migration of solution from the reaction cell into the exit tube. Omitting this closure decreases the precision.

A second modification of Maren's procedure [4] involved the use of a surfactant. Difficulty with foaming, which affects the visual detection of an end-point, was reported [4] but this problem is overcome by the surfactant, n-octanol, which is added to the reaction vessel by a thin glass rod.

Blood levels of acetazolamide generally lie in the range 1—19 μg ml^{-1} following oral administration of a single 250-mg tablet. Thus, plasma diluted 25- to 100-fold is suitable for determinations. Since plasma may also be a source of carbonic anhydrase, the effects of the dilution factor and the heating conditions (to destroy native enzyme) were studied as they influence the results of replicate determinations. Essentially identical results were achieved regardless of the dilution used (standard curves with correlation coefficients of 0.998 and equal slopes with plasma samples diluted 1:25, 1:50 and 1:100), and heating at 100 °C for 5 min produced a plasma sample which showed no influence of carbonic anhydrase, i.e. a reaction time of 60 s was observed for heated samples, indicating an absence of enzymatic activity (see Procedure). Furthermore there was no difference between determinations

performed with plasma from separate individuals (24 subjects) and pooled plasma (5 subjects).

With the modified procedure, standard curves having correlation coefficients equal to or greater than 0.998 were achieved consistently for the acetazolamide range 1—7 $\mu g\ ml^{-1}$. The accuracy and precision of the assay was assessed with plasma samples spiked as indicated in Table 1. In general, satisfactory recovery and reproducibility were achieved at all the levels analyzed.

Plasma levels for two patients treated with single oral doses of 250 mg (tablets) of acetazolamide were followed by the method described; the results are presented in Fig. 1 and are in good agreement with those reported by Bayne et al. [1].

The authors appreciate the help of Professor Thomas H. Maren during the early stages of this work. Support from the Food and Drug Administration U.S. Department of Health, Education, and Welfare, through contract 223-74-3139 is gratefully acknowledged.

TABLE 1

Accuracy and precision of determination for acetazolamide in plasma

Plasma conc. ($\mu g\ ml^{-1}$)	No. of samples	% Recovery		
		Range	Av.	s
1—2	4	93.9—111.2	104.2	9.0
3—4	5	93.5—107.3	102.1	5.1
5—6	5	90.2—111.8	102.9	7.5
7—9	9	92.4—112.8	104.4	5.7
Total	24	90.2—112.8	103.4	6.8

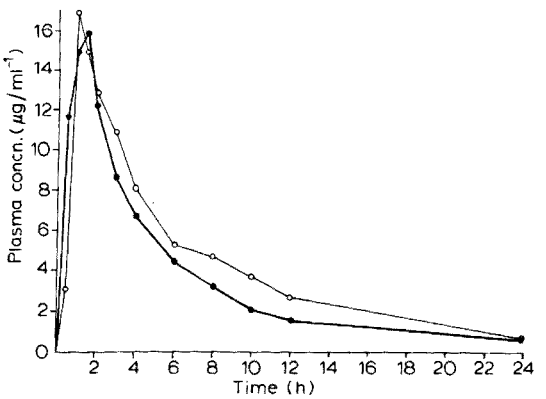

Fig. 1. Individual plasma levels of acetazolamide following oral administration of single 250-mg tablets to two patients, determined by enzymatic method.

REFERENCES

1 W. F. Bayne, G. Rogers, and N. Crisologo, J. Pharm. Sci., 64 (1975) 402.
2 S. M. Wallace, V. P. Shah, and S. Riegelman, presented at the APhA Academy of Pharmaceutical Sciences Meeting, 122nd Annual Meeting of the American Pharmaceutical Association, San Francisco, California, April, 1975.
3 T. H. Maren, V. I. Ash, and E. M. Bailey, Jr., Bull. Johns Hopkins Hosp., 95 (1954) 244.
4 T. H. Maren, J. Pharmacol. Exp. Ther., 130 (1960) 26.
5 E. G. C. Clarke, Isolation and Identification of Drugs, The Pharmaceutical Press, London, England, 1969, p. 170.

Analytica Chimica Acta, 84 (1976) 179—183

Short Communication

DETERMINATION OF GALLIUM BY ATOMIC ABSORPTION SPECTROMETRY WITH A GRAPHITE FURNACE ATOMIZER

C. PELOSI and G. ATTOLINI

Laboratorio Materiali Speciali per Elettronica e Magnetismo, MASPEC-C.N.R., 43100-Parma (Italy)

(Received 24th November 1975)

Recently there have been many reports of the determination of gallium by a.a.s. with flame techniques [1—5]. Langmyhr and Rasmussen [6] used a graphite furnace to obtain atomization from the solid state. The flame methods have poor sensitivity and their drawbacks, as well as the advantages of flameless techniques, have been discussed [7, 8].

In the work described here, the optimal conditions for the determination of gallium have been studied for aqueous solutions and for organic phases after extraction as cupferrate with butanol or chloroform; and this procedure has been used to determine gallium impurities in semi-conducting materials, e.g. $ZnIn_2S_4$. With a graphite furnace, i.e. a semi-static system, less sophisticated spectrometers are required than with dynamic techniques of flameless atomization (tungsten loop, carbon rod atomizer, etc.) which require a spectrometer with a fast response for optimal sensitivity [8, 9]. In the determination of elements with high boiling points for which only small samples are generally available, e.g. gallium, the graphite furnace technique is preferable.

Experimental

Apparatus and reagents. A Perkin-Elmer mode 306 atomic absorption spectrometer, hollow-cathode lamp operated at 20 mA, and an HGA74 graphite furnace were used, with a Hewlett-Packard model 7004B X—Y recorder. Signals were measured by the peak-height technique.

Samples (20 μl) were placed in the furnace with an Eppendorf micropipette. Separatory funnels (50 ml) with a teflon stopcock and 10-ml vessels were used to separate organic phases. To prevent adsorption phenomena, glass vessels were treated with Repellent 790 (Merck). High-purity argon and nitrogen purge gases were used.

Cupferron (Merck, p.a.), chloroform (Merck, Uvasol) and butanol (BDH, Analar) were used as received. Ammonium acetate buffer solution (pH 4.7) was prepared from Analar reagents. Deionized distilled water was used throughout.

For the standard solutions of gallium, zinc and indium (1000 p.p.m.), 1 g of the pure metal (Koch-Light 99.999 % for gallium) was dissolved in the minimum volume of 14 M HNO_3 and the solution diluted to 1 l with water.

Aqueous solutions of cupferron ($5 \cdot 10^{-3}$ M) were prepared daily to avoid oxidation.

Solvent extraction. Extraction of gallium cupferrate is quantitative in the pH range 1.5—12 when $5 \cdot 10^{-3}$ M cupferron solution is used [10] but the most suitable range was pH 4—6. Ammonium acetate buffer pH 4.7 was used. The aqueous phase was always tested before determination by a.a.s. to ensure that quantitative separation was accomplished. Shaking for 5—10 min was sufficient. Adsorption phenomena were noted at low concentrations. After the separatory funnels and vessels had been treated with repellent, the peak height and reproducibility were enhanced, e.g. the a.a.s. signal for a 2-p.p.m. extract of gallium in chloroform improved by a factor of two.

All data were obtained with equal volumes of organic and aqueous phase. Because of the solubility of butanol in water, a.a.s. measurements of these extracts necessitated a calibration against the correct volume ratio of the aqueous and organic phases.

A critical comparison was made of the various organic reagents which form extractable chelates with gallium. Cupferron was preferred because of the non-volatility of its metal chelates [10]; this is essential to avoid metal loss during the preliminary heating.

Analytical conditions. The analytical line at 287.4 nm was used with slit position 4. Figure 1 shows the signal variation for various gallium solutions when the flow rates of argon or nitrogen were increased. Argon at a low flow rate (about 1 on the flow meter, arbitrary units) gave the best sensitivity.

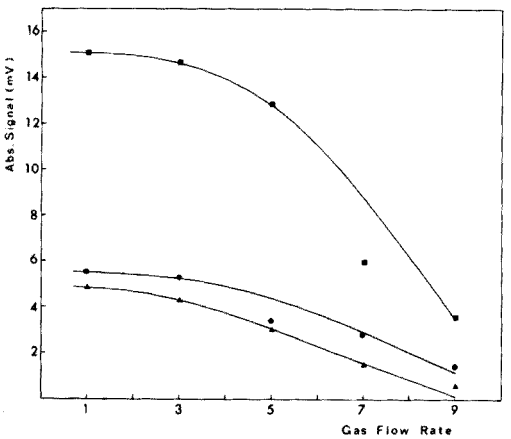

Fig. 1. Absorption signal vs. gas purge flow rate (in arbitrary units). (▲) 6 p.p.m. gallium cupferrate extract in chloroform, nitrogen flow; (●) 6 p.p.m. gallium cupferrate extract in chloroform, and (■) 6 p.p.m. aqueous gallium, argon flow.

Stopped flow and Mini-flow modes were tested; the latter was the more reproducible.

Chloroform (and some other organic solvents, e.g. benzene and carbon tetrachloride) are unsuitable for flame a.a.s. because of physical interferences [11]. The marked difference in sensitivity and detection limits may be attributed to small amounts of chlorine compounds arising from the thermal decomposition of chloroform; these compounds transport the gallium as chlorides from the centre towards the cooler ends of the furnace during thermal pre-treatment of the sample [12], according to chemical transport reaction theory [13]. To confirm this assumption, 20-μl aliquots of 10^{-2} M hydrochloric acid were added to 20-μl samples of gallium cupferrate in butanol; as expected, the absorption signal decreased strongly.

The optimal conditions for determination by a.a.s. were the following programs:

(i) for aqueous solutions, drying at 80 °C for 25 s, de-solvation at 220 °C for 20 s, and atomization at 2635 ° C for 5 s;

(ii) for butanol extracts, drying at 80 °C for 25 s, a programmed temperature rise from 220 °C to 630 °C (at about 300 °C min^{-1}), and atomization at 2635 °C for 5 s;

(iii) for chloroform extracts, only the programmed temperature stage was changed since better results were obtained in the range 220—1020 °C at 300 °C min^{-1}).

In each case, there was a final scavenging stage to eliminate interference from gallium deposited at the coldest ends of the graphite furnace.

Calibration curves and detection limits

Linearity of calibration holds up to 4 ng for the butanol extract, up to 200 ng for the chloroform extract, and up to 40 ng for aqueous gallium solutions; only slight curvature occurred for the range 4—25 ng Ga for the butanol extract or 200—400 ng Ga for the chloroform extract.

The detection limit (signal:noise = 2:1) was estimated at 0.5 ng for the aqueous solution and the butanol extract, and 5 ng for the chloroform extract under optimal conditions. Variations in the analytical response are possible because of physical conditions and ageing of the graphite tubes [14]. Sensitivities of 0.32 ng for aqueous solutions, 0.1 ng for butanol extracts and 2.5 ng for chloroform extracts were found.

Interference studies

The interference effects from zinc and/or indium were studied, to examine the applicability of the method to the determination of gallium when used as a doping element in the ternary compound $ZnIn_2S_4$. Zinc and indium nitrate were added, 1000 and 5000-fold, to 0.2-p.p.m. gallium solutions, and the mixtures were examined both directly in aqueous solution and after

extraction of gallium cupferronate in butanol. When the aqueous solutions were used, the absorption signal was masked; attempts were made to obtain selective volatilization with thermal programming but these proved unsuccessful. Determination of gallium was possible with butanol extracts; Fig. 2 shows the shape of the absorption peaks in the presence of various zinc and indium concentrations. It is evident that zinc does not interfere because it is only very slightly co-extracted in the organic phase and is volatilized selectively during the pre-atomization heating. When indium was present, a peak preceding the gallium absorption signal was noted. These double peaks, however, were well resolved and the light scattering from the atomization of indium gave no interference for the amounts used.

Single crystals of $ZnIn_2S_4$, weighing a few milligrams, were grown by the iodine chemical transport method [15]. After the addition of aliquots of gallium standard solution, the crystals were dissolved by slow heating in the minimal volume of 1 M nitric acid. Separation of the colloidal sulfur, which formed during the dissolution, was not necessary. The solutions obtained were transferred to a 10-ml volumetric flask and diluted to the mark. The analysis followed the procedure described previously for the extraction and determination of gallium; aliquots (1ml) were analysed by the standard addition method. In this way 10—30-mg samples containing down to 300 p.p.m. of gallium in the matrix could be analysed with an average deviation of 15 % (Table 1).

Conclusions

In the analysis of small single crystals of $ZnIn_2S_4$ doped with gallium, a microsampling technique was suitable. Since systematic work on the determination of gallium by flameless graphite furnace a.a.s. was not found

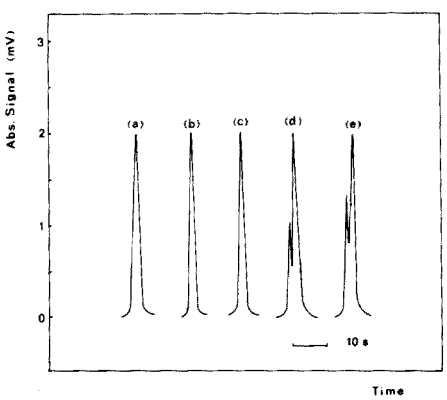

Fig. 2. Effect of an excess of zinc and indium added on the absorption signal of 0.2 p.p.n gallium extracted as cupferrate in butanol. (a) Gallium only, (b) and (d) 1000-fold amoui of zinc and indium, respectively, (c) and (e) 5000-fold amount of zinc and indium, respectively.

TABLE 1

Determination of gallium in single crystals of $ZnIn_2S_4$ (Three analyses of each sample were made)

$ZnIn_2S_4$ (mg)	Gallium (p.p.m.)		
	Added	Found	Error(%)
10.3	2427.0	2544.3	+4.0
26.9	929.3	947.3	+2.0
25.7	534.7	1031.0	+6.3
18.7	534.7	574.8	+7.5
31.7	315.4	362.0	+14.7

in the literature, a study was undertaken to find the optimal conditions for aqueous solutions and for chloroform or butanol extracts of gallium cupferrate. Chloroform was not a suitable extractant because of low-temperature transport reactions of gallium by chlorine compounds formed during the heating processes.

Optimized parameters and analytical systems for gallium were tested for the determination of gallium in the ternary compounds $ZnIn_2S_4$. Direct analysis of the samples after dissolution in aqueous solution failed. Matrix effects were partially eliminated by solvent extraction; light scattering by partially co-extracted indium did not interfere with the gallium absorption signal. The difference between the boiling points of gallium (2420 °C) and indium (2075 °C) was sufficiently large for a separation of gallium and indium to be avoided. This method of analysis is well-suited for routine work where only small samples are available.

The authors would like to thank the Consiglio Nazionale delle Ricerche for the support of this research.

REFERENCES

1 G. N. Lypka and A. Chow, Anal. Chim. Acta, 60 (1972) 65.
2 M. S. Cresser and J. Torrent-Castellet, Talanta, 19 (1972) 1478.
3 S. A. Popova, L. Bezur and L. Polos, Z. Anal. Chem., 270 (1974) 180.
4 Taketoshi Nakahara and Soichiro Musha, Anal. Chim. Acta, 75 (1975) 305.
5 A. Chow and W. Lipinsky, Anal. Chim. Acta, 75 (1975) 87.
6 F. J. Langmyhr and S. Rasmussen, Anal. Chim. Acta, 72 (1974) 79.
7 C. W. Fuller, Proc. Soc. Anal. Chem., 9 (1972) 279.
8 M.P. Bratzel, Jr., R.M. Dagnall and J.D. Winefordner, Anal. Chim. Acta, 48 (1969) 197.
9 G. Torsi and G. Tessari, Anal. Chem., 45 (1971) 1812.
10 J. Stary and J. Smizanska, Anal. Chim. Acta, 29 (1963) 546.
11 J. Aggett and T. S. West, Anal. Chim. Acta, 57 (1971) 15.
12 G. G. Welcher, O. H. Kriege and J. Y. Marks, Anal. Chem., 46 (1974) 1227.
13 H. Schäfer, Chemical Transport Reactions, Academic Press, 1964.
14 D. A. Segar and J. G. Gonzales, Anal. Chim. Acta, 58 (1972) 7.
15 R. Nitsche and W. J. Merz, Compt. Rend. Soc. Suisse Phys., 35 (1962) 274.
16 D. C. Hildebrand and E.E. Pickett, Anal. Chem., 47 (1975) 424.

Analytica Chimica Acta, 84 (1976) 185–188

Short Communication

THE RAPID DETERMINATION OF MERCURY IN SOLID SAMPLES BY HIGH-FREQUENCY INDUCTION HEATING AND ATOMIC ABSORPTION SPECTROMETRY

Y. KUWAE and T. HASEGAWA

Kansai Technical Centre for Environmental Pollution Control, 1, Tomishimacho, Nishi-ku, Osaka 550 (Japan)

T. SHONO

Department of Applied Chemistry, Faculty of Engineering, Osaka University, Yamada-kami, Suita, Osaka 565 (Japan)

(Received 24th November 1975)

Mercury in solid samples is often determined by digestion with sulfuric and nitric acids, reduction and vaporization into an atomic absorption spectrometer [1—6]. Combustion in the presence of a metal oxide catalyst in a quartz tube in an air or oxygen flow has been recommended recently [7, 8].

In the method described below, high frequency (h.f.) induction heating is used for the rapid release of mercury. Optimal conditions for the high-frequency generator voltage, heating interval and flow rate of the carrier gas (nitrogen) are described. The proposed method and a conventional digestion method were used simultaneously to analyse a standard mercury-containing sample; under optimal conditions, the recovery of mercury was 99.4 % on average compared with that by the wet digestion method, which was assumed to give 100.0 % recovery in the range studied (0.025—0.150 μg). Polluted soil and sediment were also analysed, the recoveries of mercury being 99.7 and 98.8 %, respectively. The proposed method is convenient, and about 5 min is adequate for prior treatment of samples.

Experimental

Chemicals. All the chemicals used, except for the standard sample, were commercially available materials of adequate purity.

The absorbent solution (0.5 % potassium permanganate in 0.5 M sulfuric acid) was prepared as described previously [9]. Iron sponge (99.99 % purity), used as the ferromagnetic material, was always treated by high-frequency heating to expel mercury and other impurities before use.

Standard sample containing mercury sulfide. This was prepared as follows. Sea sand was ground in a vibration mill, and heated at 900 °C in an electric furnace for 1 h to expel moisture. Mercury sulfide and the ground sand were

mixed with an electric blender, to give a 1.42 ± 0.03 $\mu g\ g^{-1}$ of Hg standard mixture. The content of mercury was determined by the wet digestion method.

Apparatus and procedure. The high-frequency induction furnace (Kokusai Electric Company), consisted of a high-frequency generator (13.56 M Hz), heating chamber, voltage regulator and other parts (Fig. 1). The heating chamber consists of a h.f. induction coil and a fusion pot which contains 1 g of iron sponge. Between the induction coil and the pot, there is a quartz tube through which nitrogen gas flowed. The fusion pot could be taken in and out easily.

Mercury in the fusion pot is expelled by heating and carried to the absorbent solution in the impinger (e). Mercury absorbed is then vaporized after addition of 1 ml of 10 % hydroxylamine solution and 2 ml of 10 % tin(II) chloride solution, into the atomic absorption spectrophotometer (Nippon Jarrel-Ash AA-1) for measurement. The assembly is shown in Fig. 2.

RESULTS AND DISCUSSION

Optimal conditions were established by measuring the recovery of mercury in the standard sample. The voltage to the high-frequency generator was regulated over the range 10—130 V; above 90 V, the recoveries were between 98 and 100 %, and 5 min sufficed for each sample. Measurement of the

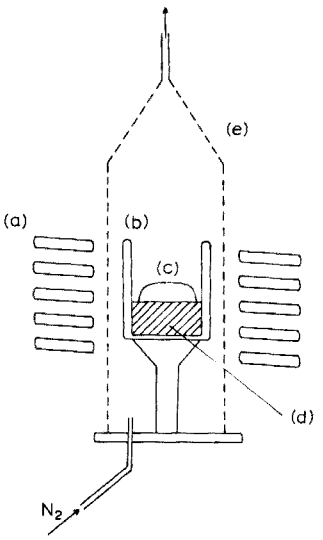

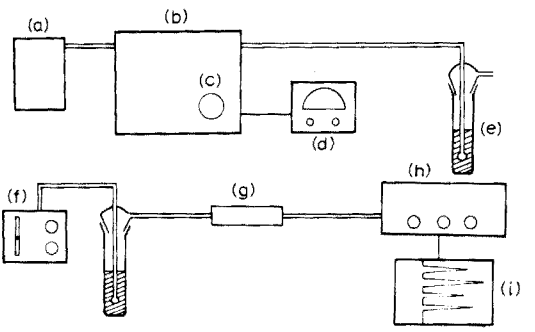

Fig. 1. The h.f. induction furnace (a) H.f. induction coil, 75-mm diam.; (b) fusion pot, 23-mm diam.; (c) sample; (d) iron; (e) quartz tube, 30-mm diam.

Fig. 2. Measurement assembly (a) N_2 gas supply; (b) heating unit; (c) timer; (d) voltage regulator; (e) impinger containing 20 ml of absorbent solution; (f) pump; (g) $Mg(ClO_4)_2$; (h) spectrometer; (i) recorder.

furnace temperature was rather difficult because of the slow response of the thermocouple (Pt—Pt/Rh, 13 %) and the inaccuracy caused by the h.f. self-induction.

The flow rate of carrier gas was examined over the range 0.15—1.00 l min^{-1}. The optimal flow rate was 0.30 l min^{-1}, which agrees with earlier results [9], but there was little difference in the recoveries when the flow rate varied from 0.2 to 0.4 l min^{-1}.

Calibration curve. A calibration curve for mercury in the standard sample was obtained under the following optimal conditions: voltage added, 110 V (a.c. 1.2 kW, 60 Hz); heating interval, 5 min; flow rate of carrier gas 0.3 l min^{-1}. Accurately weighed standard samples, containing mercury in the range 0.025—0.150 μg, were placed in the fusion pot and measured; several samples were analyzed at each level. A straight-line relationship was obtained over the range mentioned, recoveries being 99.2—99.6 % (av. 99.4 %). In these measurements, the relative standard deviations were ca. 3 %.

Analysis of raw samples. Polluted soil and sediment were dried over phosphorus pentoxide for 16 h; 100-mg samples were analysed. The results obtained are compared with those by the wet digestion method in Table 1. For these samples, 99.7 and 98.8 % recoveries* were obtained. The proposed method is adequate for routine testing of the above kinds of samples.

These results show that total mercury in solid samples can be determined satisfactorily by the h.f. induction heating method. Mercury sulfide, the most stable mercury-containing species, was used to establish the optimal conditions for analysis. Samples rich in organic mercury were not studied.

TABLE 1

Comparison of the results by two methods[a]

Sample		Present method	Digestion method
Soil	$\bar{x}$ (p.p.m.)	3.25	3.28
	s(p.p.m.)	0.061	0.052
	s_r(%)	1.9	1.6
	N	30	20
Sediment	$\bar{x}$ (p.p.m.)	6.07	6.15
	s(p.p.m.)	0.098	0.097
	s_r(%)	1.6	1.6
	N	30	20

[a] x = mean result. s = standard deviation. s_r = relative standard deviation. N = number of determinations.

*Recovery (%) = $\frac{\bar{X} \text{ by the present method}}{\bar{X} \text{ by the wet digestion method}} \times 100$ (%)

No prior chemical treatment of the sample is required. The present method is recommended for the rapid determination of mercury in solid samples such as polluted sand or soil, and is capable of successive operation.

REFERENCES

1 D. C. Manning, At. Absorption. Newslett., 9 (1970) 97.
2 Mercury in the National Environment: A review of recent work, Geological Survey of Canada, M 44-70-57 (1970) 39.
3 Mercury Contamination in Man and His Environment, Tech. Rep. Ser. No. 137 (1972).
4 I. K. Iskandar, J. K. Syers, L. W. Jacobs, D. R. Keeney and J. T. Gilmour, Analyst (London), 97 (1972) 388.
5 J. W. Hamm and J. W. B. Stewart, Commun. Soil Sci. Plant Anal., 4 (1973) 233.
6 J. E. Hawley and J. D. Ingle, Jr., Anal. Chem., 47 (1975) 719.
7 R. Tsugine, S. Ueda and T. Morita, Analyst (Japan), 22 (1973) 591.
8 R. J. Thomas, R. A. Hagstrom and E. J. Kuchar, Anal. Chem., 44 (1972) 512.
9 Y. Tanaka, K. Ikebe, R. Tanaka and N. Kunita, J. Food Hyg. Soc. Jap., 15 (1974) 386.

Analytica Chimica Acta, 84 (1976) 189—193

Short Communication

SPECTROPHOTOMETRIC DETERMINATION OF OSMIUM WITH DIETHAZINE HYDROCHLORIDE

H. SANKE GOWDA and P. G. RAMAPPA

Post-graduate Department of Chemistry, University of Mysore, Manasa Gangotri, Mysore (India)

(Received 30th October 1975)

Various chromogenic reagents proposed for the spectrophotometric determination of osmium have been reviewed [1—3]. New procedures for the trace determination of osmium based on its catalytic effect in specific redox reactions have been proposed [4, 5]. Recently, procedures based on the osmium complexes with ferrozine [6], β-benzoyl-α-(*o*-tolyl)thiourea [7], quinoxaline-2, 3-dithiol [8], rubeanic acid [9] and 2R acid [10] have been suggested.

Diethazine hydrochloride (DH, 10-[2-diethylaminoethyl]-phenothiazine hydrochloride) is a tranquilizing agent. It has been proposed for the spectrophotometric determination of palladium(II) [11] and as a redox indicator in vanadametry [12]. Microgram amounts of osmium(VIII) react with DH in hydrochloric or sulphuric acid medium to give a red coloured complex, and DH has been developed as a sensitive reagent for the spectrophotometric determination of osmium(VIII) with the advantages of simplicity, reasonable sensitivity, insensitivity to temperature, and rapid determination in high acid concentrations without the need for extraction or heating.

Experimental

Reagents. Osmium tetroxide (1 g: Johnson, Matthey Ltd., London) was dissolved in about 100 ml of 0.2 M sodium hydroxide solution and diluted to 1 l with doubly distilled water. The stock solution was standardized as described [13] by Ayres and Wells; working solutions were prepared, as required by dilution.

A stock solution of DH was prepared as described previously [11]. All other chemicals were of analytical-reagent grade.

Apparatus. A Beckman Model DB spectrophotometer with stoppered 1-cm silica cells was used.

Standard procedure. Transfer the sample solution containing 10—135 μg of osmium(VIII) to a 25-ml volumetric flask. Add sufficient hydrochloric

acid to make the final solution 3.0 M in hydrochloric acid. Add 5 ml of 0.2 % DH solution, dilute to the mark with doubly distilled water and mix. After 10 min, measure the absorbance at 515 nm against a reagent blank solution. Calculate the osmium concentration of the sample by reference to a previously prepared calibration curve.

Results and discussion

Diethazine hydrochloride is highly soluble in water and forms a red coloured complex with osmium(VIII) in the presence of hydrochloric or sulphuric acid. The maximum colour development takes place at room temperature. The sensitivity and stability of the red complex depend on the nature and concentration of the acid; the sensitivity is in the order HCl> H_2SO_4>H_3PO_4≫HAc. Although colour development is rapid initially, a period of 8, 10, 20 or 30 min is required to attain maximum absorbance in HCl, H_2SO_4, H_3PO_4 or HAc, respectively. Thereafter, the red Os—DH complex is stable in 3.0 N HCl, H_2SO_4, H_3PO_4 and HAc for 35, 10, 5 and 3 min respectively. Hydrochloric acid medium has therefore been selected. Nitric acid cannot be used as it oxidizes DH to a red coloured radical.

The absorption spectra of the Os—DH complex and of the reagent in 3 M hydrochloric acid are shown in Fig. 1. The maximal absorbance of the complex is at 515 nm, where the reagent does not absorb.

The effect of the hydrochloric acid concentration on the absorption of the complex was studied at 515 nm with solutions containing 50 μg of osmium and 5 ml of 0.2 % DH in 25-ml volumetric flasks. The absorbance increases gradually from 0.1 to 1.5 M acid and reaches a maximum in the range 2.0—4.0 M; at higher acidities the reagent slowly undergoes oxidation to a red radical and so 3.0 M was chosen for all further work.

The colour of the complex develops fully in 8 min after mixing, and an essentially constant absorbance is obtained over at least 35 min. The order of addition of the reagents is not critical.

The effect of varying reagent concentration was investigated by measuring the absorbance at 515 nm of solutions containing 50 μg Os. A 56-fold molar excess of the reagent over osmium was required for maximal absorbance; 5 ml of a 0.2 % reagent solution in a final volume of 25-ml sufficed for less than 5.4 p.p.m. of osmium.

The absorbance values were insensitive to temperature in the range 5—60 °C. Above 60 °C the absorbance gradually decreased.

Calibration, range and sensitivity. The Os—DH complex obeys Beer's law over the concentration range 0.4—5.4 p.p.m. of osmium (10—135 μg per 25 ml). The optimal working range is about 1.0—5.0 p.p.m. The molar absorptivity is $1.22 \cdot 10^4$ l mole^{-1} cm^{-1}, and the Sandell sensitivity is 0.0156 μg Os cm^{-2}.

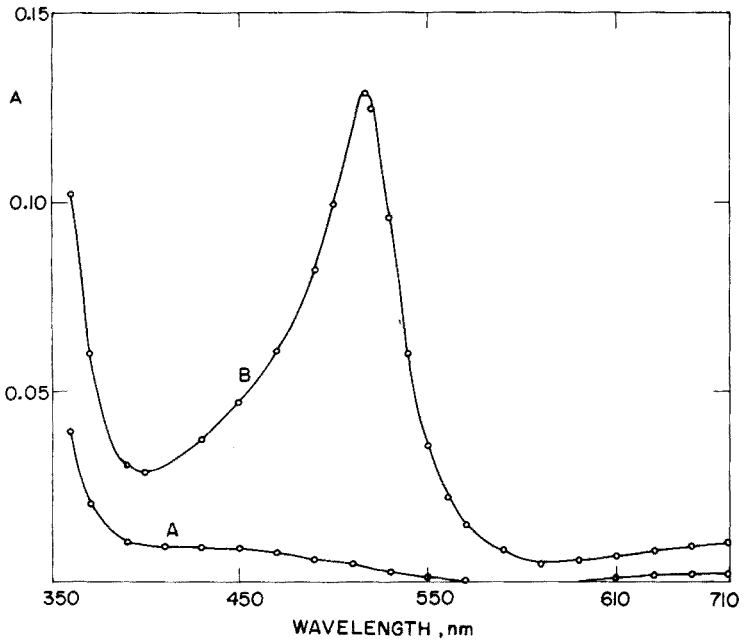

Fig. 1. Absorption spectra. A, Reagent blank vs. water; B, Os—DH complex vs. reagent blank [Os] = 10 μg, [DH] = $1.0 \cdot 10^{-4}$ M.

The sensitivity of the proposed method is greater than that of 0-β-benzoyl-thioureidol benzoic acid [14], 2-mercaptobenzothiazole [15], 1-carbamidine-3-methyl-5-pyrazolene [16], tiron [17] and β-benzoyl-α-(*o*-tolyl)thiourea [7] which have been proposed as sensitive spectrophotometric reagents for osmium(VIII). The sensitivity of the DH method is less than that of the catalytic methods [1, 2] or the rubeanic acid [9], ferrozine [6] and anthranilic acid [18] methods. In these methods, however, the formation of the complexes is quite slow in aqueous media at room temperature, and conditions for obtaining reproducible colour development are usually critical.

Composition and nature of the complex. The composition of the complex was studied by Job's method [19, 20] of continuous variations with equimolar solutions, and by the mole ratio method [21]. Both methods indicate the formation of a 1:2 complex between the metal and the reagent. The red solution of Os—DH was retained on Dowex 50W-X8 cation-exchange resin and not retained by Dowex 1-X8 anion exchange resin; this indicated that the complex is cationic.

Effect of diverse ions. In order to assess possible analytical applications of the reaction, the effects of some ions which often accompany osmium were

studied. Different amounts of ionic species were added to 50 μg of osmium in solution in 25-ml volumetric flasks and the colour was developed as in the procedure. The tolerance limits for various ions are shown in Table 1.

Determination of osmium in ores. Synthetic mixtures containing platinum metals (e.g., corresponding to osmiridium or syserkite) were prepared and the osmium content was determined. The results are shown in Table 2.

TABLE 1

Effect of diverse ions on the determination of osmium (Amount of Os(VIII) taken: 50 μg/25 ml)

Ion added	Tolerance limit[a] (μg ml^{-1})	Ion added	Tolerance limit[a] (μg ml^{-1})
Pt(IV)	10	Fluoride	2000
Rh(III)	10	Chloride	2000
Ru(III)	4	Bromide	1000
Ir(III)	10	Iodide	4
Pd(II)	2	Nitrate	1200
Au(III)	2	Sulphate	2500
Fe(III)	4	Phosphate	2000
Ag(I)	2	Oxalate	1000
V(V)	3	Acetate	800
Ce(IV)	2	EDTA	50
Ni(II)	100	Thiosulphate	4
Co(II)	50	Dichromate	4
Cu(II)	100	Permanganate	2
UO_2(IV)	100	Chloramine-T	4
		Chlorate	2

[a] Amount causing an error of less than 2.5 %.

TABLE 2

Determination of osmium in synthetic mixtures corresponding to osmiridium or syserkite

Osmium present (p.p.m.)	Ir (p.p.m.)	Ru (p.p.m.)	Pt (p.p.m.)	Osmium found (p.p.m.)
2.00	0.50	0.30	0.10	1.99
3.00	0.75	0.45	0.15	2.98
4.00	1.00	0.60	0.20	4.02

REFERENCES

1 F. E. Beamish and J. C. Van Loon, Recent Advances in the Analytical Chemistry of the Noble Metals, Pergamon, Oxford, 1972, p. 306.

2 F. E. Beamish, The Analytical Chemistry of the Noble Metals, Pergamon, Oxford, 1966, p. 366.
3 D. F. Boltz and M. G. Mellon, Anal. Chem., 46 (1974) 234R.
4 H. Mueller and M. Otto, Z. Chem. Lpz., 14 (1974) 159; Anal. Abstr., 27 (1974) 3299.
5 N. M. Lukovskaya and A. V. Terletskaya, Ukr. khim. Zh., 40 (1974) 1193; Anal. Abstr., 28 (1975) 323.
6 S. K. Kundra, M. Katyal and R. P. Singh, Curr. Sci., 44 (1975) 548.
7 S. K. Bhowal, Curr. Sci., 44 (1975) 157.
8 H. F. Janota and S. B. Choy, Anal. Chem., 46 (1974) 670.
9 S. K. Bhowal, Anal. Chim. Acta, 69 (1974) 465.
10 B. V. Agarwala and A. K. Ghose, Talanta, 20 (1973) 129.
11 H. Sanke Gowda and P. G. Ramappa, Indian J. Chem., 13 (1975) 418.
12 H. Sanke Gowda and R. Shakunthala, Z. Anal. Chem., 276 (1975) 80.
13 G. H. Ayres and W. N. Wells, Anal. Chem., 22 (1950) 317.
14 A. K. Majumdar and S. K. Bhowal, Anal. Chim. Acta, 35 (1966) 479.
15 B. C. Bera and M. M. Chakrabartty, Microchem. J., 11 (1966) 420.
16 S. N. Poddar and J. N. Adhya, Sci. Cul., 30 (1964) 50.
17 A. K. Majumdar and C. P. Savariar, Anal. Chim. Acta, 21 (1959) 146.
18 A. K. Majumdar and J. G. Sen Gupta, Anal. Chim. Acta, 30 (1964) 40.
19 P. Job, Ann. Chim., 9 (1928) 113.
20 H. Irving and T. B. Pierce, J. Chem. Soc., (1959) 2565.
21 J. H. Yoe and H. L. Jones, Ind. Eng. Chem., Anal. Ed., 16 (1944) 111.

Analytica Chimica Acta, 84 (1976) 195—199

Short Communication

EXTRACTION—SPECTROPHOTOMETRIC DETERMINATION OF COPPER IN TANTALUM AND NIOBIUM METALS WITH ZINC DIBENZYLDITHIOCARBAMATE

TSUTOMU FUKASAWA and TAKESHI YAMANE

Department of Applied Chemistry, Faculty of Engineering, Yamanashi University, Takeda 4, Kofu-shi (Japan)

(Received 29th September 1975)

Several spectrophotometric methods with reagents such as diethyldithiocarbamate [1], bathocuproine [2], dithizone [3] or 1-(2-pyridylazo)-2-naphthol [4] have been developed for the determination of copper in tantalum and niobium metals. In these methods, close control of acidity is usually necessary, and the procedures are not sufficiently sensitive for the analysis of high-purity tantalum and niobium metals.

In this communication an extraction-spectrophotometric method with zinc dibenzyldithiocarbamate (DBDTC) is described for the determination of copper in high-purity tantalum and niobium metals. The proposed method has the advantage that copper can be extracted from strongly acidic solution; close control of acidity is unnecessary. The method is simple and free of interference from other elements normally found in the samples. As little as 0.2 p.p.m. of copper can be determined with satisfactory precision and accuracy.

EXPERIMENTAL

Standard copper solution (500 μg Cu ml^{-1}). Dissolve 0.500 g of copper metal (99.9 %) in 15 ml of (1 + 1) nitric acid, and add 10 ml of (1 + 1) sulfuric acid followed by heating on a sand-bath; then dilute to 1 l with 30 ml of (1 + 3) sulfuric acid and water. Prepare more dilute solutions from this stock solution by dilution.

All the chemicals used were reagent grade.

Apparatus. A Hitachi Model EPU-2A spectrophotometer with 1-cm glass cells or 5-cm micro-cells was used for the studies. An Iwaki KM-shaker was used.

Recommended procedure. Transfer 1 g of the sample to 100-ml platinum dish, cover with a polyethylene cover and dissolve by gentle heating in 5 ml of

(1 + 1) hydrofluoric acid with dropwise addition of 3 ml of (1 + 1) nitric acid. After complete dissolution, wash the cover and inside of the dish, add 5 ml of (1 + 1) sulfuric acid and heat on a sand-bath until hydrofluoric acid and nitric acid are almost expelled. Avoid over-heating, because white precipitates may be produced; if this happens, dissolve the precipitate by addition of small amounts of (1 + 1) hydrofluoric acid, and heat on a sand-bath again. Cool the solution and add 10 ml of 25 % (w/v) tartaric acid solution and 5 ml of 4 % (w/v) boric acid solution. Transfer the solution to a 100-ml separating funnel and dilute to about 50 ml. Add 10.0 ml of a 0.03 % (w/v) zinc—DBDTC solution in carbon tetrachloride and shake for 3 min. After phase separation, drain the organic solution through a filter-paper into the cell. Measure the absorbance at 438 nm against a reagent blank.

RESULTS AND DISCUSSION

Figure 1 shows the absorption spectra of the organic phases obtained by the Zn—DBDTC—carbon tetrachloride extraction from a solution containing 5 μg of copper, from a sample solution prepared by dissolution of 1 g of tantalum metal, and from the reagent blank solution, respectively. The copper complex with DBDTC shows maximal absorbance at ca. 438 nm. The presence of tantalum caused some increase in absorbance at wavelengths shorter than 370 nm, probably because of partial extraction of a tantalum complex. However, there was no shift of the wavelength of maximum absorbance for the copper complex for any of the solutions. A second extract of the sample solution after the aqueous solution had been washed with carbo tetrachloride, showed virtually no absorption at 438 nm. A single extraction is therefore sufficient for the quantitative extraction of copper, even in the presence of tantalum. Similar results were obtained in the presence of niobium

The sulfuric acid concentration in the aqueous phase did not affect the extraction of copper; a constant absorbance value was obtained over the range

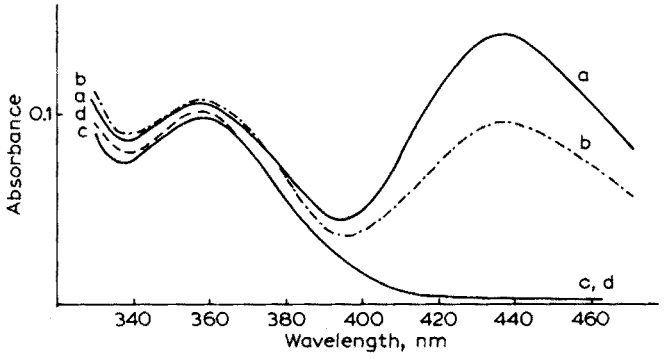

Fig. 1. Absorption spectra. a, Extraction of 5 μg of copper (standard solution); b, first extraction of copper in the presence of 1.00 g of tantalum; c, reagent blank; d, second extraction of copper in the presence of 1.00 g of tantalum. Reference: carbon tetrachlorid

0.25—3 M sulfuric acid. Hydrofluoric acid remained in the sample solution; up to 20 ml of (1 + 14) hydrofluoric acid, did not interfere with the extraction and determination of copper.

No significant interference was observed from 500 μg of Fe(III), Ni, Co, Mn(II), Al, Ti(IV), Ca, Mg, Pb, Cd, Cr(III), As(III) or W(VI), or from 150 μg of Ag, Mo(VI) or V(V). Bismuth interfered seriously at the 10-μg level, but this interference could be eliminated by washing the organic phase with 7 M hydrochloric acid after the extraction. Accordingly, the recommended procedure can be described as free from interference by other trace metals commonly contained in tantalum and niobium metals.

The copper complex with DBDTC in carbon tetrachloride obeyed Beer's law over the range 0—25 μg (with 1-cm cells) or 0—5 μg (with 5-cm microcells) of copper and the color of the complex was stable for at least 2 h.

The proposed method was applied to the determination of copper in high-purity powdered tantalum and niobium samples. These results are given in Tables 1 and 2. The results in Table 1 for sample 1 are in good agreement with the results obtained by other methods which were proposed for the JIS Committee on Analysis of Tantalum [5].

TABLE 1

Determination of copper in tantalum by the proposed method[a]

Sample	Taken	Cu added	Cu found	Cu in sample		Mean	S.d.
	g	μg	μg	μg	(p.p.m.)	(p.p.m.)	
1	1.000		0.2	0.2	0.2	0.2[a]	0.07
	1.000	5.0	5.2	0.2	0.2		
	1.000	10.0	10.3	0.3	0.3		
	1.000	15.0	15.1	0.1	0.1		
1[b]	1.001		0.2	0.2	0.2	0.2[a]	0.04
	1.457		0.4	0.4	0.3		
	1.001	1.0	1.2	0.2	0.2		
	1.000	2.0	2.2	0.2	0.2		
	1.000	3.0	3.2	0.2	0.2		
2	0.635		1.9	1.9	3.0	3.2	0.1
	1.004		3.2	3.2	3.2		
	1.500		4.6	4.6	3.1		
	1.001		3.2	3.2	3.2		
	0.618	5.0	6.9	1.9	3.1		
	1.000	5.0	8.3	3.3	3.3		
	1.500	5.0	9.9	4.9	3.3		
	0.998	10.0	13.2	3.2	3.2		

TABLE 1 (continued)

Sample	Taken g	Cu added μg	Cu found μg	Cu in sample μg	Cu in sample (p.p.m.)	Mean (p.p.m.)	S.d.
3	0.500		9.5	9.5	19.0	18.6	0.2
	1.000		18.5	18.5	18.5		
	1.000		18.6	18.6	18.6		
	1.000	5.0	23.4	18.4	18.4		
	0.500	5.0	14.4	9.4	18.8		

[a]Comparison with other methods [5].
Diethyldithiocarbamate-photometry, Cu < 1 p.p.m.; flameless atomic absorption spectrometry, 0.3; atomic absorption spectrometry after anion-exchange separation, 0.15; anodic stripping voltammetry, 0.22.
[b]5-cm micro-cells were used.

TABLE 2

Determination of copper in niobium by the proposed method

Sample	Taken g	Cu added μg	Cu found μg	Cu in sample μg	Cu in sample p.p.m.	Mean (p.p.m.)	S.d.
10	1.013		12.0	12.0	11.8	12.0	0.3
	1.005		11.8	11.8	11.7		
	0.998		12.4	12.4	12.4		
	0.643		7.7	7.7	12.0		
10[a]	0.819		9.8	9.8	12.0	12.1	0.1
	0.819		10.0	10.0	12.2		
	0.410		5.0	5.0	12.2		
	0.410		4.9	4.9	12.0		
11	1.000		4.8	4.8	4.8	3.9	0.6
	1.000		4.0	4.0	4.0		
	1.000		3.5	3.5	3.5		
	1.000		3.2	3.2	3.2		
11[a]	0.963		3.5	3.5	3.6	3.6	0.1
	0.963		3.6	3.6	3.7		
	0.963	5.0	8.6	3.6	3.7		
	0.963	10.0	13.4	3.4	3.5		
	0.963		3.5	3.5	3.6		
12[a]	0.922		4.1	4.1	4.4	4.5	0.2
	0.922		4.2	4.2	4.6		
	0.922	5.0	8.9	3.9	4.2		
	1.383		6.3	6.3	4.6		
	1.383		6.4	6.4	4.6		

[a]Samples taken were 8.192 g, 9.626 g and 9.224 g for samples 10, 11 and 12, respectively. The sample was dissolved in hydrofluoric acid and nitric acid as described above and then diluted to 100 ml. From this sample solution 5-, 10- or 15-ml aliquots were transferred to platinum dishes and treated as described in the recommended procedure.

There were significant differences in the analytical values for copper from the same niobium sample (Table 2, Sample 11). This difference was attributed to segregation of copper in the sample. Therefore, a large sample was dissolved and different aliquots of the sample solution were used for determination; there were then no significant differences in the results for copper.

The reproducibility of the method is very good and the recovery of added copper is also good. The method is applicable to the analysis of tantalum and niobium metals containing as little as 0.2 p.p.m. of copper by the use of 5-cm micro-cells and the standard addition method.

REFERENCES

1 J. Hastings, T. A. McClarity and E. J. Broderick, Anal. Chem., 26 (1954) 379.
2 E. M. Penner and W. R. Inman, Talanta, 10 (1963) 407.
3 V. A. Nazarenko, E. A. Biryuk, M. B. Shustova, G. G. Shitareva, S. Ya. Vinkovetskaya and G. V. Flyantikova, Zavod. Lab., 32 (1966) 267.
4 O. Grossmann and H. Grosse-Ruyken, Z. Anal. Chem., 233 (1968) 14.
5 Data from the JIS Committee on Analysis of Tantalum 1974.

Analytica Chimica Acta, 84 (1976) 201—202

Short Communication

SPECTROPHOTOMETRIC DETERMINATION OF TRACES OF WATER IN ORGANIC SOLVENTS (OXYGEN-FREE MOLECULES)

ERVIN JUNGREIS

Department of Inorganic and Analytical Chemistry, The Hebrew University of Jerusalem, Jerusalem, (Israel)

(Received 16th October 1975)

The color change of cobalt compounds upon hydration is the basis of a photoelectric method for the estimation of moisture in fuel gases [1—3]. The liberation of acetylene from calcium carbide on reaction with water, can be followed by colorimetric measurement of copper(I) acetylide [4]. Formation of orange—red $LiCuCl_3$ has been utilized for moisture determination [5]. Water has also been determined spectrophotometrically with solvatochromic dyes [6] and with the magnesium perchlorate—isobutyl methyl ketone—potassium bichromate system [7].

The simple method presented here is based on hydrolysis of $NH_4Al(SO_4)_2 \cdot 12H_2O$ and on subsequent liberation of iodine from a potassium iodide—iodate mixture. As the liberated iodine gives a coloration in organic solvents such as benzene, benzine, carbon tetrachloride, chloroform, dichloroethane, hexane, and toluene, spectrophotometric measurement of moisture in these solvents is feasible without any further iodine reagent. This reagent system does not react with water in oxygen-containing solvents, such as ethers, alcohols, ketones, nitro compounds, dimethylsulfoxide and ethyl acetate. Most probably, coordination of the water molecule to the oxygen atom causes this inactivity.

Experimental

Reagent powder I. Ammonium aluminium sulphate (Baker "AnalaR" pulverized).

Reagent powder II. Finely powdered potassium iodate (Baker "AnalaR") was heated to incipient fusion in a quartz crucible to convert the iodate partially to iodide. The cooled mass was pulverized.

Procedure. The determination was carried out in 10- ml volumetric flasks. Calibration curves were prepared for dry benzene, toluene, chloroform, carbon tetrachloride, dichloroethane, hexane and benzine containing 0.01 %, 0.02 %, 0.05 % and 0.1 % water.

Reagent powders I and II (50 mg of each) were added to the sample and mixed thoroughly. The color was formed fully in 2—3 min, and remained stable for hours. The absorbance was measured at 530 nm. Beer's law was obeyed in the range 0.01—1 % of water.

For example, the calibration curve for carbon tetrachloride containing various amounts of water is based on the following measurements of absorbance:

% Water in CCl_4	0.00	0.01	0.02	0.05	0.10
Absorbance	0.00	0.015	0.032	0.072	0.135

Interferences. The presence of more than 1 % of an oxygen-containing solvent partially or totally inhibits iodine formation. This effect was observed for the following solvents: methyl, ethyl, propyl, butyl, and amyl alcohols, acetone, 1,4-dioxane, diethyl ether, ethyl acetate, nitromethane, and dimethylsulfoxide.

REFERENCES

1 R. J. Pfister and D. J. Kesley, Amer. Soc. Test. Mater. Bull., 127 (1944) 17.
2 B. L. Ferguson and N. M. Coulter, Proc. Indiana Acad. Sci., 63 (1953) 124.
3 A. Taiichi, Anal. Chem., 40(3) (1968) 648.
4 H. Hartley and H. R. Raikes, J. Chem. Soc., 127 (1925) 524.
5 E. Jackwerth and H. Specker, Z. Anal. Chem., 171(4) (1959) 270.
6 S. Kumoi, H. Kobayashi and K. Veno, Talanta, 19(4) (1972) 505.
7 C. L. Luke, Anal. Chim. Acta, 54 (1971) 447.

Analytica Chimica Acta, 84 (1976) 203—205

Short Communication

A SENSITIVE COLORIMETRIC DETERMINATION OF 2-PHENYLPHENOL*

K. L. BAJAJ**, I. R. MILLER and I. S. BHATIA

Department of Chemistry and Biochemistry, Punjab Agricultural University, Ludhiana (India)

(Received 23rd June 1975)

2-Phenylphenol is used [1] as a fungicide for the post-harvest treatment of citrus fruits and as a preservative for paints, cosmetics and sizing materials [2]. This communication describes a sensitive colorimetric method for the micro determination of 2-phenylphenol with 4-aminoantipyrine (4-aminophenazone) and chloramine-T which is more sensitive and accurate than the methods in which potassium hexacyanoferrate(III) is used as the oxidizing agent [3—4].

Experimental

Reagents and equipment. Solutions were prepared from analytical-grade reagents. Organic solvents were distilled before use. Aqueous solutions were prepared from twice-distilled deionized water.

For the stock 2-phenylphenol solution (0.001 M), of 17 mg of 2-phenylphenol was dissolved in 100 ml of dioxane.

A Spectronic 20 Bausch and Lomb colorimeter with 10-mm cell was used.

Calibration curve. Take appropriate amounts of the stock solution of 2-phenylphenol (0.01, 0.02, 0.04, 0.06, 0.08, 0.1 and 0.12 ml) in 25-ml-measuring flasks. Add 4 ml of aqueous 1 % (w/v) chloramine-T solution followed by 0.5 ml of aqueous 0.4 % (w/v) 4-aminoantipyrine solution and dilute to the mark with sodium carbonate—hydrogencarbonate buffer (pH 9.7). Prepare the blank similarly, without 2-phenylphenol, and read the absorbance at 520 nm against the blank. The color is stable for at least 3 h.

Results and discussion

The reaction product of 4-aminoantipyrine with 2-phenylphenol in the presence of chloramine-T as oxidizing agent has a sharp absorption maximum at 520 nm. Beer's law holds in the range $0.17—2.4 \cdot 10^{-5}$ g of 2-phenylphenol

*Paper presented in the 43rd Annual Meeting of the Society of Biological Chemists. (India), Ludhiana, November, 1974.

**Present address: Tocklai Experimental Station, Jorhat-8, Assam, India.

per 25 ml of the final solution.

When aliquots (0.06 ml) of the stock solution of 2-phenylphenol were treated with 2, 4, 6 and 8 ml of chloramine-T solution, the presence of excess of chloramine-T did not interfere with the absorbance, and 4 ml was used in subsequent determinations. Similarly, an excess of 4-aminoantipyrine did not affect the absorbance, and 0.5 ml of its solution was used subsequently.

Since the reaction of 4-aminoantipyrine with phenolic compounds takes place at alkaline pH [5], aliquots (0.06 ml) of 2-phenylphenol solution were treated with carbonate—hydrogencarbonate buffers of pH 9.2, 9.7, 10.2 and 10.7. No change in absorbance in this pH range was observed, and pH 9.7 was used subsequently, as recommended by previous workers [3—4].

The results of replicate analyses (Table 1) show that the method is accurate and reproducible.

TABLE 1

Reproducibility of the determination of 2-phenylphenol

Weight taken (μg)	5.1	20.4
Mean value found (μg) (5 determinations)	4.98	19.52
S.d.	0.0374	0.0316
R.s.d.	0.75 %	0.16 %

Percentage recovery from thin-layer chromatograms. T.l.c. is often used for the separation of 2-phenylphenol. The stock solution of 2-phenylphenol (10 μl) was applied to an activated silica gel G plate, which was developed in chloroform—acetone (1 : 1) and viewed under u.v. light to locate the 2-phenylphenol, which was eluted with dioxane. The solution was concentrated and the volume made up to 5 ml. For 10-μl aliquots, the recovery was 99.7 ± 1.5 (4 determinations).

Determination of 2-phenylphenol in urine. A known volume of a concentrated ethyl acetate extract of rat urine was subjected to t.l.c. as described above. The concentration of 2-phenylphenol found by this method in 0.1 ml of the eluate was 18.8 μg; when hexacyanoferrate(III) was used as an oxidizin agent (λ_{max} 510 nm) a value of 16.6 μg was obtained.

Sensitivity and interferences. The minimum quantity of 2-phenylphenol detected by this method was $6.8 \cdot 10^{-8}$ g ml^{-1}, hence the method is more sensitive than those employing [3, 4] potassium hexacyanoferrate(III) as oxidant. This method is also more convenient than that recently proposed by Rajzman [6].

Since the method is based on the Emerson reaction [5], phenolic compounds give different colour reactions when treated with 4-amino-antipyrine and chloramine-T, e.g. phenol (red), pyrogallol and resorcinol

(brown) and 4-phenylphenol, salicylic acid and benzidine (pale yellow). Aromatic compounds lacking a phenolic or amino group do not give any colour reaction, so this method can be used to estimate 2-phenylphenol in the presence of biphenyl. In the presence of other phenolic compounds, the separation of 2-phenylphenol by t.l.c. is required.

REFERENCES

1 A. Rajzman, Analyst (London), 95 (1970) 490.
2 P. H. Caulfield and R. J. Robinson, Anal. Chem., 25 (1955) 982.
3 R. Mistres, M. Dudieuzers-Priu, J. C. Gaillard and J. Tourte, Ann. Fals. Expert. Chim., 60 (1967) 331.
4 E. Kroller, Dt. LebensmittRdsch., 63 (1967) 242.
5 E. I. Emerson, J. Org. Chem., 8 (1943) 417.
6 A. Rajzman, Analyst (London), 97 (1972) 271.

Analytica Chimica Acta, 84 (1976) 207—210

Short Communication

THE THERMOMETRIC DETERMINATION OF SOME ALDEHYDES BY HYDRAZONE FORMATION WITH UNSYMMETRICAL DIMETHYLHYDRAZINE

L. S. BARK and P. PRACHUABPAIBUL*

Ramage Laboratories, University of Salford, Salford M5 4WT (England)

(Received 14th January 1975)

The few reported determinations of aldehydes by thermometric methods [1—6] have generally involved reaction with phenylhydrazine [2, 3]; 2,4-dinitrophenylhydrazine [4, 5]; bisulphite [6]; or hydroxyammonium chloride [6]. The advantages of addition of known excess of reagent, and then determination of the excess, for reactions which are mainly non-ionic, have been previously discussed [5], and direct titrations have been reported only for a very restricted range of compounds. The various reactions which have been used in the determination of aldehydes have been extensively reviewed; Siggia's work [7] is generally regarded as definitive in this area.

Unsymmetrical dimethylhydrazine (UDMH) reacts rapidly with aldehydes to give the corresponding hydrazones, and it is well established that many hydrazones of aromatic aldehydes are only weakly acidic compared to the free hydrazine. It is thus possible to have a serial titration involving an acid-base system in which the free hydrazine is titrated before the hydrazone.

Siggia [7] has reported that the reactions between UDMH and the aldehydes proceed better in polar solvents, but because of the relatively low solubility in water of most samples containing aromatic aldehydes, the use of water is severely restricted. Ethylene glycol is a polar solvent which is suitable for solubility reasons, and in which reactions occur relatively readily. This solvent does not, however, favour electrometric methods of equivalence-point detection, and visual methods are not generally viable in the coloured industrial samples often encountered. Thus thermometric methods are considered to have potential in such circumstances.

Investigation of the reaction times for aldehydes with UMDH indicated that whilst most of the aliphatic aldehydes reacted completely at room temperature within 30 min, aromatic aldehydes required more than 2 h. In all cases, the reaction was apparently complete if the reactants were refluxed for approximately 30 min; this procedure was therefore adopted.

*On leave from the University of Chiengmai, Thailand.

Several aliphatic and aromatic ketones were subjected to the same procedure. In agreement with previously reported work [7], the presence of excess of the hydrazine could not be detected in the presence of the hydrazone.

Experimental

Apparatus. The apparatus [8] consisted essentially of a d.c. Wheatstone bridge having a 10 kΩ thermistor acting as one of the arms and as a temperature sensor in the titration vessel. The titrant was delivered by a multiroller peristaltic pump; temperature changes in the titration vessel were recorded on a strip chart potentiometer.

Reagents. Aldehydes and ketones were purified by distillation or recrystallization, as appropriate, until the m.p. or b.p. agreed with published values. The aldehydes used are listed in Table 1.

An approximately 0.75 M solution of UDMH in ethylene glycol was standardized thermometrically with a standard solution of hydrochloric acid in methanol. (The actual molarity of the solution was 0.737 ± 0.002 M).

An approximately 1.5 M solution of hydrochloric acid in methanol was standardized thermometrically against tris(hydroxymethyl)aminomethane.

Procedure. Add a known weight of the aldehyde to an excess of UDMH solution and reflux for 30 min. After complete reaction, transfer the mixture quantitatively with methanol to the titration vessel. Titrate with the hydrochloric acid solution at a rate of 0.442 cm^3 min^{-1}, recording the temperature change on the chart potentiometer (10 mV f.s.d.) at a chart speed of 30 mm min^{-1} (corresponding to a distance of 67.8 mm cm^{-3} of titrant added). Calculate the volume of titrant added from the approximate length of the trace. Run blank determinations in the same manner, and calculate the amount of aldehyde from the difference between the blank and sample determinations.

Results and discussion

Results for the aldehydes studied are shown in Table 1.

By analogy with the well-established behaviour of substituted benzoic acids and many other compounds, it is to be expected that the basic character of the hydrazones will be affected by the position and nature of the substituent in the benzaldehyde nucleus, and that various divisions of hydrazones will be apparent, depending on the differences in the basicities of the hydrazone and the unreacted UDMH. Three types of enthalpogram were obtained for the titration of the excess of UDMH in the presence of the aldehyde hydrazones (Fig. 1). Enthalpograms of Type 1 are expected of hydrazones which have an extremely low basicity compared to that of UDMH.

TABLE 1

Thermometric determination of aldehydes

Samples	Type	Amount taken (g)	Amount found (g)	Recovery %
Acetaldehyde	2	0.0165	0.0162	98.2
		0.0275	0.0268	97.45
3-Phenylpropenal	3	0.1609	0.1575	97.9
(Cinnamaldehyde)		0.1249	0.1207	96.6
Butanal		Not possible		
2-Butenal[a]	2	0.0161	0.0143	88.8
(Crotonaldehyde)		0.0404	0.0354	87.6
Furfural	3	0.1507	0.1484	98.4
		0.1294	0.1282	99.0
Benzaldehyde	2	0.1414	0.1426	100.9
		0.1216	0.1223	100.6
2-Hydroxybenzaldehyde	1	0.1392	0.1376	98.9
(Salicylaldehyde)		0.2884	0.2836	98.4
3-Hydroxybenzaldehyde	2	0.0608	0.0617	101.5
		0.1004	0.1021	101.7
4-Hydroxybenzaldehyde	3	0.1004	0.1001	99.7
		0.1410	0.1431	101.5
2-Methoxybenzaldehyde	2	0.0740	0.0741	100.2
		0.1130	0.1138	100.7
4-Methoxybenzaldehyde	2	0.1384	0.1400	101.15
(Anisaldehyde)		0.1661	0.1680	101.1
3,4-Dimethoxybenzaldehyde	2	0.1574	0.1597	101.4
(Veratraldehyde)		0.1614	0.1629	101.0
3,4-Methylenedioxy-benzaldehyde	2	0.1272	0.1266	99.55
(Piperonaldehyde)		0.1939	0.1914	98.71
3-Methoxy-4-hydroxy-benzaldehyde	2	0.1099	0.1133	103.09
(Vanillin)		0.1439	0.1459	101.38
3-Nitrobenzaldehyde	1	0.1136	0.1156	101.76
		0.2102	0.2130	101.33
4-Chlorobenzaldehyde	2	0.1274	0.1281	100.5
		0.1421	0.1447	101.8

[a]The purity of this sample was found to be 88—90 % by other methods.

Thus a sharp break is seen at the equivalence point, and the hydrazone does not react with excess of acid. Type 2 represents those hydrazones which have a noticeable basicity, but which are still significantly less basic than UDMH. After the UDMH has been neutralized, the hydrazone reacts with the acid, and a second end-point is obtained. This can be used to confirm the amount of aldehyde present in the sample. Type 3 is obtained when the basicity of the hydrazone approaches that of the unreacted UDMH and the equivalence point must be located by extrapolation. However, the

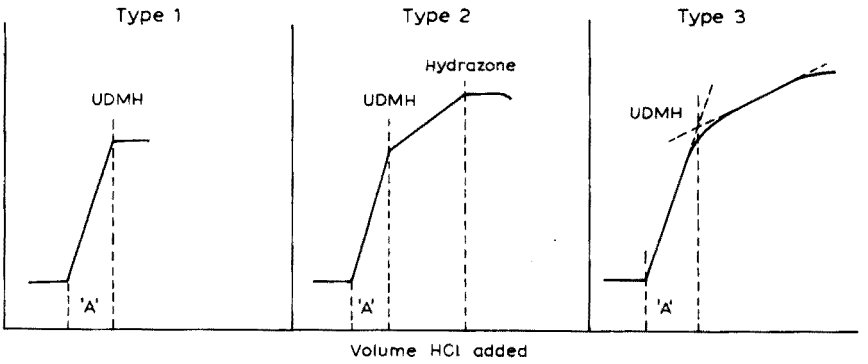

Fig. 1. Types of enthalpogram obtained.

method, is still applicable and the equivalence point can be located to within ±1 %.

Butanal (butyraldehyde) and the ketones react to form hydrazones, but on titration of the excess of UDMH, both the unreacted UDMH and the hydrazone react simultaneously with the hydrochloric acid and the result is the same as for the blank. It is therefore possible to titrate the other aldehydes in the presence of butyraldehyde and some ketones. Titration of each of the benzaldehydes alone and in the presence of up to a 10-fold amount of acetone gave the same results within 1.5 %.

The method has potential application for the determination of these aldehydes in mixtures with other materials, as long as these do not contain reducible groupings. The presence of hydrocarbons, ethers and alcohols has no effect on the precision and reproducibility of the method.

One of us (PP) thanks the British Council for the award of a Colombo Plan Fellowship for the period during which this investigation was made.

REFERENCES

1 I. M. Korenman, F. R. Sheyanova, B. A. Nikolaev, O. B. Abramov, Tr. Khim. Khim. Tekhnol., 4 (1961) 753. (C. Abs. 58 (1963) 9678 h).
2 R. R. Ledesma and C. A. Reynolds, Abstract of Paper, 155th A.C.S. Meeting (1968) page 85
3 R. R. Ledesma, Ph. D. Thesis, Iowa University 1969.
4 L. S. Bark and P. Bate, Proc. 3rd Int. Conf. Rom. Chem. Soc., Brasov, 4 (1971) 335.
5 L. S. Bark and P. Bate, Analyst (London), 97 (1972) 783.
6 R. A. Henry., Ph. D. Thesis, Pennsylvania State University 1968.
7 S. Siggia, Quantitative Organic Analysis via Functional Groups, John Wiley, New York and London. 1963, pp. 87—93.
8 L. S. Bark and P. Bate, Analyst (London), 96 (1971) 881.

Analytica Chimica Acta, 84 (1976) 211–215

Short Communication

THE DISSOCIATION CONSTANTS OF CORYPALLINE AND ISOCORYPALLINE IN ACETONITRILE

JOHN T. STOCK and GEORGE A. SHIA

Department of Chemistry, University of Connecticut Storrs, Connecticut 06268 (U.S.A.)

(Received 20th October 1975)

On electrolytic oxidation in acetonitrile solution, corypalline (7-hydroxy-6-methoxy-N-methyl-1,2,3,4-tetrahydroisoquinoline) yields principally a dimer-type product with a carbon—carbon linking. A minor isomeric product involves carbon—oxygen linkage [1, 2]. Under similar conditions, isocorypalline (6-hydroxy-7-methoxy-N-methyl-1,2,3,4-tetrahydroisoquinoline) yields a dimer in which the linkage is carbon—oxygen—carbon [1]. It can be argued that isocorypalline should tend to undergo C—O—C, rather than C–C, linking. However, the sharp difference in the behavior on oxidation of corypalline and of isocorypalline cannot really be explained by these arguments [1].

As background to the electro-preparative and biosynthetical aspects of isoquinoline alkaloids [3], the respective properties of corypalline and isocorypalline are being examined. The anodic voltammetric and cyclic voltammetric properties of these two compounds are similar [3]. Studies of adsorption on pyrolytic graphite lead to the conclusion that both compounds are adsorbed in the "flat-on" configuration [3]. The dissociation constants, $K_{BH^+} = [B][SH^+]/[BH^+]$, where B is corypalline or isocorypalline and S is acetonitrile, have now been determined.

Experimental

Reagents. Corypalline [1] was recrystallized three times from chloroform (m.p. 168 °C; lit. 168 °C). Isocorypalline was recrystallized three times from absolute ethanol (m.p. 164 °C; lit. 164—165 °C). Picric acid was purified by the procedure of Kolthoff and Chantooni [4]. Acetonitrile, purified by the procedure of Coetzee et al. [5] was stored in the dark. The water content by (Karl Fischer titration) was approximately 5 mM.

Corypalline picrate was prepared by titrating a saturated aqueous solution of corypalline with picric acid until just past the equivalence point. After partial evaporation and cooling to 10 °C, the solid was collected, washed with water, then twice recrystallized from absolute ethanol and dried in vacuo at 100 °C (m.p. 179 °C; lit. 178 °C). Isocorypalline picrate (m.p. 183 °C)

was prepared in a similar manner. Tetraethylammonium picrate was prepared as described by Coetzee and Padmanabhan [6]. Tetraethylammonium perchlorate (TEAP; Eastman Organic Chemicals) was twice recrystallized from water and dried in vacuo at 70 °C. All solid reagents were stored in vacuo over phosphorus pentoxide.

Equipment. The stoppered three-compartment potentiometric cell was similar to that described by Coetzee and Padmanabhan [6]. A Corning type 476021 glass electrode with silver—silver chloride internal electrode, and a Leeds-Northrup type 7401 pH meter were used. The linear response of this system, in conjunction with a Leeds-Northrup saturated calomel electrode, was checked in a range of aqueous buffer solutions that covered the pH range 3.55—12.55. The response was 59.0 ± 0.2 mV per pH unit at 25 °C. All potentiometric measurements in acetonitrile were directly referred to the Pleskov (Ag, 0.010 M $AgNO_3$ in acetonitrile) electrode.

Procedure. Measurements were made at 25.0 ± 0.5 °C. The junction of the reference electrode dipped into 0.0100 M TEAP in acetonitrile contained in the left-hand compartment of the cell. The same solution was placed in the center compartment, while the glass electrode dipped into the buffer solution in the right-hand compartment. Liquid levels were made as nearly equal as possible. All compartments were immediately stoppered. The cell voltage was read 10 min later, then checked for stability. Successive runs within a given working period were made by draining only the right-hand compartment. This was rinsed with acetonitrile and then with a little of the next buffer solution to be examined. All buffer solutions were made in 0.0100 M TEAP in acetonitrile.

Results and discussion

Measurements on picric acid—0.500 mM tetraethylammonium picrate buffers that were 0.0100 M in TEAP are listed in Table 1. Least-squares treatment of all data leads to a linear E(mV) vs. log $\{[HPi]/[Pi^-]\}$ plot of slope 58.9 ± 0.6. The paH^+ values were calculated by the method of Coetzee and Padmanabhan [6], with Kolthoff and Chantooni's value of 10.9 for the pK value of picric acid in acetonitrile [7]. Least-squares extrapolation of E to zero paH^+ gives E_0 = 708 ± 7 mV. Despite the long extrapolation, the uncertainty of the E_0 value is not excessive.

Results obtained with corypalline—0.500 mM corypalline picrate buffers that were 0.0100 M in TEAP are given in Table 2. The paH^+ values are calculated from the relationship $paH^+ = (708 - E)/59.0$. Table 3 concerns analogous measurements made on the isocorypalline system. Least-squares treatment of the data leads to linear E(mV) vs. log $\{[Cb]/[Cs]\}$ plots of slopes −63.5 ± 0.6 and −88.9 ± 0.6 for corypalline and isocorypalline respectively. Calculation [6] of the pK_{BH^+} values then leads to 16.9 ± 0.2 for

TABLE 1

Potentiometry of picric acid (HPi)—0.500 mM picrate buffers

[HPi],	mM	0.050	0.100[a]	0.200	0.300[b]	0.350	0.450	0.500[b]	0.600[a]
E,	mV	20	35	50	62.5	66	70	74.7	82
paH$^+$		11.7_3	11.4_3	11.1_3	10.9_6	10.9_9	10.7_8	10.7_3	10.6_6
[HPi],	mM	0.700	0.800	0.900[a]	1.00	1.10	1.40[a]	1.80	2.40
E,	mV	83	89	91.5	92	94	102.5	110	116
paH$^+$		10.5_9	10.5_3	10.4_8	10.4_3	10.3_9	10.2_9	10.1_8	10.0_5
[HPi],	mM	2.50	3.00	4.00					
E,	mV	117	122	130					
paH$^+$		10.0_4	9.9_6	9.8_3					

[a]Mean of 2 runs.
[b]Mean of 3 runs.

TABLE 2

Potentiometry of corypalline (Cb)—0.500 mM corypalline picrate (Cs) buffers

[Cb],	mM	0.050	0.100[a]	0.150	0.200	0.250[a]	0.300	0.350	0.400
E,	mV	−241	−260	−268	−280	−282	−290	−292	−298
paH$^+$		16.0_8	16.4_0	16.5_4	16.7_4	16.7_8	16.9_1	16.9_4	17.0_5
pK_{BH^+}		16.9	16.9	16.9	17.0	16.9	17.0	16.9	17.0
[Cb],	mM	0.450	0.500[a]	0.600[a]	1.00	1.30	1.50[a]	1.80	2.00
E,	mV	−299	−301	−307	−320	−328	−334	−339	−341
paH$^+$		17.0_7	17.1_0	17.1_9	17.4_2	17.5_6	17.6_6	17.7_4	17.7_8
pK_{BH^+}		17.0	16.9	17.0	17.0	17.0	17.0	17.0	17.0
[Cb],	mM	2.10	2.40	2.50	3.00	3.50	4.00		
E,	mV	−342	−346	−349	−354	−358	−360		
paH$^+$		17.7_9	17.8_6	17.9_1	18.0_0	18.0_7	18.1_0		
pK_{BH^+}		17.0	17.0	17.1	17.1	17.1	17.0		

[a]Mean of 2 runs.

corypalline and 16.7 ± 0.3 for isocorypalline. These standard deviations take into account the uncertainties of the value of E_0 and of the dissociation constant of picric acid. In acetonitrile, typical aliphatic primary, secondary and tertiary amines have pK values [8] in the range 17.9—18.8.

The results show that the contrasting electro-oxidative behavior of corypalline and isocorypalline cannot be attributed to pK differences. However, while the slope of the E vs. log $\{[C_b]/[C_s]\}$ plot for corypalline is close to the Nernstian value, that for isocorypalline is considerably larger. The occurrence of homoconjugation $BH^+ + B \rightleftharpoons BHB^+$ causes the slope to increase [9]. The expected associated effect, deviation of the plot from linearity, may be masked by the fairly narrow range of $[C_b]/[C_s]$ ratios employed in the present work.

TABLE 3

Potentiometry of isocorypalline (Cb')—0.500 mM isocorypalline picrate (Cs') buffers

[Cb'],	mM	0.050	0.150[a]	0.200	0.250[a]	0.300	0.350	0.400	0.450	0.500[b]
E,	mV	−200	−240	−250	−262	−266	−275	−278	−281	−286
paH$^+$		15.3_9	16.0_6	16.2_3	16.4_3	16.5_1	16.6_6	16.7_1	16.7_6	16.8_4
pK_{BH^+}		16.2	16.4	16.5	16.6	16.6	16.7	16.6	16.6	16.7

[Cb'],	mM	0.600	0.700	1.00[a]	1.50	2.00[a]	2.30	2.50
E,	mV	−294	−300	−314	−330	−340	−347	−350
paH$^+$		16.9_8	17.0_8	17.3_1	17.5_9	17.7_6	17.8_8	17.9_3
pK_{BH^+}		16.7	16.7	16.8	16.9	17.0	17.0	17.1

[a]Mean of 2 runs.
[b]Mean of 3 runs.

Curves obtained in the titration of aqueous solutions of corypalline and of isocorypalline with hydrochloric acid are shown in Fig. 1. Apparent pK_{BH^+} values, taken as equal to the pH at the half-titrated point, are 8.3 for corypalline and 8.4 for isocorypalline. These values are of course approximate only. They are however similar to the pK values [10] of N-methyl-1,2,3,4-tetrahydroquinoline derivatives such as morphine (8.2) and codeine (8.2). The pK value of unsubstituted 1,2,3,4-tetrahydroisoquinoline [11] is 9.4.

Attempts were made to titrate the phenol group of corypalline and of isocorypalline. As expected, titration in aqueous solution with sodium

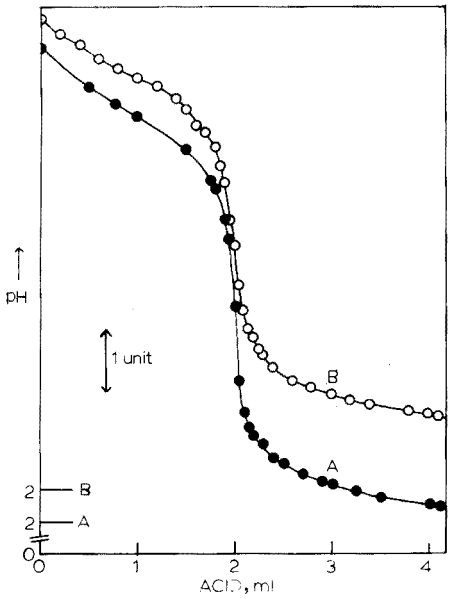

Fig. 1. Titration of 50.0 ml of base in aqueous solution (A) 0.0040 M corypalline with 0.0986 M HCl; (B) 0.00080 M isocorypalline with 0.0197 M HCl.

hydroxide gave no end-point. Titration in acetonitrile with tetraethylammonium hydroxide was also unsuccessful.

This work was carried out with the partial support of the National Science Foundation (Grant GP-30574X). We thank Professor J. M. Bobbitt for the supplies of isoquinoline compounds.

REFERENCES

1 J. M. Bobbitt, H. Yagi, S. Shibuya and J. T. Stock, J. Org. Chem., 36 (1971) 3006.
2 J. M. Bobbitt, Heterocycles, 1 (1973) 181.
3 R. D. Braun and J. T. Stock, Anal. Chim. Acta, 65 (1973) 177.
4 I. M. Kolthoff and M. K. Chantooni, J. Amer. Chem. Soc., 87 (1965) 4428.
5 J. F. Coetzee, G. P. Cunningham, D. K. McGuire and G. R. Padmanabhan, Anal. Chem. 34 (1962) 1139.
6 J. F. Coetzee and G. R. Padmanabhan, J. Phys. Chem., 66 (1962) 1708.
7 I. M. Kolthoff and M. K. Chantooni, J. Amer. Chem. Soc., 91 (1969) 6907.
8 J. F. Coetzee and G. R. Padmanabhan, J. Amer. Chem. Soc., 87 (1965) 5005.
9 J. F. Coetzee, G. R. Padmanabhan and G. P. Cunningham, Talanta, 11 (1964) 93.
10 Handbook of Chemistry and Physics, 53rd edn., CRC Press, Cleveland, Ohio, U.S.A., 1972—3, p. D117.
11 D. D. Perrin, Dissociation Constants of Organic Bases in Aqueous Solution, Butterworths, London, 1965, p. 242.

Analytica Chimica Acta, 84 (1976) 217—221

Short Communication

SOLUBILITIES OF TRIS(1,10-PHENANTHROLINE)IRON(II) SALTS IN WATER AND NITROBENZENE

YUROKU YAMAMOTO, TAKAO TARUI, ETSURO IWAMOTO and TSUNEHIKO TARUMOTO

Department of Chemistry, Faculty of Science, Hiroshima University, Hiroshima 730 (Japan)

(Received 29th September 1975)

In extensive studies of the analytical application of solvent extraction of ion pairs with the tris(1,10-phenanthroline)iron(II) cation [1], the distribution ratio of these ion pairs was found to increase with increasing size of the counter anions [2]. It was therefore considered necessary to measure the solubilities of these salts in water and in nitrobenzene, in water saturated with nitrobenzene and in nitrobenzene saturated with water. The logarithms of the solubilities were found to increase linearly with the reciprocal radius of the counter anions in water, but to decrease in nitrobenzene; a small amount of nitrobenzene in water (and vice versa) significantly affected the solubilities. Selective solvation by nitrobenzene in aqueous solution plays an important rôle in these extraction systems.

Experimental

Crystals of $Fe(phen)_3X_2 \cdot n\,H_2O$ ($X = ClO_4^-$, SCN^-, I^-, Br^-, Cl^-) were prepared as described previously [2]; purities were checked by elemental analysis. Analytical-grade nitrobenzene was washed twice with distilled water and distilled under reduced pressure after shaking with anhydrous sodium sulfate and passing through molecular sieve.

Solubilities were measured in water, nitrobenzene, water saturated with nitrobenzene, and nitrobenzene saturated with water, over the temperature range 20—50 °C in a thermostated bath (±0.3 °C). A saturated solution was made by stirring an excess of the metal chelate salt with an appropriate volume of the solvent for several days, and then filtering through G4 glass filter. An aliquot of the saturated solution was taken by weight, and diluted to an appropriate concentration, for measurement of the absorbance either at 510 nm for aqueous solutions or at 516 nm for organic solutions.

Results and discussion

The solubilities at 25 °C are listed in Table 1 and their temperature dependencies are shown in Fig. 1. The thermodynamic quantities ΔG°, ΔH° and ΔS° (Table 2) were calculated conventionally on the assumption that all the salts are completely dissociated in both phases [3].

The results show that the solubility in water decreases in the order $Cl^- > Br^- > I^- > SCN^- > ClO_4^-$, whereas in nitrobenzene, the order is $ClO_4^- > I^- > SCN^- > Br^- > Cl^-$. A small amount of nitrobenzene dissolved in water diminishes the solubilities of the iodide, thiocyanate and perchlorate, which are relatively well extracted into nitrobenzene, whereas a little water in the

TABLE 1

Solubilities in mol kg^{-1} of $[Fe(phen)_3]X_2$ at 25 °C

Solute	Solvent			
	Water	Nitrobenzene	Water satd. with nitrobenzene	Nitrobenzene satd. with water
Perchlorate	$7.90 \cdot 10^{-4}$	$2.95 \cdot 10^{-2}$	$4.50 \cdot 10^{-4}$	$3.55 \cdot 10^{-2}$
Iodide	$6.15 \cdot 10^{-3}$	$6.26 \cdot 10^{-3}$	$3.29 \cdot 10^{-3}$	$6.0 \cdot 10^{-3}$
Thiocyanate	$3.03 \cdot 10^{-3}$	$6.04 \cdot 10^{-3}$	$1.59 \cdot 10^{-3}$	$6.66 \cdot 10^{-3}$
Bromide	$5.08 \cdot 10^{-2}$	$6.7 \cdot 10^{-4}$	$5.31 \cdot 10^{-2}$	$1.27 \cdot 10^{-3}$
Chloride	$2.55 \cdot 10^{-1}$	$6.2 \cdot 10^{-4}$	$2.71 \cdot 10^{-1}$	$2.32 \cdot 10^{-4}$

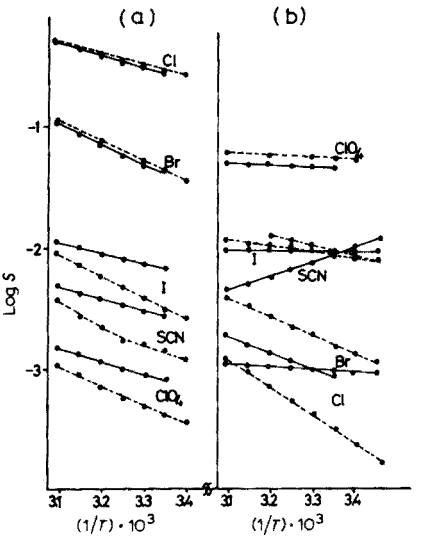

Fig. 1. Plots of the logarithmic solubilities vs. the reciprocal of the temperature. (a) in water, (b) in nitrobenzene. Solid line: in pure solvent. Broken line: in mutually saturated solvent.

TABLE 2

Thermodynamic quantities from solubility data

X^-	ΔG° (kcal mol^{-1})	ΔH° [a] (kcal mol^{-1})	ΔS° [a] (e.u.)
In water-saturated nitrobenzene[b]			
ClO_4^-	5.11	5.1	0
I^-	8.3	9.4	4
Br^-	11.0	22	37
Cl^-	14.1	32	60
In nitrobenzene-saturated water			
ClO_4^-	12.9	23	33
I^-	9.3	22	42
Br^-	4.4	22	57
Cl^-	1.5	14	42
In pure nitrobenzene			
ClO_4^-	5.44	4.6	−3
I^-	8.19	2.6	−19
Br^-	12.2	5.4	−23
Cl^-	12.3	14	6
In pure water			
ClO_4^-	11.9	17	15
I^-	8.2	16	26
Br^-	4.5	19	48
Cl^-	1.6	18	56

[a]The maximum error was ±1.0 kcal mol^{-1} or ±4 e.u.

nitrobenzene decreases the solubility of the chloride, which is the most sparingly soluble in pure nitrobenzene.

Generally, solubility is governed by both the lattice energy and the free energy of solvation of the constituent ions. Although it is very difficult to estimate the lattice energy of polyatomic salts and also not strictly possible to separate the solvation energies of the cation and anion, the problems can be eliminated by comparing the difference in the solubilities in different solvents. The opposite trends between the aqueous and nitrobenzene solutions are illustrated in Fig. 2, which shows the plot of $\log S$ vs. $1/r$, together with the solubilities of some chromium and cobalt complexes [4]. The interesting aspects in the solubilities cannot be explained in terms of Born's solvation energy equation, which predicts the sequence, $Cl^- > Br^- > I^- > ClO_4^-$, if the solid states equilibrated with the saturated solutions are of the identical lattice energy in both phases. This failure has been similarly observed in a previous thermodynamic study of the extraction system [9],

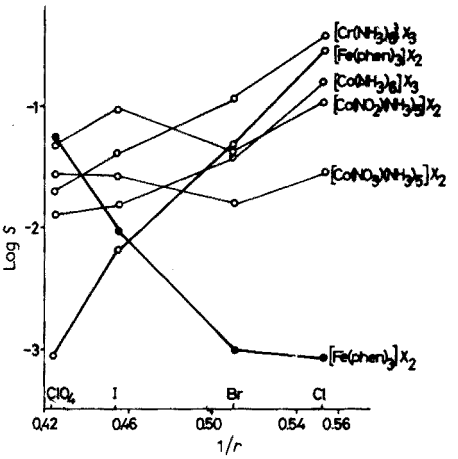

Fig. 2. Plots of the logarithmic solubilities vs. the reciprocal of the radii of the anions. ○ Aqueous solution • Nitrobenzene solution.

in which some specific interactions between the solute and nitrobenzene were considered to play an important role.

With regard to the Co(III)- and Cr(III)—hexaammine complexes, the trend of solubilities in water is quite similar to that of $Fe(phen)_3^{2+}$ but the dependencies on anion sizes are weaker. Reduced symmetry in the metal cation causes large deviations from linear relationships, as shown for $[Co(NH_3)_5NO_2]X$ and $[Co(NH_3)_5NO_3]X_2$ (Fig. 2).

The observation that traces of water in nitrobenzene (or vice versa) affect solubilities also indicates specific solute—solvent interactions, which cause changes in the activity coefficients of solute ions and in the equilibrated solid states. The nitrobenzene solvate, $Fe(phen)_3I_2 \cdot 2H_2O \cdot (C_6H_5NO_2)$, can be isolated from the nitrobenzene-saturated aqueous phase, and the amount of water [5] co-extracted with $Fe(phen)_3X_2$ into nitrobenzene increases [6] in the order $ClO_4^- < I^- < Br^- < Cl^-$. In the present study, the nitrobenzene solvate of the perchlorate was obtained in a similar way. $[Fe(phen)_3(ClO_4)_2 \cdot H_2O \cdot C_6H_5NO_2$ requires 53.9 %C, 3.3 %H, 10.5 %N; found 54.0 %C, 3.4 %H, 10.5 %N]. Similar nitrobenzene solvates could not be isolated for the bromide or chloride.

$Fe(phen)_3Br_2$ greatly increases the solubility of nitrobenzene in aqueous phases [7], probably because of the hydrophobic character of the metal chelate cation; nitrobenzene is probably bound to the $Fe(phen)_3^{2+}$ cation (association constant 15.0 [8]). It can be said that the strong hydration of bromide and chloride ions prevents the formation of nitrobenzene solvates whereas the weaker hydration of perchlorate and iodide ions does not. Such phenomena can explain the lower solubilities of the salts with the larger anions in water saturated with nitrobenzene, which is the actual solvent system in practical extractions. These suggestions are supported by the

temperature dependence of the solubilities (Fig. 1); when the water contains nitrobenzene, the dissolution reactions of the perchlorate, thiocyanate and iodide become more endothermic. A similar phenomenon occurs with the chloride in nitrobenzene containing some water; the cause of the thiocyanate results in nitrobenzene is not clear.

In conclusion, in this extraction system, a small amount of solvent dissolved in each phase plays an important role, particularly for species which are only slightly soluble in pure solvent. Thus the transfer of the perchlorate salt into nitrobenzene is promoted by inter-saturation of the water and nitrobenzene phases.

The authors are grateful to the Japan Society for Promotion of Science for grants for fundamental research in chemistry.

REFERENCES

1 (Part L). Y. Yamamoto, T. Kumamaru, Y. Hayashi and M. Yamamoto, Anal. Chim. Acta, 69 (1974) 321.
2 Y. Yamamoto, T. Tarumoto and E. Iwamoto, Chem. Lett., (1972) 255.
3 Y. Yamamoto, E. Sumimura, K. Miyoshi and T. Tominaga, Anal. Chim. Acta, 64 (1973) 225.
4 A. Seidell and W. F. Linke, Solubilities of Inorganic and Metal Organic Compounds, 3rd edn., Vol. 1, Van Nostrand, New York, 1940, p. 427.
5 E. Iwamoto, T. Tarumoto, T. Tarui and Y. Yamamoto, Chem. Lett., (1972) 755.
6 Y. Yamamoto, T. Tarumoto and T. Tarui, Bull. Chem. Soc. Jpn., 46 (1973) 1466.
7 E. Iwamoto, M. Yamamoto and Y. Yamamoto, Inorg. Nucl. Chem. Lett., (1972) 755. 1069.
8 T. Tarui, E. Iwamoto and Y. Yamamoto, Inorg. Nucl. Chem. Lett., 11 (1975) 323.
9 Y. Yamamoto, T. Tarumoto and E. Iwamoto, Anal. Chim. Acta, 64 (1973) 1.

Analytica Chimica Acta, 84 (1976) 223—224

Book Reviews

Investigation of Rates and Mechanisms of Reactions: Part I. General Considerations and Reactions at Conventional Rates (Vol. VI of *Techniques of Chemistry*, edited by A. Weissberger), Wiley-Interscience, New York, 1974, xiii + 838 pp., price £21.00.

It is sad, but true, that reaction kinetics are not beloved of Analytical Chemists. It is sad because kinetic factors are often important in the whole spectrum of chemically based methods, as well as in pyrolytic techniques, and in environmentally important processes. Usually, only necessary kinetic measurements are tolerated (enzymic methods, for example). It is also sad because they will find it unnecessary to use the present text. It (and Part II) provides a comprehensive but lucid account of all aspects of kinetics as they apply to most types of chemical reaction, and much of the information is relevant to the chemical processes used in analytical chemistry.

Part I covers mainly theoretical, data production and interpretive aspects of reactions with "conventional" rates (Part II will be concerned with fast reactions). It deals with current theories of kinetics in solution and in the gas phase, of isotope and stereochemical effects, and also discusses the kinetics and mechanisms of inorganic and complexing reactions, and of homogeneous (including enzymic) and heterogeneous catalysis. Chapters on the use of computers and linear free-energy relationships are included. Particularly useful is the section, From Kinetic Data to Reaction Mechanism, often a difficult problem in kinetics, and a discussion on Pitfalls in Kinetics (p. 187) which presents many a cautionary tale. This is a well produced book, which is likely to be a standard reference on reaction kinetics for many years.

Alan Townshend

Determination of Gaseous Elements in Metals, edited by L. M. Melnick, L. L. Lewis and B. D. Holt, Wiley, New York, 1974, viii + 744 pp., price £19.25.

The mechanical and physical properties of metals and alloys can be affected seriously by small amounts of gaseous elements such as hydrogen, oxygen and nitrogen. The methods necessary to determine these are exacting; many of the reactions involved are still not fully understood. This book, which appears as Vol. 40 in the Kolthoff—Elving Chemical Analysis series, provides detailed information on the many techniques that have been used. After two general chapters, the particular applications of activation analysis, fusion methods, electrical discharge extraction methods, and optical and

mass spectrometry are surveyed. Three chapters are then devoted to analyses for hydrogen, nitrogen and oxygen, and ten chapters to the metals and alloys that have been analyzed. The final chapter deals with surface analysis by nuclear and ion-beam techniques.

As occurs so frequently with multi-author volumes, some of the reference lists are more up-to-date than others. Although there is some duplication, it can be of interest for the same problem to be examined from different angles. The treatment is remarkably homogeneous, possibly because the editors, with V. A. Fassell, contributed 9 of the 20 chapters. This book maintains the established reputation of the Kolthoff—Elving series, and will be the standard work on the subject for many years.

Spectroscopic and Chromatographic Analysis of Mineral Oils, by S. H. Kagler, IPST, Jerusalem—J. Wiley (Halsted Press), New York, 1974, xiii + 559 pp., price £24.85.

The contents of this translation of a German book are better described by its original title *Neue Mineralölanalyse: Spektroskopie und Chromatographie in Grundlagen, Geräten und Anwendung.* The spectroscopy ranges from x.r.f. and emission to n.m.r. and m.s., and all types of chromatography, except h.p.l.c., are also covered. For each technique a discussion of basic principles is followed by descriptions of instrumentation and practical hints; the length of these sections is excessive, in view of the numerous general texts and monographs now available on these topics. The paragraphs on applications to mineral oils and their products are straightforward literature reviews, with very little detail, except in the cases of infrared spectroscopy and gas chromatography, where full discussions are included. In 1969, the original German text was of value to chemists in the oil industries, but this English edition, which is a direct translation with no attempt at updating, is too expensive and out-of-date to attract interest.

Analytica Chimica Acta, 84 (1976) 225

Announcements

XXVIth International Congress of Pure and Applied Chemistry Tokyo, Japan, September, 1977

The XXVIth International Congress will be held on September 4—10, 1977 in Tokyo (Akasaka area), Japan, under the auspices of the Science Council of Japan. The Congress will consist of Joint Symposia and Division Sessions. The Joint Symposia have been organized in the recognition that the future of mankind and its prosperity are largely dependent on the progress of fundamental and applied chemistry, and that interdisciplinary cooperation between specialists is urgently needed.

Joint Symposia will be arranged under the following titles: Selectivity and Specificity in Chemical Reactions; Phase Boundaries and Multiphase Systems; Biologically Active Substances; Separation and Detection of Trace Species, Modern Aspects of Industrial Materials and Resources. Sessions on physical, analytical, organic and macromolecular chemistry will also be arranged.

The official language of the Congress is English, although presentation can be made in any language. Those who wish to offer papers should do so not later than August 31, 1976; abstracts must be submitted by March 15, 1977. Further information can be obtained from: XXVIth Congress of IUPAC, P.O. Box 56, Kanda Post Office, Tokyo 101-91, Japan.

Trace Analysis of Environmental Materials TARC International Symposium III

The third of a continuing series of international conferences on analytical chemistry will be held on August 4—6, 1976 at Dalhousie University, Halifax, Nova Scotia. The conference is co-sponsored by the Chemical Institute of Canada and the Trace Analysis Research Centre at Dalhousie University. Papers on all aspects of trace analysis of environmental samples will be presented. Information on the conference may be obtained by writing to: Professor D. E. Ryan, Trace Analysis Research Centre, Dalhousie University, Halifax, Nova Scotia, B3H 4J1, Canada.

Guide to the use of Ion-Selective Electrodes

A comprehensive 40-page guide, which includes information on electrode characteristics, methods of measurement, performance data, storage and maintenance of electrodes is available, on request, from: Philips Science and Industry Division TQ 111-4, Eindhoven, The Netherlands, or from Philips Electronic Instruments, 750 South Fulton Avenue, Mount Vernon, N.Y. 10550, U.S.A.

Analytica Chimica Acta, 84 (1976) 226—229

ERRATUM Corrected / V.P. 18 Jan. 1977

R. Belcher, S.L. Bogdanski, I.H.B. Rix and A. Townshend, Molecular Emission Cavity Analysis: Stimulation of Metal Halide Emissions, *Anal. Chim. Acta*, 81 (1976) 325—336.

The upper sections in Figs. 1—7 were reproduced incorrectly or omitted. The correct figures are:

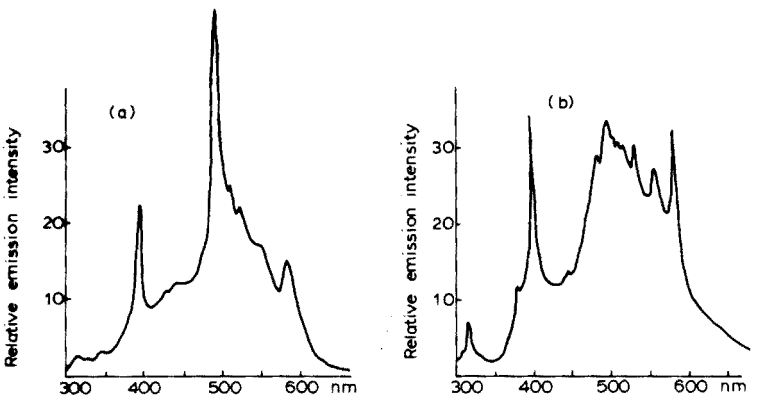

p. 327. Fig. 1. MECA spectra of (a) $MnCl_2$, (b) $MnBr_2$.

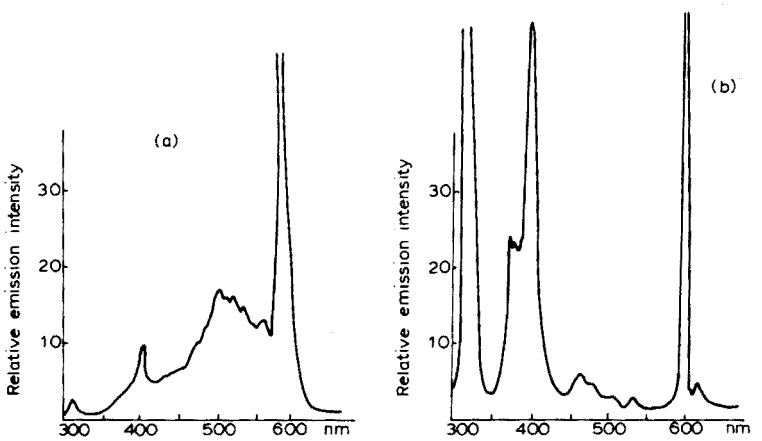

p. 328. Fig. 2. Spectra of MnI_2 by (a) MECA, (b) aspiration.

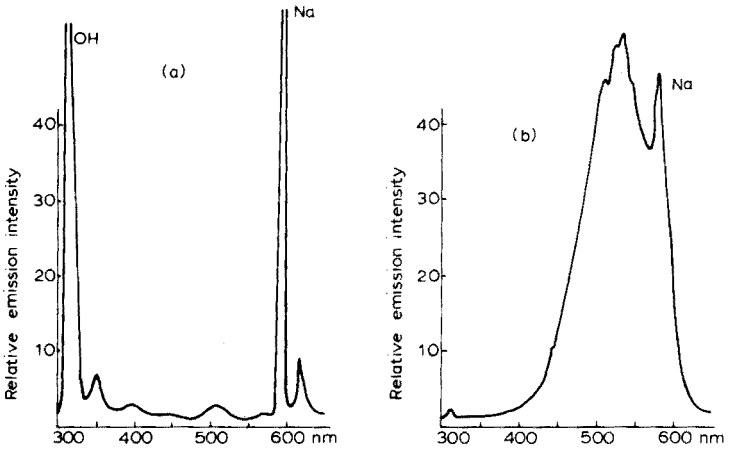

p. 329. Fig. 3. Spectra of CoI_2 by (a) aspiration, (b) MECA.

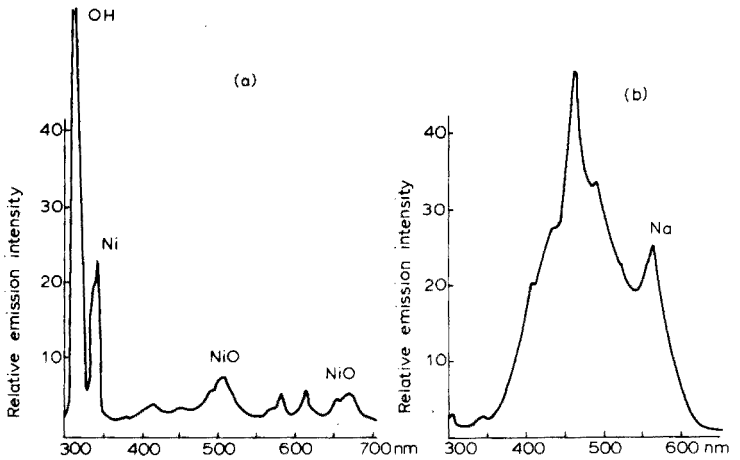

p. 330. Fig. 4. Spectra of (a) $NiCl_2$ by aspiration, (b) $NiBr_2$ by MECA.

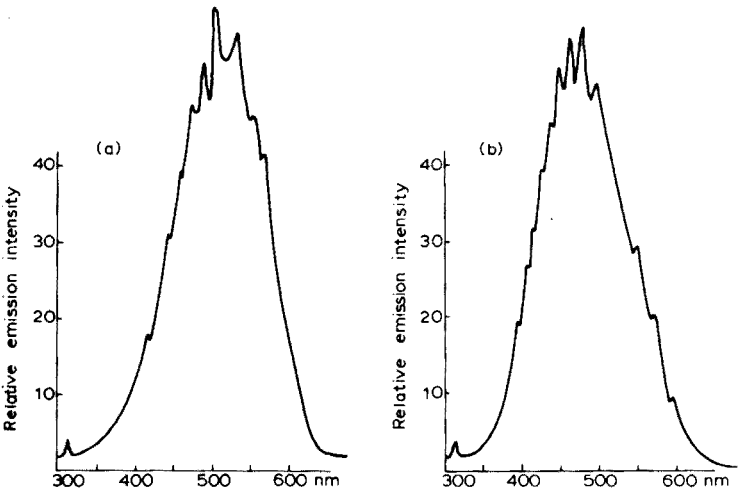

p. 331. Fig. 5. MECA spectra of (a) $PbBr_2$, (b) $PbCl_2$.

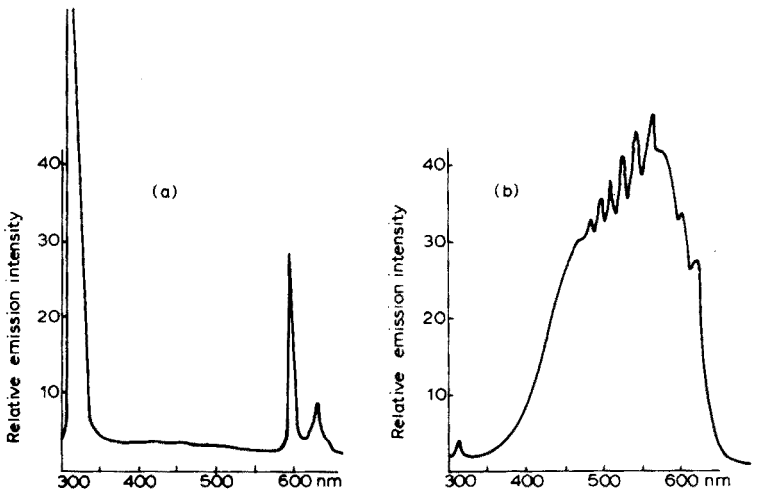

p. 331. Fig. 6. Spectra of PbI_2 by (a) aspiration, (b) MECA.

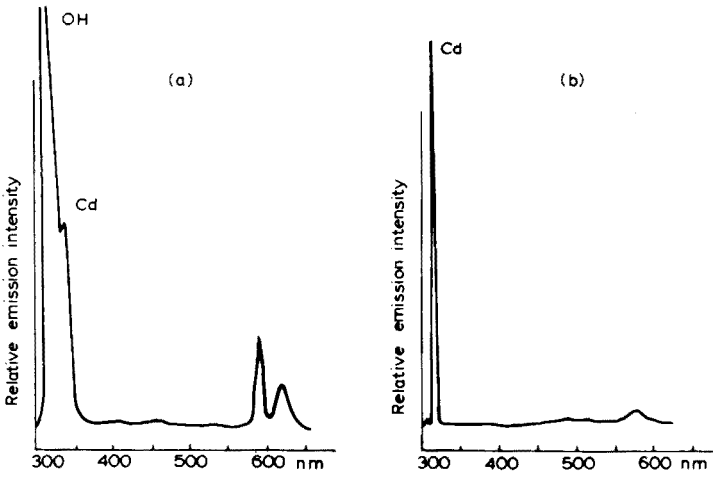

p. 333. Fig. 7. Spectra of $CdCl_2$ by (a) aspiration, (b) MECA.

Corrected
V.P.
18. Jan. 1977

RECENTLY PUBLISHED BIBLIOGRAPHIES IN CHROMATOGRAPHY

BIBLIOGRAPHY OF PAPER AND THIN-LAYER CHROMATOGRAPHY 1970-1973

And Survey of Applications

edited by K. MACEK, I.M. HAIS, J. KOPECKÝ, V. SCHWARZ, J. GASPARIČ, *and* J. CHURAČEK.

Supplementary Volume No. 5, published in conjunction with the Journal of Chromatography.

1976. xviii + 744 pages.
US $76.95/Dfl. 200.00.
ISBN 0-444-41299-9
Subscription price:
US $47.95/Dfl. 125.00

This volume is the continuation of earlier bibliographies covering developments of both paper and thin-layer chromatography. It contains 5601 references of authors and titles of papers or books (translated titles for papers in languages other than English, French or German), appearing from the beginning of 1970 to the middle of 1973. A General Part covers general reviews and books and provides a detailed classification of techniques and applications. A Special Part is subdivided into approximately 500 chapters according to the chemical structure of the compound, or exceptionally, according to their biological activity (vitamins, antibiotics, pesticides, pharmaceuticals), physical properties (dyes), or technical importance (plastics, antioxidants). Cross references are given in cases where papers contain data which could be included in several chapters. The subject matter is gathered from a systematic search of journals which regularly publish papers of chromatographic interest, as well as from material available in other journals, reprints, etc. The bibliography contains an author index and an extensive list of 20,000 compounds chromatographed.

BIBLIOGRAPHY OF ELECTROPHORESIS 1968-1972

And Survey of Applications

edited by Z. DEYL, J. KOPECKÝ, J. DAVÍDEK, M. JURICOVÁ *and* R. HELM.

Supplementary Volume No. 4, published in conjunction with the Journal of Chromatography.

1975. xvi + 862 pages.
US $76.95/Dfl. 200.00.
paperback.
ISBN 0-444-41225-5
Subscription price:
US $47.95/Dfl. 125.00

This volume complements preceeding publications on paper, thin-layer and column chromatography and presents many diverse problems of electrophoretic separations. It contains exhaustive information on theoretical separational techniques selected from work scattered throughout various journals. The reader is provided with a quick reference to the particular compound of his interest, consequently saving many hours of disastrous literature search. In the first section special emphasis is laid on the electrophoretic estimation of molecular weight of macromolecular substances. Papers dealing with instrumentation, and those dealing with new media for electrophoresis are presented. The second part concentrates on application, and contains specialised chapters stressing the vast area of application of electrophoretic techniques in biochemistry, clinical chemistry, physiology as well as biology. This comprehensive work should be a welcome asset to the libraries of investigators and research workers in the field. The bibliography contains an author index and an extensive list of compounds electrophoresed.

BIBLIOGRAPHY OF COLUMN CHROMATOGRAPHY 1967-1970

And Survey of Applications

compiled by Z. DEYL, J. ROSMUS†, M. JUŘICOVÁ, *and* J. KOPECKÝ.

Supplementary Volume No. 3, published in conjunction with the Journal of Chromatography.

1973. xix + 1067 pages.
US $69.25/Dfl. 180.00.
Subscription price:
US $51.95/Dfl. 135.00.
paperback.
ISBN 0-444-41008-2

BIBLIOGRAPHY OF PAPER AND THIN-LAYER CHROMATOGRAPHY 1966-1969

And Survey of Applications

compiled by K. MACEK, I.M. HAIS, J. KOPECKÝ, J. GASPERIČ, V. RABEK, *and* J. CHURAČEK.

Supplementary Volume No. 2, published in conjunction with the Journal of Chromatography.

1972. xvi + 992 pages.
US $76.95/Dfl. 200.00.
Subscription price:
US $57.50/Dfl. 150.00.
ISBN 0-444-40953-X

BIBLIOGRAPHY OF PAPER AND THIN-LAYER CHROMATOGRAPHY 1961-1965

And Survey of Applications

edited by K. MACEK, I.M. HAIS, J. KOPECKÝ *and* J. GASPARIČ.

Supplementary Volume No. 1, published in conjunction with the Journal of Chromatography.

1968. only available in microfilm
US $57.50/Dfl. 150.00.

ELSEVIER SCIENTIFIC PUBLISHING COMPANY

P.O. Box 211, Amsterdam, The Netherlands

Distributed in the U.S.A. and Canada by:
ELSEVIER/NORTH-HOLLAND INC.,
52 Vanderbilt Avenue, New York, N.Y. 10017

The Dutch guilder price is definite. US $ prices are subject to exchange rate fluctuations

(Continued from page 4 of cover)

Printed in The Netherlands

CONTENTS

(continued on inside page of the cover)